3D LOCALIZATION TECHNIQUES FOR WIRELESS SENSOR NETWORKS

A THESIS SUBMITTED TO AUCKLAND UNIVERSITY OF TECHNOLOGY
IN FULFILMENT OF THE REQUIREMENTS FOR THE DEGREE OF
DOCTOR OF PHILOSOPHY

By
Tanveer Ahmad
School of Engineering, Computer and Mathematical Sciences

July 2019

Attestation of Authorship

I hereby declare that this submission is my own work and that, to the best of my knowledge and belief, it contains no material previously published or written by another person nor material which to a substantial extent has been accepted for the qualification of any other degree or diploma of a university or other institution of higher learning.

Signature of candidate

Acknowledgements

God never spoil any effort. Every piece of work is rewarded according to the nature of the devotion for it. I am extremely thankful to **ALMIGHTY ALLAH**, Who in spite of numerous difficulties and acute frustrations enables me to complete the study and present the humble piece of scientific work. I offer my humblest thanks to **Holy Prophet Muhammad** (peace be upon him) who is the beacon of enlightenment and biggest benefactor of the mankind ever had.

It gives me immense pleasure to express my deepest gratitude and sincere thanks to my respected supervisor **Dr. Xue Jun Li** Senior Lecturer, School of Engineering, Computer and Mathematical Sciences, Auckland University of Technology, New Zealand, for his special attention, consistent encouragement, expertise suggestion and constructive criticism without which, I really would never have been able to complete this manuscript. I would also like to thank my secondary supervisor, **Dr. Boon-Chong Seet** Associate Professor, SECMS who despite of his busiest timing routine work acted as guided me through this journey. Last but not least I owe to acknowledge the understanding, encouragement, spiritual and financial support given by my beloved, affectionate and great Father, my sweetest Mom who left this world during this journey of Ph.D and my lovely wife Komal Abid, for her endless love and prayer. No words no phrases can really express my feeling that I have for my beloved parents.

I dedicated it to my lovely Parents. May their soul be in rest, peace and heaven (Ameen)

Abstract

Location information is crucial for the correct interpretation of data collected through wireless sensor networks (WSNs). The de facto system for wireless localization, Global Positioning System (GPS) does not work properly in indoor environment, thus researchers are thriving to find other localization schemes for indoor WSNs. The main goal of this work is to study and design three-dimensional (3D) wireless localization schemes for indoor applications.

In this thesis, a new and accurate, efficient and cost-effective algorithm, called parametric loop division (PLD) has been proposed for localizing static nodes within a WSN. In the proposed technique, reference points can help to produce new parametric points by calculating the mid points and by taking step size that falls within the network boundary. The objective of PLD scheme is to estimate the actual localization volume and find the node position in 3D space by using subdivision method. In each step, triangles are subdivided into pairs with the addition of extraordinary nodes in its control ring matrix. Parametric points are generated by using the step size and RSSI is compared with threshold value for localization. The work involves the development of novel solution which utilizes the anchor node position information to calibrate nodes with unknown target, allowing it to work even in a changing environment with increased reliability and accuracy.

Subsequently, PLD is evaluated in presence of different types of noises. Firstly, the localization accuracy was tested without the addition of noise in distance measurement.

Like other schemes, PLD is adversely affected by the noise, which reduces the accuracy of the system. A new framework with extended kalman filtering (EKF) is proposed to refine the nodes coordinates affected by the noise. Furthermore, an analytical framework is presented with the detailed study of lower bound of the localization accuracy. The PLD is tested for naive, Gaussian and intelligent noise. The anchor node is modelled by only using the knowledge information of coordinates to redesign the distance vertex from anchor to parametric points.

Finally, we consider the mobile based localization scheme, which has become popular recently with the development of autonomous robots and unmanned aerial vehicles. We designed an extended centroid based localization system that use the weight on distance to compute the signal power. A fuzzy logic approach is adopted for computation. The design is divided in to In the first phase, RSSI is mapped to fuzzy membership function. The mobile anchor exchange beacon and measure distance using RSSI data. The target node position is computed in a circle within the sensing region for a mobile anchor node, which moves on a random walk for broadcasting beacons. RSSI and signal power is used as an input for fuzzy system. In the second phase, for accurate node positioning a perpendicular bisector is drawn from rough estimation to circle drawn previously. Like EKF, fuzzy logic works well in nonlinear estimation of target nodes locations.

Localization problem is evolving with the advance of mobile technologies and this thesis contributes to the fast development of this topic. However, there are still some issued left out as future study, mainly on the effect of anchor node localization error, implementing mobile anchor in a PLD algorithm and energy-aware localization schemes in WSNs.

Contents

List of Tables

List of Figures

Glossary and Notations

Glossary

2D	Two Dimensional
3D	Three Dimensional
AoA	Angle of Arrival
ABC	Assumption Based Coordinates
AFL	Anchor Free Localization
APS	Ad-hoc Positioning System
APIT	Approximation Point in Triangulation
AVPLE	Auxiliary Variables Pseudo-Linear Estimator
AGN	Additive Gaussian Noise
AWGN	Additive white Gaussian Noise
BWRS	Berkeley Wireless Research Centre
BSN	Body Sensor Network
BPN	Back Propagation Network
BPSK	Binary Phase Shift Keying
CS	Control Segment
CL	Centroid Localization
CGCS	China Geogetic Coordinate System
CRLB	Cramer-Rao Lower Bound
CFP	Convex Feasible Problem

CWLS	Constrained Weight Least Square
CPU	Central Processing Unit
CoG	Center of Gravity
CDF	Cumulative Distribution Function
CDF	Central difference filter
DSS	Direct Spread Spectrum
DARPA	Defence Advance Research Project Agency
DSN	Distributed Sensor Networks
DME	Distance Measurement Error
EGM96	Earth Gravitational Model 1996
EGC	Equal Gain Combining
EKF	Extended Kalman Filter
FIM	Fisher Information Matrix
FLMSL	Fuzzy-logic based Multilateration Scheme for Localization
FAF	Floor Attenuation Factor
FL	Fuzzy Logic
GPS	Global Positioning System
GSM	Global System for Mobile
GHS	Grouping Hierarchy Structure
GHT	Geographic Hash Function
GNSS	Global Navigation Satellite System
GDOP	Geometric Dilution of Precision
GMM	Gaussian Mixture Modelling
GCC	Generalized Cross Correlation
IoT	Internet of Things
IEEE	Institute of Electrical and Electronic Engineering

IPS	Indoor Positioning System
IC	Integrated Circuit
ICL	Improved Centroid Localization
ITS	Intelligent transportaton systems
KNN	K Nearest Neighbour
KF	Kalman Filter
LA	Location Assistance
LBS	Location based Service
LoS	Line of Sight
LR-WPANS	Low Rate Wireless Personal area Networks
LLS	Linear Least Square
LNSM-DV	Log-normal Shadowing Model with Dynamic Variance
LAN	Local Area Network
LQI	Link Quality Indicator
LMS	Least Mean Square
LE	Localization error
MEMS	Micro Electro Mechanical Systems
MCDS	Minimum Connected Dominant Set
MLE	Maximum Likelihood Estimator
MVE	Minimum Variance Estimators
MVU	Minimum Variance Unbiased
MSE	Mean Square Error
MCL	Monte Carlo Localization
MDS	Multidimensional Scaling
MISO	Multi Input Single Output
MIMO	Multi Input Multi Output

MRC	Maximum Ratio Combining
MPMR	Maximum Point Minimum Rectangle
MPMD	Maximum Point Minimum Diameter
MSDS	Minimum Size Dominant Set
MAL	Mobile-Assisted Localization
ME	Mean Error
NLoS	Non-Line of Sight
NLLS	Nonlinear Least Square
OA	Outer Approximation
PDF	Probability Density Function
PLD	Parametric Loop Division
POCS	Projection onto Convex Set
PIT	Point is Triangulation Test
PLD	Parametric loop division
QFT	Quantum Field Theory
RSSI	Received Signal Strength Indicator
RF	Radio Frequency
RFID	Radio Frequency Identification
RDNL	Robust Distribution Network Localization
ROPE	Robust Position Estimation
SS	Space Segment
SA	Subspace Approach
SNR	Signal to Noise Ratio
SIMO	Single Input Multi Output
SISO	Single Input Single Output
SCCL	Self-Calibrated Centroid Localization

SSR	Secondary Surveillance Radar
SE	Sum of Error
TS	Taylor Series
ToA	Time of Arrival
TDoA	Time Difference of Arrival
TCP-IP	Transmission Control Protocol & Internet Protocol
TCL	Triangular Centroid Localization
ToF	Time of Flight
TWR	Two-Way Ranging
TWTT	Two-Way Time Transfer
US	User Segment
UTM	Universal Transverse Mercator
UPS	Universal Polar Stenographic
UDG	Unit Disk Graph
UKF	unscented kalman filter
VHF	Very High Frequency
WSN	Wireless Sensor Networks
WPAN	Wireless Personal area Networks
WGS84	World Geodetic System 1984
WCL	Weighted Centroid Localization
WAF	Wall Attenuation Factor
WLLS	Weighted Linear Least Square

Notation

G_{RX}	Receiver Gain
G_{TX}	Transmitter Gain
N	Sensor nodes
A	Anchor Nodes
Δ	Step Size
M_i	Mid-point at each PLD network.
A_i	ith anchor nodes.
P_i	ith parametric points produced after each iteration.
v_i	volume of ith parametric looped network.
k_i	Non overlapped PLD networks.
$D_{N\to N}$	Distance from a sensor nodes to all other sensor nodes.
$D_{A\to N}$	Distance from a anchor nodes to all other sensor nodes.
Δ	Step size in PLD network.
α	Parametric function of PLD network.
γ	Representation of change in center point.
$\bigotimes$	Working boundary.
φ	Target nodes in each k_i network.
$\hat{x}, \hat{y}, \hat{z}$	Cartesian coordinates of estimated node position.
η	Anchor nodes in each k_i network.
V_u	unit volume
l_i	Pre-localized Node
σ	Standard Deviation

Chapter 1

Introduction

Recent advancements in communication technology, microelectronics, and low-cost sensor technologies have empowered the expansion and emergence of wireless sensor networks (WSN) as an innovative paradigm of computer networking [1]. With low cost sensor nodes, WSNs benefit from simple deployment [2]. Applications of WSNs include maintaining and controlling environment, transportation, medical and business purposes. It is desired for WSNs to prolong their lifespan under limited constraints [3, 4]. Most nodes in WSNs can observe the environment or events in a region of interest, as well as to forward data packets according to a predefined routing protocol [5]. Some special nodes are known as sink nodes, which collect sensor data and forward them to the end user. In particular, sink nodes can disseminate control messages to common sensor nodes, which may include network-related policies, sleeping and waking-up schedule and routing updates [6].

Networking in WSNs can be established in two ways, without infrastructure (i.e., infrastructure-less) or with the aid of infrastructure. In a infrastructure-less WSN, sensor nodes collect and process sensing data, set up the network by network discovery and routing protocols. In infrastructure-based WSNs, nodes can communicate with each other through the infrastructure. Therefore, node to node connection can be varied and hence network maintenance becomes easy. In addition, infrastructure-based WSNs usually require fewer sensor nodes as compared to infrastructure-less WSNs [7, 8]. The collection of date and forwarding it to destination is a vital role of a sensor nodes. So, knowing the location of collected data is very important in WSNs. The location information can be obtained by sensor localization. Localization is basically a method to compute the sensor nodes location, that is an interesting research topic, and numerous works have been done so far. That is why, it is very crucial to develop an accurate, scalable, low-cost and energy efficient localization technique for WSNs.

1.1 Wireless Sensor Networks

Technological advancement has empowered the development of low-power, self configured, cheap, and multi-functional sensor devices. These are the self-organizing devices with cohesive communication capabilities, information processing, and sensing. A WSN consists of number of low-cost, battery operated tiny sensor nodes that are capable of sensing, actuation, networking and data processing [9].

In WSNs hundreds or even thousands of tiny, sensors nodes operated on a battery are deployed on a physical area of interest. Each sensor in a network is used to collect information, distinguishing ecological conditions such as temperature, sound, vibration, synthetic mixture, and so on. Sensors then transmit the collected data to other neighboring nodes in a network and back to the application system where data is being processed. The sensing hardware estimates parameters from nature encompassing the sensor and changes them into electrical signals. The electrical signals expose the characteristics of sensor by either object located or by demonstration of some events occurrence in the vicinity of the WSNs. The detected signals are sent by the sensor nodes, typically by means of a radio transmitter, either specifically or through a sink node or a based station.

In the past few decades, the emergence in Internet of Things (IoT) also allows the user to transfer different forms of information that helps in science, industry, education, business, and even in our daily life. WSNs also gain much popularity in civil application, process monitoring [10, 11, 12, 13, 14], military applications [15, 16, 17, 18, 19, 20], habitat environment monitoring [21, 22, 23, 24, 25, 26], structure health monitoring [27, 28, 29, 30, 31], home automation [32, 33, 34, 35, 36], health care applications [37, 38, 39, 40, 41, 42], and vehicle networks and intelligent transportation systems (ITS) [43, 44, 45, 46, 47]. Hence, the new ways of proactive computing are introduced by WSNs in which sensor automatically gain real-time data from the physical environment.

Numerous applications have been projected for WSNs, and a significant number of these applications have explicit prerequisites with extra challenges to the application designer. Each WSNs have four basic components including: (1) localized or distributed nodes; (2) a wire/ wireless interconnected network; (3) information cluster located in a central point; and (4) set of application system to process correlation data [48]. In this way the computational and sensing nodes are considered part of WSNs. Doubtlessly, the main computation is mostly accomplished within the network, because of the large amount of data, algorithms and techniques used in the system. In some cases, the communication and computation structure connected with sensor nodes are application explicit to the physical and environmental condition [48].

A typical sensor node MICAz equipped with a processor Atmel128L, having throughput of 8 million instructions per second with 8MHz operating power is shows in Figure 1.1. MICAz also featuring IEEE 802.15.4/Zigbee with acquiescent a direct spread spectrum (DSS) for RF interference, RF transceiver, with 2.4-2.4845 GHz operated frequency band and 250kbps data transfer rate [49]. The MICAz is compatible with existing sensor boards and runs on a TinyOS that easily mounted on a mote. Several types of sensors are presented in the field of control and sensing includes radio wave frequency sensors, magnetic and electric field sensors, optical sensors, infrared and

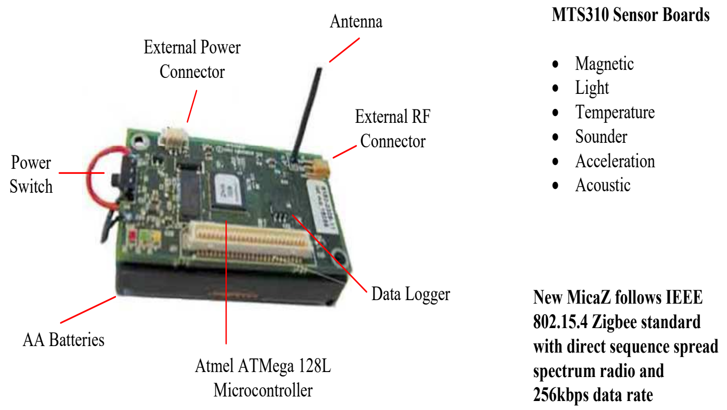

Figure 1.1: A typical hardware of MICAz Sensor mote.

electrooptic, laser and radars, environmental sensors and location/ navigation sensors. A few favorable circumstances exist for instrumenting within a territory with a WSNs:

- In a dense environment a high level of fault tolerance is attainable a large networks.
- The tiny sensor union coverage makes it possible to cover a large area of concern
- The network should cover a specific zone and territory, to defeat network boundaries/ gaps within the interested region.
- It is conceivable to gradually expand the coverage density with extra nodes deployment in the region under perception.
- The quality of the sensing is achieved by deploying multiple sensors in a dense area and by having multiple readings from different sensors. Furthermore, WSNs also helps in hostile and harsh areas where wired networks can't be deployed. For example, nodes can be dropped in a forest from the air where wired connection is almost impossible.
- WSNs are also scalable in nature so they are continuously being used in application such as health care and agriculture.

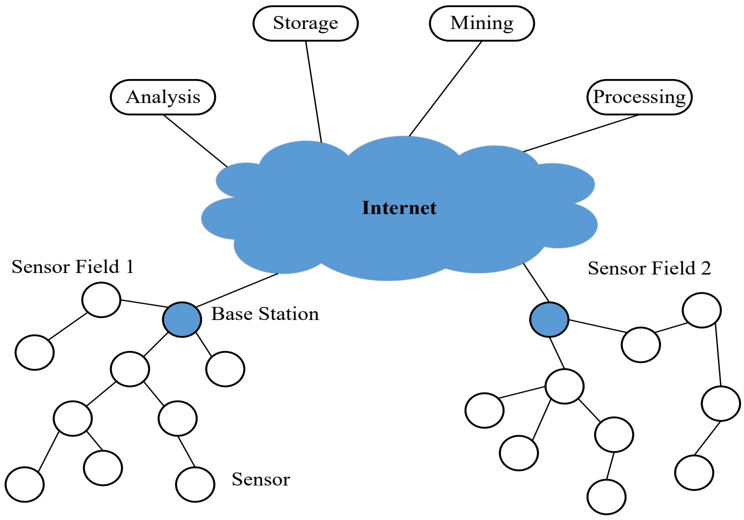

Figure 1.2: Distributed infrastructure of a Wireless Sensor Networks.

Let's take a scenario as depicted in Figure 1.2 where two sensor spaces are available for tracking of separate areas and connected with internet via base stations. This means it is not necessary to have only one sensor node to communicate with the base station. In a network there might be several complicated sensors and some may be equipped with the GPS for more precise location estimation at the expense of power [50].

1.2 Significance and Motivation

WSNs is a large scale network with thousands of wireless transducer devices typically known as sensor nodes or "mote". At first WSN was used in cold war era, where a large scale distributed network of hydrophones and radars were deployed in a region for monitoring of the oceans and skies [51]. Information broadcasting within a network is possible where network setup is predefined. However, in some worst situations this is not the case as in battle fields or volcano eruptions as networking topology is dynamically changing. This is is known as infrastructure-less WSNs, in which nodes are deployed and setup without the use of any hardware, which is a most favourable solution where no precise network setup is required. The node deployment is setup less structure may require some mobile nodes with full network coverage and low communication cost to save energy. This issue forms one motivation of this research. Large amount of deployed sensors and anchor nodes arrange themselves in ad-hoc manner with single-hop or multi-hop connection while considering distance between the nodes. Furthermore, a localization system must be energy efficient to prolong the battery life of the nodes. Several algorithms were developed to tackle energy utilization in an effective manner for sensor node life duration and performance enhancement. Data gathering is the key action in such tree-topology networks. In such approach every sensor can sense location and can send the data to the sink node. Data fusion is considered for such kinds of networks. On the one hand, if the sink node is interested in calculating the upper limit temperature in particular location, it is unnecessary to delivery packets from all the nodes to the end user. On the other hand, if data packets from all the nodes are delivered to the end user, it would lead to extra energy utilization. Therefore, data fusion may be utilized to lower complete packet broadcasting via computations at every head node and sending only the combined data set [52].

In many of the WSN localization techniques received signal strength indicator (RSSI) is used to estimate the distance between nodes. An error in RSS computation leads to incorrect distance estimation and thus localization error. The error in RSS measurement is might be due to low battery level or multipath fading. So the problem should be addressed and taken into account by solving the battery utilization at each node [53]. Localization refers to the process to estimate the absolute / relative coordinates of a sensor node with inputs such as distances to other sensor nodes in a particular coordination system. In addition, landmarks with known locations are required to localize sensor nodes with unknown location. These landmarks are known as anchor nodes (static or mobile) in a WSN. In general, in a two-dimensional plane, localization of a sensor node requires connections with at least three anchor nodes [54]. With this methodology, increased in number of anchor nodes will also increased the accuracy of the system. Localization enables WSNs to provide meaningful data, especially when visualization of data is required in a graphical user interface. However, it remains challenging to determine how accurate a localization system is? They may be due to possible damaged sensor or adverse environmental change. It is thus desired to design resilent localization systems to deal with these factors [55].

This thesis focuses on designing localization systems for WSNs while taking RSSI measurement error, energy consumption into consideration. The literature survey shows that extensive efforts have been paid to WSN localization and positioning. In some of the existing localization techniques, deployment area is divided in grids and an anchor node is deployed on each vertex of the grid , leading to the requirement of a large number of anchor nodes. Furthermore, some techniques require to deploy anchor nodes on the boundary of the network, which requires one to use less anchors to localize a target node.

In many of the aforementioned applications, sensor position is a critical piece of information in order to provide a meaningful service. This is because users not only need to know what happens, but also are interested to know the location of the event. Location based service (LBS) can be put in two categories: outdoor localization and indoor localization system [56]. GPS is the *de facto* standard for many of the outdoor systems that provides global coverage and its precision is up to $1m$ [57]. But GPS is not suitable for indoor systems due to its stringent requirements. An object or people are localized in indoor positioning system (IPS) by using magnetic field, radio waves, acoustic signals or other sensory information collected by mobile devices. A lot of IPS systems are available commercially but they are not standardized. The system use several algorithms and technologies including magnetic positioning, distance measurement to anchor nodes and dead reckoning. They either actively locate static, provide ambient location or mobile to get sensory information. The structure and design of an IPS concluded in design fragmentation with system using various radio, optical or even acoustic technologies. The IPS must be able to provide at least three independent measurements to unambiguously find a position of the node. It must also be able to compensate for stochastic errors, and methods to remove those error budget significantly. Indoor localization may work on specific scenario to boost the business market and improve the life quality. For the purpose different technologies are used in accordance to the need and system requirements. Table 1.1 summarizes the indoor positioning technologies along with their coverage and measured accuracy [58].

Table 1.1: Indoor positioning technologies.

Technology	Accuracy	Coverage (m)	Measurement Technique
cameras	0.1mm-dm	1-10	Angle measurement from images
Infrared	1cm-1dm	1-5	Active beacons
Sound	2cm	2-10	Time of arrival (ToA)
WiFi	10m	20-50	Fingerprinting
RFID	1dm-1m	1-50	Fingerprinting, proximity detection
Ultra-wide band	1cm-1m	1-50	ToA, body reflection
Pseudolites	1cm-1dm	10-1000	Carrier phase ranging
Magnetic Systems	1mm-1cm	1-20	Fingerprinting and ranging technique
Zigbee	1m	30-60m	Centroid based techniques

The accuracy and coverage of above mentioned technologies are given in Figure 1.3. Zigbee technology is basically a low cost WPAN with low data throughput and power consumption's with an approximate communicate range of $100m$ for outdoor environment and $30m$ for indoor environment. RSSI is used for distance computation between zigbee nodes. WiFi (IEEE 802.11), Bluetooth (IEEE 802.15.3), and Zigbee (IEEE 802.15.4) all are operateed in the $2.4/5.2$ GHz frequency bands [58]. Aiming at a better understanding on the indoor technologies, we build a system that is also suitable for zigbee-based sensor network for localization. We do not build a testbed using Zigbee nodes, but the features of zigbee technology were taken into account while simulating the proposed system. Since ZigBee operates in the unlicensed ISM bands, it is vulnerable to interference from a wide range of signal types using the same frequency, which can disrupt radio communication. The accuracy and power utilization of most indoor positioning solution is not accurate as those of others used for other technologies.

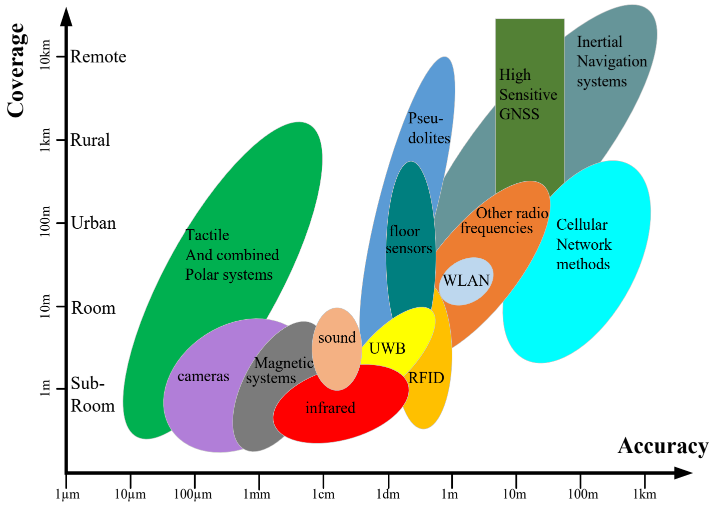

Figure 1.3: Indoor positioning technologies: Accuracy vs. coverage [58]

Many approaches were proposed to localize sensor nodes accurately and efficiently. In this thesis, we will revisit them and present a critical review based on their performance. High accuracy and low cost solution for localization is demanded by many applications. Most node localization algorithms are able to work independently as compared to hybrid based solutions, which increase the computation cost and energy utilization. Thus, localization algorithm should be able to respond to any environment as a context aware application to improve the positioning accuracy. Many algorithms use GPS as standard for outdoor usage. But it can't perform accurately in indoor environment. So, this motivates us to design a localization algorithm that does not require ranging devices like GPS. In this scenario, mobile node is also helpful for tracking [56].

1.3 Objective and Challenges

Nodes must be aware of their location information, in order to maintain a effective collaboration between sensor nodes in a distributed WSN. The location information along with associated data can help to provide the exact interpretation by sensing data and recognizing the source of data location [59]. It also can help in target movement monitoring [60], geographic routing [61], identifying network coverage [62] etc. Since a WSN always holds a large number of devices, so the localization process should be distributed among different nodes rather to executed from a central system and the process must be initiated after deployment of the network. In the same context, the main challenges for localization algorithm is fast convergence, low energy utilization, and high precision accuracy. Generally, WSN communication is through ultrasound waves or radio frequency transmission. Many of the literature suggest the use of ultrasound waves for WSNs, but its short range and very high energy consumption's make it impossible to use for low cost and energy constrained sensor nodes. On the other hand, radio frequency is a best choice that provides long range communication and does not require additional hardware. Studies also shows that, communication aspect is a main paradigm that utilizes most of the sensor energy. Therefore, a localization system must be self dependent so that less communication overhead is required between nodes for localization. The main objectives of this thesis are as follows.

1. To perform a comprehensive review of the existing state-of-the-art wireless localization algorithms while considering localization accuracy, energy and communication cost.
2. To design a three-dimensional wireless localization algorithms for Wireless Sensor Networks with data fusion and context awareness.
3. To investigate and design a wireless localization system with mobile anchor

nodes.

4. To analyze and model the performance of the proposed localization algorithms with different noisy conditions.

The development of mathematical models from data should be involuntary, since in many scenarios there is no information about the changes apprehended by sensor measurements. Furthermore, the models need to be simple, robust and cost effective in term of computation. For this propose, Sections 1.4 and 1.5 present the research questions and contributions, respectively.

1.4 Research Questions

As discussed above, many localization schemes were proposed for Wireless Sensor Networks. However, not all of them are suitable for low cost and energy efficient WSNs. Furthermore, it requires performance improvement in terms of accuracy, implementation cost, computational power and energy consumption. The following research gaps in this area are identified as follows.

- In particular, the key disadvantage with many of the techniques using anchor node deployment is that each anchor, as long as it is in the neighbourhood, will give the same RSS value regardless of its distance from the node. This means, for instance, that a beacon reception which is on the boundary of the neighbourhood may risk jumping from full presence to no presence due to fluctuations in G_{RX} and G_{TX} in the Friis' formula.
- Environment (indoor or outdoor) is a main factor while choosing the technology. Even small change in environmental factors leads high localization error.

- In the competition leading by localization accuracy, most authors do not pay much attention to communication cost. It means nodes are expected to generate a lot of radio traffic for every positioning cycle. Each node has to listen to all beacons in the neighbourhood and obtain their IDs before calculation can be performed. But in practice, nodes are limited both by battery and sometimes by computing ability.

- High Computation and power consumption exist in most 3D based localization algorithms. In particular, hybrid based localization techniques are more complex in terms of number crunching.

Identified issues of existing localization schemes motivate us to search for better localization techniques for low-rate WPANs (LR-WPANs) WSNs in terms of (1) smaller localization error, (2) lower power consumption and (3) better system scalability. This leads to the following research questions:

1. What are the most frequently applied methods in context of 2D and 3D localization for LR-WPANs? The goal is to identify the most commonly used methods and explore their drawbacks.

2. Is it possible to propose new solutions that minimize the effect of environmental changes?

3. Is it possible to design a new technique for static and mobile anchor based localization for low rate personal area networks?

4. Is it possible to reduce the noisy affect from localization algorithm in presence of fading and noise?

1.5 Thesis Contribution

The primary contribution of the thesis are as follows.

- **3D localization based on Parametric loop division and subdivision surfaces**. In a first stage of the thesis we have evaluated the different kinds of algorithms based on static nodes and static anchor localization. A novel idea based on parametric points for 3D based static networks is proposed. Anchor nodes with known position is used to form a triangle based on RSS. Triangulation can be used to compute the center point as well as reference anchor points for next iteration. These are basically parametric points that overcome the size of the space using subdivision methods described in [56] . At each parametric point the RSSI is being compared with threshold value for localization. The idea is being compared with the well-known range-free localization algorithms like APIT, MDS-MAP and DV-Hop algorithms, explained in Chapter 4 in this thesis. With the use of triangulation and subdivision in our proposed system the localization accuracy provides up to $0.89m$ with a standard deviation of $1.2m$ due to scattered data. Furthermore, network coverage problem is being analysed. The proposed scheme don't have coverage problem due to having enough anchors on the boundary of the network. This idea is published in a *25th Wireless and Optical Communication Conference (WOCC)* hosted by IEEE [63] and the detail mathematical modelling was published in *Sensor* volume 17, issues 7 [56].

- **Noise reduction scheme for parametric loop division algorithm**. In a first stage the localization accuracy was tested without the addition of noise in distance measurement. Similar as other wireless localization schemes, PLD is also influenced by the noise, which degrades the performance of the system. A new methods of extended kalman filtering is used to refine the nodes coordinates affected by the noise. Further, an analytical frame work is presented with the detail study of lower bound of the localization accuracy. By refining the node coordinates PLD scheme maintains its localization accuracy even in presence of noise. The system is simulated and tested for naive, Gaussian and intelligent noise. The PLD-EKF algorithm is also presented in *"journal of sensor and actuator network"* [64]. We found that the refinement process also provides a better localization accuracy of up to $0.42m$ and the standard deviation is also reduced to $0.26m$.

- **Mobile based Localization using Fuzzy Logic system**. Recently, mobile based WSN getting much attention towards different applications. By using mobile node a network is able to provide necessary information, like its position to the nearest mobile anchor or mobile node. We have designed a centroid based localization system by using fuzzy logic approach. The design is divided in to different stages, like in a first training phase that the RSSI is mapped to initialize fuzzy membership function. The mobile anchor exchange beacon and measure distance using RSSI data. The target node position is computed in a circle form that is a sensing region for a mobile anchor node, which moves on a random walk for broadcasting beacons. RSSI and signal power is used as a input for fuzzy system. After that, for accurate node positioning a perpendicular bisector is drawn from rough estimation to circle drawn previously. Fuzzy logic based system also work on non linear estimation same like extended kalman filtering. The simulation was performed 1000 times and localization error was recorded between $0.7m$ and $0.9m$. The Fuzzy logic algorithm is also presented in *" 2nd International Conference on Communication, Computing and Digital Systems (C-CODE' 19)"* [65].

1.6 List of Publications

J1 Ahmad, Tanveer, Xue Li, and Boon-Chong Seet. "Parametric loop division for 3d localization in Wireless Sensor Networks." Sensors 17, no. 7 (2017): 1697.

J2 Ahmad, Tanveer, Xue Jun Li, and Boon-Chong Seet. "Noise Reduction Scheme for Parametric Loop Division 3D Wireless Localization Algorithm Based on Extended Kalman Filtering." Journal of Sensor and Actuator Networks, no. 2 (2019): 24.

J3 Ahmad, Tanveer, Xue Jun Li, and Boon-Chong Seet. "Extended Kalman Filter based Localization of Static Target in Noisy Wireless Sensor Network." (Submitted)

J4 Ahmad, Tanveer, Xue Jun Li, and Boon-Chong Seet. "Clustered based Closeness Centrality for 3D WSNs Localization using Social Network Analysis." (Submitted)

J5 Ahmad, Tanveer, Xue Jun Li, and Boon-Chong Seet. "Mobile based localization using fuzzy triangulation." (Submitted)

C1 Ahmad, Tanveer, Xue Jun Li, and Boon-Chong Seet. "Fuzzy-Logic Based Localization for Mobile Sensor Networks." In 2nd International Conference on Communication, Computing and Digital systems (C-CODE), pp. 43-47. IEEE, 2019.

C2 Ahmad, Tanveer, Xue Jun Li, and Boon-Chong Seet. "3D Localization Using Social Network Analysis for Wireless Sensor Networks." In IEEE 3rd International Conference on Communication and Information Systems (ICCIS), pp. 88-92. 2018.

C3 Ahmad, Tanveer, Xue Jun Li, and Boon-Chong Seet. "3D localization based on parametric loop division and subdivision surfaces for Wireless Sensor Networks." In 25th Wireless and Optical Communication Conference (WOCC), pp. 1-6. 2016.

C4 Ahmad, Tanveer, Xue Jun Li, and Boon-Chong Seet. "A self-calibrated centroid localization algorithm for indoor ZigBee WSNs." In 8th IEEE International Conference on Communication Software and Networks (ICCSN), pp. 455-461. 2016.

1.7 Organization of the Thesis

The rest of this thesis is organized as follows.

Chapter 2 gives a brief overview of technology background. We briefly explain the WSNs design consideration, their usage in different applications and different services provided by Wireless Sensor Networks. A brief introduction about localization is also presented to lay the foundation for detailed discussions in the following chapters.

Chapter 3 reviews and critically analyzes the different aspects of localization algorithms. A detail literature review is presented into two phases. First a review of 3D based algorithms are classified in to several groups from centralized to distributed, range-based to range-free and anchor-less to anchor based localization algorithm. A localization measurements models like RSSI, ToF, AoA, ToA, TDoA along with Triangulation, Trilateration and Multilateration is explained. A taxonomy of range-free algorithms like APIT, MDS-MAP, DV-Hop is also explained. A brief overview of mobile anchor/ static node, static anchor/ mobile node, mobile anchor/ mobile node is also discussed in this chapter.

Chapter 4 is our proposed scheme based on Parametric Loop division and subdivision. We have consider a 3D static network in which we deploy anchor nodes in the boundary of the network. The proposed scheme gives high accuracy as compared to other range-free localization algorithm. The algorithm is detailed analyzed for Rayleigh fading, parametric point construction and their relationship with anchor nodes and sensor nodes is presented.

Chapter 5 presents the effect of noise factor in our proposed scheme. Initially we have not added the noise factor for PLD simulation. In this chapter different kind of noises like intelligent, naive and Gaussian noises are added to check the localization error in real time environment. An extended kalman filtering (EKF) framework is added to refine the coordinates of target nodes which provide high accuracy even in presence of noise.

Chapter 6 presents a 3D localization scheme based on mobile anchor. Nodes are deployed along with some mobile anchors having random-walk over a region of interest. Fuzzy logic based approach is used to derive non-linear coordinates into linear system.

Chapter 7 provides the concluding remarks and discusses possible future work on this topic.

1.8 Summary

WSNs enjoy great advantages because of their size, low-cost and automative nature. Sensor are not only deploy on a dangerous and cumbersome areas for interest for monitoring and controlling purpose. Different assumptions and properties of WSN are presented in literature that make them unique from other kinds of networks. In this Chapter, we started with a brief introduction to WSNs, and discussed why wireless localization techniques are important. Then, we identified a number of research gaps in 3D localization techniques, and presented our research questions. Subsequently, we discussed our contribution to the topic of 3D wireless localization techniques, followed by the organization of this thesis.

Chapter 2

Technological Background

Development of Wireless Sensor Networks (WSNs) can divided into four phases [66]. As we know, during cold war the United States of America deployed sensor and actuators for monitoring and in the first phase of WSN development radars were basically deployed over North America. The military use WSN as a driving force as with many other technologies. In the second phase of WSN development an initiative were taken in the form of launching of Defence Advance research project agency (DARPA) in 1980s. Technology elements comprises of high-level communication protocols, self-localization algorithms for nodes and acoustic sensors [67]. In phase three of WSN enhancement military application were developed during 1980s and 1990s were named as first-generation commercial products. By utilizing the simulation results of DARPA-DSN research, military approve WSN application for network-centric war. In "network-centric warfare", weapons and deployed sensors work together within a specific platform. The prior information about the movement of objects is sent to deployed sensors, that helps to localize the improve discovery of incidents through various observations, extended detection range, geometric diversity and fast response time. Nowadays, the WSN research which is in second-generation constitutes the fourth phase. The mobile system of nodes and flying robots are designed to improve the overall traditional sensors system in reasonable price and tiny sensors based on Micro Electro Mechanical Systems (MEMS). University of California at Berkeley designed extremely small sensors nodes under Smart Dust projects knows as “motes” [68]. Under smart dust project the designed sensor was merged into tiny devices, perhaps the size of a grain of a sand. Similarly, Berkeley Wireless Research Centre (BWRS) designed low power and energy efficient sensor devices under Pico Radio project [69]. The sensor are now able to power themselves from different energy sources, depending on the operating environment such as vibration or solar energy.

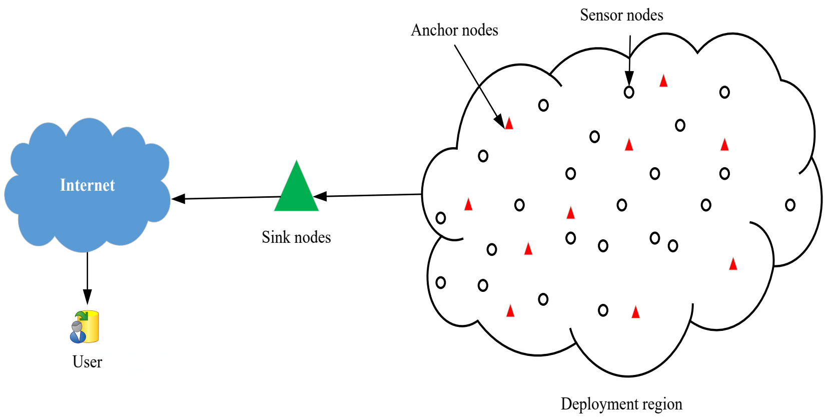

Figure 2.1: Data fusion in Wireless Sensor Networks

Figure 2.1, show the WSN architecture in distributed fashion. We noticed that the ad-hoc network protocols and structure are not ideal for WSN due to the following reasons:

1. The network scale of WSN is larger than ad hoc networks.
2. WSN nodes are prone to failure due to environmental conditions.
3. Dynamic network topology is challenging factor in WSNs.
4. WSN use broadcasting communication scenario but ad-hoc network use unicast communications.

5. Memory, computational capacity, and power in sensor nodes are limited.

2.1 WSN Design Consideration

WSN has been found in variety of applications with different characteristics and requirements [70]. That is why, it becomes more difficult to discuss about hardware requirement and software support for application. This is basically an issue with the multidisciplinary research area like WSN, where a tight collaboration between application, domain system, hardware designers, software developers and even user is needed to design an efficient system. Therefore, this issue is debatable for researchers to consider which area within a design space and one may argue in favour of adding more parameters or explicitly remove some featured from the specification list. We will discuss about existing and intended applications of WSN and can identify different phases of the design consideration in the subsequent section. Following are the key factors and considerations in designing of the WSNs.

2.1.1 Sensor Deployment

Sensor nodes deployment in a WSNs may take places in different forms like sparse deployment or dense deployment. Nodes may be dropped from air (randomly) or may installed at strategic spots. Sensor node deployment is a one-time activity, in which a sparse deployment has fewer nodes as compared to dense deployment. The model of dense deployment is adopted where more nodes can cover an interested region and where it is very significant to detect every activity. On the contrary, the sparse arrangement is used where network coverage is more important. In most of the WSNs research study, it is to be assumed that the nodes are static and do not require any mobility management that affect the vital characteristics such as node locations, node density, network topology, and dynamic of the network degree. Some nodes are also mobile in the network and require to change their location according to the given condition. In [71], the sensor deployment is targeted to determine the location with maximum network coverage. The deterministic deployment of node is shown in Figure 2.2. Dropping of sensor nodes via planes or flying robots are the best example of random placement. The simplest deterministic approach was discussed in [72] where as a more sophisticated deterministic method was presented in [73].

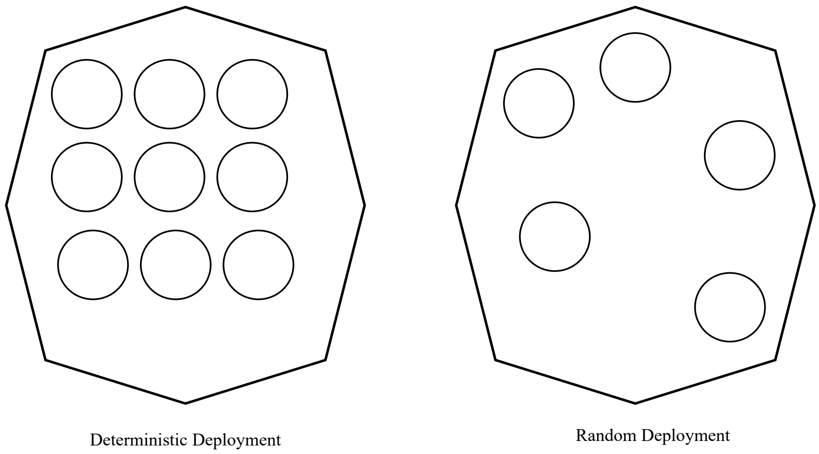

Figure 2.2: Sensor node deployment

In another deployment algorithm all the nodes can communicate with its neighbour to inform them to keep moving within maximizes coverage while maintaining connectivity [74]. The simulation runs many times to gain a very high degree of coverage of network deployment in which node lost their energy due to continuous movement. The method in [75] is the enhancement of the idea with maximum network coverage with less sensor movement. For this the authors in [76] derived all three separate protocols for network coverage, node movement and deployment time with minimum scalability.

The authors in [76] mathematically proved the sensor deployment pattern validation. It assumes that the communication range and sensing are a perfect circle and nodes are giving full network coverage.

2.1.2 Sensor Mobility

As indicated by topology and application needs, traditionally two principle kinds of sensor mobility should be taken into account, miniaturized scale and large-scale mobility. From one viewpoint, smaller scale versatility, refers to sensor mobility inside the equivalent sensor arrange area, as appeared in Figure 2.3. The mobility of nodes may be due to environmental influences such as wind, water or that the node is attached to a mobile device, which lost their trajectories [77, 78]. In 6LoWPAN networks, small scale versatility is identifies by the mobility of a sensor into the equivalent 6LoWPAN area, where the location prefix stays unchanged. Consequently, the versatility of sensor, changing its connection point from an edge switch to another inside the equivalent expanded network, which is considered as a small scale mobility [79, 80]. As we will detail more later in Chapter 3, hybrid system must also be considered where several WSN domains are under control of one operator as shown in Figure 2.4.

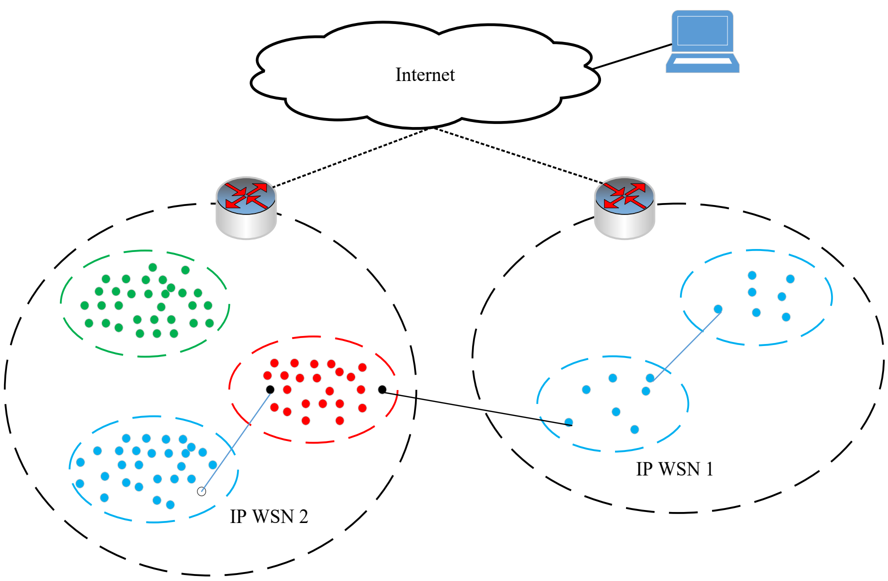

Figure 2.3: Main mobility scenario [79]

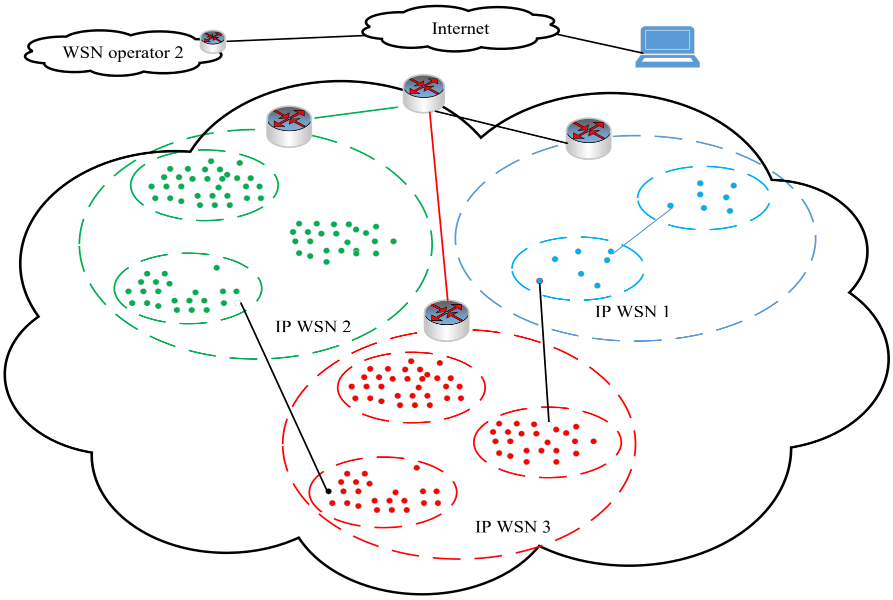

Figure 2.4: Hybrid Mobility scenarios [79]

2.1.3 Node Types

In general, there are two types of nodes in WSNs: heterogeneous and homogeneous sensor nodes. In heterogeneous network, sensor nodes with different capabilities, such as different sensing range and computing power are deployed, while in homogeneous network all nodes are with the same capabilities and functionalities. Consequently, in heterogeneous network some nodes are more powerful than others, maintaining a group of more powerful nodes known as cluster heads. As compared to homogeneous network, heterogeneous network has a topology that is more complex in nature and design. Example of homogeneous and heterogeneous nodes are given in Figure 2.5. A homogeneous set of nodes were practically used in [73] and [81] those deployed nodes with some precise distance. The author in [72], also used the homogeneous network but repeat the simulation with different sensing ranges for localization. In [82], a barrier is monitored using homogeneous network based on rectangular based coverage model.

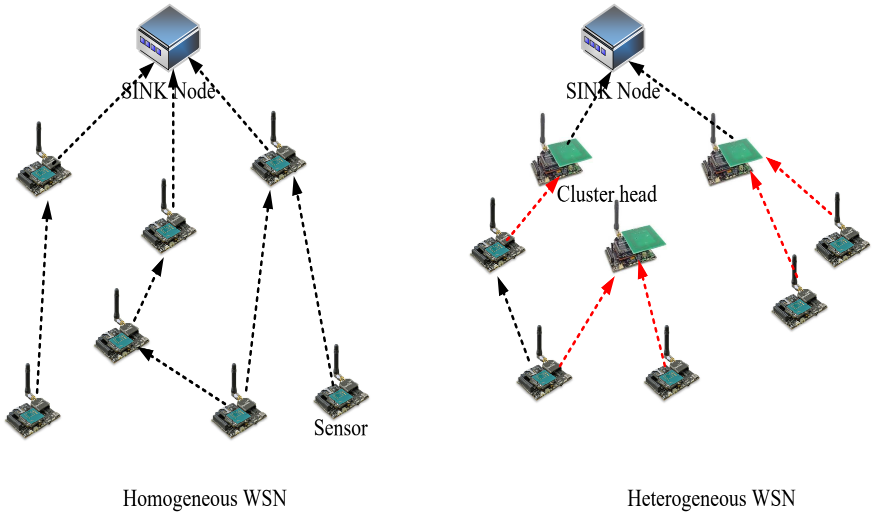

Figure 2.5: Homogeneous and Heterogeneous network

2.1.4 Network Infrastructure

WSNs can be set up with or without infrastructure. In infrastructure-based WSNs, nodes can directly communicate with base station. The number of base stations in a network is totally dependent on network coverage area and communication range. An example of this type of WSNs is smart dust [83].

In infrastructure-less WSNs, nodes can communicate with each other in an ad-hoc manner. Sensor nodes may act as a router to forward packets on behalf of other nodes. As the network infrastructure cost is always very high, and deployment may not feasible for many scenarios, infrastructure-less WSNs will be the preferable solution. Nevertheless, assuming a network infrastructure like GSM network, it may also work under different WSN applications. A combination of infrastructure-based and infrastructure-less WSNs is also feasible when a cluster head of a WSN region is connected with the wide area network through internet.

2.1.5 Network Topology

Network topology is another property of a WSN, which represents the distance, hop count and communication properties between nodes and even in a entire network. STAR topology is the simplest topology in WSNs, where the cluster head is able to communicate with all the nodes in a network. Next, a TREE or BUS topology is usually adopted in multi-hop WSNs. In BUS topology, a node who can initiate a process of communication and send message to another node. Specially, the homogeneous type of network can't afford the use of bus topology despite of its simple structure. MESH topology is difficult to implement in WSNs because of huge traffic and simplex correspondence.

In star topology all the nodes are located at one hop distance from a sink node so different sensor can send redundant data all the time. The sink node act as a cluster head that process all the information. Similarly, a multi-hop communication is taken place in tree and mesh topologies. For localization a lot of topology based algorithm like minimum connected dominant set (MCDS) is proposed, with the benefit of low energy consumption [84]. All data is being processed by a cluster head so this node is normally connected with the Internet to monitor the entire network as shown in Figure 2.6. The data processing and routing may also be dependent on network topology [85].

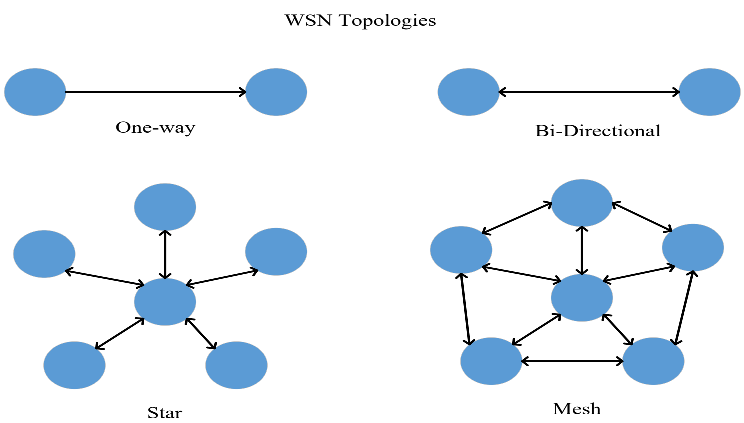

Figure 2.6: Wireless Sensor Networks topologies

2.1.6 Network Coverage

Localization algorithms always depend on network coverage [86]. Before developing a localization algorithm a research, we need to define the network coverage. Either a full coverage for entire area or blanket coverage for a subset of interested region is needed to localize. For blanket coverage, a few nodes within a field are deployed to make an ideal network. This was proposed in [87], where all the nodes are placed in r-strip, i.e., each node is r distance away from other in a neighbour.

Target coverage refer to the scenario in which fixed number of targets are being observed [88]. The author in this research not only detect the targets but also organize and track them. A lot of proposals are presented in [89, 90, 91, 92, 93], to achieve network coverage with lot of energy conservation. Last but not least, barrier coverage refers to detection of some measures and movements on a barrier of sensors. This was defined in [94].

2.1.7 Network Connectivity

Network connectivity in WSNs can be persistent or intermittent. For persistent connectivity, nodes are always active and connected to at least one neighbour node. In case of partitioned network, the connection is intermittent, whereas the connection can be sporadic, if nodes are isolated and only required to communicate occasionally [95]. The interesting fact is that, in case of node isolation, partition, and node separation in multiple area, the message and data can be delivered by mobile nodes over the network. This is the beauty of WSNs as compared to ad-hoc networks.

2.1.8 Network Size and Lifespan

The number of nodes, anchor and sink nodes included in WSNs is dependent on the system requirement, coverage area, and the sensing region. Network size may vary from several nodes to thousands of nodes. Network size also determine the scalability requirement of the network. There may be numerous difficulties in execution of WSN frameworks, such as data collection, which is also influenced by the network size if WSN is partitioned into different subsets and domains [96].

Similarly, the lifespan of WSN may vary from some hours to even some years depending on the application and power mechanism. The lifespan has a high impact on robustness, and the degree of the power consumption of the nodes [97]. Fuzzy logic based solutions seem to be appropriate as they require less energy, resulting in an increase lifespan of the network. In the proposed mobile based localization system we also used fuzzy logic approach that can save much energy and provide high accuracy of localization scenario [97, 98].

2.2 Application of Wireless Sensor Network

Numerous applications of WSNs has been envisioned in the literature [99]. These range from environmental application to military and health application to agriculture and biomedical application.

2.2.1 Environmental Applications

Environment monitoring is very important task of WSN that can be used to monitor any kind of environment, it is most frequently characterized as the perception and investigation of regular habitats [99]. Sensors are even capable to attain detailed measurements, localized objects that are hard to achieve in dense environment. Consequently, different environmental application are proposed for WSNs consisting of animal tracking, habitat monitoring, precision farming, forest-file detection and disaster relief applications [100, 101].

Let us consider a fire in a forest as illustrated in Figure 2.7. A deployed sensor node can immediately inform the management before it going to spread over a vase area and becomes uncontrollable. The incident location can be identified in a timely manner so that fire fighter can reach the scene to take further action.

Figure 2.7: Forest-fire monitoring system

Another area of environmental monitoring is precision farming [102], in which WSNs can provide spatial data to measure crop response through analyzing soil type [103]. In disaster relief, severl applications are also developed like ALERT flood-detection system [104], that relays information from multi-hop nodes by using remote field sensors, which typically include different types of sensors, like water-level sensors, rain fall sensors and other weather sensors.

2.2.2 Military Applications

WSNs play a vital role in military applications, including major tasks like computing, reconnaissance, command control, targeting systems, intelligence and surveillance. The famous military applications are targeting, ammunition and equipment monitoring, monitoring of enemy and friendly forces, nuclear weapons, and chemical and biological attack detection [105]. The tiny sensors are affixed with troops, outfit and essential weapons, vehicle and report the status to the troop pioneers [106].

The sensor nodes can also help in battlefield monitoring and pin targeting. Pointer is a test counter marksman system used to recognize and spot shooters [106]. It also used to paralyze waves from a shooter end. Sensors track their estimations to a base station to figure out the shooter's area [106, 107]. Let us consider a battle field where troops are moving in a far area and enemies tanks are on the other side as shown in 2.8. The deployed sensors in a battle field can localize the position of the enemy tanks and inform to the troops.

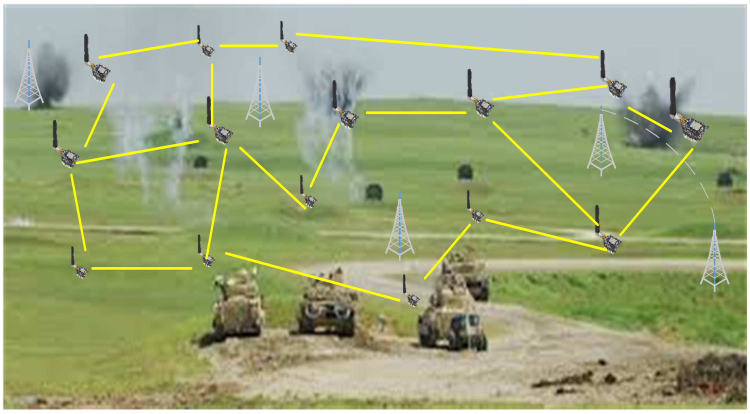

Figure 2.8: Enemy target localization and detection

2.2.3 Health Applications

WSNs are also important in healthcare applications. They can be used to monitor the patients health and even track their location by embedding a sensor chip inside clothes or in a wrist ring. This helps patients to move freely while they are under constant monitoring. In case of patient accident. WSNs can help hospital staff to localize the position of a patient

In [108], biomedical challenges and some potential applications are proposed for health monitoring, such as glucose-level monitoring that can constantly monitor the blood sugar level of a patient and display the results on a wrist watch.

2.2.4 Agriculture

WSNs are also used in several areas of agriculture to increase the efficiency of livestock and plant breeding. Sensor can monitor the plant growth factors like soil, humidity, light and temperature that influence the crop conditions. A practical example of plant monitoring is the deployment of tiny sensor in a large grape vineyard in Oregon USA [109]. Nodes are deployed over *20m* $\times$ *20m* area, connected with each other via a cable in order to get accurate reading. All the temperature, humidity and other factors that affect the grapes can be recorded and this information is sent to the laptop computer using gateways.

Sensors are also used in cattle herding [110]. An acoustic stimulus is given to cows that cross a fence line created virtually. This basically control the movement of animals. PlantCare project [111] also used WSN to control a water robot and monitor soil humidity.

2.3 WSN Services

Applications in large-scale WSN always use mutual services such as location discovery, time synchronization, data storage, data aggregation, message routing and topology management.

2.3.1 Location Discovery

The detection of location is a main service provided by WSN. Location information of sensors can be expressed in global coordinates or local coordinates according to a particular application. The importance of location discovery is widely recognized and presented in many research works [112]. In addition, location discovery can be useful for location-based routing in WSNs. A detail review of localization algorithms is further discussed in Chapter 3.

2.3.2 Data Aggregation

Data aggregation is another important factor of WSN [113]. As we know, WSNs operate on battery have limited resource, thus it is necessary to minimize the relay messages. A basic application of relaying messages is beacon, which may create ambiguities in data aggregation. To solve this problem, data fusion is required to filter duplicate data before sending it to the base station [114]. This also help to overcome the repetition in data transfer and messages relayed to the base station.

2.3.3 Time Synchronization

Another service in WSNs is time synchronization [115]. Sensor nodes need always be synchronized, in order to achieve complex sensing tasks. A synchronized system allows sensor nodes to correctly identify an event with a certain time stamp. Time synchronization may be affected by factors like "hardware clock drifting". Synchronization can also help to conserve battery life. By synchronization, nodes can power "ON" when it is needed. They may enter idle mode after sending relay message to the base station. If nodes are not synchronized, they need to wait unnecessarily to communicate with neighbours. For more details, interested readers are referred to works in [115, 116, 117, 118, 119, 120].

2.3.4 Data Storage

Data storage to store location and information data pose a challenge to WSN developers. This data might be stored in a cloud. In WSNs data can be stored in three different ways [121].

1. **Local Storage**: Whenever a node detects an event, data can be stored locally within onboard memory of the node. In this model, extra communication is not needed as the queries are flooded to all the nodes. After computation, this data can be relayed towards base station.

2. **External Storage**: In case of heterogeneous network where network is formed in some subset or domains, data might be relayed to some external cloud for processing. The advantage of this model is energy efficiency as nodes don't need to perform much computation by itself.

3. **Data-Centric Storage**: In this technique data is relayed to some especific locations. Geographic hash function (GHT) is used to route data on predefined locations.

2.3.5 Routing and Topology Management

Apart from localization information, routing protocols are also required to gain fault tolerance. As the channel bandwidth is limited in WSNs, the localization and routing protocol is designed to minimize the requirement of bandwidth. According to [122, 123], if topology construction is not carefully managed, WSNs may lead to congestion and collision.

2.3.6 Operating Systems

TinyOS is used by WSN that is an open-source operating system [124]. TinyOS is a kind of library that includes distributed services, network protocols, data-acquisitions tools, and sensor drivers. It also adopts a event-driven execution model and enable a fine-grained power mechanism. Developed by Crossbow, TinyOS is proposed in different platforms and over 1000 companies and research groups are using it [125].

2.4 Localization Problem

The data, information, including RSSI that we obtained from sensor nodes can be of great value, if the originated position is known. Therefore, almost for all WSN system location information is a fundamental requirement for many applications. The location information either from a direct source by using positioning device or from where the sensing, receiving signal is originated require some accuracy and reliability of the system. Localization information can be used not only for geographical origin, but also can used for maintenance, target tracking and coverage information.

2.4.1 Localization Requirements

Most of the applications in WSN requires high precision. If it is used in industrial robots, the requirement of accuracy becomes higher. Similarly for body sensor network (BSN) applications, where almost 128 nodes are attached to a patient for skin monitoring, accuracy becomes more vital and may even go up to few millimeters. For any localization algorithm, we need to generally consider the following requirements:

- The localization algorithm should be generic and can operate in indoor and outdoor environment.
- Node power source is always scarce, so the required communication among nodes should be energy efficient.
- The design of the system must be accurate enough, especially for applications deployed in industries.
- The localization algorithm should be scale-able so that new nodes can join the network easily.
- The localization algorithm should be feasible in terms of deployment cost.

- what are the type of coordinates used among nodes either local or global. What are the assumptions for sending data and information in particular time. Is there any synchronization involved? Also either an algorithm adopted the use of cluster head or not?

2.4.2 A General Problem Statement

Localization problem is usually defined for two dimensional ($2D$) or three dimensional ($3D$) based WSNs. In this thesis, we focus on $3D$ networks with static and mobile anchor nodes. Considering a network with $N + A$ sensor nodes deployed over a geographic region. We also assume that the location of N unknown target nodes i.e. $x_i = [x_{i1}, y_{i1}, z_{i1}]^T \in \mathbb{R}^2, i = 1, 2, ...N$ are unknown. Similarly, the position of A anchor nodes are $a_j = [x_{j1}, y_{j1}, z_{j1}]^T \in \mathbb{R}^2, j = A + 1, ..., N + A$ with known positions. First, let us consider all nodes are static and don't change their position over time. Target and known sensors can communicate with each other such that

$$\alpha_i \triangleq \{j \mid \text{Anchor node } j \text{ is in communication range of target } i\} \tag{2.1}$$

and

$$\beta_i \triangleq \{j \mid i \neq j, \text{node } j \text{ is in communication range of target } i\} \tag{2.2}$$

where α and β are set of indices representing the coordinates of the nodes. It means all reference anchors and unknown nodes can communicate with each other. Some sort of measures are also needed to take about the position of unknown nodes. The detail system model is given in Chapter 4 and Chapter 6 respectively.

The main factor for any initiative to develop an indoor positioning system is through analysing the specific application description and user requirements in order to justify the research and development in the field. The user requirement of significant application should lead to the future research. Performance parameters need to be matched with user requirements before electing the suitable positioning technology for a specific system. Current research usually focuses on two-dimensional (2D) space, three-dimensional (3D) space and mobile anchor based localization. Furthermore, we also consider energy consumption so that the proposed system utilizes less energy as compared to conventional localization techniques. The following factors are taken into account during this project.

2.5 Summary

In recent years, WSNs becomes the hotspot for information technology combines sensors, applications, processed signals information and many other areas of IoT. One of the most famous and popular research topic is sensor localization. Monitoring of the location is only possible if the location information is available. The use of sensor technology in many applications makes things possible to remotely access data and also provides some necessary functions in WSNs like routing, network topology control and data aggregation. For this reason, the study of localization become very attractive. In this chapter, we started with design consideration of WSNs, in which we explain several factors that taken into account for WSNs design like sensor deployment, type of sensor (static or mobile), network consideration like the infrastructure and topology, size of the network and their coverage. After that we described some main application of WSNs. The chapter ends with the discussion of some of the services provided by WSNs.

Chapter 3

Literature Review

Several location aware applications exist in an indoor environment, such as asset tracking, resource discovery, navigation tools for human and security. In indoor localization system, position can be determined through coordinate system such as latitude/ longitude. Whereas local system can follow up the topology of the network. Most of the local system can be deployed in such a way that they can get rigid transformation (rotation, translation, reflection) to global coordinate system. In [126], the authors studied three distributed localization algorithms which are using three-phase approach: 1) calculate the distance between nodes and anchors, 2) compute the position of nodes and 3) iteratively refine the position. Many localization techniques are presented in literature with different precision and method. Nevertheless, this topic remains attractive due to its potential applications in IoT. Researchers tirelessly study to develop a localization system with minimal cost, high accuracy, and even energy efficient system for commercial or personal use. This chapter revisits several algorithms that focus on high accuracy, energy and low computation cost with low budget. After that, we compare and summarize them in tables.

3.1 Location-aware Computing

The idea of context-aware computing [127, 128] becomes increasingly popular. According to the environmental observations, sensor networks may change their functions autonomously. The study of context-aware computing characterize as a noteworthy step in the light of ubiquitous computing. Location-aware computing systems always depend on location information and scene of the context. That is why positioning information of target and sensor nodes is essential for the application management. Location and orientation sensing, mobile computing and wireless communication are the three technical capabilities that converge together for possible implementation of location-aware computing. A simple architecture of context aware computing is presented in Figure 3.1

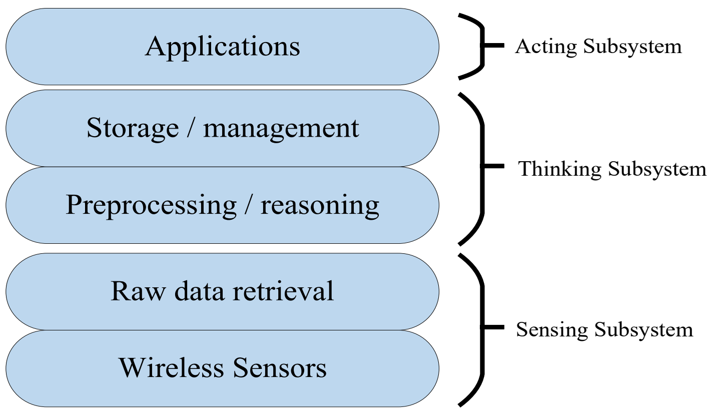

Figure 3.1: Context-aware computing layered architecture

Localization is a key task in context-aware computing. Along this, diverse frameworks appeared relying upon a few highlights like exactness, inclusion, establishment, and support cost. For example, Global Positioning System (GPS) are suitable for outdoor applications with progressively worldwide extension, however, they are costly and requires stringent time synchronization. The indoor infrared-based technology receives divider mounted sensors for catching infrared ID acquired from the labels on sensor clients. Table 3.1 summarizes the features of these localization technologies [129].

Table 3.1: Characteristics of Location-Sensing Technologies.

Technology	Technique	Attributes	Accuracy	Limitations
GPS	Radio ToF Lateration	Physical Absolute	1-5m (95-99)%	Outdoor
Active Badges	infrared proximity	Symbolic Absolute	Room size	lights interfere with infrared
Active Bats	Scene Lateration,	Physical Absolute	9cm, 95%	Ceiling sensor grid required
VHF	Angulation	Physical Absolute	1 radial 100%	LoS
Cricket	Proximity Lateration	Symbolic Absolute	4×4 ft region	high computation
MSR-RADAR	Triangulation	Physical Absolute	3-4.3 m 50%	Wireless NICs requirement
Smart floor	physical proximity	Physical Absolute	100%	Not suitable for large area
Wireless Andrew	802.11 proximity	Symbolic Absolute	100m indoor	Wireless NICs requirement
E911	Triangulation	Physical Absolute	150-300 m 95%	works if cell coverage available
SpotON	Ad-hoc lateration	Physical Absolute	Area dependent	Attenuation less, better then ToF

3.2 Localization in Wireless Sensor Networks

Localization is important in many research fields, consisting of vehicle navigation and autonomous robot [130, 131], virtual reality systems [132], mobile robots [133], and user tracking and positioning in cellular networks [134]. Location information can be used for routing in WSNs. For instance, transmission range and location information allows geographic routing algorithms used to propagate and transport information via multi-hop WSNs [135, 136, 137]. However, in many cases the position of node may not be available due to lack of infrastructure support. That is why it is very important to have mechanism to compute the sensor position after deployment. GPS is suitable for outdoor localization, but it is not feasible for indoor environment [56]. Based on the limitations of GPS discussed in Chapter 1, we focus on the development of GPS-less techniques for indoor localization.

In view of the WSN application scenarios, designing of a localization system is more challenging than other domains of sensor networks, because sensor nodes are very small and often unable to perform sophisticated computing because of low power consumption. So, the low power cost and low consumption is a major necessities for ideal localization system. Sensors are deployed remotely, in Springbrook rain forst, a project taken in the laboratory of University of Queensland, Australia where a long term sensor network is deployed for monitoring of regrowth of forest [138].

3.2.1 Localization Terminologies

localization techniques use different source of information and terminologies. Some common terms are used throughout this thesis:

1. Anchor node: a node whose position is already known in a system. An anchor node often functions as a reference node and transmits beacons. Anchor nodes can be static or mobile.

2. Mobile anchor node: A node with mobility, which traverses over the interested region. It can also transmit beacons regularly.

3. A blind node: An unknown target node that needs self-localization using multiple beacon packets.

4. A static node: A node whose position is fixed. In this thesis, all blind nodes are static nodes.

The core process of localization can be taken places by using GPS or coordinate systems explained below.

3.2.2 Global Positioning System

GPS is a Global Navigation Satellite System (GNSS) designed by US Department of Defence, consisting of three major segments space segment (SS), control segment (CS) and user segment (US). Space vehicle and orbiting satellites is a part of SS while CS is used to manage and control the flight paths of satellite from CS location on earth. GPS receiver is the part of user segment [139]. As shown in Figure 3.2, a GPS receiver requires line-of-sight connections to four satellites in order to localize itself.

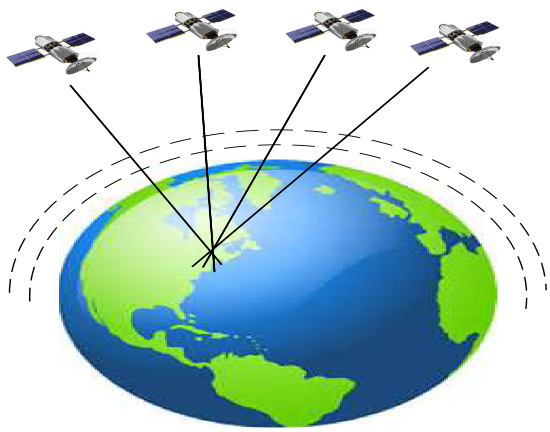

Figure 3.2: Localization using GPS

3.2.3 Coordinate System

Coordination system is defined to determine the position of an object. The most famous standard is World Geodetic System Developed in 1984 and known as WGS84 [140]. It is same as GPS coordinate system but uses the reference ellipsoid described by Earth Gravitational Model 96 (EGM96) [140]. China Geodetic Coordinate System 2000 (CGCS2000) is another famous coordinate system [141]. Universal Transverse Mercator/ Universal Polar Stenographic (UTM/ UPS) is a coordinate system used for two-dimensional (2D) space localization and positioning system [142].

3.3 Localization Estimators

For wireless localization, there are three well-known estimation measures, namely the Geometric Dilution of Precision (GDOP) [143], Cramer-Rao lower Bound (CRLB) [144], and Maximum Likelihood Estimator (MLE) [145]. Furthermore, a zero-mean

Gaussian estimator and linear model also provide the computation facility for simulated based localization. The localization problem proposed in Section 2.4, can be optimized as follows:

$$min_{X \in \mathbb{R}^{d \times A}} \;\; l(X, a) \tag{3.1}$$

where $a \triangleq \{a_{i,j}\}_{j \in \alpha_A U \beta_A}$, and $l(X, a)$ is a loss function and computed through static or geometric interpretation. In this section, we discuss two major estimation approaches, statistical estimator and geometrical estimators, as summarized in Figure 3.3.

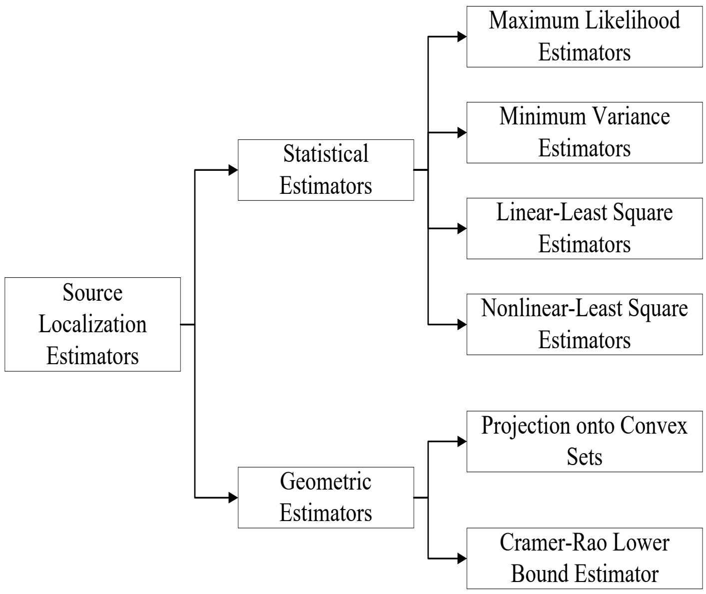

Figure 3.3: Flow diagram of source localization estimators

3.3.1 Statistical Estimator

The general thoughts of estimation hypothesis is to reduce the vague parameters dependent on a lot of discrete estimation information [146]. Consider a set of angular data

$$\theta = (\theta_1, \theta_2, \theta_3, ..., \theta_n)^T \tag{3.2}$$

dependent on discrete data:

$$\mathbf{Y} = \{y[0], y[1], ..., y[A-1]\} \tag{3.3}$$

This discrete data is found in sampling process of localization parameter, which are dependent on vector information of angle θ. This dependency is written as:

$$\hat{Y} = f(\theta, y_i) \tag{3.4}$$

where $\hat{Y}$ is approximately right observation of y and represents the model output. The internal parameters are denoted in a vector position, i.e., $\vec{y_i}$. The data will also be affected by noise η taken as a random variable. In this thesis noise is considered as a additive nature, however we also test our system for white and Gaussian noise. The model in (3.4), then can be expressed as:

$$Y = \hat{y} + \eta = f(\theta, y_i) + \eta \tag{3.5}$$

θ is a statistical estimator and computed on the basis of relative data. So, the estimation function for computing the value of θ can be of the form

$$\hat{\theta} = \mathbf{g}(y, y_i, \eta) \tag{3.6}$$

This fulfils the statistical criteria of θ contingent to C_η, which is a co-variance of the additive noise [146]. Some well-known statistical estimation techniques are least square approximation (both linear and non-linear) and maximum likelihood estimators.

3.3.1.1 Maximum Likelihood Estimator (MLE)

For non-linear system it often becomes impossible to compute unbiased estimators due to complexities in the non-linear estimator. In this case, the reliable way is to use maximum likelihood estimator, which provides approximate efficiency for a set of large data such that $Y = y[0], y[1], ..., y[A-1]$ with $A \to \infty$.

Consider a probability density function (PDF) of α and β from the problem statement.

$$\hat{\theta} = \mathbf{g}(y, y_i, \eta) \tag{3.7}$$

$$A_{i,j} \triangleq \begin{cases} f(y_i, a_i) + \eta_{i,j} & j \in \alpha_{i,j} \\ f(y_i, x_i) + \eta_{i,j} & j \in \beta_{i,j} \end{cases} \tag{3.8}$$

$$\prod_{i=1}^{A} \prod_{j \in \alpha_i \beta_i} f(A_{i,j}; y) \tag{3.9}$$

The MLE of a target location can be obtained as follows [147, 148]. Where ";" shows the likelihood relationship among anchor nodes and target nodes.

$$\hat{Y} = \underset{y \in \mathbb{R}^{d \times A}}{arg} \mid \sum_{i=1}^{A} \sum_{j \in \alpha_i \beta_i} \log f_i(a_{i,j}; y) \mid \tag{3.10}$$

Here, we noticed that the optimization problem in (3.10) is not convex and quite complicated to explain and solve. In some cases the MLE tends to an average value to accurate position for high signal to noise ration (SNR) for large number of observations. The MLE in synchronization form can be represented through time of arrival estimator that shows zero-mean Gaussian errors as represented as follows.

$$\hat{Y} = \underset{y \in \mathbb{R}^{d \times A}}{arg} \sum_{i=1}^{A} \mid \sum_{j \in \beta_i} \frac{1}{\sigma_{i,j}^2} (\hat{d}_{i,j} - \parallel y_i - y_i \parallel)^2 + \sum_{j \in \alpha_i} \frac{1}{\sigma_{i,j}^2} (\hat{d}_{i,j} - \parallel y_i - a_i \parallel)^2 \mid \tag{3.11}$$

where σ^2 is Gaussian errors. It is to be considered that the localization problem is affected by additive noise, path loss exponent, and transmission power. The noise factor can be removed by manipulating measurement and can be considered separately with the estimated position of unknown nodes [149, 150, 151, 152, 153].

3.3.1.2 Minimum Variance Estimators (MVE)

To solve the optimal criteria of statistical estimators, a natural solution is Mean Square error (MSE). Consider the example given in (3.2):

$$MSE(\hat{\theta}) = V\left[(\theta - \hat{\theta})^T(\theta - \hat{\theta})\right] \tag{3.12}$$

The optimization of the MLE in (3.12) can be further explained as follows.

$$=\mid \theta - V(\hat{\theta}) \mid_2^2 + V(\mid V(\hat{\theta}) - \hat{\theta} \mid_2^2) \tag{3.13}$$

$$=\mid V(\hat{\theta}) - \theta \mid_2^2 + est\,(C_{\hat{\theta}}) \tag{3.14}$$

where $C_{\hat{\theta}}$ is a co-variance matrix and $V()$ represents the expected outcomes in Euclidean normalization form. The bias in the MSE is computed by:

$$\mathbf{b} = V(\hat{\theta}) - \theta \tag{3.15}$$

Definition 1. If $V(\hat{\theta}) = \theta$, it is unbiased estimation.

To compute the value of biased parameter b the exact location of target nodes must be known after estimation. So, this is only theoretically true but not possible to measure practically. The value of co-variance matrix is biased. MSE is thus not generally realizable. Furthermore, $C_{\hat{\theta}}$ is only function that is unknown parameter on θ, the set of all parameter is said to be minimum variance unbiased (MVU).

3.3.1.3 Linear Least Square Estimators (LLS)

In WSNs localization problem is also considered as non-convex problem. There are two least square strategies. One is to achieve the solution by approximating the problem to a convex state, e.g., getting a accurate coarse positioning estimation and by following suitable relaxations. This can also be achieved by refining the coordinates of the nodes using some well-known techniques like kalman filtering and fuzzy logic. The other solution is to attain a high SNR by CRLB to linearized the computation based on target node position and then apply LLS criterion. Many of the system has been proposed in the literature deriving linear estimation [150, 151, 154, 155, 156, 157, 158]. According to [156], to form a LLS model, a derivation of linear signal model is required for unknown parameters. In presence of nuisance parameter, such as noise and unknown clock in time of arrival (ToA) or RSSI based techniques, the unknown factors like θ also contains nuisance parameters. To reduce this a linear model is needed to solve the vague parameters from mathematical model. Considering that the error is small with a distance between i and j and it is computed as:

$$\hat{d}_{i,j} = d(y_i, a_j) + \eta_{i,j} \quad j \in \alpha_i \tag{3.16}$$

where, η is a measurement noise or nuisance parameter having variance $\sigma^2_{i,j}$. Assuming that the noise is small and with zero-mean. If noise function $\eta_{i,j}$ is not zero, we need to solve (3.16) for noise by subtracting $\eta_{i,j}$ from both side:

$$\hat{d}_{i,j} \triangleq \hat{d}^2_{i,j} - \parallel a_j \parallel^2 = \left[-2a_j^T\right] \eth_i + 2d(y_i; a_j)\eta_{i,j} + \eta^2_{i.j} \tag{3.17}$$

$$\eth_i = \left[y_2^T \parallel y_i \parallel^2\right]^T \tag{3.18}$$

From (3.18) a semi-linear model on target node y_i is obtained. Further assuming the noise factor is very small so,

$$\hat{d}_{i,j} \triangleq \left[-2a_j^T\right] \eth_i + 2d(y_i; a_j) \quad j \in \alpha_i \tag{3.19}$$

the set of linear function

$$d_i = A_i \eth_i + V_i \tag{3.20}$$

where:

$$d_i \triangleq \left[\hat{d}^2_{(i,j)1} \hat{d}^2_{(i,j)2} ..... \hat{d}^2_{(i,j)k}\right]^T$$

$$A_i \triangleq \begin{bmatrix} -2a_{j1}^T \\ . \\ . \\ -2a_{jk}^T \end{bmatrix}$$

and

$$V_i \triangleq [2d(y_i, a_j 1)\eta_{i,j1}, ..., 2d(y_j, a_{jk})\eta_{i,jk}]^T$$

Therefore,

$$\hat{\eth}_i = (A_i^T C_{V_i}^{-1} A_i)^{-1} A_i^T C_{V_i}^{-1} d_i \tag{3.21}$$

where C_V is a weighted matrix and computed by [159]. For real computation of C_V the exact distance between target and anchor node is needed. Furthermore, we observed that the position is sub optimal in (3.21), so some techniques like relaxations are required to refine the estimator. One can employ Taylor series expansion given in [152]. The (3.21) is further expanded to

$$\left[\hat{\eth}_i\right]_1 = y_{i1} + s_1,\ \left[\hat{\eth}_i\right]_2 = y_{i2} + s_2,\ \left[\hat{\eth}_i\right]_3 = y_{i3} + s_3 \tag{3.22}$$

where $\eta = [s_1 s_2 s_3]$ is error estimation, i.e., $\eta = \hat{\eth}_l - \eth_l$ and $y_i = [y_{i1}\ \ y_{i2}]^T$. Taking square on both side of (3.22), we get;

$$\left[\hat{\eth}_i\right]_1^2 \cong y_{i1}^2 + 2y_{i1}\ s_1,\ \left[\hat{\eth}_i\right]_2^2 \cong y_{i2}^2 + 2y_{i2}\ s_2,\ \left[\hat{\eth}_i\right]_3^2 \cong y_{i3}^2 + 2y_{i3}\ s_3 \tag{3.23}$$

Note that in our parametric loop division (PLD) method [56] is also assumed that the noise is nominal and the co-variance matrix only records the parametrized nodes position along with reference anchor position. Therefore, we also use estimation method in Tayler series form to obtain co-variance data values.

3.3.1.4 Nonlinear Least Square Estimators (NLLS)

In [160], a TDoA based NLLS estimator was proposed. Initially LLS provides a accurate solution for normal imperative straight least square and dependent on the deployed area. NLLS is used to improve accuracy. Consider the problem definition;

$$\hat{Y} = \underset{y\ \in\ \mathbb{R}^{d\times A}}{arg}\ \ min \sum_{i=1}^{A} \left[\sum_{j\in\alpha_i} (V_r^a(i,j))^2 + \sum_{j\in\beta_j} (V_r^t(i,j))^2 \right] \tag{3.24}$$

To find positioning estimation $\hat{Y}$ of Y based on region and volume $V_r^a(i,j)$. Usually NLLS method is suitable for (3.24). We observed that the variance of positioning error is available, so NLLS can be converted to weighted NLLS form expressed as:

$$\hat{Y} = \begin{matrix} arg \\ y \in \mathbb{R}^{d \times A} \end{matrix} \quad min \sum_{i=1}^{A} \left[\sum_{j \in \alpha_i} \left(\frac{V_r^a(i,j)}{\sigma_{i,j}} \right)^2 + \sum_{j \in \beta_j} \left(\frac{V_r^a(i,j)}{\sigma_{i,j}} \right)^2 \right] \tag{3.25}$$

where $\sigma_{i,j}^2$ is a variance of noisy function $\eta_{i,j}$.

3.3.2 Geometric Estimators

Another well-known formulation is to consider the geometric interpretation between nodes for localization measurement. Consider a distance between target and known node $\hat{d}_{i,j} = d(y_i, y_j) + e_{i,j}$ and $j \in \alpha_i \beta_j$, where $e_{i,j}$ is an estimation error. If there is no error, it is assumed that both i and j nodes lie in the intersection of a circle with a radius of $\hat{d}_{i,j}$. Let us assume, $e_{i,j}$ is non negative and $e_{i,j} \geq 0$. The disc centered is represented as

$$D_{i,j} \triangleq \left\{ y \in \mathbb{R}^2 \mid \hat{d}_{i,j} \right\} \quad j \in \alpha_i \beta_j \tag{3.26}$$

where y_i lies in the intersection of D_i of the circle $D_{i,j}$

$$\hat{Y} \in D_i \triangleq \bigcap_{j \in \alpha_i \cup \beta_j} if \;\; e_{i,j} \geq 0 \tag{3.27}$$

Figure 3.4 illustrate the above mentioned phenomenon including unknown nodes for the PLD network shown in Figure 3.5.

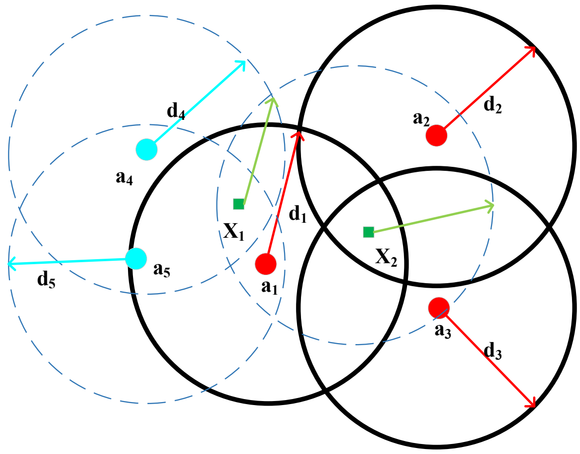

Figure 3.4: Distance measurement with non-negative errors

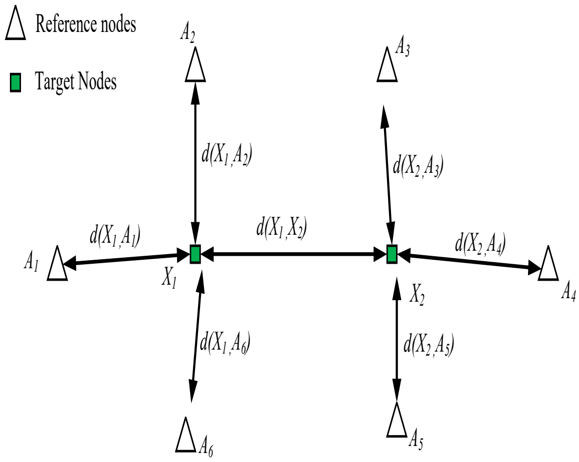

Figure 3.5: A cooperative PLD model with target and reference anchor nodes

The problem of NLLS can be further enhanced to convex feasible problem, (CFP) in case of non cooperative scenarios. This problem can also be taken by outer approximation (OA) or projection onto convex sets (POCS).

3.3.2.1 Projection onto Convex Sets (POCS)

CFP's are solved by POCS [161, 162]. Most of the projection sets are applied to image restoration problems [163, 164]. POCS have two variations, sequential and parallel. In a sequential method, a data set is selected followed by other sets in an iterated system according to algorithm rules and data structure, which construct next iterated data sets. The parametric points calculation based on first reference node sets is also an example of projection in our model. On the contrary, in parallel projection method all current points are projected to all the sets and then all projected estimation will be generated at the same time as shown in Figure 3.6.

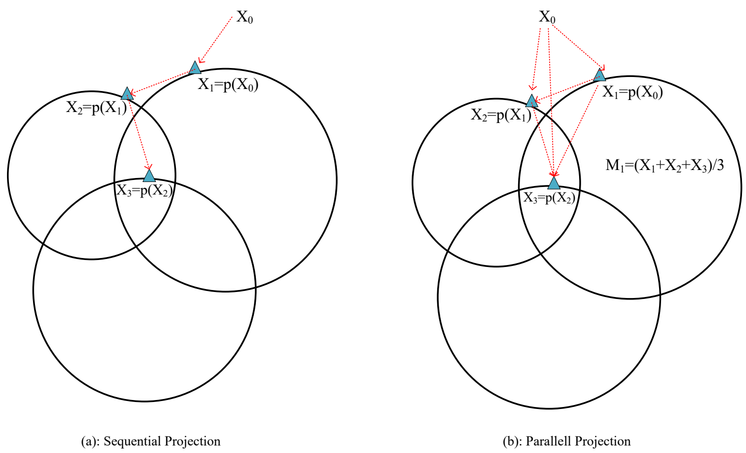

Figure 3.6: Example of Sequential and Parallel projection

Other than image transformation, POCS approaches are first used in [165, 166] for sensor localization and in [167, 168] for sensor network convergence.

3.3.2.2 Cramer-Rao Lower Bound

(CRLB) [144], is very well known in describing the lower limit of unbiased estimators. The MVU is also computed through CRLB, but CRLB is a benchmark against efficiency of any unbiased estimator. Assume the data is given in vector form that is $y \in \mathbb{R}^a$. The known MLE parameters $(\theta = \theta_1, \theta_2, ..., \theta_n)^T$ of y and the PDF is $p(y; \theta)$, where y is dependent on unknown deterministic parameter θ. The flow of data y is also taken w.r.t $p(y; \theta)$ as a function of angular parameter and represented by $\mu(\theta)$. The CRLB is computed through the following theorem [146].

Theorem 1. *Considering that the PDF, $p(y; \theta)$ satisfies the regularity state.*

$$T\left[\frac{\partial lnp(y;\theta)}{\partial\theta}\right] = 0 \text{for all } \theta \tag{3.28}$$

computation expectation is taken w.r.t $p(y;\theta)$. So,

$$\frac{\partial ln(y;\theta)}{\partial\theta} = \left(\frac{\partial lnp(y;\theta)}{\partial\theta_1}, \frac{\partial lnp(y;\theta)}{\partial\theta_2}, ..., \frac{\partial lnp(y;\theta)}{\partial\theta_q}\right) \tag{3.29}$$

The co-variance matrix $C_{\hat{\theta}}$ satisfies the unbiased estimators

$$C_{\hat{\theta}} - F^{-1} \geq 0 \tag{3.30}$$

where F is a fisher information matrix (FIM) expressed by $F(\theta)$:

$$F(\theta)_{i,j} = -T\left[\frac{\partial^2 lnp(y;\theta)}{\partial\theta^i\partial\theta^j}\right] \tag{3.31}$$

$$\left[\frac{\partial^2 lnp(y;\theta)}{\partial\theta}\right]^T = F(\theta)(g(x) - \theta) \text{ satisfies } 3.30 \tag{3.32}$$

Definition 2. An estimator is said to be efficient if and only if it is unbiased and follows CRLB estimation.

3.4 Classifications of Localization Algorithms

Many WSNs localization algorithms have been proposed so far. They can be classified into different groups based on a number of criteria.

3.4.1 Centralized vs Distributed Approaches

To localized a sensor nodes, the measurement process can be taken either by centralized or by distributed approach. In centralized approach, complete data is directed to the central node or point primarily referred as sink or a beacon node. The central node will determine the actual nodes position and reply to the requested node. The main advantage of this approach is low energy cost for those nodes to be localized as most of the computation is done at the central node. Multidimensional scaling [169], linear programming [170] and stochastic optimization [171, 172]. In case of distributed approaches, there is separate localization process of each node with one to one communication with anchors and no central node is required.

Several optimization techniques like geometric models or dual/ primary decomposition methods are used in distributed approaches with fast convergence and accomplishes in two steps: signal broadcasting and combining the local estimation at each node. The broadcasting stage is always costly. According to the rule of thumbs, the power requirement of broadcasting 1 bit over $100m$ distance is almost the same as what is used to process 3 million instructions [173]. Therefore, to determine the algorithm complexity, the number of broadcasts should always be taken into account.

3.4.2 Range-based vs Range-free Approaches

Based on whether actual distance measurement between nodes is required, localization algorithms can be divided into range-based and range-free localization techniques. Range based algorithms provide precise better localization accuracy as compared to range-free ones [174]. Ranged based localization makes use of information about the distance to neighbour nodes.

In range free localization algorithms, there is no hypothesis about the availability of absolute distance between the sensor nodes. Instead, the sensor node location can be estimated through radio connectivity information or sensing capabilities of each sensor. Anchor nodes may be used in this kind of algorithms. The detail of these techniques is presented latter in this chapter. Range free is better option when cost is the main concern. For example, mobile and static localization algorithms proposed in [126] can provide high performance with heterogeneity features. Table 3.2 compares range free and range based algorithms based on different parameters.

Table 3.2: Comparison of Range-based and Range-free Localization Algorithm.

Algorithm Types	Estimation Technique	Accuracy	Computation cost	Hardware cost
Range-Based Techniques	RSSI	Medium	Low	Low
	TDoA	High	Low	High
	AoA	High	Low	High
Range-Free Techniques	Per hop distance	Medium	Low	Medium
	Single neighbour techniques	Low	Low	Low
	Multi neighbour techniques	Low	Low	Low

3.4.3 Anchor-based vs Anchor-free Approaches

The precision of anchor-based localization is directly proportional to the density of anchor nodes. More anchor nodes will lead to less error in localization, hence higher accuracy. These algorithms with known positions transmit their data to neighbours. The performance of anchor-based algorithms will be dependent on the anchors arrangement in sensor environment [175]. In [176], an anchor based approach was discussed where anchors selection is done using advanced RSSI table for distance estimation between anchors and anonymous nodes. These anonymous nodes with updated location are utilized as novel anchors primarily known as pan-anchors. Another work was discussed in order to enhance virtual anchor nodes by making use of additional rational slide based on smallest hopping track approach without addition of substantial anchors [176].

In anchor unrestricted algorithms no presupposition is required concerning nodes positions. Thus, relative range rather than absolute range is determined with respect to nodes. In [177] ladder diffusion node localization technique was proposed specifically with anchor independent criteria. This approach was successful in terms of low broadcasting determination error, low delay and acceptable budget.

In anchor-free localization there are no beacon nodes, in other words, location of all sensor nodes is unknown. An assumption based coordinate (ABC) algorithm was proposed in [178]. Initially, four nodes within the communication range initiate the process. Then location of the remaining nodes is determined with the defined position of the four nodes. The benefit of this scheme is its simplicity and robustness in computation. However, this approach also has some limitations, such as poor localization accuracy, inefficient coordinate assignment and unguaranteed graph localization.

Robust distributed network localization (RDNL) scheme was proposed in [179]. This approach discusses node localization in presence of noise. This is a cluster based approach in which each node acts as cluster head and determines the distance to the nodes in its neighborhood. The advantage of this technique is that the nodes are even localized in presence of noise. Low node connectivity is a main limitation of this system. In [180], anchor free localization algorithm (AFL) was presented in which the coordinate information of all nodes is computed and processed in parallel. Initially, the coordinates to the nodes are assigned based on the connectivity among nodes and the localization errors are corrected using a mass spring optimization.

3.4.4 GPS vs Non-GPS Approaches

GPS dependent approaches are the most expensive approaches due to GPS receiver installation requirement at every node but it offers the best performance for outdoor localization [126, 181]. In [182], a GPS-dependent approach was explained with trilateration measurement. In GPS less approaches, distance estimation is done through information exchange of sensor nodes [183].

3.4.5 Fine-grained and Coarse-grained

Fine-grained approaches adopt RSSI, whereas coarse-grained approaches do not rely on RSSI. In [184], an RSSI based approach was discussed with emphasis on indoor channel response. The researchers in [185] discussed an RSSI technique where node locations are geometrically determined through distributed process.

In [186], discusses several approaches which are applicable in indoor as well as outdoor scenarios. By considering different channel models like log-normal shadowing model with dynamic variance, LNSM-DV approach was proved to be successful as far as localization errors are concerned [187]. But for indoor scenarios, Gaussian Mixture Modelling and Maximum Likelihood Estimation (GMM-MLE) algorithm is a good choice [188]. Room confinement localization is accurate using co-variance approach [188]. The aforementioned techniques are summarized in Table 3.3.

Table 3.3: Different Localization Techniques.

Ref.	Proposal
[179]	2D system with noisy range measurement with graph planner
[189]	Use of grey prediction method in WiFi
[190]	APS based localization system, using distance vector routing, self positioning system
[191]	Complex shapes and non-uniform deployment.
[126]	N-hop multilateration for ad-hoc sensor network
[192]	Monte carlo localization (MCL) based system. more accurate than the original MCL
[193]	GPS anchors using mere connectivity and MDS system
[194]	used of connectivity information within a range. MDS with some anchor positions and $O(n^3)$ node complexity
[195]	simulated annealing and self localized system
[196]	multi-hop localization system, used RSSI and self localization
[197]	Improved APIT, with radio pattern and randomly deployed nodes
[198]	bits and flops system using n-hop wsn localization
[199]	distributed ad-hoc system, discrete model of random deployment
[200]	system with globally accessible beacons with 26% accuracy
[201]	Manual measurement of RSSI with distributed node and GPS based anchor positions
[202]	localization using spatial map
[203]	use of proximity distance map and MDS to self localization

Continued on next page

[204]	SHARP, new relative approach using distance measurements and absolute coordinates system
[205]	Radio interferometric geo-location
[206]	Radio interferometric system of localization using pairwise distance with minimal use of hardware
[207]	localization using interferometric ranging, RSSI and relative distance
[208]	Distance measurement error (DME) and CRLB, using UWB channel measurement
[209]	stochastic approach based on deductive and inductive methods, reduction of training phase for self and indoor localization

The detailed classification of different proposals with their characteristics is given in Table 3.4

Table 3.4: Classification of Localization Algorithms.

Ref.	Centralized/ Distributed	Anchor-based/ Anchor free	Range-based/ Range-free
[126]	Distributed	Anchor-Based	Both
[179]	Distributed	Anchor-Free	Range-Free
[189]	Both	Anchor-based	Range-based
[190]	Distributed	Anchor-based	Range-based
[191]	Distributed	Anchor-Free	Range-Free
[192]	Distributed	Anchor-Based	Range-Free
[193]	Centralized	Anchor-Based	Range-Free
[194]	Centralized	Anchor-Free	Range-Free
[195]	Centralized	Anchor-Based	Range-Free
[196]	Centralized	Anchor-Based	Range-Based
[197]	Distributed	Anchor-Based	Range-Free
[198]	Distributed	Anchor-Based	Range-Based
[199]	Distributed	Anchor-Based	Range-Free
[200]	Distributed	Anchor-Free	Range-Free
[201]	Distributed	Anchor-Free	Range-Free
[202]	Distributed	Anchor-Free	Range-Free
[203]	Distributed	Anchor-Based	Range-Free
[204]	Distributed	Both	Range-Based
[205]	Distributed	Anchor-Based	Range-Based
[206]	Distributed	Anchor-Free	Range-Based
[207]	Distributed	Anchor-Based	Range-Based
[208]	Distributed	Anchor-Based	Range-Based
[209]	Distributed	Anchor-Based	Range-Based

3.5 Range-based Localization Algorithms

In range-based localization algorithms, angle or distance between target and anchor nodes is estimated, then the position of unknown node is computed by means of some statistical or geometrical algorithms [210, 211, 212]. Figure 3.7 shows our taxonomy of localization algorithms based on the type of anchor node, static or mobile.

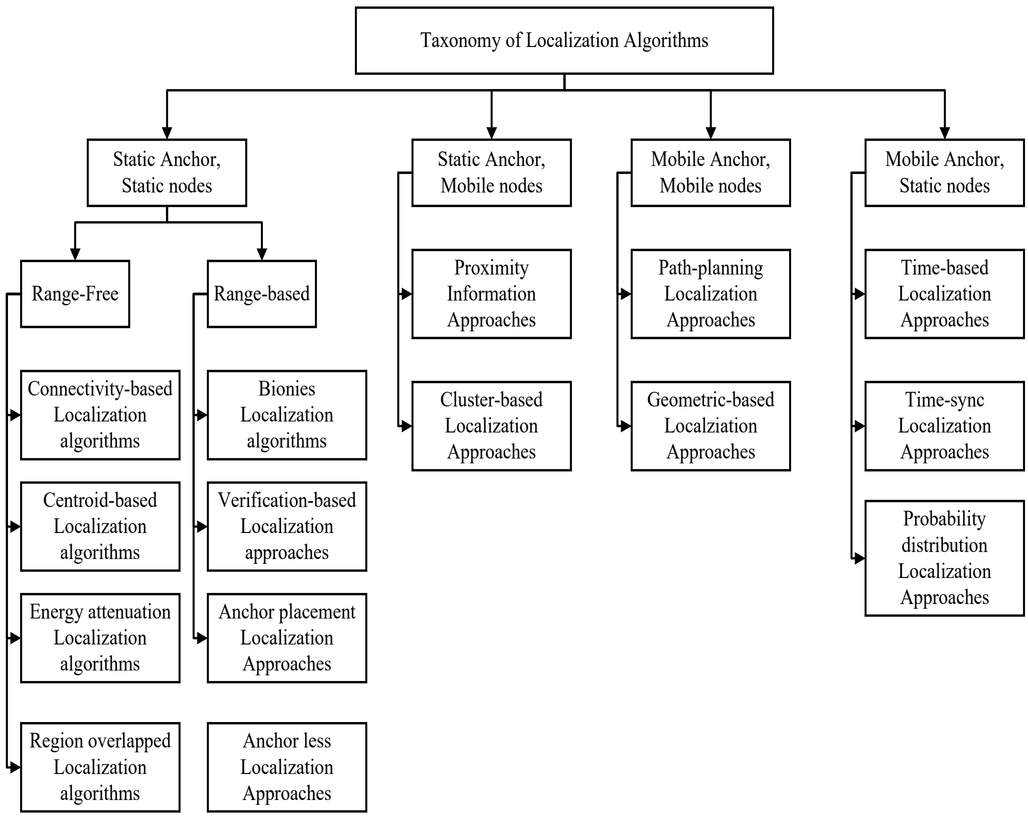

Figure 3.7: Taxonomy and survey of Localization Algorithms

The type of algorithm operated in a WSN applications can be determined using measurement technique. In WSN, measurement can be dependent on coordinates of the sensors denoted by:

$$Y = h(X) + e \tag{3.33}$$

where X is a real coordinated values of the target nodes, e is a directional error and Y is the particular vector from anchor node to a target node. MLE [145] was used to minimize optimization. If the error f_e is known in distribution measurement, then

$$\hat{X} = arg\ min(\log f_e(Y - h(\hat{X}))) \tag{3.34}$$

As we discussed in optimization, illustrated in section 3.3.2.2, the FIM is used to solve known distribution measurement.

$$Q(X) = E(\nabla_x^T \log f_e(Y - h(X))\nabla_x \log f_e(Y - h(X))) \tag{3.35}$$

where ∇_x is used for partial derivation w.r.t. X. The location accuracy is then computed by CRLB [144]

$$Cov(\hat{X}) = E(X - \hat{X})(X - \hat{X})^T \geq Q^{-1}(X) \tag{3.36}$$

CRLB highlights the presence of unbiased estimators of sensor locations. This should provide the measurement phenomenon that is used to compute the lower-bound of the localization.

3.5.1 Proximity

Many systems used proximity for localization. This can be accomplished using different techniques such as "*in radio range*". Other systems use detection of a sound, pressure sensor in floor [213], and RF or light source in a building or room for proximity with accuracy of 30cm to 3m. The proximity describes the geo-location and relationship between anchor and sensor node and used when ranging is costly and difficult. The scenario behind localization becomes very simple with proximity. For example, if a node A senses the presence of node B in a mobility scenario (e.g., magnetic field, infrared, acoustic, radio, etc). Furthermore, node A has information about node B in in its neighbour. Thus, the distance from node A to B is represented as follows:

$$d_{AB} \leq R_A \tag{3.37}$$

where R_A represents the sensing range of node A. A binary ranging represents 0 for out of R_A and 1 for in-range in range-free localization techniques. This idea of centroid based localization is implemented in [214]. For triangulation, a target node j can select other k neighbours with reliable communication and link quality. The localization is calculated as gravity centre for k selected anchor nodes as

$$(\hat{x}_j, \hat{y}_j) = \left(\sum_{i=1}^{k} X_i/k, \sum_{i=1}^{k} Y_i/k \right) \tag{3.38}$$

The centroid technique is further improved in weighted centroid localization (WCL) [215], MSL [216], and LANDMARC [217] by assigning weight to the link. WCL and LANDMARC use RSSI for distance estimation.

$$(\hat{x}_j, \hat{y}_j) = \left(\frac{\sum_{i=1}^{k} w_{ij}(X_i, Y_i)}{\sum_{i=1}^{k} w_{ij}} \right) \quad \text{where,} \quad w_{ij} = \frac{1}{(d_{ij})^{\eta}} \tag{3.39}$$

where w_{ij} is a weight to RSSI link and η represents the path-loss factor. A complex design for static and mobile node localization was proposed in [216], which adopts a partial filter to compute the location. Another interested work that we describe latter in range-free localization algorithm is APIT [218], which used the anchor node proximity as presented in Figure 3.8.

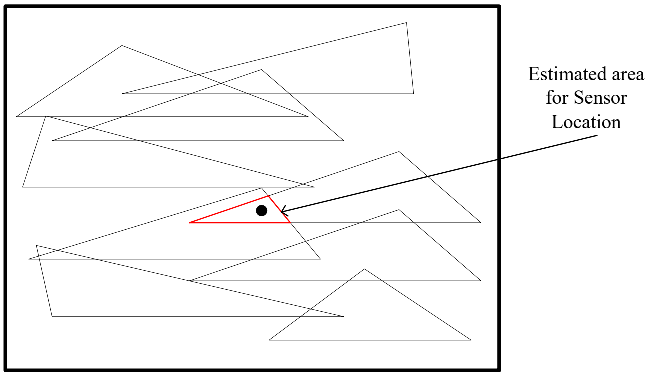

Figure 3.8: Triangular Coverage Based on Proximity: APIT

Centroid [214] and APIT [218] showed that low cost sensor nodes are localized efficiently in proximity based range-free schemes.

3.5.2 Received Signal Strength Indicators (RSSI)

RSSI values have been widely used in location estimation through computing the distance between neighbours. The theoretical properties of RSSI can be directly derived from the Friis' free space transmission equation, the RSS decreases quadratically with the distance to the transmitter.

$$P_{RX} = P_{TX} \cdot G_{RX} \cdot G_{TX} \left(\frac{\lambda}{4\pi d} \right)^2 \tag{3.40}$$

where, P_{RX} is a received power and P_{TX} is transmission power of sender. G_{RX} and G_{TX} are the gain of receiver and transmitter, respectively. Equation (3.40) shows that most power lost occurs at higher frequencies. This means that for antenna with specified gains, there will be higher energy transfer at lower frequencies. Due to various signal path factors, the path loss in the wireless communication is different from (3.40). By merging the constants, adding losses and using logarithmic power values, (3.40) can be re-written as follows [219].

$$d = d_0 \cdot 10^{(P_0 - P_{RX} + E_\sigma)/10\eta} \tag{3.41}$$

where d_0 is a reference distance corresponding to a reference transmission power P_0. There is also a path loss factor η which is typically between $1.6 - 1.8$ for outdoor deployments and $2 - 4$ for indoor deployments [219]. The RSSI value from a receiving device can be expressed, using logarithmic power values.

$$RSSI = k \cdot (P_{RX} - P_{ref}) \tag{3.42}$$

Combining (3.41) and (3.42) will give an expression whereby distance can be calculated solely from RSSI. The two constants k_0 and k_1 can be empirically estimated.

$$d = d_0 \cdot 10^{-k_1 \cdot \frac{RSSI}{RSSI_{max}} \cdot 1 + E_\sigma} \tag{3.43}$$

In most implementation of RSSI measurements, the RSSI is an 8 bit unsigned integer value corresponding to the range $0 \sim 255$. However, depending on the implementation, the significant value range might be less, e.g., $25 \sim 175$ or $0 \sim 100$ [219]. In such cases, the RSSI value and $RSSI_{max}$ will need to be scaled accordingly. The error factor E and standard deviation bring many issues with RSSI. As part of its Network Management Services, IEEE 802.15.4 and ZigBee specifies the LQI. It is only accessible via "$mgmt\_lqi$" command, whose response gives all the LQI values of neighbours in the form of a table [220]. The correlation between RSSI and LQI is presented in [221] and [222]. Therefore, we can assume a new LQI-based expression, in which d_{ij} represents the distance from a sensor node i to node j.

$$d_{ij} = k_0 \cdot 10^{-k_1 \cdot Q_{ij}} \quad \text{where} \quad Q_{ij} = \frac{LQI_{ij}}{LQI_{max}} \tag{3.44}$$

Since the condition of Q_{ij} will not be accurate for extreme situations, we cannot simply set $LQI = 0$ thus eliminating k_1 and be able to isolate k_0. Instead, k_0 and k_1 must be fitted to empirical data points by the least square method or similar methods. From [221] and [222], two other expressions have been suggested, of which (3.45) is a variant of (3.44) and (3.46) is a third order polynomial.

$$d_{ij} = \sqrt[N]{\frac{a}{Q_{ij}}} \tag{3.45}$$

$$LQI_{ij} = k_3 \cdot d_{ij}^3 + k_2 \cdot d_{ij}^2 + k_1 \cdot d_{ij} + k_0 \tag{3.46}$$

In wireless local area networks (WLANs), several RSSI measurements are taken from all visible points, e.g., sniffing devices, and access points in WLAN at each sample points [223]. Each sample point is mapped to RSS probability distribution or RSS vector from the collected information. This helps to develop its own RSS fingerprint that is further transferred to central station. The central station then compare the RSS vector with RSS model based on the nearest neighbour technique [224] or probabilistic technique [225], which helps to determine non-anchor network localization. Different from the method proposed in [224], another technique based on RSS profiling is the area based localization that measures the area of network not having anchor node in proximity [226]. It is also observed that a dense sampling with medium localization error of $3m$ is gained for devices using 802.11 standard.

A 3D localization technique was proposed in [227], which is based on the RSSI. Firstly, measures the beacon nodes present in the neighbourhood area by using RSSI and then the positional data through optimization iterations is achieved. Iterative streamlining can enhance the location precision, however, the division of regions is effectively influenced by RSSI estimation errors. In [228], authors have proposed the RSSI based technique for localization based on the fuzzy logic, with a name as the fuzzy logic based Multilateration scheme for localization (FLMSL). In this algorithm, the variables used are *High,Medium,Weak* and *Near,Far,Intermediate*. Logic rules are then defined after optimization. In the third phase, Jacobi's defuzzifier technique is then used for phase de-fuzzification,

$$D_k = (a, , b, c) = \frac{\sum L_n}{\mid L \mid} \tag{3.47}$$

In [229], authors contemplated the effect of various types of spatial assorted qualities on the accuracy of localization in indoor situations while changing the shadowing impact. Three framework models outlining the spatial differing qualities were considered: diversity based on the transmission through multi input single output (MISO), diversity based on received values through single input multi output (SIMO) and the diversity based on the received and transmission values through multi input multi output (MIMO). It is determined that the localization accuracy is enhanced as compare with the single receiving antenna framework through single input single output (SISO). The wireless channel is obtained by:

$$y = hx + n \tag{3.48}$$

where h is the channel gain and n is the noise. Error probability is modelled as:

$$P_e = exp- \mid h^2 \mid SNR/2 = \frac{1}{1 + \frac{SNR}{2}} \tag{3.49}$$

The average error rate is analyzed by utilizing distinctive differing qualities consolidating techniques at the receiver named as Equal Gain Combining (EGC) method, Maximum Ratio Combining (MRC) method, and Selection combining (SC) method. In MRC methods, RSSI measurement is modelled as:

$$RSSI_{MRC} = \left(\frac{1}{\sum_{i=1}^{n} R_i} \right) \cdot \sum_{i=1}^{n} (R_i)^2 \tag{3.50}$$

In [230], author proposed a new idea based on RSSI. Signal strength can provides a way to select RSSI and a propagation model is used to apply RSSI value for calculating distance. In this algorithm, there would be a self-calibration that doesn't require human intervention. The author then used the model floor attenuation factor (FAF) and wall attenuation factor (WAF) as shown in (3.51).

$$L(d) = l_0 + 10\beta \log d = WAF + FAF, \quad WAF = \sum_{i=1}^{N} k_i l_i \tag{3.51}$$

where $L(d)$ is a path loss, β is path loss exponent and l_0 is the path loss in reference distance. In [231], authors proposed a new technique to improve the accuracy. They claimed that this technique can be simulated with RSSI, ToA and TDoA. Polarization angle was determined by using an accelerometer. Then, an error correction formula was proposed and semi-automatic trial that calibrated the entire system is presented. Author, in [232] presented an improved RSSI based localization algorithm for children tracking and park lighting based on distributed localization. The error was $4m$ in an area of $60m \times 60m$ for child tracking. Log normal model was used for range measurements and Maximum Likelihood technique was adopted for location estimation. This can basically be used in a Min-max model to localized blind node overlapped under three or more rectangular areas as shown in Figure 3.9.

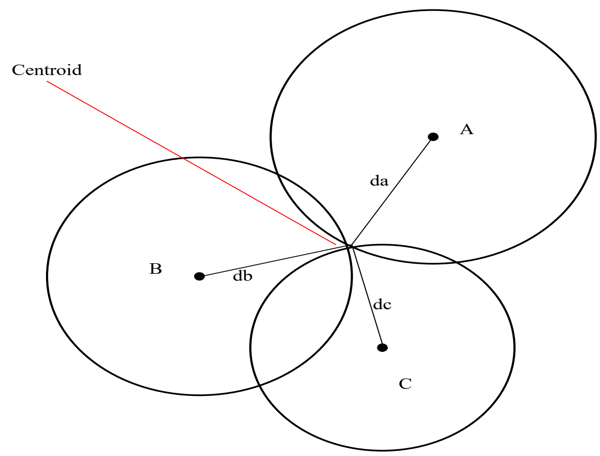

Figure 3.9: Min-Max Model

In [233], an effective range based localization algorithm was proposed, which used the shadowing effects in RSSI signals to improve localization accuracy. For initial simulation, the authors used 122 sensor nodes to monitor health equipment's in a power substation. The author in [234] considered RSSI method in three baseline WSNs with several experiments. Results showed that RSSI methods were not good enough to achieve high localization accuracy and stability. In [235], the authors proposed an idea based on log-normal shadowing model, giving better results in comparison to Maximum likelihood estimation method. They found that average RSSI value did not decrease as a function of distance, therefore propagation parameters were changed among anchor nodes. In other words, anchor nodes should not be considered statistically identical.

The algorithm proposed in [236] investigated a mechanism using dependable RSSI for distance estimation. Through practical experiment, a threshold is defined, and a distance between blind node and anchor node is computed by shortest path algorithms. The rationale behind defining a threshold for RSSI value includes two points: (1) large RSSI demonstrate high SNR ration, so practically they are not suitable for log-normal path loss model, (2) there is a large localization error even with a small error in RSSI measurement.

Hybrid localization algorithms, which combine RSSI based algorithms and centroid localization (CL) algorithms, were also proposed. Examples of these algorithms include Triangular Centroid Localization (TCL) [237], the WCL [215], Improved Centroid Localization Algorithm (ICL) [238], and easy to deploy indoor positioning system (EDIPS) [239]. The TCL algorithm operated with two beacon nodes and estimated position of unknown nodes to form a triangulation. The distance estimation in WCL is also performed by using the RSSI/ LQI. Under WCL, the position of an unknown node would be estimated by (3.39).

Authors in [240] proposed Robust Position Estimation (ROPE), which allowed sensors to estimate their locations without assistance from a centralised computation facility. Self-localization and calibration algorithms are explained in [70, 241]. [242] is another RSSI based system where path loss model is used for RSSI. This model was good for outdoor environment. The proposals of well-known RSSI based localization algorithms are summarized in Table 3.5.

Table 3.5: Proposals of RSSI based localization algorithms.

Ref.	Proposal
[187]	use of propagation model and self-adaptability.
[70, 241]	GMM model and self-calibrated node localization using RSSI and LQI.
[233]	Mitigation of shadowing effect using RSSI.
[242]	RSSI measurement with better result in outdoor environment.
[196, 231]	RSSI based calibration and use of specific propagation models.
[236]	Effect of antenna polarization and pattern recognition using RSSI values.
[237, 238, 239]	Mobile based localization methods using RSSI measurements.
[71, 200, 209, 211]	Self-localization in large scale network using RSSI.

A brief summary of RSSI based method algorithms are given in Table 3.6.

Table 3.6: Summary of RSSI based Localization Algorithms.

Ref.	Context of the paper	Methodology	Focus area/ Review
[70]	Guassian mixture model GMM	MLE and RSSI	GMM-MLE high accuracy
[71]	incremental self-deployment	RSSI, self-system	Energy consumption
[187]	RSSI, LNSM model, dynamic nature	Least square (LS) and LNSM-DV	Better with LNSM-DV as compared to LNSM
[196]	simple calibration	no deployment info require	Average system, only suitable for indoor
[200]	Self-localization	RSSI, global Coordinates, MLE	High computation cost
[209]	Hybrid localization	RSSI, stochastic approach	High energy utilization
[211]	self-organized network	RSSI, secrete key sharing	High energy utilization, low accuracy
[231]	RSSI, Interference	virtual calibration, worse for WSN	Accuracy depend on anchor node density
[233]	LNSM, Multilateration	moving beacons and clusterization	self-positioning, high accuracy
[236]	Indoor, clear	Trilateration, 8 anchor nodes	Low accuracy, polarization
[237]	Indoor	trigonometric figures, TCL	High computation cost
[238]	Mobile	Weighted centroid, RSSI	Low accuracy, coverage
[239]	indoor, mobile	Weighted centroid, RSSI	Low accuracy

Continued on next page

[241]	Self-calibration	RSSI, LQI measurement	SCCL high accuracy in centroid
[242]	Trilateration method and RSSI	LS, Pathloss model	Good for outdoor

3.5.3 Time of Flight (ToF)

Measuring the ToF of the signal is another important ranging technique. If ToF is accurately measured, the travel distance can be computed. For distance estimation, authors in [225] used the ToF with cooperation of RF signals and ultra sound signal. Both signals of RF and ultra sound are broadcast at the same time. But they arrived at different time because sound signals travel slower as compared to radio signals. Then the time resolution for the signals is computed by:

$$c = 299792458m/s \quad \approx \quad 0.3mm/ps \tag{3.52}$$

$$v_s \approx 1238km/h \approx 344m/s = 0.344mm/\mu s \tag{3.53}$$

where c is a speed of light and v_s is a speed of sound in air. The pToF is another alternatives for measuring time variables by affixing an offset known as pts. This is basically a start of a specific clock t_0, and the emission time. Figure 3.10 shows the time variables for ToF and offset variable for pToF.

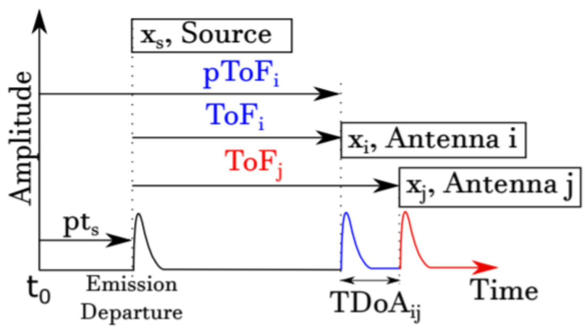

Figure 3.10: ToF, TDoA and pseudo-time of flight (pToF) notations for arbitrary receiver and source x_s.

Authors in [243] considered a burst mode and exploits the method of two-way ranging (TWR) that nearly approaches the hypothetical lower bound for extending accuracy in a noise restricted environment and accomplishes meter level preciseness in environments with multipath. Estimations are taken at numerous frequencies and consolidated together to relieve the effect of multipath channel attributes. TWR method uses the Two-way time transfer (TWTT) that minimizes the errors of clock synchronization [244] described as:

$$\hat{T} = \frac{t_A - t_B}{2} \tag{3.54}$$

where $t_A = t_{SA} - t_{RA}$ and $t_B = t_{SB} - t_{RB}$. Both A and B are responsible for measuring the time delay and use local clock for this purpose. t_{SA} is the time sent by the A while t_{RA} is the time received by the A.

3.5.4 Angle-of Arrival (AoA)

AoA is another type of range based localization algorithms, which adopts angular estimation instead of distance. The AoA data are typically gathered by using radio or microphone arrays [245, 246] that helps the receiver to determine the direction of a transmitter. AoA is not a new idea. Smart synchronization [247] and phased array radars used AoA methodology have been widely used in civil and military applications. However, use of AoA in WSN localization is not trivial as the measurement of angle is much harder to measure than distance. Details of AoA methods can be found in [247] and [248]. Nevertheless, researchers have contributed much effort in AoA localization in WSN including (1) effective noise mitigation [145, 146, 149, 249, 250], (2) practical angle measurements [128, 200, 251, 252], and (3) anchor placement and limitation of AoA [73, 136, 253]. The first assemblage of AoA measurement is known as "*beamforming*" based on the polarization pattern of antenna [254]. Signal wavelength can effect the size of measurement unit as shown in Figure 3.11.

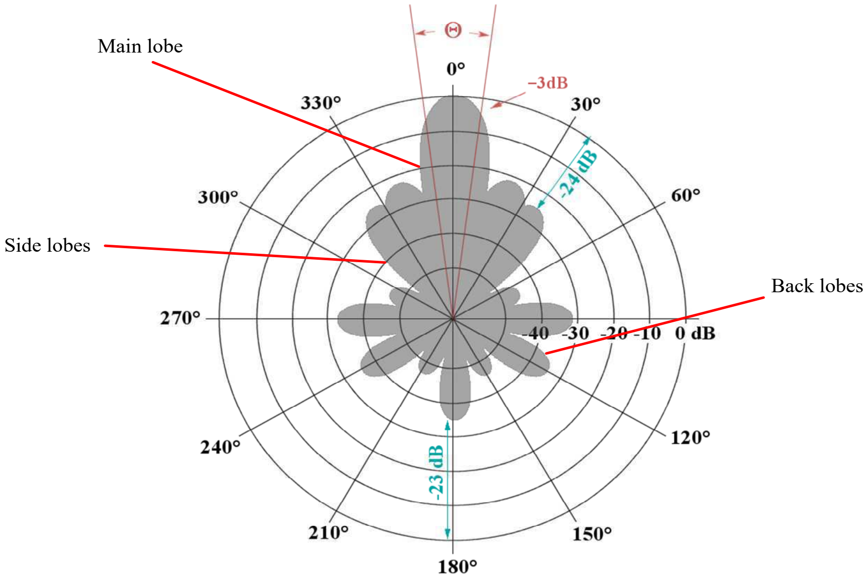

Figure 3.11: Horizontal antenna lobes with AoA measurement.

The transmitter direction is considered as the maximum RSS, when antenna beam is rotated mechanically or electronically. The beam width and receiver sensitivity helps to determine the measurement accuracy. By rotating the antenna beam, the receiver cannot differentiate the signal strength. Parabolic fitting functions can easily be stored in a wireless sensor node and its inverse function can be utilized for accelerating the procedure of node localization. Practical implementation is performed for ALRD by considering the indoor area of $10m \times 10m$ having two beacon nodes. Experimental results showed a localization error of $124cm$ [255]. Two other schemes are also proposed, namely maximum point minimum rectangle (MPMR) and maximum point minimum diameter (MPMD) for minimizing the localization error. Proposed technique gathers more beacon signals in order to locate all the estimated locations. Experimental results in [255] suggested that proposed techniques can minimize the location estimation errors by 29% to become $89cm$.

In [256], authors considered an agreeable localization in WSNs comprising of numerous anchor nodes outfitted with a direct reception antennas cluster of M components, a control unit (CU) and a single antenna target. Synchronous network along with the flat frequency channels is taken into account for proposed scheme. The triangulation strategy and the most likelihood (ML) based estimations are typically implemented for (AoA) based localization in WSNs. However, the localization precision of the triangulation is low, and the MLE requires an initial prepossessing near the exact position to evade the issue of convergence. In [257], two productive AoA schemes are extracted from adequate complementary variable strategy.

$$\hat{\beta}_j = \beta_j + \delta\beta_j, \tag{3.55}$$

where β_j is the accurate measurement of AoA from j^{th} beacon and noise is measured by Gaussian distribution with zero mean and σ_j^2 we get:

$$\delta\beta_j \approx \S(0, \sigma_j^2) \tag{3.56}$$

then the relationship between neighbour beacon and unknown nodes is presented in the following form

$$\tan(\theta + \beta_j) = \frac{b_j - y}{a_j - x}, \quad j - 1, 2, ..., N \tag{3.57}$$

where b_j and a_j is the position of the j^{th} beacon, and θ is the orientation of the unknown node. In [258], authors proposed a new method for user-centric ultra network (UDN) using cloud computing. Azimuth AoA was considered for distance estimation and LoS path between multi transmission reception point and a device. The result of this technique shows a some meter localization accuracy by deploying ULAs with four antenna per TRPs.

3.5.5 Time of Arrival (ToA)

ToA based localization algorithms estimate the location of a node based on the received time of arrival packet from another node. Considering that both nodes are perfectly synchronized. The distance is measured by multiplying the propagation speed of a signal by its propagation time. The receiver notes the time of signal arrival from its clock. For example, let us suppose a receiver knows the exact packet transmission time, and then it can calculate the total time for the packet transmission and propagation delay. Usually ultrasound signals are deployed in ToA based localization systems as shown in Figure 3.12(a). The distance between each anchor node and mobile object is calculated by:

$$d = \left(\frac{(t_3 - t_0) - (t_2 - t_1)}{2} \right) \cdot v \tag{3.58}$$

where t_0, t_1, t_2, t_3 and v are the transmission time at the transmitter, reception time at the receiver, transmission time at receiver and receiving time at transmitter and ultrasound signals velocity, respectively. In ToA, the multipath fading, time synchronization and additive noise are the main source of errors. However, the following techniques can substantially reduce these errors: (1) Error due to multipath: ToA can be adjusted to be the time such that cross correlation between transmitted signals and received signals first crosses the threshold. (2) Error due to un-synchronized clocks: All nodes are required to synchronize their clocks to a reference clock before localization starts. (3) Error due to additive noise: Cross correlation is used to calculate ToA. To overcome this limitation a mobility assisted node localization approach was proposed in [259] which does not require any time synchronization. The author assumed that all anchor-target links have same SNR for homogeneous network.

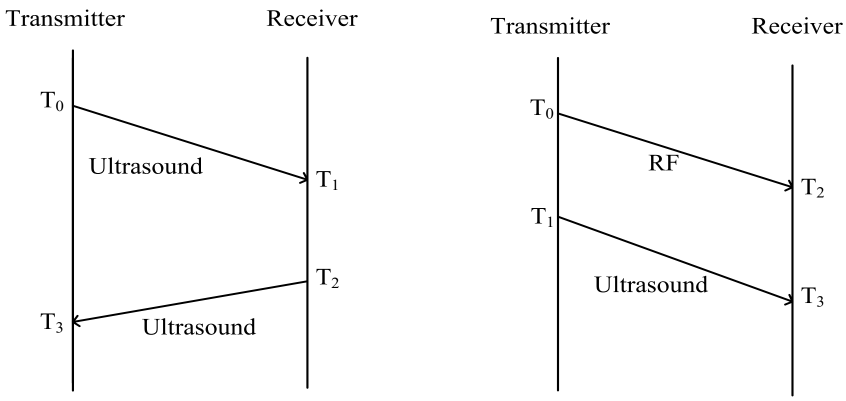

(a): ToA (b): TDoA

Figure 3.12: ToA and TDoA methods

Linear approach based on localization is also another methodology to locate the position of source node. Four other linear methodologies known as Weighted Linear Least Squares (WLLS), Subspace Approach (SA), Linear Least Squares (LLS), and two phase Weighted Linear Squares (WLS) are presented in [260].

- LLS technique uses the least square method for calculating the position of unknown node.
- Subspace approach uses the ToA statistics in form of matrix for calculating position of unknown node.
- Weighted linear least square uses the weighted symmetrical matrix for the calculation of position of unknown node.

LLS approach is represented as $r = f(x) + n$ mathematically. The distance between the kth sensor and source node denoted by d_k is a ToA form d is presented by :

$$d_k = \parallel \mathbf{X} - \mathbf{X}_k \parallel_2 = \sqrt{(x - x_k)^2 + (y - y_k)^2}, \quad k = 1, 2, ..., K \tag{3.59}$$

In [261], a semi-definite relaxation (SDR) method was approached based on ToA distance measurement. It resembles a hybrid approach that first use MLE with minimization of constrained weight (CWLS).

A critical analysis of the localization of multiple transmitting signals sensors that are using ToA based calculations in WSNs are discussed in [262]. Multiple source localization is quite complicated problem as compare to the single source localization, as anchor nodes are not aware of link between the source nodes and calculated signals. In this case it is not conducive to apply prevalent single source customization methodologies to solve the problems related to the multiple source localization. This complex problem of multiple source localization is addressed through optimization. ToA of the source j is measured by the i^{th} sensor is presented by:

$$t_{i,j} = \frac{1}{c} \parallel X_i - Y_j \parallel + \tau_j + \eta_{i,j}, \quad \forall \; i = 1, 2, ..., N, \;\; j = 1, 2, ..., M \tag{3.60}$$

where c is a speed of light, τ is a initial transmission time for j which is not known and $\eta_{i,j}$ is a ToA based noise measurement. Another work in [263] is based on quantum field theory (QFT) with single time observer. The only difference in this technique is the use of Newton-Wigner operator rather than CRLB. The accuracy was limited as the focus area was energy based system.

3.5.6 Time Difference of Arrival (TDoA)

TDoA is much similar to ToA in the sense that the receiver still requires the arrival time of signals, but in TDoA it can receive two signals with different frequencies as shown in Figure 3.12. Usually an acoustic and radio signal is used for TDoA method. Upon receiving a RF signal, the receiver time is started to measure the elapsed time until acoustic signal is received. Therefore, global time synchronization is not required among the sensor nodes. The distance d between a receiver and a transmitter can be calculated as:

$$d = ((t_3 - t_2) - (t_1 - t_0)) \cdot \left(\frac{v_{RF} \cdot v_{US}}{v_{RF} - v_{US}} \right) \tag{3.61}$$

where $t_0, t_1, t_2, t_3, v_{RF}$ and v_{US} are the transmission times of RF signal at transmitter, ultrasound transmitter time, RF receiving time, ultrasound signal receiving time, the speed of RF and ultrasound signals, respectively. In [264], the accuracy and correctness of $3D$ localization is critically analyzed for the indoor environment and hardware designed for this purpose. It is further demonstrated that accuracy is an essential characteristic of localization systems and it also influences the other components based on quality of service like latency and update rates. To minimize consumption of energy, network sensor node pairing methodology is implemented to gather the TDoA based estimations while ensuring the quality of node localization [265]. Proposed solution in [265] included finding a minimum size dominant set known as (MSDS) for a multi hop graph.

$$\hat{t}_{i,j} = d_{i,j}/v + e_{i,j} \;\; \text{where} \;\; d_{i.j} = \parallel \mathbf{X}_i - \theta \parallel \;\; \text{and} \;\; x_i = [X_i, Y_i]^T \tag{3.62}$$

where $e_{i.j}$ is a TDoA estimation. A novel technique based on the utilization of neural networks and TDoA technique for localization of source node was presented in [266]. Two neural network based models named as Radial Basis Function (RBF) and Back Propagation Network (BPN) model were simulated for the source localization. The root mean square of this system is calculated as follows:

$$rmse = \frac{\sqrt{(x_i - \hat{x}_i)(y_i - \hat{y}_i)}}{n} \tag{3.63}$$

where (x_i, y_i) are the original coordinates of the i^{th} data nodes and $(\hat{x}_i, \hat{y}_i)$ are the coordinates for the estimated position of i^{th} node. The work in [267] is an hybrid technique based on TDoA and RSSI with improved convergence accuracy and preciseness by adding RSSI measurements collaborative communications between sensor networks and Wi-Fi. Two estimation expansions based on the maximum likelihood (ML) and Taylor series (TS) were proposed to solve the non-linear TDoA and RSS based equations. Received signal power is calculated as follows:

$$P_i^r = K^i \cdot (P_i^t / d_i^a) \text{ where } i = 1, 2, ..., N \tag{3.64}$$

where K^i is a factor that affect signal power, P_i^r is a received signal power, while P_i^t is a transmission power and d_i^a is a distance of source from receiver.

Authors in [268] discussed the performance of TDoA based localization methodologies by considering the binary phase shift keying (BPSK) signals. The cross correlation among the temporary sensors is employed for the estimation of TDoA based localization. Major benefit of using generalized cross correlation (GCC) as compare to the cross correlation (CC) is that GCC gives considerable resistance against the interference of noise and capability of solving the multi path problems. By two-signal detection and sample counting methods, time synchronization necessity can be removed [269], while maximum resolution based on time can be accomplished. A mathematical model for expressing the TDoA between A and B is as follows.

$$T_{AB} = \frac{1}{v}(d_{AB} - d_{AA}) - (T_{B2S} - T_{A2S}) \tag{3.65}$$

where d_{AB} is a distance between speaker of $\acute{A}s$ and microphones of $\acute{B}$ whereas d_{AA} is used to denote the distance from $\acute{A}$s speaker to $\acute{A}$ microphone.

3.5.7 Triangulation

Triangulation is a process of computing the angle β information of an unknown node from two anchor nodes A_1 and A_2 as shown in Figure 3.13. The distance between anchor nodes is also known, then the localization is estimated through sine or cosine rules:

Sines Rule:

$$\frac{A}{\sin\alpha} = \frac{B}{\sin\beta} = \frac{C}{\sin\gamma} \tag{3.66}$$

Cosines Rule:

$$C^2 = A^2 + B^2 - 2AB\cos(\gamma) \tag{3.67}$$

$$B^2 = A^2 + C^2 - 2AC\cos(\beta) \tag{3.68}$$

$$A^2 = B^2 + C^2 - 2BC\cos(\alpha) \tag{3.69}$$

where α and γ are the known angles at anchor nodes.

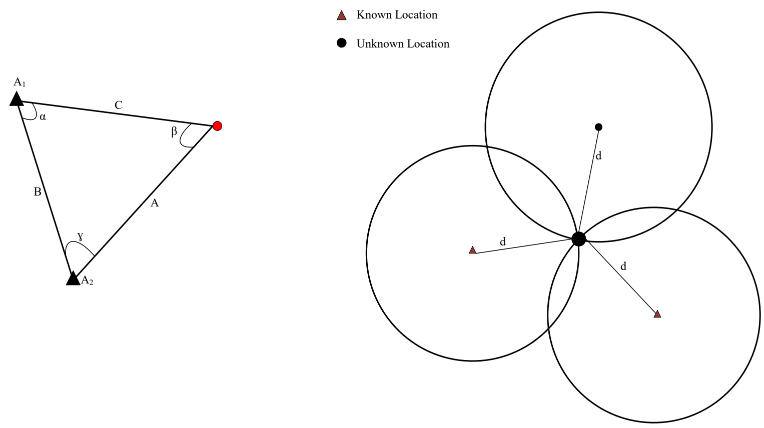

Figure 3.13: Triangulation method

Another localization technique with minimum number of anchor nodes was presented in [270]. However, it is expected that the detecting scope of every sensor can be broadened to ensure certain triangulation, thus just three anchor nodes are needed to localized nodes in $2D$ plane. Similarly, the author in [271] used triangulation scheme for mobile robot localization.

3.5.8 Trilateration

A most fundamental form of position estimation is trilateration. The location is computed through finding the intersection of three or more circles, where anchor nodes in the center and radius is used as a distance between sensors and anchor nodes. It is based on the fact that the sensor node should lie within the intersection of the three circles. This phenomenon is illustrated in Figure 3.14.

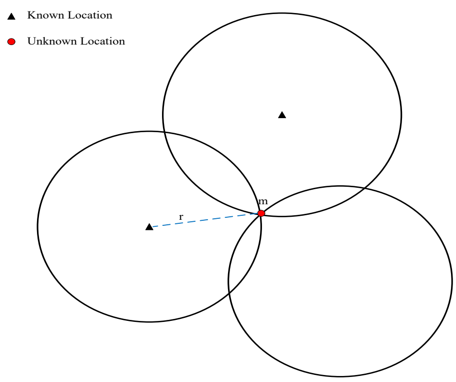

Figure 3.14: Trilateration method

Assume we have an accurate distance at three anchor nodes with a position $(x_i, y_i), i = 1, 2, 3$, the Euclidean distance between three anchors and unknown node is given by:

$$(x_i - x_{un})^2 + (y_i - y_{un})^2 = r_i^2 \tag{3.70}$$

where x_{un} and y_{un} are the coordinates of unknown nodes.

3.5.9 Multilateration

Multilateration is related to the standard developed by Secondary Surveillance Radar (SSR). The complete description of such standard is given in [272]. Initially these systems were designed for airport surveillance system, including for surface vehicle and air crafts. In this technique receiving stations are also deployed within the area of interest. Two types of transmission the Mode A/C and Mode S is used in multilateration. Then the received signal is transmit to the Central processing unit (CPU) where the target position is estimated. The standard version of multilateration is used by TDoA as shown in Figure 3.15.

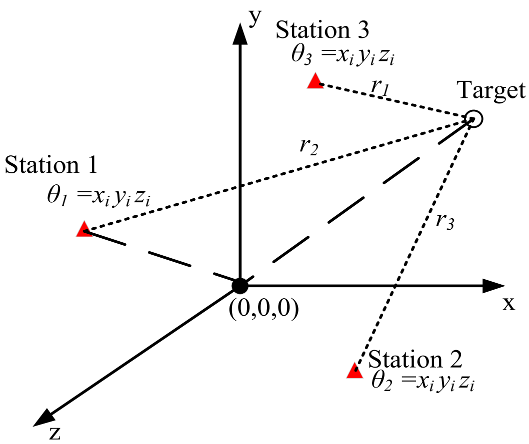

Figure 3.15: Multilateration System

3.6 Range-Free Localization Algorithms

In range free localization algorithms, there is no hypothesis about the availability of absolute distance between the nodes. Hence, the sensor node location can be estimated through the radio connectivity information of each sensor.

Range-free approaches simply used sensing features such as localization event detection, wireless connectivity and beacon proximity [197, 272], providing low cost techniques with reasonable accuracy. RSSI becomes unstable with the use of RF signals that are vulnerable to environmental effects [273]. As a well-known range-free localization technique, fingerprinting based localization will be accomplished in of offline and online phases. In first phase, RSSI is collected from each access point and stored in a database. In online phase the collected data set is used to determine the node position. Fingerprinting is grouped into several different methods such as the ray tracing model [274], support vector machine [275], data mining techniques [276], probabilistic methods [277] and some others based on kalman filtering [278]. In an indoor environment the idea of fingerprinting may have poor accuracy due to multipath fading. The RSS fluctuates in the presence of multipath fading. This may occur due to several factors, such as building structure and presence/ movement of people.

3.6.1 Centroid Algorithms

Range-free localization schemes such as centroid localization (CL) [197, 214] were proposed due to simplicity and robustness to changes in wireless propagation properties such. Anchor nodes are used to transmit known location periodically to all neighbours within a communication range. The node will be in the communication range of an anchor node if it receives enough messages. Consequently, the average of x and y coordinates of several anchor nodes is calculated from beacon to neighbours. This is known as centroid and is used as the estimated location for the node. The centroid based algorithms only relies on the connectivity information.

In the two-dimensional and linear CL, anchors with known positions A_j send their position coordinates A_{jx} and A_{jy} along with their *IDs* to nodes N_i, with coordinates N_{jx} and N_{jy}, in their neighbourhood. Nodes can now calculate their position based on the anchors around them according to the following formula:

$$\acute{N}_i = \frac{1}{N}\sum_{j=1}^{n} A_j \tag{3.71}$$

with the error:

$$E_i = \sqrt{(\acute{N}_{ix} - N_{ix})^2 + \acute{N}_{iy} - N_{iy})^2} \tag{3.72}$$

In [279, 280], author used CL for applications such as vehicle and luggage trolley tracking in airports. One drawback of CL method is that the random noise can be reduced but not fully eliminated in centroid based techniques. Another drawback with CL is that the nodes are expected to exchange many data packets for every positioning cycle. To improve the calculation in real implementations, weighted centroid localization [215] was proposed. In WCL, weightings are introduced to scale importance of anchor nodes in the neighbourhood depending on their distance to the node as shown in Figure 3.16. The expression (3.71) is expanded to include weight on the neighbour gateways described in (3.39). WCL algorithm has several disadvantages due to its time consuming and high maintenance cost issues.

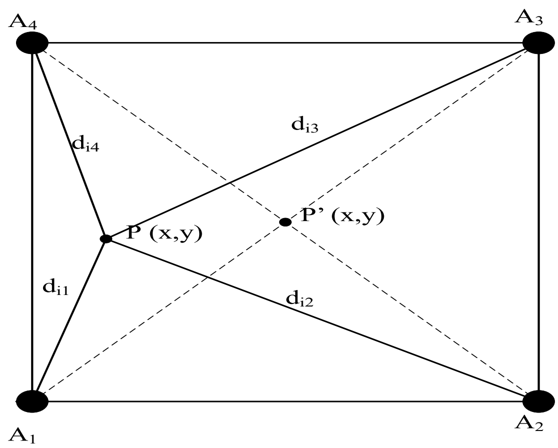

Figure 3.16: Weight calculation in WCL

1. In WCL beacons with known positions $A_j(x, y)$ send their *IDs* and positions to nodes $N_i(x, y)$ in their neighbourhood. However, this means that the nodes will have to spend significant amount of radio time in listening and receiving information from anchor nodes as the mobile anchor nodes move around the

area. They also have to compute their positions before sending those over to the gateways. This means devices operated on battery utilize much energy and may shut down early. This was already true with CL, but the situation even exacerbates for WCL since the nodes are now undertaking the additional burden of calculating the weights from LQI readings. Hence, a practical WCL system will not be energy effective and will suffer from high maintenance costs. Furthermore if weighted value is set to 1, the WCL algorithm fall into centroid algorithm that also effect on overall performance of the system as CL methods don't use LQI ranges being calculated at the start of the system.

2. Due to the large distance-dependent variations in the path loss exponent in (3.39), we do not have a consistent method for all distance measurements. A practical system cannot use different path loss exponents for short distances and for long distances, unless one modifies the path loss exponent dynamically as a function of distance.

3. The distance is also part of the equation to derive the weightings. A mechanism is required to calculate distance that is an extra burden to system. Thus we need an expression to derive the weighting directly from the LQI ranging.

4. If there is a change in environment, re-calibration of the weights is needed, resulting in delays in the system and put further load on the nodes.

. In [281, 282], authors proposed a trigonometric method that does not require any special hardware or time synchronization, known as Triangular Centroid Localization algorithm (TCL). Simulation shows that TCL improves the performance of CL by 54% and WCL by 64%. With LQI values, TCL get 38% improvement over CL and 64.98% over WCL.

3.6.2 DV-Hop Algorithms

DV-hop is a distributed localization technique based on distance vector routing and connectivity measurements. Although DV-Hop is more complex, but it provides more accurate estimation [247, 272] than CL. DV-hop algorithm localizes sensor nodes in two steps. In first step anchor nodes broadcast beacon messages throughout the network to exchange localization information and count the number of hop among them. After getting these information's, anchor node compute the physical distance for 1-hop as follows:

$$\hat{d}_{hop} = \frac{\sum_{i \neq j} dis(n_i, n_j)}{\sum_{i=j} hop(n_i, n_j)} \tag{3.73}$$

where $hop(n_i, n_j)$ and $d(n_i, n_j)$ are the minimum number of hops between n_i and n_j and physical distance, respectively. In the second phase, an arbitrary node v_i can compute its physical distance to anchor node as:

$$\hat{dis}(v_i, n_i) = \hat{d}_{hop}.hop(v_i, n_i) \tag{3.74}$$

A localization error of $0.2 \sim 0.45$R is reported in an isotropic network with 100 nodes and average node degree of 7.6 [247]. Therefore, in DV-hop system each node computes its position based on average hop length and shortest path to each anchor distance as shown in Figure 3.17.

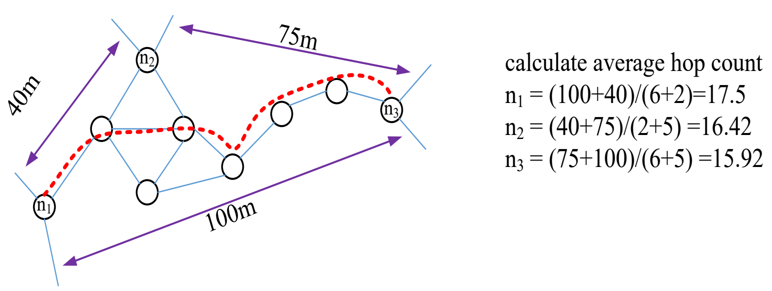

Figure 3.17: Hop count in DV-hop algorithm

In [283], authors used a similar method for hop-based distance measurements known as Hop-TERRAIN. An iterative refinement step was introduced for location adjustment based on radio range and local sensing results. At any iteration w, the position of arbitrary node v_i can be recomputed based on neighbour position obtained from iteration $w - 1$ as well as sensing results. The refinement step can enhance the localization accuracy and performance. Hop-TERRAIN summarizes three further guidelines: (1) a high connectivity, (2) reasonable anchor within a particular region, and (3) anchor nodes deployment on a right place, i.e., at the boundary of the network to solve coverage problem. Amorphous design is another technique can compute the hop-distance from sensor to remote anchor [284] known as Amorphous design. As compare to DV-hop, Amorphous can be computed by:

$$\hat{d}_{hop} = R.(1 + e^{-n_{local}} - \int_{-1}^{1} e^{-\frac{n_{local}}{\pi}(arccos(t) - t.\sqrt{1-t^2}} dt) \tag{3.75}$$

where R is a unit disk graph (UDG) radius and n_{local} is a neighbourhood size. According to the (3.75), each distance hop is dependent on n_{local} rather than total nodes in a network. Amorphous design also improves the hop-based distance computation described as follows:

$$s(v_i, n_i) = \frac{\sum_{v_j \in N(v_i)} hop(v_j, n_i) + hop(v_i, n_i)}{\mid N(v_i) \mid +1} \tag{3.76}$$

where n_i is a 1-hop neighbour, $s(v_i, n_i)$ is a distance between target and anchor node. The performance analysis of DV-hop [247], Hop-TERRAIN [283], and Amorphous design [284] is given in [126].

3.6.3 APIT Localization

In [218], authors proposed a localization technique that iteratively compute the position by testing the node location within the chosen triangle. Two criteria, including area and minimum angle, were used to select an optimal triangle. This procedure was repeated until the distance threshold was reached. This system is not good especially for outdoor environments. APIT test is basically a division of area into multiple triangles as shown in Figure 3.8. The anchor nodes are deployed on the edge of triangle that forms a vertices of the triangulation region. The test is also repeated for all sensors as well as anchor nodes. After that, the localization is measured using center of gravity (CoG) on overlapped triangles. APIT has the following steps:

1. Obtain the location of n anchor nodes.
2. For each unknown node, perform point of triangle (PIT) test.
3. If the node is inside, the triangle add it to *InsideSet*.
4. Break the test and gain RSS from anchor nodes.
5. Estimate the position as CoG, i.e., $CoG(\bigcap T_i \in InsideSet)$

If the node is not *InsideSet* move it to the inside triangle. In case of static network where node can not move, PIT is defined as

Definition 3. If no neighbour node is close to all three anchors. The node is assumed to be inside the triangle.

The two different proposition of PIT test is shown in Figure 3.18. If the node is close to point M and lies between the triangle of anchor nodes the node is *InsideSet*. To overcome the problem of *In-To-Out* and *Out-To-In* error, an improved version of APIT was presented in [285] shown in Figure 3.19. Large number of anchor nodes and overlapped triangles are the main drawbacks of APIT scheme.

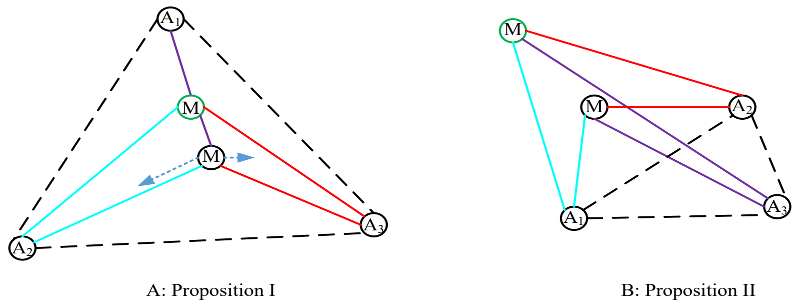

Figure 3.18: Point in triangulation test in two proposition

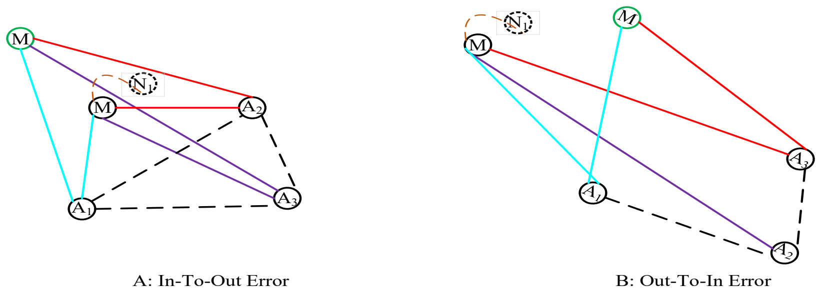

Figure 3.19: Error scenario of APIT test

Voronoi diagram based overlap region localization algorithms related to APIT algorithms were presented in [286].

3.6.4 Fingerprinting

Fingerprinting is another popular method in wireless localization. Refs [223, 224, 287] explained how to use RSSI as fingerprints. In general, fingerprinting consists of offline site survey and online location estimation. During offline phase, the central database is filled with the fingerprints of each location. During the online phase, a node sends queries to the database for its locations and the k nearest neighbour (kNN) is used to find out which fingerprints from the database respond to the received signal. This scheme measures the Euclidean distance in signal space between the received signal and record in the database. The location with the minimum distance is chosen as the estimated location of the localized node.

A system utilizes fingerprinting data to characterize a model that partners to the deliberate information of positions where they are made. To this end, a fingerprinting database containing RSSI measures for each reference node related to its position is built. The model then used RSS techniques and built a database table. These RSSI measurements are utilized with the characterized model to assess the information about nodes. The online and offline mode is shown in Figure 3.20 and Fig 3.21.

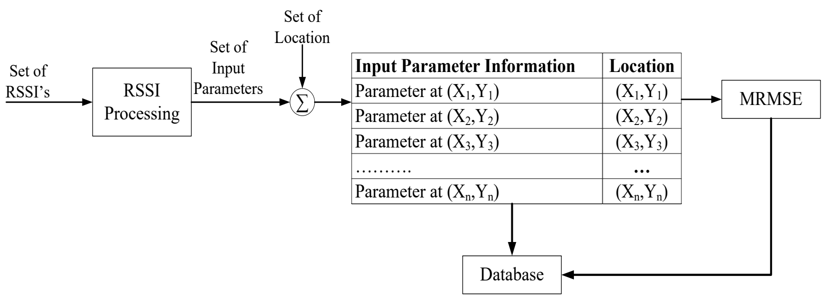

Figure 3.20: Fingerprinting in online mode

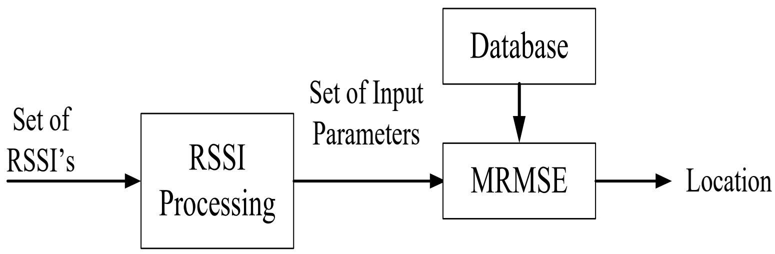

Figure 3.21: Fingerprinting in offline mode

3.6.5 MDS-MAP

Multidimensional scaling [169] was designed to use in mathematical psychology. This scheme have many variations according to the network structure, deployment and environmental factors. The most famous and well-known scheme is MDS-MAP [191], that is a simplest form of multidimensional scaling. The main idea is to arrange different object in a space with different dimensions and size that can be used to reproduce the dissimilarities in the object. In adaption to a localization algorithm, the objects are basically the nodes and dissimilarities are the distance estimates. By applying the linear algebra and law of cosines, the MDS reconstruct the relative estimation based on distance computation. At last, a relative map is transformed to an absolute MAP based on location information of anchor nodes. The following steps are taken in MDS-MAP scheme.

1. Estimate shortest path between all pairs of nodes. The values of shortest path is stored in matrix D.

2. MDS is applied to the distance matrix D to construct 2D and 3D relative map depending on the network structure.

3. Make sure the network have enough number of anchor nodes. Relative map is transformed to absolute MAP obtained is step 2.

Shortest path can be computed through Dijkstra's or Floyd's algorithm. The time complexity of shortest path computation is $O(n^3)$. According to [169], the accuracy and performance of MDS-MAP is highly dependent on the connectivity information between the nodes. A high density of node (a minimum of 12 nodes) is required to reduce the error. Another point to consider is that the high accuracy is achieved if range information is used, but not the connectivity information. MDS-MAP is first tested in 7×7 grid network as shown in Figure 3.22 taken from [288].

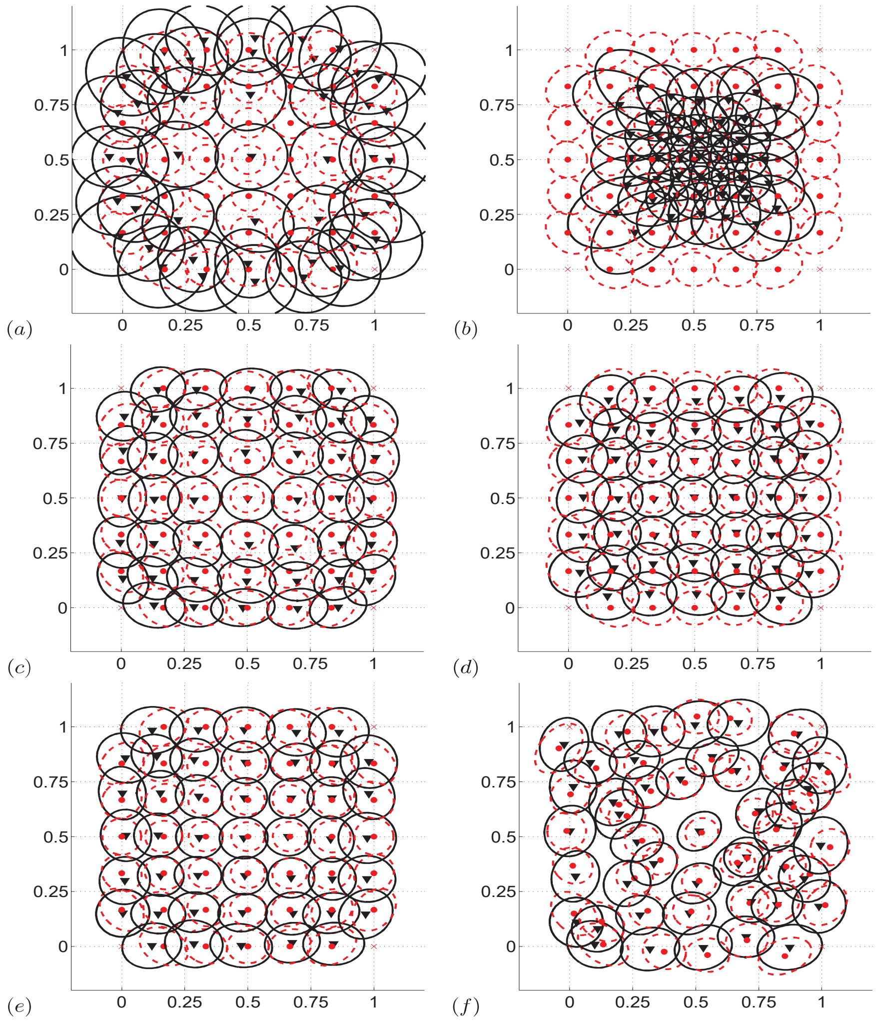

Figure 3.22: MDS-MAP testing with R=0.5

Progressive MDS known as hierarchical MDS or HMDS was proposed for 2D localization estimation having three stages named as cluster creation, localization based on the intra-cluster, and merger of coordinates that are obtained in the intra cluster localization step. The primary disadvantage of this algorithm is that if there are numerous disjoint clusters in the framework exists, then it will be difficult to perform mapping between local and global coordinates system. So the error rate is high in case of shortest distance calculation, which generates the high localization errors [289]. MDS and trilateration were used simultaneously in [290] to solve the energy problem in

WSNs. When all distance are acquired, further calculation for discovering positions does not require correspondence among nodes. MDS is certainly not only energy efficient but also promising for any improvement system. Benefits of employing trilateration after initial processing are that it estimates locations accurately and gives good initial localized points.

3.7 Mobile based Localization Algorithms

In this section, localization algorithms addressing mobility in WSNs are reviewed. For simplicity, we divide mobility based methods into three different parts: 1) algorithms with mobile anchor nodes for static target localization, 2) algorithms proposed for mobile sensor nodes by using static anchor, and 3) algorithms having mobile anchors to localize mobile sensor nodes.

The performance analysis of static anchor and static network localization algorithms is given in Table 3.7.

Table 3.7: Comparative study of static anchor and static nodes localization Algorithms.

localization Technique	Ref.	Accuracy	Energy	Anchor Density	Node Density
Connectivity based algorithms	[272]	Medium	High	Low	High
	[157]	Average	Average	Average	High
Centroid based algorithms	[121]	Medium	High	Low	Low
	[215]	Average	High	High	Low
	[230]	Medium	Average	Average	Low
Energy attenuation algorithms	[89]	Average	Average	Average	Average
	[181]	Medium	High	Average	Average
Region overlap algorithms	[290]	Average	Average	Average	Low
	[291]	Medium	Low	High	Low
verification based algorithms	[235]	Average	Average	High	Average
Anchor placement algorithms	[116]	Medium	Low	Low	Average
Anchor upgrade algorithms	[70]	Average	High	Low	Low

3.7.1 Mobile Anchors and Static Nodes

In WSNs, some techniques used mobile anchor nodes to compute the location of static nodes according to specified trajectories. For this purpose, localization requires two parts to accomplish. One part is to localize nodes using some geometric method [292, 293, 294, 295] and the other part is path planning [296, 297, 298]. The development of path planning is beyond the scope of this thesis. However, we review main trajectories for path planning to provide a way for mobile anchor-based localization. In mobile-assisted localization (MAL), distance is computed through a mobile node between different pair of nodes. In [296], authors follow a periodic trajectory and mobile anchors broadcast its location information to all static nodes. Then, the RSSI is used to calculate distance between static and mobile location assistance (LA) node. Further, for finding the node position. According to the simulation result with the error distance of 10% of the communication radius, the positioning accuracy is 11.2%. The requirement of LA equipment is a drawback of this technique. Another technique proposed in [293] is a sphere-based localization that change the whole scenarios into linear system to measure the coordinates of unknown nodes. The benefit of this scheme is that it does not require any LA device, so the nodes only localize themselves by interacting with mobile nodes as shown in Figure 3.23.

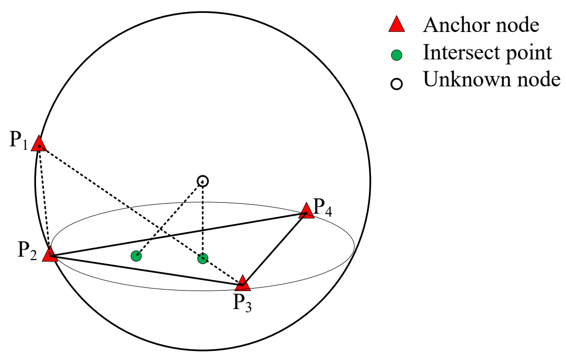

Figure 3.23: Sphere-based localization algorithm

According to the Figure 3.23, the mobile node broadcast its location information on different points P_1, P_2, P_3 and P_4, then a sensor node N estimate its distance coordinates based on these four beacons. Another flying anchor method was proposed where all anchors are equipped with GPS receiver [294]. Each unknown node calculates its location based on geometry principles after receiving packets from mobile anchor nodes. From intersected circle, there are two lines perpendicular to intersection circle. Thereafter, the intersection point is the estimated position of the node as shown in Figure 3.24. According to the simulation results, the error is $1.6m$ with a radius of $15m$. However, in case of centroid based methods, the error rises to $2.4m$.

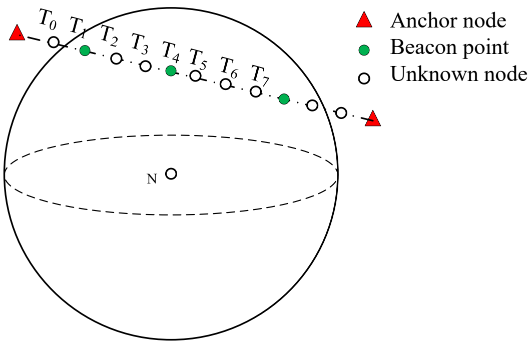

Figure 3.24: Mobile anchor localization with GPS receiver

A mobile anchor node can moves along a specific trajectory and send information beacon in path planning algorithms. A **S** shape trajectory was proposed in [299]. In a sensing region, the unknown node receives beacon periodically from mobile anchors to estimate its coordinates. A well known algorithm for 3D network with three different trajectories, namely SCAN, DOUBLE SCAN, and HILBERT was proposed in [300] as shown in Figure 3.25. The length of SCAN is shorter but many mobile anchors broadcast beacon same time when it moves to the straight line. DOUBLE SCAN increases the path on y-axis that solves the co-linear problem, but the positioning accuracy is average. Therefore, HILBERT increase the path turns to increase the localization accuracy. For initial simulation, an area of $420m \times 420m$ was taken that gives a an error distance of

$0.86m$ for SCAN with trajectory length of $3780m$. In DOUBLE SCAN, the counted error distance is $0.85m$ for $4080m$ of trajectory length, and for HILBERT, its has an error distance of $0.88m$ and a trajectory length of $3840m$. The comparison of mobile anchor and static node localization algorithms is given in Table 3.8.

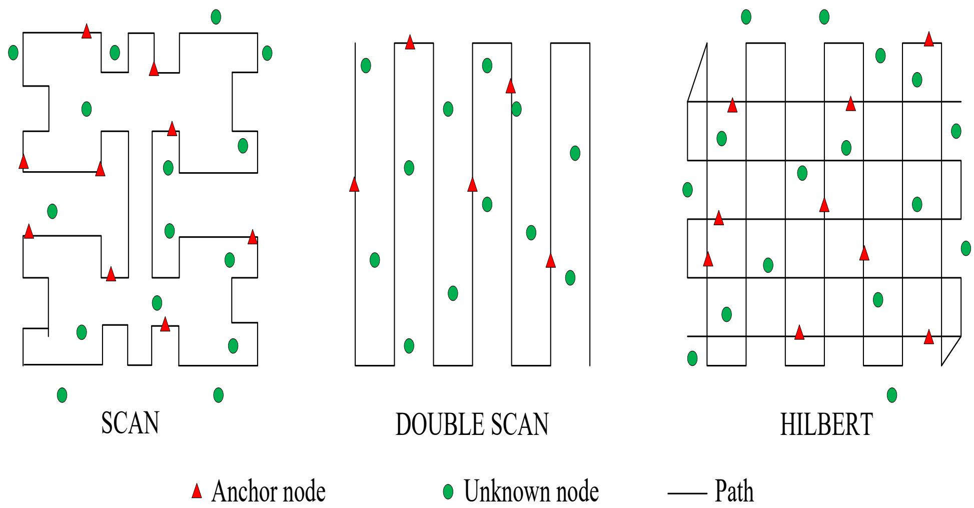

Figure 3.25: Three different trajectories for path planning

Table 3.8: Comparison of mobile anchor and static target localization algorithms.

Ref.	Accuracy	Node Density	Path length	Travelling speed	Energy
[293]	Good	Average	Average	Fast	Medium
[294]	Good	Medium	Average	Fast	Medium
[296]	Average	N/A	Short	Medium	Low
[297]	Good	Low	Average	Average	Average
[298]	Average	Low	Average	Medium	Low
[299]	Good	Low	Low	Fast	Medium

3.7.2 Mobile Anchors and Mobile target

In this kind of schemes both anchor and target nodes are mobile. The topic of mobile anchor and mobile target is not a major concern of this thesis, so we briefly explain the idea to complete our discussion. From the literature study, we have divided these algorithms in to two categories: probability distribution localization [121, 272] and time based localization algorithm [300, 301]. In probability based schemes, the unknown nodes can only predict their coordinates information using probability distribution function. The best example of this scheme is MCL [133, 192], in which node can detect neighbour position. The network coverage is the main issue for this kind of localization algorithms. Similarly, in time-based localization algorithms, the system only relies on continuous movement of mobile anchor to identify the mobile target. The idea to localize mobile target node is to find the coordinate information in a very short interval of time [300]. The comparison of this kind of algorithms is given in Table 3.9.

Table 3.9: Comparison of mobile anchor and Mobile target localization algorithms.

Ref.	Accuracy	Node Density	Path length	Travelling speed	Energy
[133]	Good	Low	Low	Average	High
[192]	Good	Low	Low	Low	High
[300]	Average	High	High	High	High

3.8 Summary

Generally speaking, range-based and range-free are two groups of localization in WSNs. Time synchronization at both sending and receiving devices is a strict requirement in range-based algorithms. However, the algorithms presented in range-free group are much easier to implement. The fundamental localization techniques are triangulation, trilateration, MLE, and multilateration.

Different criteria were taken in classifying the localization algorithms, such as single-hop versus multi-hop, centroid versus distributed, anchor versus non anchor and GPS based etc. The high computation power is needed for centralized algorithms but can execute complex mathematical operations. This helps sensors to send data to a central server for further operation. APIT, DV-Hop and MDS are range-free algorithms that provides higher accuracy as compared to range-based systems.

Mobile based algorithms are also classified based on the network infrastructure. Based on the comparative study, mobile based systems are classified into static nodes and mobile anchor, mobile anchor and mobile target and static anchor and mobile target. Mobile anchor-based algorithms requires trajectories to operate. However, network coverage and power consumption are main issues with this kind of algorithms. Techniques like fuzzy logic and kalman filtering can be used to refine the coordinates of the nodes and provide high accuracy even in presence of noise.

In this Chapter, we started with the description of localization problem statement and describe the localization in WSN in a bit detail. The localization estimators including statistical and geometric estimators are explained in detail, along with their types, algorithm and implementation in different scenarios is also being discussed. The main focus of this Chapter is the classification of localization algorithms that is classified and explained including, centralized versus distributed, range-based versus range-free, anchor-based versus anchor-free, GPS versus non-GPS and fine-grained and coarse-grained. A detail study of range-free and range-based algorithms along with their localization measurements and models is also a part of this chapter. In a range-free algorithms the well-known localization schemes including APIT, MDS-MAP and DV-hop is discussed in detail. Finally, we also presents a taxonomy and survey of mobile based localization algorithms, which classify in to mobile anchor and static nodes, static anchors and mobile nodes and mobile nodes and mobile sensors. The comparison analysis of all the proposals are also presented and being compared in the form of tables.

Chapter 4

Localization using Parametric Loop Division Method

This chapter mainly focuses on the sensor localization using parametric loop division (PLD) and subdivision surface methods. Subdivision surfaces becomes popular in many areas, such as geometric modelling, games and mostly in pattern recognition and image processing due to their capabilities of transforming any shape to one spline surface. The generation of subdivision surface is through refining and transferring control to next level and by reducing the surface area. Therefore, subdivision surface are computed by refining the points known as parametric points in iterative form. Interpolation of surfaces is also possible if the refine coordinates compute mesh parametric points known as interpolating schemes.

The most famous subdivision schemes are presented in literature such as Doo-Sabin scheme [302], Catmull-Clark scheme [303], and Loop division scheme [304]. Whereas, Butterfly scheme [305], and Kobbelt scheme [306] are the interpolating schemes. The main difference between Loop division methods and interpolating subdivision schemes is the generation of next parametric points in Loop subdivision while the computation of new vertex is in the interpolating methods. Interpolating is easy and simple to implement because of its capability of handling mesh vertices in a large networks. However, it is not possible to move vertex after its initial computation so it is not suitable for mobility networks.

On the other hand, Loop subdivision does not interpolate their points in a control mesh. Therefore, it is possible to use these kinds of schemes in mobile networks. One way is to compute global optimization by creating a global linear system having fair constraints to eliminate biased values [307, 308]. In a large scale networks the computation cost is the main factor that degrades the quality of the network. To avoid such cost, methods like two-phase subdivision were proposed [309]. A method proposed in [310] used Catmull-Clark subdivision, which avoids to solve a system of linear equation by using similarity concept in points construction phase.

All the subdivision methods only interpolate approximate points to compute linear surfaces. None of the methods is available to measure the parametric points and reduce the surface size at the same time. That is why a 3D localization scheme based on parametric points and subdivision surface is proposed in this thesis. Our main focus is to improve localization accuracy by minimizing the computation cost and mitigating the deployment of anchor node dependencies. Loop division approaches were never used for WSN localization and it is a first time to be used for localization purposes due to its simple rules, triangular controllable meshes, and excellent continuity [311]. This is basically a 3-order B-spline and surface split approach, in which parametric points are computed with the help of control vertices within the 3D earth space and step size.

Definition 4. Triangulation mesh is used for pre-localized nodes. This is different from APIT, which gets localization information from overlapped triangles.

4.1 Theory of B-splines and Subdivision

In numerical analysis, B-spline also known as basis spline, which is a function of spline with minimal support with respect to given smoothness, degree, and domain partition. The degree of spline function is a major factor that can be defined as a linear combination of B-splines. These B-splines are used for numerical differentiation and curve fitting of experimental data. These knots or curve fitting points are known as central points in computer graphics and computer-aided design. In a spline function, a degree d spline curve f can be obtained through n control points $(c_i)_{i=1}^{n}$ and $n + d + 1$ knots $(t_i)_{i=1}^{n+d+1}$ and it can be written by

$$f = \sum_{i=1}^{n} c_i B_i, d \tag{4.1}$$

where $\{B_i, d\}$ are B-splines.

Definition 5. Let $t = (t_j)$ be a vector sequence and d be a non-negative integer, then t is the non-decreasing sequence up to $d + 2$. Then, the B-spline is defined as

$$B_{j,d,t}(x) = \left(\frac{x - t_j}{t_{j+d} - t_j}\right) B_{j,d-1,t}(x) + \left(\frac{t_{j+1+d} - x}{t_{j+1+d} - t_{j+1}}\right) B_{j+1,d-1,t}(x) \tag{4.2}$$

The value of $B_{j,0,t}(x)$ is 1 if $t_j \leq x < t_{j+1}$ and 0 otherwise. Let us assume if B-spline degree is 1, then we have:

$$B_{j,1}(x) = \left(\frac{x - t_j}{t_{j+1} - t_j}\right) B_j(x) = \begin{cases} (x - t_j)/(t_{j+1} - t_j) \\ (t_{j+2} - x)/(t_{j+2} - t_{j+1} \\ 0 \end{cases} \tag{4.3}$$

Figure 4.1 shows that B-spline contains polynomial pieces with different breaks (step size) in a knots (vertex). In Fig 4.1(b) the knots are identical and $B_{j,0} = 0$. The subdivision rules of B-spline curve in case of uniform spline are related to binomial coefficient. How local averages are subdivided in to different surfaces are presented in [312].

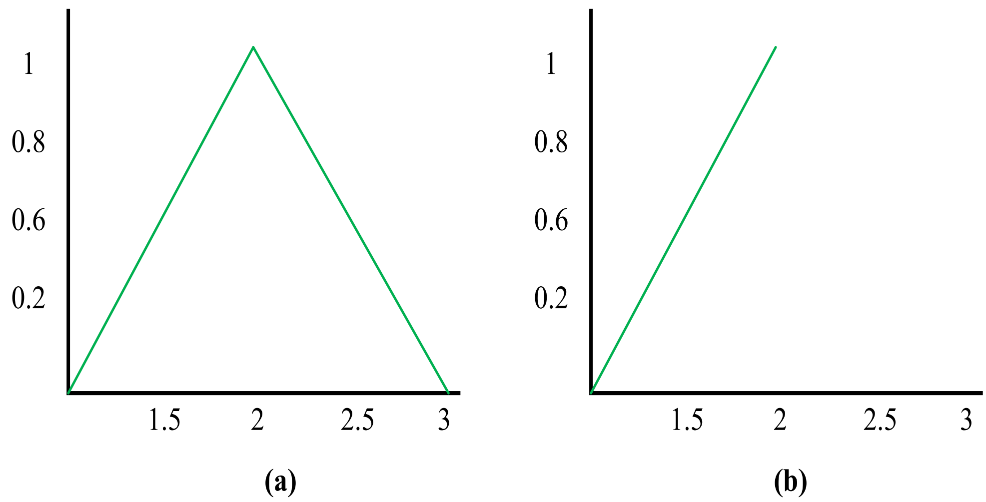

Figure 4.1: A linear B-spline with (a) simple knots (b) double knots.

According to the algorithm presented in [312] control vertices are subdivided as follows

$$......, P^{\circ}_{-2}, P^{\circ}_{-1}, P^{\circ}_{0}, P^{\circ}_{1}, P^{\circ}_{2}, ... \tag{4.4}$$

in Δ step size linear subdivision is expressed as

$$P^1_n = \begin{cases} P^{\circ}_{n/2} \\ (P^{\circ}_{(n-1)/2} + P^{\circ}_{(n+2)/2} \end{cases} \tag{4.5}$$

The new control vertices are generated using $d-1$ average step sizes.

$$P^k_n = \frac{1}{2}(P^{k-1}_n + P^{k-1}_{n+1}), \quad k = 2, ..., d \tag{4.6}$$

we proposed a more desirable approach to calculate parametric points even for a circular network or any form of network as explained in section 4.4.2. We observed that degree of nodes, deployment, step size and control vertex are the main elements to subdivide the surface for computation of node localization. For the localization and triangulation, we need to take the average of three nodes to compute control vertex and to form a convex combination of these nodes.

Definition 6. Let us consider n points, the convex combination $(c_i)_{i=1}^{n}$ is expressed as $(\lambda_1 c_1 + \lambda_2 c_2 + ... + \lambda_n c_n)$, where λ denotes the average of control vertices, mid point and degree of nodes.

The convex of two points is denoted by a straight line, whereas a triangle is used to express the three convex points. In general, the convex hull of different points are shown in Figure 4.2.

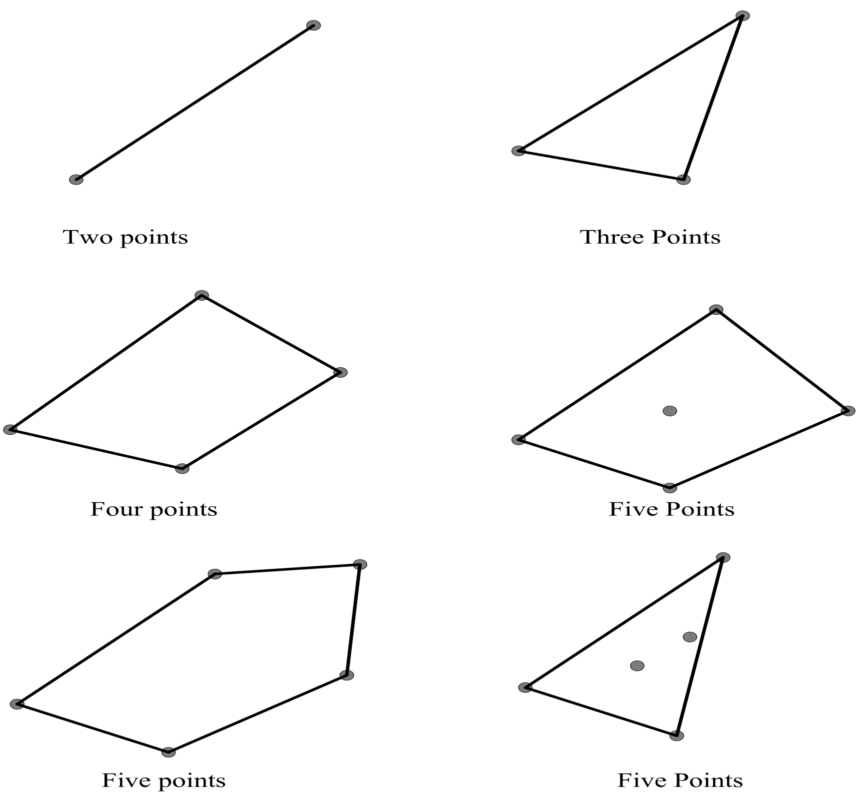

Figure 4.2: Initial formation of different convex hull (parametric) points.

4.2 Related work

Development of an indoor positioning system (IPS) requires a detailed analysis of deployment area, user requirement and application description to prove the research and development in the field. Generally, a localization algorithm should be robust, accurate, and efficient in terms of communication cost, energy, and computation cost. A localization technique should also be reliable and tolerant to the node failure.

A very well-known technique based on approximate point in triangulation test (APIT) was proposed in [218]. The idea is based on overlapped triangles and interpolation of nodes. The concept of the APIT is seems as subdivision surfaces but it is based on geometric estimators. A target node in APIT is chosen and select three beacon nodes to test whether it is in the triangle or not. The test is performed in different steps, in which a node can exchange reference points and perform PIT test. After that, these points are aggregated to compute approximation. Then, the center of gravity (CoG) is used to calculate node position through centroid localization. Simulation shows that APIT provides better results as compared to other range techniques with lower communication overhead and random node deployment.

APS [247] and MDS-MAP [169] are also famous range-free localization schemes. Initially, Multilateration was not possible under APS because none of the sensor node received enough beacons from at least three anchor nodes. A combination of technique like distance vector and GPS triangulation was used to perform localization. For distance computation, immediate neighbour were used to estimate distance between anchor and neighbour nodes. This scheme is based on distributed network that does not rely on any special infrastructure.

MDS-MAP [169] is based on pure mathematics psychology, which shows a structure of nodes as a geometrical picture. MDS-MAP require different steps such as estimation of distance between the possible pair of nodes, determination of node localization and normalization of coordinates using anchor node information.

4.3 Proposed PLD Algorithm

4.3.1 Basic idea of PLD algorithm

The objective of PLD scheme is to estimate the actual localization volume and find the node position in 3D space. A brief example of subdivision was explained in [311] where 3D images are generated using triangulation subdivision approach. In each step triangles are subdivided into pairs with the addition of extraordinary nodes in its control ring matrix. For the triangulation purpose, three nodes are elected at every initial step. A node starting the operation of PLD is known as reference anchor, which further helps to produce parametric points. The work involves the development of novel solution which utilizes the anchor node position information to calibrate nodes with unknown target. This allows localization scheme to function even in a changing environment that increased reliability and accuracy of the proposed scheme.

In a proposed technique, reference points can helps to produce new parametric points by calculating the mid-points and by taking step size that falls within the network boundary. The distribution of parametric points, which divide the complete region using Loop division are shown in Figure 4.3.

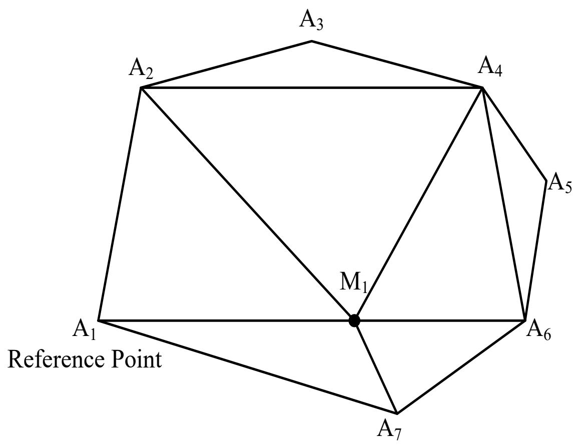

Figure 4.3: Nodes distribution in PLD and mid-point calculation.

The deployment of the anchor nodes on the boundary of the network helps our solution to solve the problem of network coverage. That is why PLD scheme helps to localize sensor nodes in random and uniform distribution of anchor nodes. Within the PLD, network region can localized a number of sensor nodes distributed in 3D space after each iteration. It is also possible that there is no node within a region due to not having enough node or node failure. In this case, a control is transferred to next iterative mode. That is the beauty of the parametric points, provides continuity in the operation. Moreover, the total number of nodes in each PLD network is determined and estimate localization. By this parametrization process, each node in a network have information about sum of received power from all the anchor node. The combination of mid-point and parametric node position with adjustable step size can helps to form triangles within the region.

As stated earlier, the sum of RSS recorded at each parametric point is being compared against a pre-defined threshold. If the sum of the RSS is smaller than the threshold value, the RSS value of corresponding parametric point is recorded in the storage matrix. Otherwise, the point will be discarded. The loop will be terminated when all pre-localized nodes are found against each anchor node and mid-point is shifted up and down through the value of step size Δ. The localization volume is estimated from storage matrix after recording the step size upward or downward. The position of each unknown node is also computed through centroid based formula and localization error is calculated.

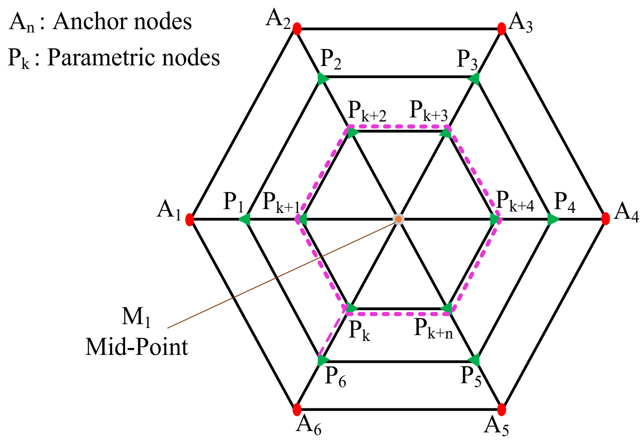

Figure 4.4: Generation of parametric points in Loop division.

Let us consider the network shown in Figure 4.4, assuming that triangle $\triangle M_1A_1A_2$ is the selected region for repeating the above mentioned process. After completing the first iteration with the base function, a similar region of triangle $\triangle M_1P_1P_2$ is produced with parametric points. This process generates similar triangulation structure in continuous paramterization of Loop. The control will be transferred from one to another triangle with the help of base function parameter, that shrinks the volume of the region. Midpoint is also recalculated with parametric points. For a fair system, $A + 1$ anchor nodes are deployed followed by A^{th} anchor nodes in each network. The key notations used in a PLD scheme are summarized in Table 4.1.

Table 4.1: List of key notations used in PLD.

Notation	Explanation
M_i	Mid-point at each PLD network.
A_i	i^{th} anchor nodes.
P_i	i^{th} parametric points produced after each iteration.

Continued on next page

v_i	volume of i^{th} parametric looped network.
k_i	Non-overlapped PLD networks.
$D_{N\to N}$	Distance from a sensor node to all other sensor nodes.
$D_{A\to N}$	Distance from an anchor node to all other sensor nodes.
Δ	Step size in PLD network.
α	Parametric function of PLD network.
γ	Representation of change in center point.
$\bigotimes$	Working boundary.
φ	Target nodes in each k_i network.
$\hat{x}, \hat{y}, \hat{z}$	Cartesian coordinates of estimated node position.
η	Anchor nodes in each k_i network.

4.3.2 Problem Formulation and Assumptions

The idea of PLD localization scheme is different from APIT [218]. In APIT, the triangles were overlapped that increased the communication as well as computation cost for localization. Therefore, in the proposed PLD scheme, we maintain a system of non-overlapped triangles. Let us assume a non-overlapped network $K = k_1, k_2, ..., k_n$ with a network volume of $V = v_1, v_2, ..., v_n$. Assuming that A anchor nodes and N sensor nodes are randomly deployed in a interested region. Every sensor node preserves a set of parameters as:

$$\mathbf{N} = \{N_i(x_i, y_i, z_i), A_i(x_i, y_i, z_i), D_{N\to N}, D_{N\to A}\},\ i = 1, 2, 3, ..., n \tag{4.7}$$

where x_i, y_i, z_i are the i^{th} node coordinates. Correspondingly, each anchor node preserves a set of parameters as:

$$\mathbf{A} = \{N_i(x_i, y_i, z_i), A_i(x_i, y_i, z_i), D_{A\to N}, D_{A\to A}\},\ i = 1, 2, 3, ..., n \tag{4.8}$$

Two kinds of nodes are involved in a system, anchor and sensor nodes. Anchor nodes have known position information. The A anchor nodes and N sensor nodes can compute the position in a 3D space denoted by:

$$\mathbf{n_i} = (x_i, y_i, z_i)^T \text{for } i = 1, 2, ...N + A \tag{4.9}$$

Furthermore, assuming that each PLD network has φ target nodes in each network ring such that $\varphi \subseteq N$. Similarly, there might have η anchor nodes in each network such that $\eta \subseteq A$. So the possible number of anchor and sensor nodes are computed by $k \times \varphi$ and $k \times \eta$, respectively. Generally, the value of η is chosen fixed, i.e., $\eta \geq 4$ for proper triangulation and parametric loop formation. The physical distance between two sensor nodes is computed by Euclidean distance formula i.e. $\mathbf{d_{ij}} = \sqrt{(\mathbf{n_i} - \mathbf{n_j})^2}$. The proximity information among sensor nodes is $P_{ij} \in \beta_k = \{1, 2, ..., \varphi + \eta\}$. Anchor nodes $\mathbf{n}_\eta$ and physical distance d_{ij} also have a respective proximity. The proximation information helps to compute localization of target node $\mathbf{n}_\varphi$ in each iteration and $\varphi \in \{\eta + 1, \eta + 2, ..., \eta + \varphi\}$. Let us consider that each PLD network chooses a constant number of anchor nodes defining the subset of network with no repetition of anchor node position. The number of PLD network is computed by

$$\left(\frac{N}{K}\right) \leq N_k \leq N \tag{4.10}$$

where N_k denotes each PLD network. The following terms are defined to help readers to understand the PLD algorithm.

Definition 7. Reference node: A node who initiate, the process of localization in a PLD scheme is known as reference node. In PLD, this should be a anchor node.

Definition 8. Ring Control Matrix: Anchor node position vector forms the boundary of a network.

Definition 9. Step Size: Distance between the network boundaries, which is at each iterative step.

Definition 10. Working Boundary: Th difference between maximum and minimum of anchor/ parametric coordinate values in a PLD network.

4.3.3 Algorithm Design

The PLD algorithm is accomplished in the following steps.

4.3.3.1 Network size, mid-point and parametric points

Assuming a set of anchor nodes with positioning vector (x_i, y_i, z_i) be
$A = \{A_1, A_2, ..., A_m\}$, where $m \geq 4$. A reference anchor can select two other nodes in a network to form a triangle. The network size must be greater than 3 for proper execution of PLD algorithm. To compute a parametric node position, the measurement of a mid-point is the first step in the proposed scheme. From Figure 4.4, let $\vec{A}_1$ be selected as a reference anchor node, and the total distance is between the k^{th} selected node is computed by (4.11). Here, the reference points are denoted in the form of a vector because during the first iteration all anchor nodes formed the working boundary.

$$\mid \vec{D}_{1k} \mid = \sum_{k=2}^{m} \mid \vec{D}_{Ak} \mid \tag{4.11}$$

The operation of computing mid-point in our scheme is slightly different than the one presented in projection point calculation [311]. From reference node to other anchor in a network a distance is computed as shown in Figure 4.5 using Euclidean distance formula $A_1 \rightarrow A_2 = \sqrt{(A_{2x} - A_{1x})^2 + (A_{2y} - A_{1y})^2 + (A_{2z} - A_{1z})^2}$. We noticed that the distance between A_1 and A_3 is very high. So the mid point is computed by $M_1 = \frac{1}{2}(A_1 + A_3)$.

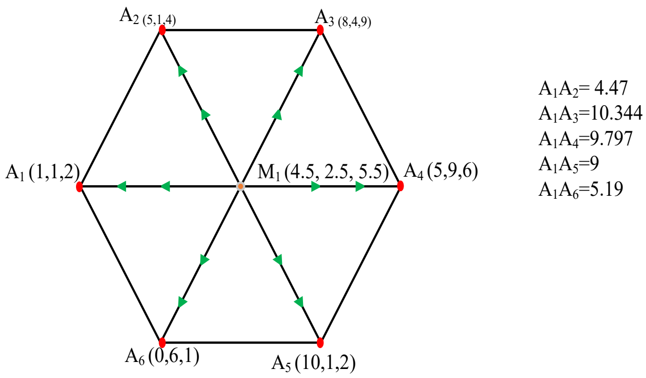

Figure 4.5: Mid-point calculation in PLD algorithm.

The next step is to measure the parametric points, to transfer the control to next level as shown in Fig 4.6. Anchor nodes act as a control vertex during the first iteration. The parametric point is computed by the following formula.

$$\vec{P}_{ik} = \frac{3}{8}(\vec{M}_1 + \vec{A}_k) + \frac{1}{8}(\vec{A}_{k-1} + \vec{A}_{k+1}) \tag{4.12}$$

Practically, after getting the mid-point value, the first parametric point is generated by $P_1 = \frac{3}{8}(M + A_1) + \frac{1}{8}(A_2 + A_6)$. Similarly, all other parametric points are generated in a similar way.

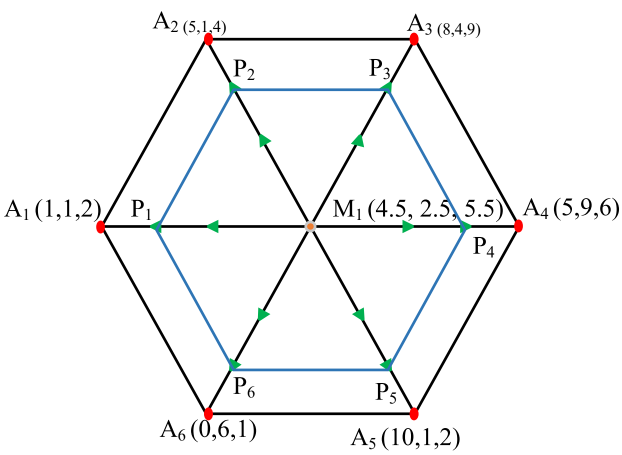

Figure 4.6: Explanation of parametric point calculation.

4.3.3.2 Selection of pre-localized nodes, step size and storage matrix

Subsequently, the RSSI from each parametric point is measured at corresponding anchor node. The RSSI is calculated by the following relationship.

$$RSSI = P_T - P_L + F_D \tag{4.13}$$

where P_T, P_L and F_D are the transmission power from an anchor node, path loss model and fading, respectively. The upward and downward increment on the mid-point is adjusted by addition and subtraction of step size over a working boundary. After summing up the RSSI, if its smaller than threshold the node is selected as a pre-localized node, stored into storage matrix and the iteration stops at this point. Spherical distance is calculated using the PLD coordinates C_k:

$$\mathbf{C}_k = \begin{bmatrix} x_{1,k} & y_{1,k} & z_{1,k} \\ x_{2,k} & y_{2,k} & z_{2,k} \\ \vdots & \vdots & \vdots \\ x_{i,k} & y_{i,k} & z_{i,k} \end{bmatrix} \tag{4.14}$$

4.3.4 Estimation of node position

The storage matrix contains the values of each coordinates along with its maximum and minimum values. This will help to measure the localization volume of the network. The product of difference between the maximum and minimum values on each axis determines the network volume, which is computed by

$$V = (x_{\max} - x_{\min})\,(y_{\max} - y_{\min})\,(z_{\max} - z_{\min}) \tag{4.15}$$

The number of localization points are measured by taking the fraction of volume of pre-localized nodes boundary and unitary volume. The node boundary is calculated in

Cartesian coordinate form which makes it possible to compute in 2D paradigm. This basically makes computation more simple and robust.

$$V_u = \frac{V}{N} \tag{4.16}$$

where V_u represents the unit volume. The volume of pre-localized node boundary is stored in a matrix. These values are used for centroid based methods which gives the nodes estimated position.

$$(\hat{x}, \hat{y}, \hat{z})_{l_i} = \prod [V_u, \mathbf{C}_k(a_j)] + (x, y, z)_{min} \tag{4.17}$$

where l_i denotes the pre-localized node. The proposed PLD algorithm is summarized in Algorithm 1.

Algorithm 1 Description of PLD Algorithm

take a network size φ
for $i = 1 : K$ **do**
    calculate mid point of the k^{th} network.
    take step size Δ
    divide the minimum axis difference into equal φ parts
    for $i = 1 : K$ **do**
        for $i_{differ} = 1 : min_{axis}$ **do**
            for $icase = 1 : min_{axis}/\varphi$ **do**
                if $i_{differ} \geq min_{axis}/2$ **then**
                    accept positive step size
                    $minpoint = midpoint + \Delta$
                    calculate the pre-localized points using Algorithm 2
                else
                    accept negative step size
                    $midpoint = midpoint$ returning to old midpoint
                    $minpoint = midpoint - \Delta$
                    calculate the pre-localized points using Algorithm 2
                end if
            end for
        end for
    end for
    find out each axis maximum and minimum points from the storage matrix
    calculate the volume of localization
    calculate the φ with the help of unit sensing volume.
    divide the storage pre-localized points to η
    for $i_{loc} = 1 : \eta$ **do**
        find a minimum and maximum coordinates from cluster of pre-localized points
        calculate difference between minimum and maximum points
        calculate the sensor position by adding difference and minimum co-ordinate of cluster
    end for

After getting the storage matrix values from Algorithm 1, we need to compute the pre-localized nodes and their estimated position by using Algorithm 2.

Algorithm 2 Calculation of pre-localized nodes

for $i = 1 : \eta + 1$ **do**

    for $j = 1 : \eta$ **do**

        calculate parametric points

        calculate distance between parametric points and each anchor nodes

        calculate the sum of RSS from each anchor nodes

        if $sum(RSS) \leq RSS(threshold)$ **then**

            take a first parametric point corresponding to each anchor nodes

            break

        else

            nodes with least sum of RSSI considered as pre-localized. Stored them in a matrix

        end if

    end for

end for

After that, localization error is computed by 3D based centroid formula. From the algorithm structure, we noticed that PLD used non-overlapped triangulation meshes for estimation of parametric points. Therefore, it is different from the APIT scheme where location information is obtained from overlapped triangles. The proposed system has several advantages as compared to other range-free schemes.

APIT adopts rectangle-like C-shaped topology. So, if the communication radius increases the performance of the system degrades. Furthermore, the network coverage of APIT does not reached 100%. In PLD, settlement of step size helps the proposed solution to work within a working boundary that solves the problem of network coverage. Moreover, the use of mesh triangle can reduce the communication as well as computation cost. The node distribution in PLD is also free from angle, connectivity, and other information that were pre-requisite is for many of the localization scheme.

Despite of the above mentioned advantages, the accuracy of PLD scheme is dependent on the number of deployed anchor nodes. In addition, if the deployment is not homogeneous, some nodes maybe far from the mid point. As a result, anchor node estimated far from step size. The standard deviation will increase in this case as the data points are spreads out over a region of interest..

4.4 Analysis and Discussion

In this section, we presents the detailed analysis of PLD algorithm with different sets of anchor deployment and mathematical modelling.

4.4.1 Calculation of Initial mid-point and working boundary

Let us consider a set of anchor nodes $\mathbf{A} = \{\vec{A}_1, \vec{A}_2, \vec{A}_3, ..., \vec{A}_m\}$ in a PLD network with reference anchor node $\vec{A}_i$. The distance between reference anchor node $\vec{A}_i$ to all other anchor nodes$\vec{A}_j$ is given by Euclidean distance formula and stored in a matrix form we have:

$$\mid D_{ij} \mid= \sqrt{(X_i - X_j)^2 + (Y_i - Y_j)^2 + (Z_i - Z_j)^2} \tag{4.18}$$

Reference anchor node in a network is selected using two criteria. One is done before deployment and the other is through proximity information. For the sake of simplicity, we use proximation information in selection of reference anchor node. The main idea for proximity information is to localize a node with high accuracy through using any addition hardware. The reference anchor $\vec{A}_i$ for initial mid-point calculation is determined by the fact that reference must have a higher distance to any of the node from a set of other anchor nodes $\vec{A}_i$ in a network.

$$\vec{A}_k = \underset{\vec{A}_j \in \mathbf{A}}{\arg\max} |D_{ij}| \tag{4.19}$$

After selecting the reference node, the distance from reference to all other anchors is calculated. For initial calculation, anchors on the boundary of the network are considered. After having all these distance, we select two anchors, one is reference anchor and the other that gives longer distance from reference node. These two are selected to estimate mid-point for the first PLD network.

$$M_1 = \frac{1}{2}(A_i + A_k) \tag{4.20}$$

The mid-point will deviate if the anchor deployment is random as compared to fixed deployment.

Lemma 4.1. If the deployment of anchor node is in regular distribution, the initial mid-point becomes the centroid of PLD network.

By deploying anchor nodes in a regular distribution mode, PLD results in regular shapes in a 3D space. The regular shape 3D object has diagonal of equal length, where an intersection of all diagonals lies in the same place known as centroid points or center of mass point. The working boundary is calculated by:

$$\xi = \mid f_{max}(x_k, y_k, z_k) - f_{min}(x_k, y_k, z_k) \mid \tag{4.21}$$

4.4.2 Center Points and Parametric Points Calculation

In this stage, we need to store all points in a storage matrix. Assuming that M_i is a mid-point in a working boundary. As the triangulation requires at least three anchor node, for the K^{th} anchor node, the $k \times 3$ vertices are stored in a matrix. The new parametric points generation is based on sub-division method [311] that provides an advantage of picking the close location as extraordinary node. The extraordinary nodes matrix has a dimension of $(K + 1) \times 3$ in a PLD network.

$$\mathbf{B} = \begin{bmatrix} x_{M_i} & x_{A_1} & x_{A_2} & \cdots & x_{A_k} \\ y_{M_i} & y_{A_1} & y_{A_2} & \cdots & y_{A_k} \\ z_{M_i} & z_{A_1} & z_{A_2} & \cdots & z_{A_k} \end{bmatrix} \tag{4.22}$$

The parametric nodes are generated by (4.12). The values of $\vec{P}_{ik}$ is mainly dependent on center point because of the static anchor node deployment. If the anchor nodes are mobile in PLD network, the mid-point needed to re-calculate at every stage of the trajectory. Furthermore, the calculation of center point is also dependent on step size and parametric factor. Every new center point has the effect as described in Lemma 4.2.

Lemma 4.2. In a regular distribution of anchor nodes, the parametric factor becomes constant. The first iteration center point and all other center points in different iteration lies at the same point.

From (4.12), for the selection of same midpoint at each iteration in PLD, the adverse effect of irregular node distribution is managed as shown in Appendix A. The anchor node distribution in a ring structure is shown in Figure 4.7.

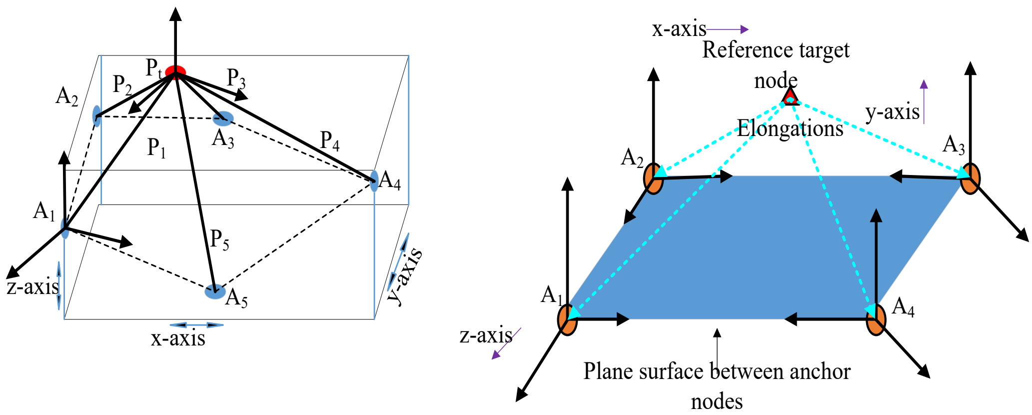

Figure 4.7: Triangulation and mid-point measurement in PLD network.

Lemma 4.3. If the parametric factor is changed, the mid-point will shifted to another point.

The mid-point angle between anchor nodes is dependent on parametric factors. If there are K number of anchor nodes, there will be a_i number of angles which are dependent to the node distribution. In case of regular distribution of anchor nodes, all angle are acute angle except $k = 3$ and $k = 4$, but the angle become obtuse angle if the node distribution is random. The angle information is more crucial in localization process, so for PLD algorithm we consider corresponding angle values for initial simulation. The sum of all angles to all sides will $360°$. In case of four or more anchor nodes the parametric factor varies from 0.765 to 0.516 and angle ranges is between $90°$ to $0°$. The first element is obtained by assuming constant distribution and the second one is derived from the average value of different parametric factor. Center point is needed to shift if it does not lie on a same point as in the first iteration. The shifting requires some derivation as explained in Appendix B.

4.4.3 Movement of Midpoints in PLD network

According to the mathematical formulation of mid-point derivation, the mid-point lies exactly in the center of network if the deployed anchors are properly distributed. The calculation of CoG is another way to compute the mid-point, but it requires parametric node position. The center point always varies within a working network, so we do not need exact position of the mid-point. The step size Δ on each axis coordinate gives random movement of medium points. The variations is determined by

$$M_1 = \{(M_x \pm \Delta), (M_y \pm \Delta), (M_z \pm \Delta)\} \tag{4.23}$$

$$N_{mov} = \frac{\xi}{\Delta} \tag{4.24}$$

where N_{mov} is a change in sensor node location.

Lemma 4.4. Parametric factor does not affect by the change in mid-point location.

Midpoint shifting either upward or downward is considerable change in a working boundary of PLD networks. The shifting of mid-point as shown in Figure 4.8 also reflects a minor change in an angle of position. This also introduces a minor change in the parametric factor calculation. The parametric factor is deviated as follows.

$$\sigma_{\alpha_k} = \frac{3}{16}(\cos\theta_{max} - \cos\theta_{min}) + \frac{1}{8}(\cos^2\theta_{max} - \cos^2\theta_{min}) \tag{4.25}$$

In an experimental study, it is noticed that the performance of localization process does not affect by the change in mid-point. Assuming a change of $5°$ upward and $5°$ downward for up to six anchor nodes. The parametric factor produces negligible change. Furthermore, as the exact position of mid-point is not necessary, the change is a Cosine angle that does not affect the accuracy of the localization calculation. Therefore, we assume that PLD is independent of such mid-point and angle variations that may affect the value of parametric factor.

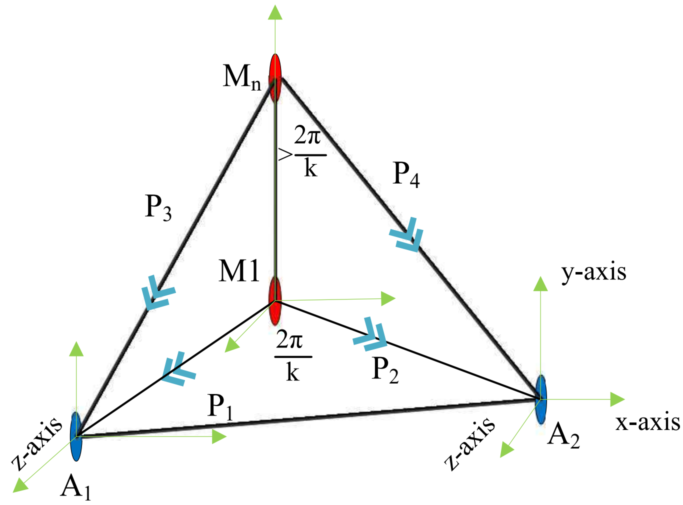

Figure 4.8: Effect on parameterization with various parametric factors.

4.4.4 Computation of Pre-localized Nodes

In an entire calculation of pre-localized nodes, PLD can compute several parametric points in each iteration by a parametrization process near to extraordinary nodes. After getting the parametric points, the RSSI is checked corresponding to that point and the distance between parametric point and sensor nodes is recorded. Path loss in RSSI is determined by

$$PL(d)[dB] = PL_F(d_o) + 10n\log(\frac{d}{d_0}) \tag{4.26}$$

The RSSI is represented by Gaussian random complex variable according to the central limit theorem. The Rayleigh fading is computed by:

$$f_X(x) = \frac{x}{\sigma^2}.e^{-\frac{x^2}{2\sigma^2}} \tag{4.27}$$

The obtained distance and RSSI have a certain relationship derived from [313].

$$RSSI(dB) = -23.28 \times \log_{10} d(m) - 2.4225 \tag{4.28}$$

The sum of RSSI at each node is:

$$\sum RSSI = \sum_{k=1}^{K} \acute{D}_{RSSI} \tag{4.29}$$

$$\acute{\mathbf{D}}_{RSSI} = \mid \vec{\mathbf{P}}_{ik} - \vec{\mathbf{A}}_{ik} \mid$$

In the next step the obtained RSSI values are stored in a matrix form:

$$f(P_{RSSI}) = \begin{Bmatrix} Preloc_{cord} & (P_{RSSI}) \leq \text{threshold} \\ * & \text{otherwise} \end{Bmatrix} \tag{4.30}$$

4.4.5 Storage Reduction factor and Actual Node Calculation

The regular distribution of anchor nodes deployment helps to perform triangulation on distance vertex with step size Δ. But for fair analysis, the anchor or node distribution is always random. In practice we introduce another parameter that distribute current working boundary in several levels that gives $K+1$ pre-localized nodes in each iteration. The reduction in storage capacity and complexity is very important in PLD networks. The value of step size Δ is also reduced, which is important to minimize localization error.

Let τ be a storage matrix having the values of pre-localized nodes in each working boundary. Step size helps to move the position of mid-point on all over the space of the networks. The value of step size helps to transfer the control to next PLD network and compute the number of pre-localized nodes. The dimension of storage matrix is $3 \times [\tau \times (K+1)]$.

$$PreLoc_{cord} = \begin{bmatrix} x_{p\tau 0} & x_{p\tau 1} & \dots & x_{p\tau k} \\ y_{p\tau 0} & y_{p\tau 1} & \dots & x_{y\tau k} \\ z_{p\tau 0} & z_{p\tau 1} & \dots & z_{p\tau k} \end{bmatrix} \tag{4.31}$$

For computation of localization volume, maximum and minimum coordinates points are computed from matrix having pre-localized nodes values on each axis.

$$V_{localization} = x_\zeta * y_\zeta * z_\zeta \tag{4.32}$$

The volume of pre-localized node boundary is derived from the following relation.

$$V_{pre\ Loc} = \int_{x_{min}}^{x_{max}} \int_{y_{min}}^{y_{max}} \int_{z_{min}}^{z_{max}} f(x, y, z)\mathrm{d}x\mathrm{d}y\mathrm{d}z \tag{4.33}$$

Then, the working boundary is divided in to N-clusters, and each cluster has maximum and minimum value of coordinates stored in a storage matrix. The difference between the cluster is computed by:

$$(x_{n(\zeta)}, y_{n(\zeta)}, z_{n(\zeta)}) = \left[x_n \mid \begin{matrix} max \\ \\ min \end{matrix}, y_n \mid \begin{matrix} max \\ \\ min \end{matrix}, z_n \mid \begin{matrix} max \\ \\ min \end{matrix} \right] ;\ \text{where } n = 1, 2, ...N \tag{4.34}$$

This will help PLD networks to estimate the position vector of i^{th} localized nodes.

$$(x_{L_{Pi}}, y_{L_{Pi}}, z_{L_{Pi}}) = (\frac{x_{n_\zeta}}{2}, \frac{y_{n_\zeta}}{2}, \frac{z_{n_\zeta}}{2}) + (x_{n_{min}}, y_{n_{min}}, z_{n_{min}}) \tag{4.35}$$

4.4.6 Relationship between Anchor, Parametric and Pre-localized Nodes

Let us assume that the value of step size Δ is a fixed constant, then the RSS value of two pre-localized node will be same as step size. To prove this let us consider, two consecutive nodes as:

$$P_N = \{P_{N-1}\} \pm \Delta \tag{4.36}$$

P_N basically provides subdivision of earth surface in anchor nodes deployment and Δ is a difference between two points. The maximum increment and decrements on upward and downward direction on parametric points result in the same coordinate points on M_1. Then (4.36) can be written as:

$$P_N = M_1 \tag{4.37}$$

$$M_1 = P_{1i} \pm \sum_{j=1}^{N-1} \Delta \tag{4.38}$$

If there is any change in the working boundary, like that a nearest anchor node is damaged or stop responding due to node failure, then the change in the control vertices also changes the value of mid-point. The change in mid-point is represented as:

$$\gamma = \acute{M}_{j+1} - \acute{M}_j \tag{4.39}$$

$$= \alpha_k(\acute{M}_j - \acute{M}_{j-1}) + (1 - \alpha_k)(\Delta) \tag{4.40}$$

Therefore, if the difference among two node is Δ, then the (4.39) is written as:

$$\gamma = \Delta \tag{4.41}$$

The angle of deviation is independent of points from Loop division as represented in (4.35). That describes the relationship between parametric point and mid-point. The parametric point with RSSI less than threshold are the pre-localized points. The PLD scheme only stores pre-localized node information of each anchor as shown in Figure 4.9.

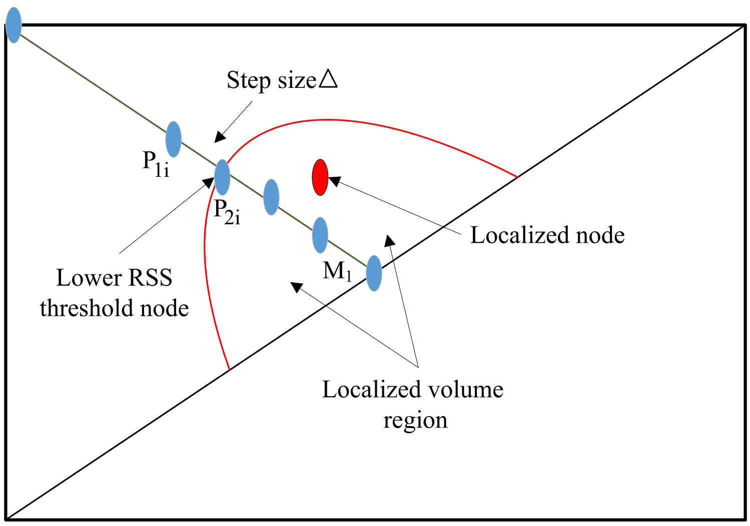

Figure 4.9: Localized volume region along with localized node.

The target node position is computed by (4.35). The number of actual nodes in 3D depoloyment in each unit volume is computed by:

$$(\hat{x}, \hat{y}, \hat{z}) = [(K+1)P_L] \times \tau * \frac{N}{k} \tag{4.42}$$

$$Sum(LE) = \sum_{i=1}^{N} \sqrt{(x_i - \hat{x}_i)^2 + (y_i - \hat{y}_i)^2 + (z_i - \hat{z}_i)^2} \tag{4.43}$$

where LE is a mean localization error and x_i is the target point and $\hat{x}_i$ is the estimated point. The general flow diagram of PLD algorithm is shown in Figure 4.10.

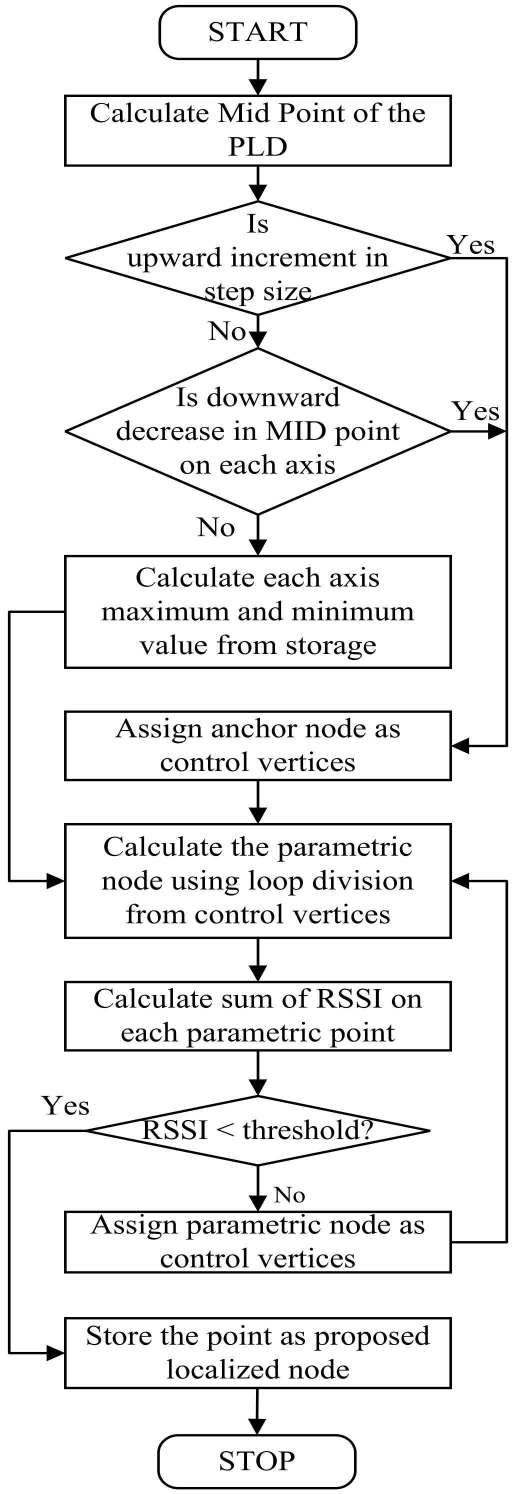

Figure 4.10: Flow diagram of PLD algorithm.

4.5 Simulation Results

In this section, we provides a comprehensive simulation study of the PLD algorithm in Matlab. For the initial simulation, random anchor nodes are deployed over a 3D space of $100m \times 100m \times 100m$. Furthermore, six anchor nodes are used in each iteration with the knowing information that the position of anchor nodes is changed randomly to test the system reliability. The simulation was run for 1000 iterations. Moreover, a constant $80000m^3$ volume space is adjusted on each axis. The total distance is then calculated by (4.44).

$$d = \sqrt[3]{80000} = \sim 95m \tag{4.44}$$

The lower bound of the localization error is computed by the following equation.

$$l = \frac{0.955\sqrt{V}}{8\pi^2 m(K+1)} \tag{4.45}$$

where, V denotes the total localization volume, m is the midpoint values and K denotes the number of PLD networks.

4.5.1 Topology Construction

We have assumed that all anchor nodes are connected with each other node for mid-point calculation, then the number of connection pairs is given by binomial coefficient we have:

$$^{n}C_2 = \frac{n!}{2!(n-2)!} = \frac{n(n-1)}{2} \tag{4.46}$$

Note that each pair of vertex denoted by V for all m anchor nodes has a binomial correlation with the anchor node position. Therefore, for further iterations of PLD, the vertex information is also correlated to parametric points distribution. For all other nodes in a PLD, we perform the following routines for topology construction.

Algorithm 3 Topology construction at the first step of anchor node deployment

```
s=0
for t = 1 : to m do
    if A_V(1) ~ A_V(2) then
        s++
        pair ← V_t (Actual pairs for 1 ≤ s ≤ g
    else
        Control might be at parametric node position
        pair ← V_p (Parametric ring)
    end if
end for
g ← s =0
```

4.5.2 Localization Accuracy

Localization volume plays an important role in accuracy analysis of the PLD algorithm. The volume of pre-localized nodes are directly proportional to the number of localized points. Mean localization error (MLE) is computed by taking the fraction of number of nodes and sum of error distance. The random deployment of anchor nodes produces four localized points (targets) are shown in Table 4.2. In initial experiment, sum of error and MLE were found as $3.57m$ and $0.89m$, respectively.

Table 4.2: Localization error of four nodes in each PLD network.

$\hat{x}$	$\hat{y}$	$\hat{z}$	**x**	**y**	**z**	**Error** (m)
14.47	7.66	14.11	15.90	8.20	15.27	1.91
15.54	9.93	14.90	15.54	9.93	14.90	1.53
15.73	10.65	15.25	15.79	10.63	15.27	0.05
16.93	11.85	16.45	16.94	11.85	16.15	0.08

For the same scenario, we obtained different values in each iteration as shown in Table 4.3. In simulation, iteration is changed for different number of unknown nodes. In the first iteration, only 1 node was localized with an average localization error of $1.55m$ and $1.43m$ in case of 5 and 6 anchor nodes, respectively. Similarly, for 2, 3 and 4 target nodes, localization error of $1.58m$, $1.45m$ and $1.26m$ is recorded for 5 anchor nodes and $1.36m$, $1.12m$, $0.9m$ is recorded for 6 anchor nodes. The localization error will gradually decreases if we deploy more anchor nodes for a given environment. Furthermore, if a proper distribution of anchor node is followed during deployment, the error will also decrease even with less anchor nodes. So, the anchor deployment is a crucial factor in PLD.

Table 4.3: Mean error of 10 different trials of PLD network with $r = 3m$.

$N = 1$		$N = 2$		$N = 3$		$N = 4$	
$A = 5$	$A = 6$	$A = 5$	$A = 6$	$A = 5$	$A = 6$	$A = 5$	$A = 6$
1.06	0.84	2.01	1.5	1.42	1.48	1.77	0.77
1.2	1.08	1.99	1.36	1.77	1.08	1.22	0.76
1.44	1.62	1.93	1.38	1.68	1.10	0.91	0.89
1.45	1.60	1.57	1.47	1.64	1.12	1.52	0.95
1.84	1.78	1.30	1.57	1.72	1.23	1.44	0.82
2.16	1.75	1.69	1.56	1.12	1.24	1.41	1.01
1.99	1.66	0.96	1.57	1.54	1.20	0.76	0.99
2.08	1.57	1.25	1.61	1.12	0.95	0.78	0.97
1.47	1.26	1.73	0.77	0.99	0.96	1.42	0.96
0.88	1.18	1.43	0.80	1.59	0.92	1.43	0.96

The localization accuracy might be affected by the value of step size Δ. If the value of the step size is high for small volume networks, the computation cost becomes higher as the number of iterations increases. Our step size value was high for 5 anchor nodes as compared to 6 anchor nodes. For the authenticity of PLD algorithm, an average, minimum and maximum error is also recorded against $A = 5$ and $A = 6$ as shown in Table 4.4. The accuracy plot for different localization volume is shown in Figure 4.11.

Table 4.4: average, maximum and minimum localization error at each PLD network with $A = 5$ and $A = 6$.

Number of	e_{avg}		e_{max}		e_{min}	
Localization points	$A = 5$	$A = 6$	$A = 5$	$A = 6$	$A = 5$	$A = 6$
N=1	1.55	1.43	2016	1.78	1.28	0.84
N=2	1.58	1.364	2.01	1.61	1.05	0.77
N=3	1.45	1.128	1.77	1.48	0.78	0.92
N=4	1.265	0.908	1.77	1.01	1.01	0.76

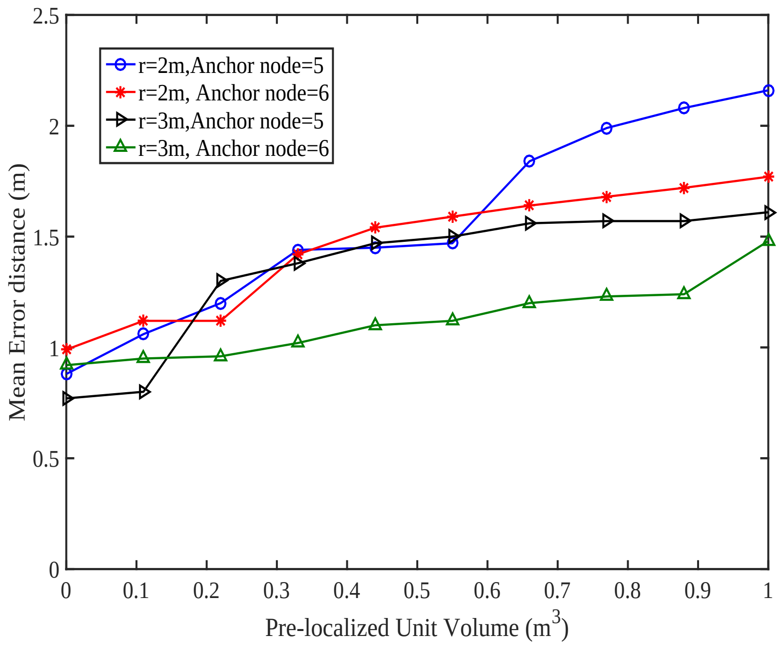

Figure 4.11: Mean error analysis with different volumes of PLD.

4.5.3 Effect of Rayleigh fading

In RSSI computation, Rayleigh fading is also considered that makes localization process challenging. Variations in signals amplitude over time and frequency can affect the properties of RSSI. In simulation, the power samples are to be multiplied by a factor r_f^2, if Rayleigh fading is taken into account. The factor r_f is a random variable to account the fading amplitude. This random variable is modelled with a probability density function (PDF) derived in (4.27). The value of path loss factor is needed to adjust from (4.26), which reflects the two main properties of radio irregularity known as continuous and non-isotropic variations. The adjustment is accounted by the relationship

$$d = d_0 + N(\mu, \sigma) \tag{4.47}$$

where μ represent mean and σ denotes standard deviation.

The Rayleigh fading is added in the RSSI to compute the effect multipath fading on localization as shown in Figure 4.12. σ^2 is assumed to be $\frac{1}{2}$ in (4.27) that given $E[r_f^2] = 2\sigma^2 = 1$, representing no attenuation in terms of power, we have:

$$RSSI = RSSI + 20\log_{10} r_f \tag{4.48}$$

where r_f is a multipath factor represents Rayleigh fading.

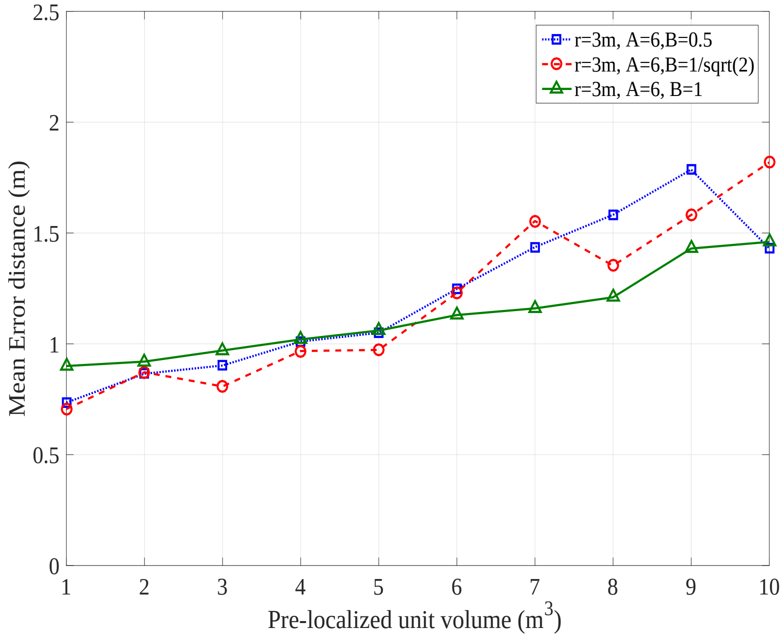

Figure 4.12: Effect of Multipath Fading on Localization Error.

4.5.4 Effect of Anchor Node Density

The deployment of nodes is crucial in any localization scenario. It should be random or through regular distribution according to the system requirement. It should be optimized to provide a complete network coverage, power optimization and less computation cost. Figure 4.13 shows the anchor, target and estimated target nodes after 10 iterations. Random deployment of nodes results in spread of nodes across the deployment region, which solves the problem of network coverage and power optimization.

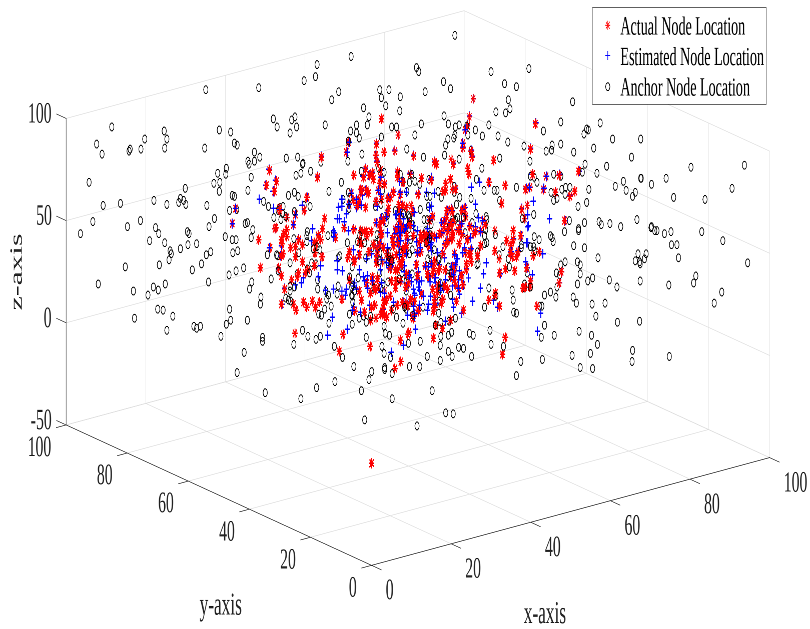

Figure 4.13: Location of anchor nodes, actual sensor nodes and estimated sensor nodes in 3D environment.

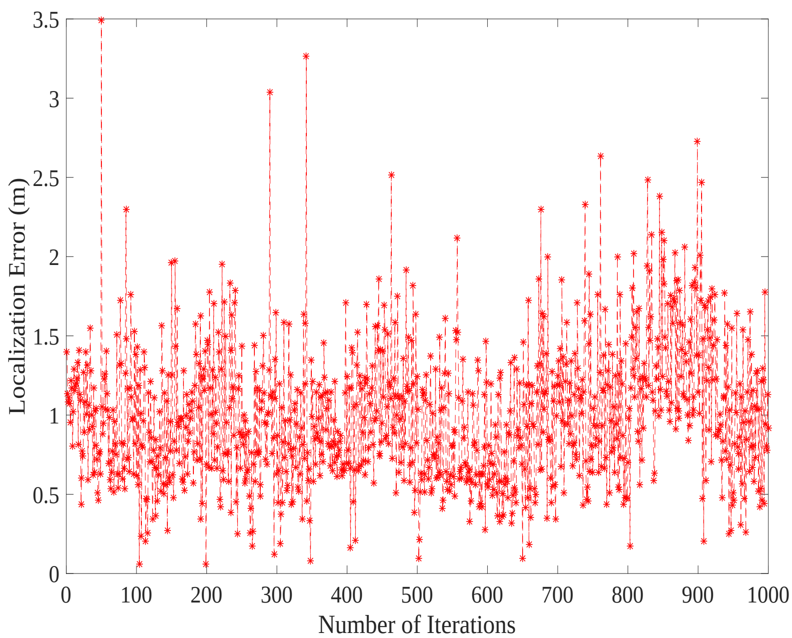

Figure 4.14: Average localization error after 1000 iterations.

Simulation with the algorithm is run for 1000 iterations. Figure 4.14 shows that the algorithm is quite reliable. The average localization error falls between $0.9m$ and $2.5m$ for 1000 iterations with $A = 6$. The main reason of this error reduction is that PLD uses all ranges between target and anchor nodes. As the three anchor nodes participate in triangulation process, a good localization accuracy is achieved with lower error bound.

The increase in anchor node density will increase the accuracy in PLD algorithm. The localization error is tested using different percentage of anchor volume as shown in Figure 4.15. The error was gradually decreased when the deployment region have 21% of anchor nodes. However, in certain cases localization error can be reduced by varying the anchor nodes in numbers or changing their positions. Fig 4.16 shows that the variation in anchor node density with maximum localization error. The maximum anchor nodes density is recorded up to 24% to 30% , resulting in reduction of localization error.

The standard deviation is calculated to check the variation of localization error within the network region. Figure 4.17 shows that a range of 1% to 11% of anchor volume leads to high standard deviation. To overcome this problem, we can increase the anchor node density with proper deployment with regular distribution. The main reason for the higher standard deviation is that the nodes are deployed with improper distribution, and some nodes are out of pairs in our topology construction routines. Therefore one can find the upper bound on the volume of anchor node for localization. The percentage standard deviation is calculated by:

$$\%SD = \frac{\sqrt{E(D_i - \mu)^2} \times 100}{\sum D_i} \tag{4.49}$$

where,

$$D_i = \sqrt{(P_{LP_i} - P_{eP_i})^2} \tag{4.50}$$

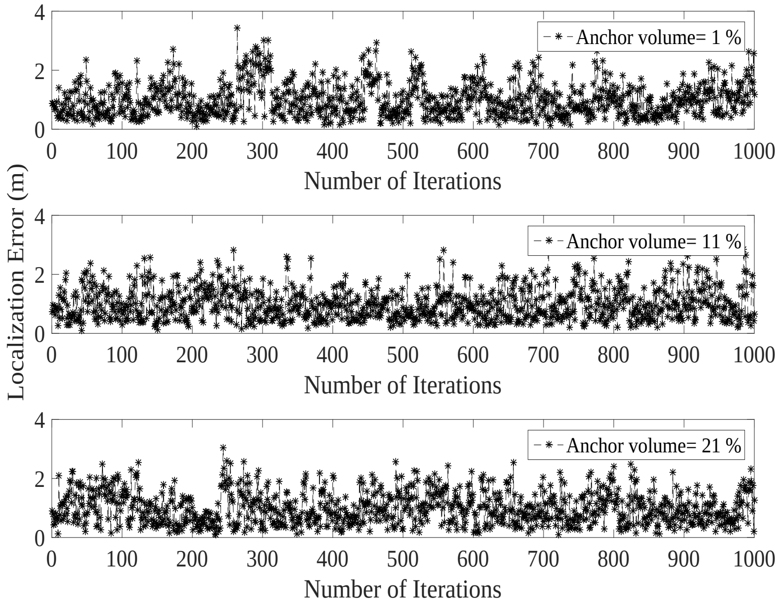

Figure 4.15: Localization error vs varying percentage of anchor node density.

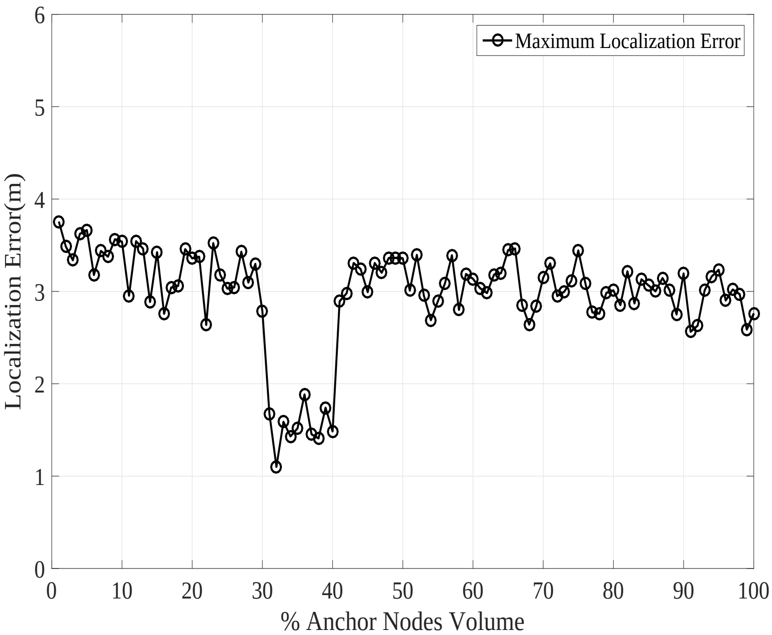

Figure 4.16: localization error under different percentage of anchor node density.

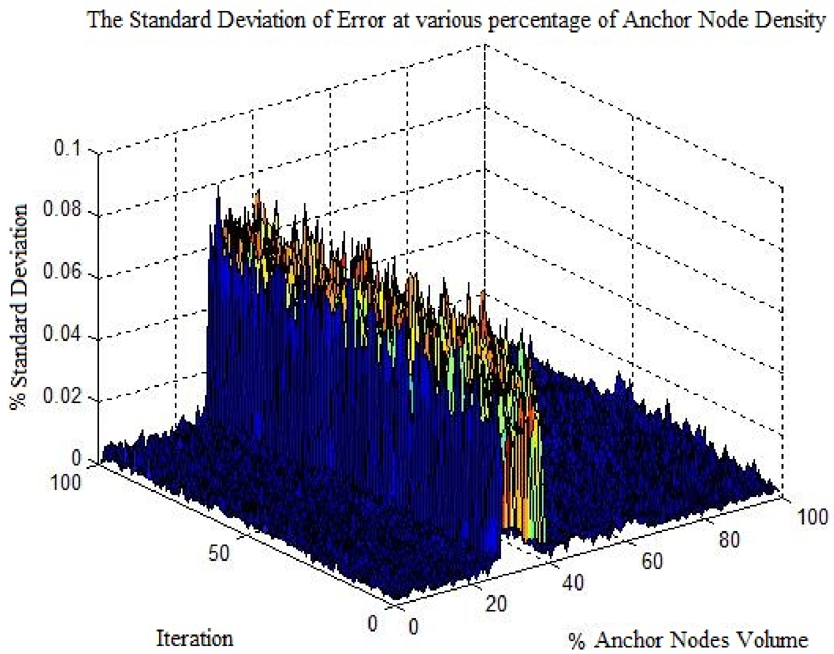

Figure 4.17: Percentage maximum standard deviation with varying anchor node volume.

4.5.5 Comparison with existing methods

The accuracy of localization algorithms depends on many factors like number of anchor nodes, model and deployment (like regular or random distributed), radio range and many other as per requirement of the application. In addition, node density and degree of connectivity also affect the localization accuracy.

The simulation of PLD algorithm was run for 1000 times to obtain an overall localization error. PLD algorithm shows superior performance as compared to other well-known range free schemes like APIT [218], MDS-MAP [169], and DV-Hop [247] as shown in Figure 4.18. For fair comparison, the same network space is considered for all schemes. In DV-Hop algorithm, the number of nodes were changed from 50 to 300, the average network connectivity value of 18.66. If the number of nodes are fixed to 200 and varying the communication range varied from 50 to 200, the network connectivity value of 8.38 is obtained. Same parameters are applied to APIT and the connectivity value was 18.13 while by changing the number of nodes, we obtained connectivity range of 8.53. For other algorithms like centroid [214], it is 18.47 and for MDS-MAP it is 8.49. We set a RSSI threshold value of $-40dBm$ for our PLD scheme.

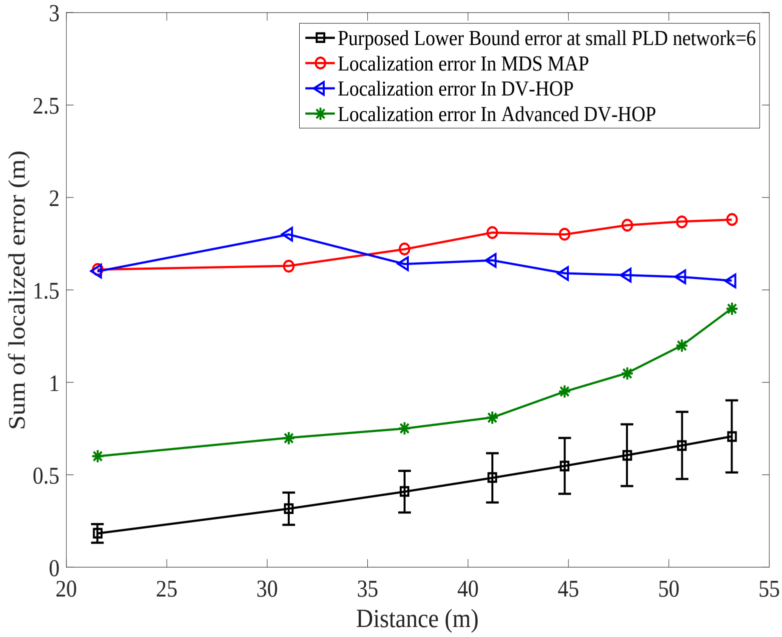

Figure 4.18: Comparison of lower bounds PLD network error to existing systems.

Moreover, PLD algorithm is simulated with different anchor node density as compared to DV-Hop method shown in Table 4.5. In each iteration, we increased the number of anchor nodes. As we can see from Table 4.5, accuracy of PLD scheme improves as the anchor node density increases, while DV-Hop even stops responding in some cases if there are not enough anchor nodes. This is due to the fact that DV-Hop needs to compute number of hops in each steps. Therefore, if there are not many node in proximity, it becomes hard to count the number of hops.

Table 4.5: SE (sum of error) and ME (mean error) of $N = 1, 2, 3, 4$ point over $r = 3m$ and $A = 6$.

WSN	@ 20% *anchor nodes*			@ 25% *anchor nodes*			@ 30% *anchor nodes*		
A	e_{max}	e_{min}	e_{avg}	e_{max}	e_{min}	e_{avg}	e_{max}	e_{min}	e_{avg}
PLD $A = 5$	1.7827	0.8057	1.265	1.1884	0.5372	0.8433	0.8913	0.4029	0.4573
PLD $A = 6$	1.0172	0.7654	0.9145	0.6782	0.5103	0.6097	0.5086	0.3827	0.4573
DV-HOP C-shaped	2.2	1.38	1.68	1.86	1.35	1.48	2.18	1.55	1.78

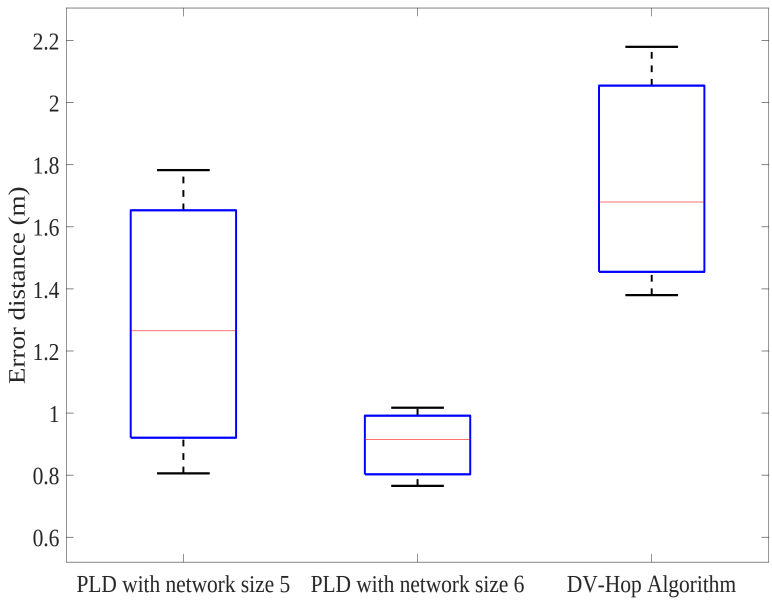

Figure 4.19: Comparison of the average position error of PLD with DV-Hop at 20% anchor nodes.

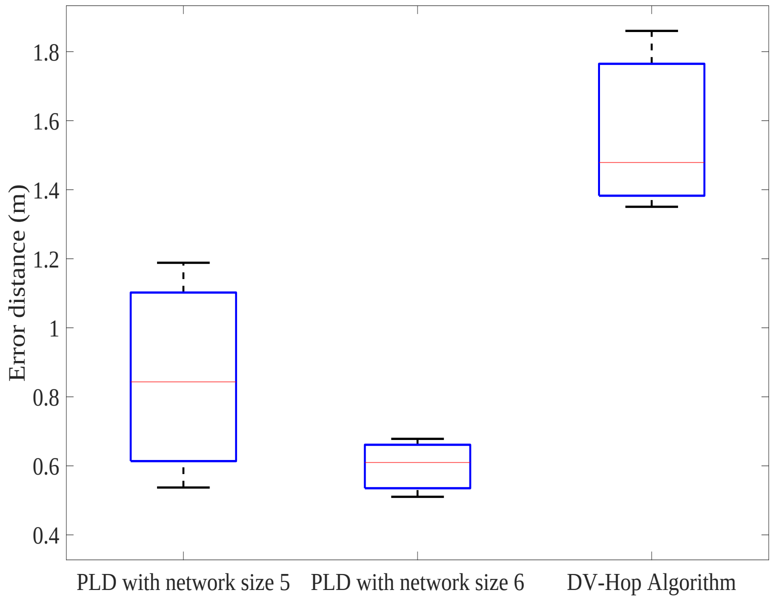

Figure 4.20: Comparison of the average position error of PLD with DV-Hop at 25% anchor nodes.

The PLD algorithm is being tested with DV-Hop algorithm with varying anchor nodes density. Figure 4.19 shows that when there are 20% of anchor nodes, the localization error of PLD algorithm is between $0.5m$ to $1.2m$. An average localization accuracy of up to $0.89m$ is achieved while in case of it is almost $1.8m$. Similarly, with a node percentage of up to 25%, the average localization error for PLD reduces to $0.6m$ and $1.5m$ for DV-Hop algorithm as shown in Figure 4.20. The interesting fact is that if we further increased the number of anchor nodes while keep number of unknown nodes to fixed value, the DV-Hop loses the accuracy as more computation is required to count the number of Hop. We try to increase the number of anchor nodes up to 30%, the PLD still keeps increasing its accuracy as ring vertex computes a mid point, that is close to the value of step size. So we do not need to make any upward and downward increment to change the position of mid-point. As shown in Figure 4.21 in case of 30% of anchor nodes, PLD and DV-Hop have localization error of $0.35m$ and $1.9m$, respectively.

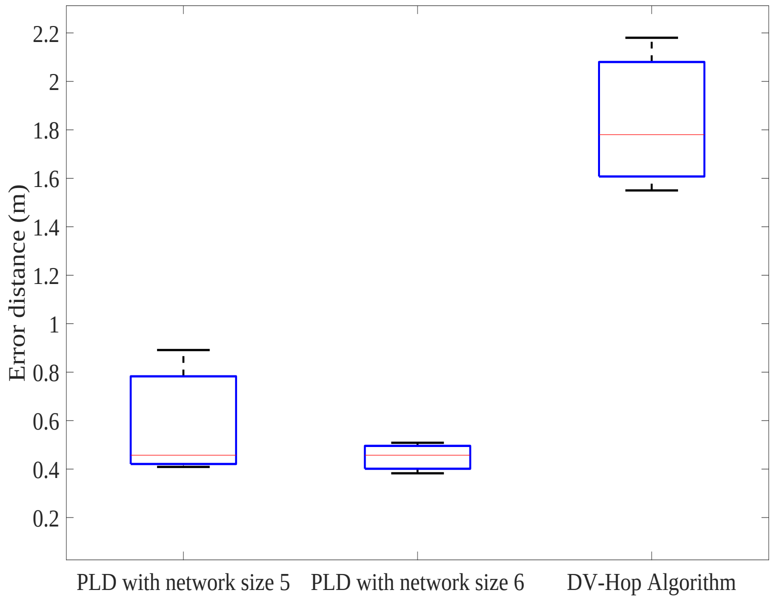

Figure 4.21: Comparison of the average position error of PLD with DV-Hop at 30% anchor nodes.

4.5.6 Accuracy analysis of PLD algorithm

The expected localization error in PLD utilizes equal probability at each node over a deployment region. Since all the nodes follow same uniform distribution of anchor deployment over a 3D space. The CDF of of localization is defined as $e(r) = P(D < r)$ where PDF is computed in each unit volume. Assuming nodes are distributed uniformly on a region space R, then the unit volume PDF is estimated as:

$$f(x, y, z) = \frac{1}{V_R} \tag{4.51}$$

$$\varrho = \frac{2 \times \text{Error distance on each axis}}{\text{Distance}_{N \longrightarrow N}} = \left\{ \frac{1-U}{2}, \frac{1+U}{2} \right\} \tag{4.52}$$

where ϱ is unit transmission ratio. The PDF calculation at unit volume radius plays a vital role in analyzing the accuracy of PLD network. For the accuracy analysis, we choose two difference radii of $r = 2m$ and $r = 3m$. Here we needed to compute the transmission range under sensing radius between any of two nodes. We noticed that the transmission range of $r = 2$ and $r = 3$ is $4m$ and $6m$, respectively. The minimum worst case accuracy of PLD is 0.653 and 0.681 with $A = 5$ and $A = 6$ networks and transmission range of $d = 0.76346$. It shows a high tolerance level as compared to [314], which gives up to 0.2887 and 0.28286 for [315], which is shown in Figure 4.22. The sum of error on each sides of the axis along with mean square error (MSE) is recorded against $A = 5$ and $A = 6$ in a region of $r = 3m$. Table 4.6 shows MSE and sum of error for $A = 6$ along with $N = 1, 2, 3, 4$. We found that the average localization error is $1.434m, 1.364m, 1.128m, 0.9m$ for $N = 1, 2, 3, 4$, respectively.

Table 4.6: SE (sum of error) and ME (mean error) of $N = 1, 2, 3, 4$ point over $r = 3m$ and $A = 6$.

$r = 3m, N = 1, A = 6$		$r = 3m, N = 2, A = 6$		$r = 3m, N = 3, A = 6$		$r = 3m, N = 4, A = 6$	
SE	**ME**	**SE**	**ME**	**SE**	**ME**	**SE**	**ME**
0.84	0.84	3.01	1.55	4.44	1.48	3.08	0.77
1.08	1.08	2.73	1.36	3.26	1.08	3.07	0.76
1.62	1.62	2.76	1.38	3.3	1.1	3.56	0.89
1.6	1.6	2.95	1.47	3.38	1.12	3.8	0.95
1.78	1.78	3.15	1.57	3.69	1.23	3.31	0.82
1.75	1.75	3.13	1.56	3.72	1.24	4.06	1.01
1.66	1.66	3.14	1.57	3.61	1.2	3.99	0.99
1.57	1.57	3.22	1.61	2.86	0.95	3.91	0.97
1.26	1.26	1.55	0.77	2.91	0.96	3.86	0.96
1.18	1.18	1.6	0.8	2.78	0.92	3.84	0.96

Table 4.7: SE (sum of error) and ME (mean error) of $N = 1, 2, 3, 4$ point over $r = 3m$ and $A = 5$.

$r = 3m, N = 1, A = 5$		$r = 3m, N = 2, A = 5$		$r = 3m, N = 3, A = 5$		$r = 3m, N = 4, A = 5$	
SE	**ME**	**SE**	**ME**	**SE**	**ME**	**SE**	**ME**
1.06	1.06	4.03	2.01	4.27	1.42	5.33	1.77
1.2	1.2	3.99	1.99	5.32	1.77	4.88	1.22
1.44	1.44	3.87	1.93	5.05	1.68	3.65	0.91
1.45	1.45	3.14	1.57	4.92	1.64	6.09	1.52
1.84	1.84	2.64	1.32	5.17	1.72	5.78	1.44
2.16	2.16	3.38	1.69	3.36	1.12	5.63	1.4
1.99	1.99	1.92	0.96	4.64	1.54	3.07	0.76
2.077	2.074	2.45	1.25	3.37	1.12	3.12	0.78
1.47	1.47	3.46	1.73	2.98	0.99	5.69	1.42
0.88	0.88	2.86	1.43	4.79	1.59	5.74	1.43

Similarly, Table 4.7 shows the mean square error (MSE) and sum of error for $A = 5$ along with $N = 1, 2, 3, 4$. We found that the average localization error is $1.556m, 1.588m$, $1.459m, 1.265m$ for $N = 1, 2, 3, 4$, respectively.

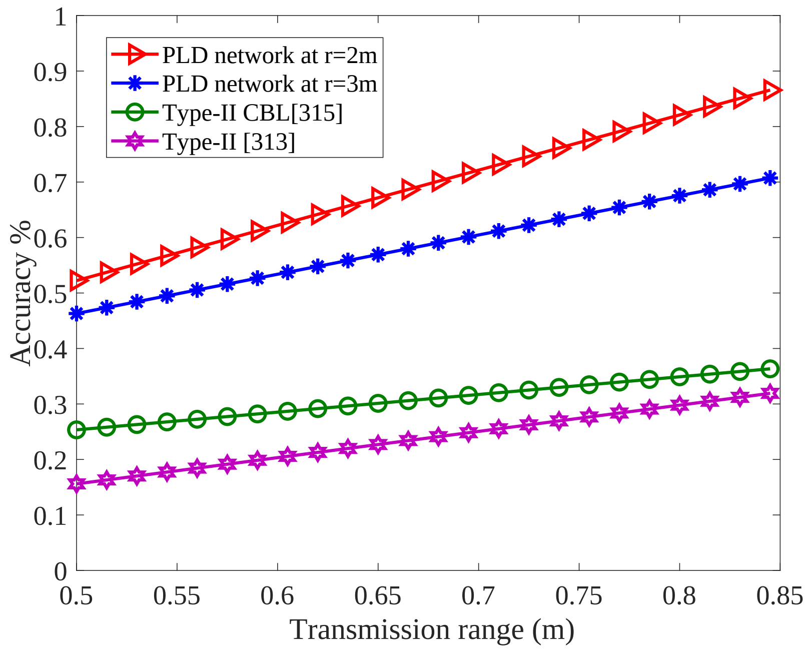

Figure 4.22: Impact of transmission range and localization accuracy of PLD with different network size.

For further accuracy analysis, assuming that a region of 3D space R is subdivided into several networks. All of these networks are overlapped, i.e., $R = \{R_1, R_2, ...R_k\}$ with volume V, i.e., $V = \{v_1, v_2, ...v_k\}$. A node within any ring matrix ρ with localization error $l_e = (x, y, z)$ lies in a real position at any subdivided region R_i.

$$\rho(V_i) = \frac{v_i}{V} \quad and \sum_{i=1}^{k} \rho(V_i) = 1 \tag{4.53}$$

if $l_e(R_i)$ is an error of a target node $\rho(x, y, z)$ distributed uniformly, then the total sum of error $E[l_e]$ is computed as:

$$E[l_e] = \sum_{i=1}^{k} \rho(V_i) l_e(R_i) \tag{4.54}$$

$$l_e(R_i) = \frac{1}{v_i} \int\int\int_{R_i} \sqrt[3]{X_{i(\zeta)} \times Y_{i(\zeta)} \times Z_{i(\zeta)}} \mathrm{d}x\mathrm{d}y\mathrm{d}z \tag{4.55}$$

where $l_e(R_i)$ is derived from (4.35). Substitute (4.55) in to (4.54) we have:

$$E[l_e] = \sum_{i=1}^{k} v_i l_e(R_i) \tag{4.56}$$

where ζ denotes the difference between the coordinates. The working volume is transferred to 2D form by that make computation more easy. This also proves the accuracy of PLD algorithm. The variation in localization volume can also result in variation of PDF. In accuracy measurement, we take a constant value of step size and mid-point. The PLD localization accuracy with respect to unit transmission is shown in Figure 4.23.

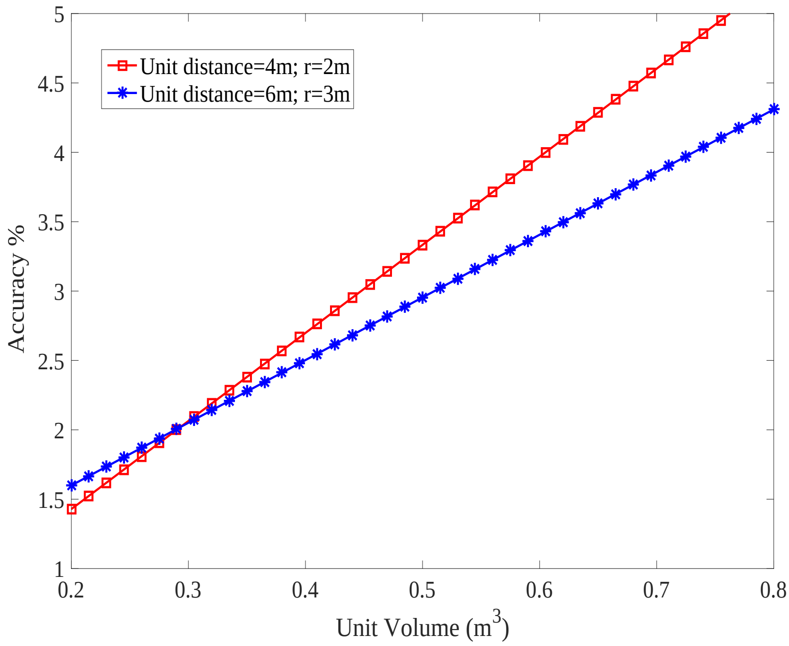

Figure 4.23: Accuracy of PLD network with different volume of PLD network.

The probability density of PLD is also computed after 1000 random experiments with each experiment have 10 iterations in $10m$ spherical distance. This spherical helps PLD to perform computation in 2D form. The probability density function (PDF) in [314] which has $PDF = 1$, while in PLD have a probability of 0.5 and 0.333, respectively having $10,000$ of iterative values in each PLD network. The cumulative PDF is shown in Figure 4.24. We noticed that PLD have a low error probability in low sensing radius. The trade-off between radio coverage and unit sensing radius exists in PLD network.

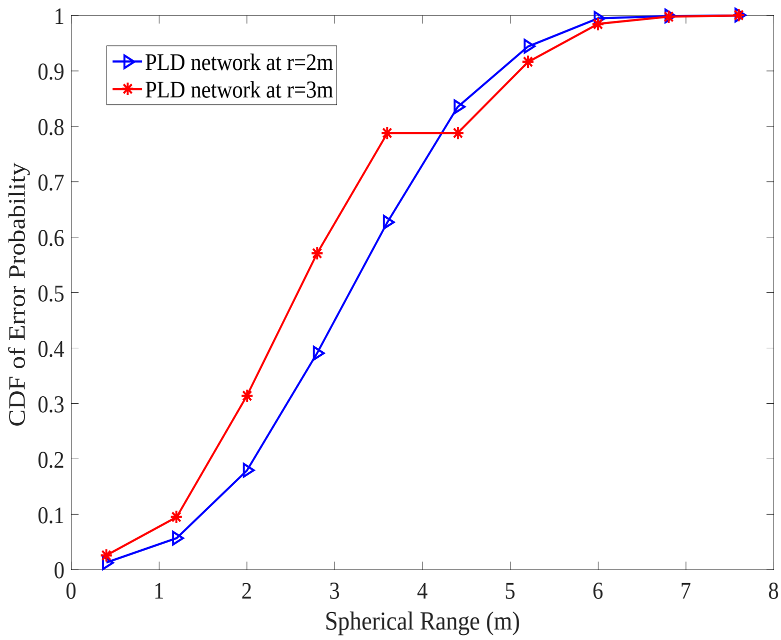

Figure 4.24: Cumulative error probability in PLD network with $r = 2m$ and $r = 3m$.

4.5.7 Effect of Node Position

In the literature, the anchor node placement, topology construction and effect of anchor node movement are often recognized, but left as a future study. Mostly algorithms only stated that nodes are deployed randomly except those deployed nodes practically using some source like drones and planes with accurate information. In [73, 180, 194], it was described that the co-linear anchor nodes "represent a rather unlucky selection" without auxiliary suggestion. Therefore, for PLD algorithm, the proper deployment of anchor nodes are taken place. At first, we drop some node using random deployment, later on a distribution of nodes are derived in the form of topology construction as explained in

Algorithm 3. Then we can analyze what a perfect anchor node position is and how the change in position can affect the overall localization error. We know that for different distances between target and estimation node, the localization error is different. To achieve higher accuracy, anchor node must be deployed so that it can help the PLD network to provide full coverage. Hereafter, we can test whether anchor node position can affect the PLD accuracy or not. During the testing phase, we also see that how to overcome worst anchor node position and how the system respond in case of node failure. If the anchor node failed to respond, the next nearest possible anchor can make a pair with corresponding anchor and measure the initial distance. In this case, it might be possible that localization error may fluctuate. To overcome this issue, when a anchor node failed to respond, a corresponding anchor responds to the back system for such changes. In simulation, we can change the position of reference anchor in cm in each side to test the robustness of the algorithm. We noticed that if the variation of anchor node is less than $15cm$, the localization error will not be affected much. However, when an anchor node position is shifted between $15cm$ to $40cm$, the average localization error gradually increases up to $1.1m$ as shown in Figure 4.25. Major changes occurs when a reference anchor node moves up to $2m$ on each side of the surface. An average localization error of up to $1.2m$ is recorded with such changes.

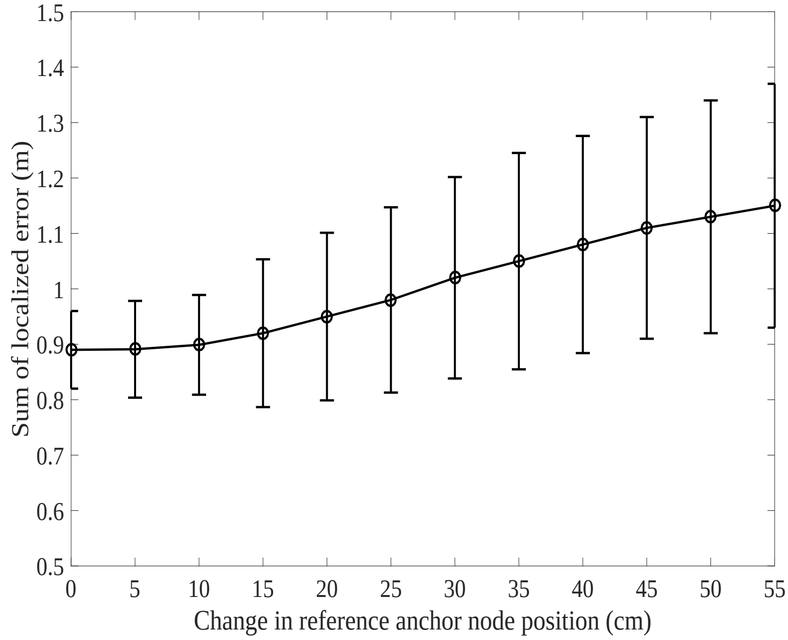

Figure 4.25: Influence of reference anchor node position vs localization error.

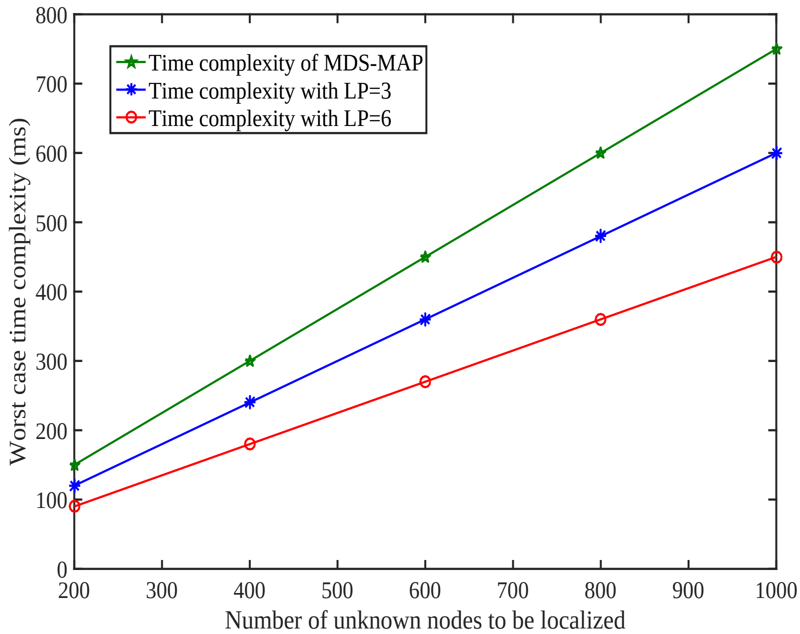

Figure 4.26: Complexity comparison between PLD and MDS-MAP.

4.5.8 Time complexity and Lower Bound Derivations

The computational complexity of any localization algorithm is referred to as the time consumption. Assuming that PLD algorithm has minimum $\frac{N}{k}$ to maximum N number of PLD networks in a 3D space. Each PLD network computes the number of pre-localized nodes in each iteration and generates ξ nodes in a matrix. The number of anchor nodes is $(\frac{N}{K} \times \xi) \leq N_{PLDnetwork} \times \xi \leq N \times \xi$. Let us assume that there are 400 target nodes with 50 anchor nodes, pre-localized in each iteration. Let five simultaneous anchor nodes can be localized in each ring network, then $N = 4$. Then, the number of target nodes are $(50 + 10 \times 5) = 100 \leq (50 + 50 \times PLD_{network} \times 5) \leq (50 + 50 \times 5) = 300$. The requirement of number of anchor nodes against with each volume of PLD network is shown in Figure 4.27. Here, the complexity of the PLD is reduced by 25% but with $N = 7$ the complexity is completely in control. The complexity of PLD is also compared with MDS-MAP as shown in Figure 4.26.

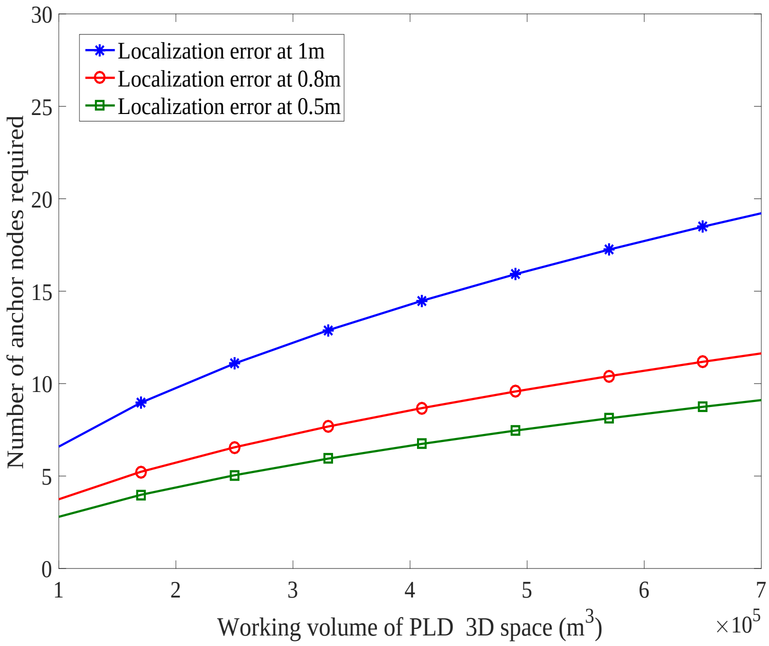

Figure 4.27: Number of anchor nodes required and their corresponding lower bounds.

To compute the lower bound derivation, let $le(C)$ be the value of $l_e(R_i)$. For regular unit shape sh_{R_i} defined as $e_{sh_{R_i}}$ is derived by

$$e_{sh_{R_i}} = \frac{le(R_i)}{le(C)} = 0.9554 \tag{4.57}$$

We have scaler values if each deployment region is divided in unit sphere, we have:

$$e_{sh_{R_i}} = \frac{le(R_i)}{m \times le(C)} = 0.9554 \tag{4.58}$$

where $m = \frac{v_i}{c}$. By substituting the above value into the sum of error equation, we get

$$E[le] = \frac{1}{V} \sum_{i=1}^{k} \frac{v_i}{C} e_{sh_{r_i}} le(C) \tag{4.59}$$

We have a minimum value of sphere volume as $\frac{1}{8\pi^2}$. The worst case error can be calculated through $l = \frac{0.955\sqrt{V}}{8\pi^2 m(K+1)}$, where V is the numerical value and the number of networks is $k = \frac{0.955\sqrt{V}}{8ml\pi^2} - 1$.

The mean, maximum and minimum localization error of PLD algorithm with $A = 5$ and $A = 6$ is shown in Figure 4.28 and Figure 4.29, respectively. Different iterations of PLD is shown in Figure 4.30 that used lower bound error formulation. The comparison of PLD among different range free localization algorithms is shown in Figure 4.31.

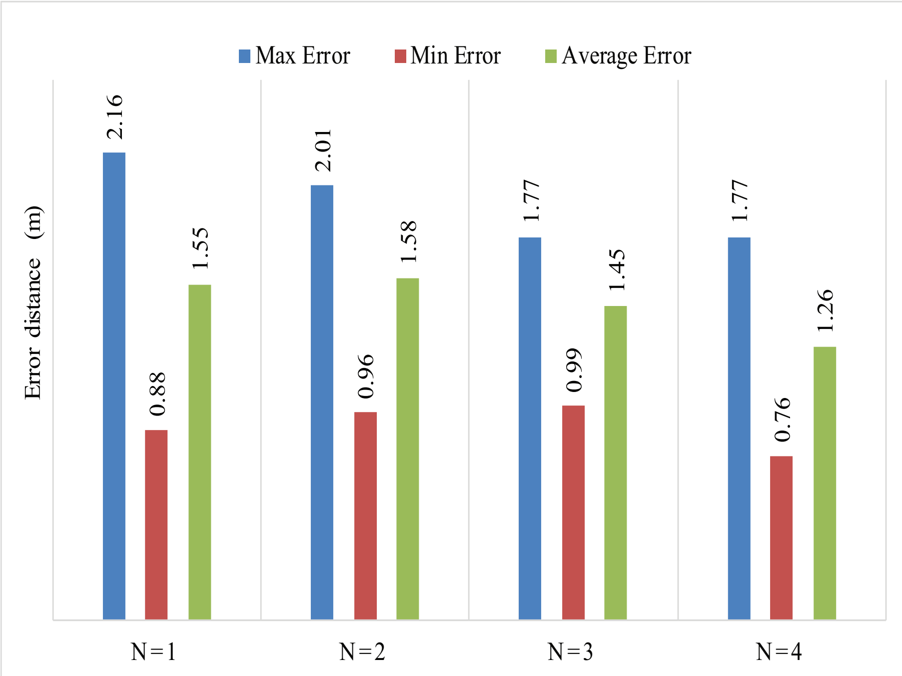

Figure 4.28: Localization error distance of PLD with A=5.

Figure 4.29: Localization error distance of PLD with A=6.

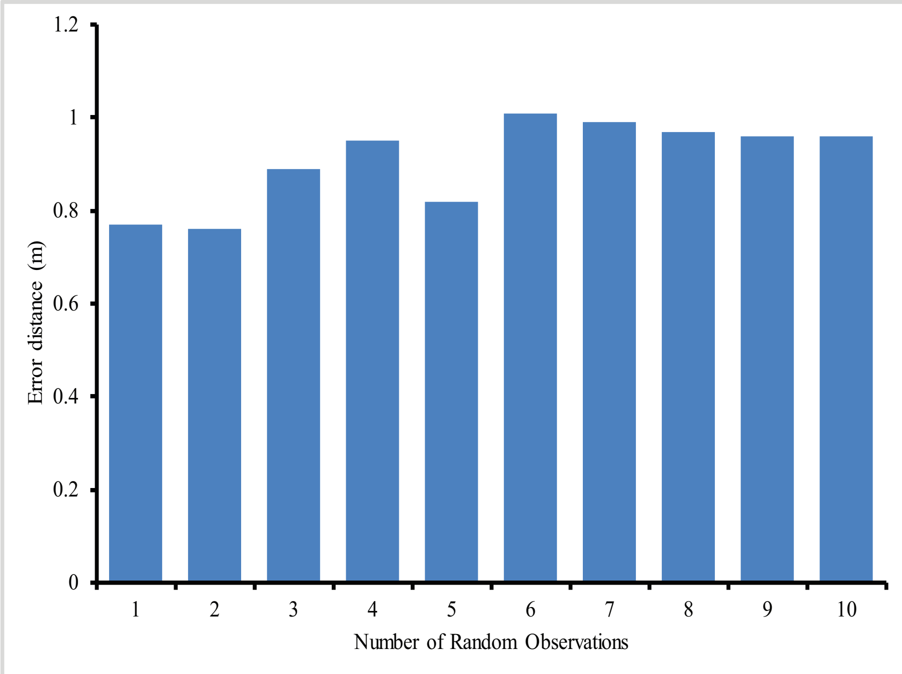

Figure 4.30: Random experiment of localization error of PLD with six anchor nodes in each cluster.

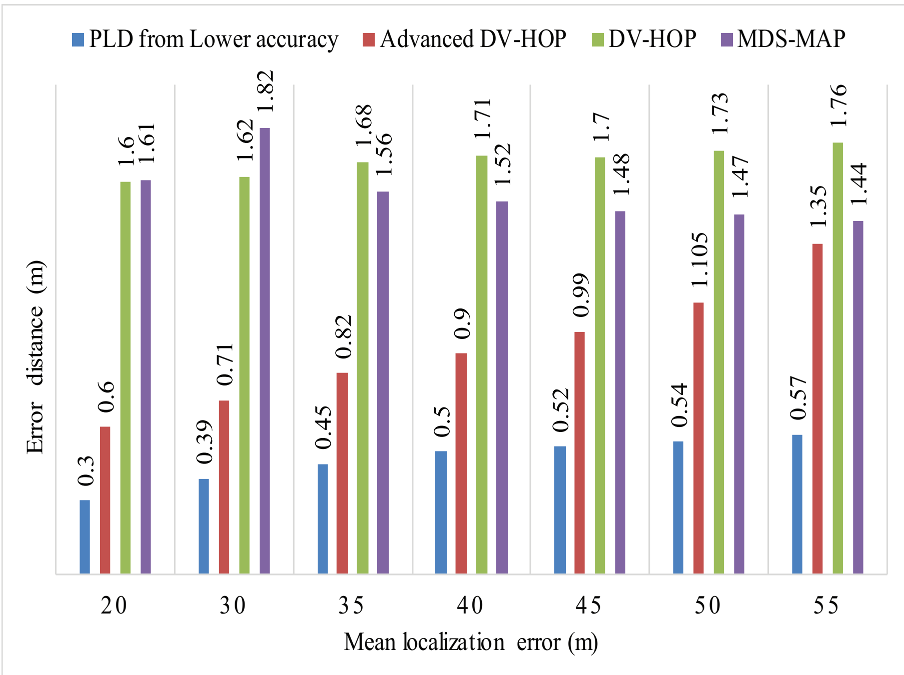

Figure 4.31: Mean localization error of PLD, DV-Hop, Advanced DV-Hop and MDS-MAP.

4.6 Summary

In this chapter, we proposed a new algorithm for 3D based localization algorithm. The proposed technique is based on Parametric Loop division and subdivision surfaces for 3D space. In a PLD scheme, a region of network is subdivided into pairs with the addition of extraordinary nodes in its control ring matrix. Three nodes are selected to complete a triangulation. For generating a parametric point, mid point is computed and by taking step size that falls within the network boundary.

The proposed technique provides superior localization accuracy and network coverage, due to having enough anchor nodes in a boundary of the network. Even if a node failure or not having enough node in each iteration of PLD network, the control is still transferred to the next iteration, resulting in continuity of operation. Parametrization process also helps in low computation cost and energy saving. The proposed algorithm provides better localization accuracy as compared to existing range-free solutions presented in the literature.

Chapter 5

PLD Denoising with Extened Kalman Filtering

In Chapter 4 we presented the parametric loop division (PLD) localization method. In this chapter, we will enhance the PLD method using extended kalman filtering (EKF) in presence of noise, especially for additive Gaussian noise (AGN), white noise and intelligent noise that considered in recent localization algorithms. The effect of noise in measurement of WSN localization is significant, as [316] presented a flip and flex ambiguities of noise measurement for distributed WSN. To minimize noisy distribution, authors in [316] described a robust idea of clusters and quadrilaterals. But in case of large-scale network the complexity and energy increases, which leads to a major drawback. Researchers has also identified the influence of noise in many localization systems, but there is no standardized solution to avoid noisy measurement data during localization process. This is basically dependent on the type of sensor and even environmental factor.

Noise is considered in some measurement techniques, like latreration, angulation and proximity. In lateration, all three circle intersect at one point, which is the location of the target node if the noise is not considered. But in presence of noise, all these circles overlapped and target node may not be inside the intersection region. Similarly, in angulation process, if noise is fairly considered, the target will never intersect at the same point, instead a region is defined where the target node is likely to be. Some algorithms used combination of techniques to reconstruct localization coordinates using well-known techniques like extended kalman filtering. In this Chapter, we enhance our PLD algorithm using extended kalman filtering to deal with noisy data in computation. The EKF presents best estimation for data in presence of different kind of noise like AGN, white noise and intelligent noise. For the sake of clarity, we referred to our PLD algorithm as classic-PLD on which we are adding EKF to deal with noise in the system.

5.1 Distance Estimation

Most localization algorithms only depend on the availability of distance from an anchor node to the target node. The statistical feature of the algorithm is only based on distance estimation properties. In order to perform accurate computation, it is very important to know all distance measurements along with signal strength values and weight. Let us review the well-known distance estimators for AGN and long-normal models with their statistical properties.

5.1.1 Additive Gaussian Noise (AGN) Model

Assuming that a distance measurement is effected by a noise that gives a right positioning of the system. The model of the distance is written as:

$$b = d + \eta \tag{5.1}$$

where η is a random variable representing the characterization of noise, d is an accurate distance and b represents measured distance. If a measurement is modelled in this way, then we can construct a distance estimator such as $\hat{d} = b$. Thus, using some hardware specific source of technology, the estimator can be defined as:

$$\hat{d} = d + \eta \tag{5.2}$$

The true distance is automatically calculated if the error estimator $E[\eta] = 0$ that gives us unbiased estimator as described in Chapter 3. The error η is usually considered as normally distributed, i.e., $\eta \sim N(0, \sigma^2)$. Similarly, $\hat{d}$ is also considered as normally distributed i.e. $\hat{d} \sim N(d, \sigma^2)$. The derivation is proved by considering the likelihood of measurement b.

$$l(b, d) = \frac{1}{\sigma\sqrt{2\pi}} exp\{-\frac{1}{2}\frac{(b-d)^2}{\sigma^2}\} \tag{5.3}$$

The logarithm of likelihood is taken as:

$$L(b, d) = -\ln(\sigma\sqrt{2\pi}) - \frac{(b-d)^2}{2\sigma^2} \tag{5.4}$$

After that fisher information (FIT) is computed by (3.30).

5.1.2 Additive White Gaussian Noise (AWGN) Model

AWGN is basically due to the random variations of atoms in transceivers circuit, which added unwanted signals in time of arrival (ToA) estimation process. In (5.1), the log normal distribution of $\eta \sim N(0, \sigma_i^2)$ is a white Gaussian noise. The standard deviation is constant and independent of true distance d, presented in vector form, i.e.

$$\hat{d} = [\hat{d}_1, \hat{d}_2, ..., \hat{d}_N]^T \tag{5.5}$$

The effect of AWGN on original signal is shown in Figure 5.1.

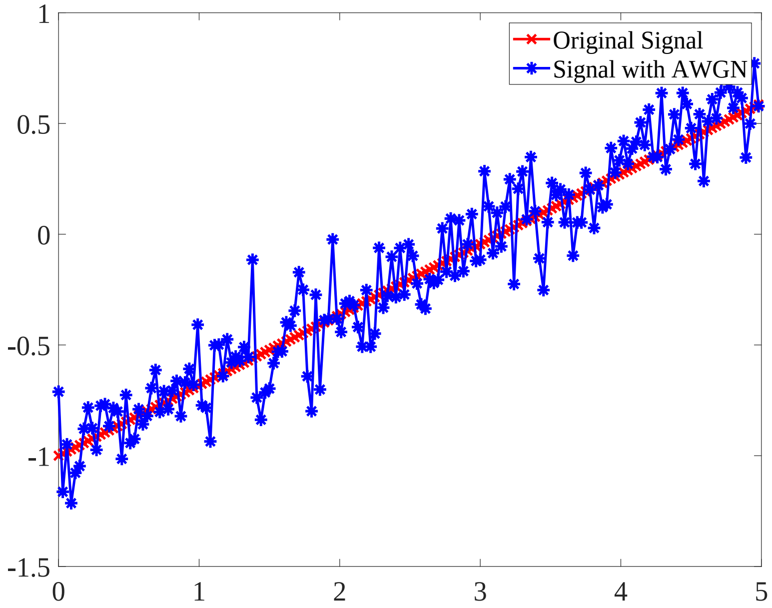

Figure 5.1: The effect of AWGN on original signal.

5.1.3 Multiplicative Noise Model

Assuming our model of distance estimation from (5.1)

$$z\hat{\tau}_i = z\tau_i + z\bar{\eta}_i \tag{5.6}$$

where z denotes the multiplicative variation in measured distance, noise and estimated distance, $\bar{\eta}$ denotes the Gaussian noise. Then the ToA estimator is written by CRB as [317]:

$$\sigma^2(\hat{\tau}) \geq \frac{1}{8\pi^2\beta^2 SNR} \tag{5.7}$$

where β is effective bandwidth of i^{th} anchor node given by [318].

$$J_i = J_t \frac{\varrho}{d_i^{\alpha}} \tag{5.8}$$

where ϱ is a loss related to frequency, antenna height or other physical effects. α is path loss exponent with a value between $(2.0$ and $5.0)$ and J_t is transmitted power. SNR is an fraction of transmitted power and power of noise, i.e., $SNR = \frac{J_i}{\eta_0}$. From (5.4, 5.5, 5.6), the standard deviation is computed by:

$$\bar{\sigma}_i = \Upsilon \cdot d_i^{\alpha/2} \tag{5.9}$$

where

$$\Upsilon = c\sqrt{\frac{\eta_0}{8\pi^2\beta^2 J_t \varrho}} \tag{5.10}$$

Finally, the estimator model of (5.1) is written as:

$$\hat{d}_i = d_i + \Upsilon d_i^{\alpha/2}\omega \tag{5.11}$$

Where ω is noise with mean of zero and unit variance. Therefore, the model (5.11) is multiplicative because of $d_i^{\alpha/2}\omega$

5.2 Kalman Filters

The uncertainty spreads data across region which causes many problems in a localization system. Kalman Filtering (KF) is an optimal solution to gather data on a defined area and even rectify the coordinates for nodes. Many researchers use KF in localization but do not get optimal estimator because KF is a statistical tool that estimate stochastic state from noisy sensor measurement.

1. KF is an optimal tool because it leads to optimal results with respect to certain criteria, like MSE. In addition, KF it gets all the information for computation.

2. KF is recursive, which means that all data are not required to be stored in a matrix

and new values are reproduced when needed. For PLD, this is why we are using EKF that supports this property of recursion. Only those items are stored along with noise signal will be used to calculate the RSS.

3. KF can filter out those unnecessary data not needed for distance measurement, e.g., angle information.

5.2.1 Kalman Filter in WSN Localization

KF is based on an iterative approach, in which knowledge of noise in distance estimation is used to filter the noise parameters from original signal. However, this system gives problems when noise modelling is needed. Therefore, by using KF we can only measure the noise by approximation but do not approach the real noisy distribution. The KF is suitable for linear stochastic processes, but our model of PLD is based on non-linear optimization and computation. Thus, extended kalman filtering (EKF) is a suitable choice for noise measurement in PLD.

There are many parameters that that EKF uses to model PLD. The anchor node is modelled by only using the knowledge information of coordinates to redesign the distance vertex from anchor to parametric points. In 3D space, the distance is measured using the form $d = \sqrt{(x - x_i)^2 + (y - y_i)^2 + (z - z_i)^2}$, where x_i, y_i, z_i are the coordinates of anchor nodes. A major question arises–Why do we need EKF? First KF is only used for Gaussian distribution. Furthermore, KF only works on linear functions PLD is non-linear and involves multiplication. If we give AGN with non-linear parameter, the output will not be Gaussian. Thus, we need to consider nonlinear functions, which does not follow Gaussian distribution. The only solution is Taylor series that only comes with EKF.

In PLD, the proposed solution uses non-linear estimation to compute the location of target nodes in the area covered by a set of anchor nodes. If these nodes are not properly distributed, leads to a non-rigid graph with a non-linear distribution. In presence of noise, classic-PLD might result in large localization error. Therefore, refinement of node coordinates is required that deteriorates the PLD accuracy, seriously weakening the localization process in presence of noise. The lower bound accuracy is estimated for the given idea along with its analytical framework. By simulating the noise factor combining with PLD algorithm, the node refinement using EKF achieves better positioning accuracy regardless of the shape of the network topology, deviation of noise statistics, distance, and the node degree of the network, with localization error distance of $0.42m$ and standard deviation of $0.26m$.

5.2.2 EKF for WSN Localization

EKF is most widely used to linearizes the data observation in case of nonlinear observational models. In the literature the application of EKF was found in neural networks [319], robotics [320], depth recovery [321], and satellite system [322]. EKF remains the same in all the applications but its computation complexity gradually varies, depending upon how state information is explained and updated. Some other KF are also described in literature, like Iterated EKF, Central difference filter (CDF) and unscented kalman filter (UKF). All of these filters are based on EKF with some variations.

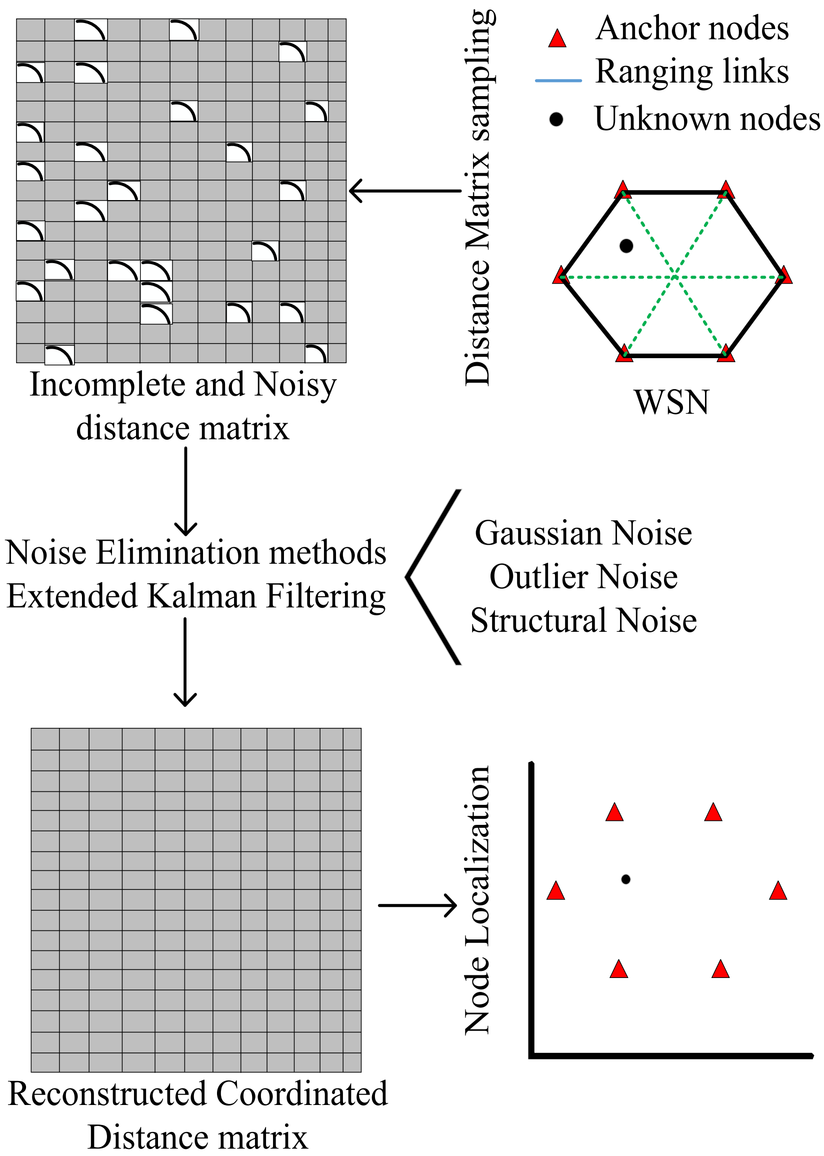

Figure 5.2: Noise-toleration in WSNs Localization.

5.3 Problem Statement and System Model

5.3.1 Problem Statement

Nodes are randomly deployed in a 3D space used for environmental monitoring and event detection. Some of the nodes are anchors with known position. In presence of noise, the distance will be corrupted and needed to be refined through certain process. Generally, as shown in Figure 5.2, a localization scheme in case of noisy data, will be accomplished in three phases: 1) sampling of data that is basically a distance matrix from anchor node to target node, 2) reconstruction of distance matrix after refining the incomplete and noisy data and 3) computation of localization of target nodes.

For noise modelling in PLD, a distance matrix of incomplete and noisy data is drawn, and nodes coordinates are estimated using EKF framework for achieving higher accuracy. The key idea of PLD is already explained in Chapter 4.

5.3.2 System Model

In the system modelling, the EKF framework is added to the classic-PLD, algorithm. In classic-PLD the non-overlapped network [**K**] was considered with volume [**V**]. It was assumed that nodes are deployed randomly in a 3D sensing space as described in (4.7) and (4.8). The distance between two nodes will be calculated by $d_{ij} = \sqrt{(n_i - n_j)^2}$. The distance computation is carried out using statistical RSSI measurement model.

Let φ denotes the number of nodes with unknown position and η as the number of anchor nodes, giving k$\times$ φ and k $\times$ η nodes in each PLD network. For proper formation of Looping triangle, a constant ρ is taken, whose value should be not less than 4. Nodes have proximity information, such that $P_{ij} \in \beta_k = \{1, 2, ...\varphi + \eta\}$, anchor nodes n_η, geographic physical distance d_{ij} are used to compute the position of n_φ, where $\varphi \in \{\eta + 1, \eta + 2, ...\eta + \varphi\}$ for every PLD network. Assuming a system having n small PLD network, and no repetition in anchor nodes coordinate information, so there will be (N/K) number of possible ring matrices which satisfy $(\frac{\mathrm{N}}{\mathrm{K}}) \leq N_p \leq N$. The Euclidean distance matrix (EDM) data may be incomplete or corrupted due to noise for LOS and NLOS scenario. The system for noise in case of LOS and NLOS is modelled as:

$$\eta_{i,j} = \begin{cases} v_{i.j} & LOS; \\ v_{i.j} + b_{NLOS} & NLOS; \end{cases} \tag{5.12}$$

$$\rho_{\eta_{i,j}}^{LOS} = \frac{1}{\sqrt{2\pi\sigma_{i,j}^2}} \exp(\frac{\eta_{i,j}^2}{2\sigma_{i,j}^2}) \tag{5.13}$$

$$\rho_{\eta_{i,j}}^{NLOS} = \frac{1}{\sqrt{2\pi\sigma_{i,j}^2}} \exp(-\frac{(\eta_{i,j} - \mu_b)^2}{2\sigma_{i,j}^2}) \tag{5.14}$$

$$\rho_{\eta_{i,j}}^{NLOS} = \frac{1}{\beta} \lceil \tau \left(\frac{\eta_{i,j} - n_{max}}{\sigma_{i,j}} \right) - \tau \left(\frac{\eta_{i,j} - n_{min}}{\sigma_{i,j}} \right) \rceil \tag{5.15}$$

where $v_{i,j}$ representing the noise measurement, i.e., $v_{i,j} \sim \eta(0, \sigma_{i,j}^2)$ which follows some spatial distributions such as Gaussian, uniform and exponential distribution. β denotes NLOS fractional noise computed by $\beta = n_{max} - n_{min}$ with CDF τ. The b_{NLOS} explained the Gaussian non-linear distribution, i.e., $v_{i,j} \sim \eta(\mu_b, \sigma_b^2)$. Hence the PDF for NLOS is changed to (5.14), while in case of exponential distribution function $(b_{NLOS} \sim \eta(\lambda)$, the PDF of $\eta_{i,j}$ is given by:

$$\rho_{\eta_{i,j}}^{NLOS} = \frac{\lambda}{2} \exp[-\lambda \left(\eta_{i,j} - \frac{\lambda^2 \sigma_{i,j}^2}{2} \right) \phi \left(\frac{\lambda^2 \sigma_{i,j}^2}{\sqrt{2\sigma_{i,j}}} \right)] \tag{5.16}$$

where, ϕ represents a complementary error function and λ is a positive constant. Indoor environment assumes uniform distribution because of huge RSSI variations and multipath transmission as described in Appendix C.

5.4 EKF Framework for Noisy PLD Algorithm

Assuming a set of anchors $A = A_1, A_2, A_3, ...A_m$ with positive vector (x, y, z) are deployed over a region of interest, where $m \geq 4$. A reference anchor node can select another two anchor nodes to from a triangulation. The mid-point is measured within a control ring network for proper operation. Let $\vec{A}_1$ be a reference node, the distance from reference node and all other nodes with the addition of noise is computed as follows:

$$\mid \vec{D}_{ik} \mid = \sum_{k=2}^{m} \mid \vec{D}_{A,k} + \eta_{A,k} \mid \tag{5.17}$$

where, η denotes the Gaussian noise based on path loss exponent value. The noise factor is computed by random function with both LOS and NLOS scenarios. There are two environmental conditions that affect the value of path loss which are LOS and NLOS condition. The range of path loss exponent is $1-2$ and $2-5$ for LOS and NLOS conditions respectively. The noise factor random function is given by:

$$\eta_{A,k} = \begin{cases} LOS^T + rand(m,1); \\ LOS = randi([n_{min} n_{max}], 1, m) \\ NLOS^T + rand(m,1); \\ NLOS = randi([n_{min} n_{max}], 1, m) \end{cases} \tag{5.18}$$

In a classic-PLD algorithm where localization error does not affect the noise parameters the computation of step size is given by (4.12). After that, we check RSSI values that can be recorded at each parametric point

$$f(P_{RSSI}) = \begin{Bmatrix} Preloc_{cord} & (P_{RSSI}) \leq \text{threshold} \\ * & \text{otherwise} \end{Bmatrix} \tag{5.19}$$

If the sum of RSSI values are smaller than the threshold value, it is chosen as a pre-localized node (A_{ik}) and the iteration stops at this point. The RSSI will fluctuate due to noise factor that always affects the performance of localization algorithms. To overcome this effect of noise, the weighting concept is introduced along with EKF framework for intelligent, AGWN and AGN naive noise as derived in Appendix D. The derivation is nonlinear, which is why an EKF framework is adopted for computation of localization. For most indoor localization having adverse effect on non-linear optimization, EKF is a best solution to use. Furthermore, we have a multiplicative noise effect in PLD, which spreads data element and surely affects the accuracy of the PLD. The refinement of node coordinates using EKF really stabilizes the system even in the presence of noise. EKF framework has three variations namely, P-model (position), PV-model (position, velocity) and PVA-model (position, velocity, acceleration) [323]. The PLD algorithm only uses reference coordinates, RSSI, and distance to compute node position, therefore, P-model EKF is appropriate for PLD algorithm. For refinement of node coordinates in PLD, EKF framework is completed in three phases, namely, initialization, prediction and update states described below.

Initialization State: This step is basically modelled using EKF algorithm as follows:

$$\begin{cases} x_k = f(x_{k+1}) + W_{k-1} \\ x_k = f(x_{k+1}.t_k) + W_{k-1}.t_{k-1} \\ z_k = h(x_k) + v_k \\ z_k = h(x_k).t_k + v_k.t_k \end{cases} \tag{5.20}$$

where, W_{k-1} is a noise factor of EKF having normal distribution with average of zero and its co-variance matrix Q_k and R_k, i.e., $W_{k-1} \sim \eta(0, Q_k)$ and $W_{k-1} \sim \eta(0, R_k)$. x_k and x_{k-1} are the state vector at time instants t_k and t_{k-1}. Whereas f is a non-linear function used for prediction of data information depending on previous measurement. This is used to described non-correlation state function h between x_k and z_k.

Prediction State: After initialization, the variable needed to predict used in step 1. Priori state $\hat{x}_{k|k-1}$ is another factor that determines the historical data information from posteriori state, we have:

$$\begin{cases} \hat{x}_{k|k-1} = F.\hat{x}_{k-1|k-1} + B_k.u_k \\ P_{k|k-1} = F.P_{k-1|k-1}F^T + Q \end{cases} \tag{5.21}$$

where, F is a transition or iterations, u_k represents the input system and B_k is a input matrix. The variable of $P_{k|k-1}$ and $P_{k-1|k-1}$ are the information state gain from covariance data matrix Q.

Update State: In this step, an innovation vector $\hat{Y}_k$ from (5.20) is revised as :

$$\begin{cases} \hat{Y}_k = z_k - h(\hat{x}_k) \\ S_k = H_k.P_{k|k-1}.H_k^T + R_K \\ \hat{x}_{k|k} = \hat{x}_{k|k-1}.K_k.\hat{Y}_k \\ K_k = P_{k|k-1}.H_k^T.S_k^{-1} \\ P_k = (l_d - K_k.H_k).P_{k|k-1} \end{cases} \tag{5.22}$$

where H_k represents the Jacob matrix based on expected computation result given by $h(\hat{x}_k)$. The posteriori state is an estimated computation from EKF framework taken from (5.22). Noisy distance in PLD algorithm is used as a parameter for computing target node estimation. To reduce the noise, EKF is added to filter out the PLD estimation mixed with unbiased parameter noise. There are two computation steps, first estimation is taken from PLD algorithm based on pre-localized node boundary (which added some noise to classic PLD). The second phase is to improve the estimation output in update state using EKF framework. The initial estimated results are linearized by using EKF. The EKF with the combination of PLD also described in a same way based on estimation update (output) from PLD algorithm with noise addition.

$$x_k = PLD_{RSSI,\eta}[f(x_i y_i z_i)] \tag{5.23}$$

In PLD algorithm, initially five to six anchor anchors are considered for initial simulation. The reference distance values from target to anchor node are taken within a working boundary $z_k = [d_1 d_2 ... d_n] \rightarrow \sum d_n$. The resulted coordinates from PLD with noise modelling can be used for co-variance matrix for EKF framework, derived as:

$$P_0 = \begin{bmatrix} \sigma^2 x_{PLD,\eta} & 0 & 0 & 0 & 0 \\ 0 & \sigma^2 y_{PLD,\eta} & 0 & 0 & 0 \\ 0 & 0 & \sigma^2 z_{PLD,\eta} & 0 & 0 \\ 0 & 0 & 0 & 0 & 0 \\ 0 & 0 & 0 & 0 & 0 \end{bmatrix} \tag{5.24}$$

All the variables, including initialization state and co-variance matrix declared in priori state are now predicted using

$$x_k = PLD_\eta[x_i \ y_j \ z_k] * F \rightarrow f = \begin{bmatrix} 1 & 0 & 0 & 0 & 0 \\ 0 & 1 & 0 & 0 & 0 \\ 0 & 0 & 1 & 0 & 0 \\ 0 & 0 & 0 & 0 & 0 \\ 0 & 0 & 0 & 0 & 0 \end{bmatrix} \tag{5.25}$$

$$P_k = F * P_0 * F^T + Q \rightarrow Q = P_0 \tag{5.26}$$

where, Q denotes the co-variance matrix and P_k denotes the co-variance information. The output after predicting the state from (5.25) and (5.26) is an updated data information multiplied with filtering gain K_k we have:

$$K_k = P_k.H_k^T.S_k^{-1} \tag{5.27}$$

where H_k represents the observation data from resultant Jacobin matrix. This can be obtained by comparing data coordinates $x_{PLD,\eta}$ $y_{PLD,\eta}$ $z_{PLD,\eta}$ with estimated distance effected with noise factor (PLD_η) we have:

$$H_{k_\eta}^{\sigma} = \begin{bmatrix} \frac{x_1-\hat{x}_1}{d_1} & \frac{y_1-\hat{y}_1}{d_1} & \frac{z_1-\hat{z}_1}{d_1} \\ \frac{x_2-\hat{x}_2}{d_2} & \frac{y_2-\hat{y}_2}{d_2} & \frac{z_2-\hat{z}_2}{d_2} \\ \cdots & \cdots & \cdots \\ \frac{x_n-\hat{x}_n}{d_n} & \frac{y_n-\hat{y}_n}{d_n} & \frac{z_n-\hat{z}_n}{d_n} \end{bmatrix} \tag{5.28}$$

$$d_n = \sqrt{(x_i - \hat{x}_i)^2 + (y_j - \hat{y}_j)^2 + (z_k - \hat{z}_k)^2} \tag{5.29}$$

The final co-variance matrix S_k is arranged by combining a co-variance matrix P_k with noise co-variance distance R_k gain from original estimation and can be derived as follows:

$$\begin{cases} S_k = H_k.P_k.H_k^T + R_k \\ R_k = diag(\sigma^2 d_1 \ \sigma^2 ... \sigma^2 d_n \\ P_0 = (P_k - K_k * H_k) * P_k \end{cases} \tag{5.30}$$

The posterior state as the estimation result of EKF algorithm (X_{EKF}, Y_{EKF}) is represented as:

$$\begin{cases} Y_k = z_k - h_k \\ h_k = [d_1 d_2 ... d_n] \\ X_{k+1} = X_k + K_k.Y_k \end{cases} \tag{5.31}$$

The flowchart of the proposed PLD scheme with EKF is shown in Figure 5.3.

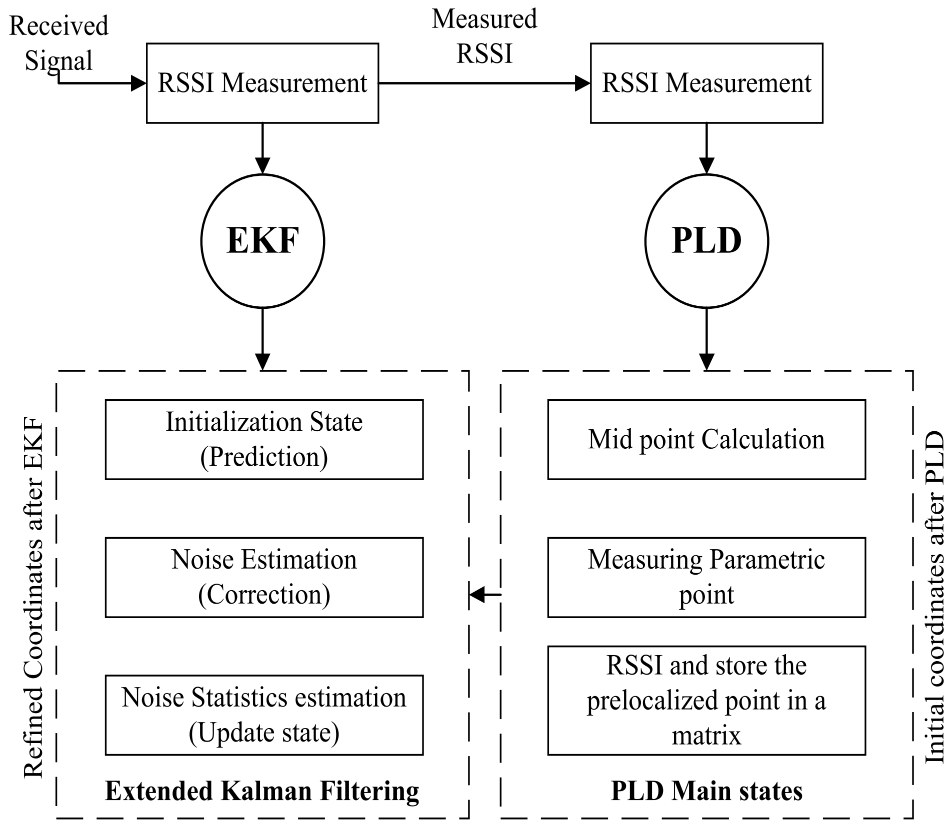

Figure 5.3: PLD and EKF structuring.

5.5 Simulation Results

In this section, we analyze the accuracy of PLD algorithm by simulating EKF framework in Matlab. In a 3D space of $1000m \times 1000m \times 500m$, 50 anchor nodes are deployed randomly and at each iteration and location of anchor node is changed randomly. A total of 100 iterations are executed that allow a 3D space to cover almost 5000 anchor nodes. The localization computation that generate four localized point as the target node in case of classic PLD algorithm is shown in Table 4.2. In an initial simulation, the sum of error of 3.57 and a MLE of $0.89m$ is recorded. The localization error is affected by the step size Δ in a classic PLD algorithm. Therefore, assuming that this value should not be high for small coverage space, otherwise the target node cannot be pre-localized in a region. For the authenticity of classic PLD algorithm, an average, minimum and maximum error is also recorded against $A = 5$ and $A = 6$ as shown in Table 4.4 of Chapter 4. We analyze the accuracy of PLD algorithm by combining EKF framework with different noisy environments, such as naive weighting noise and intelligent weighting noise. RSSI may fluctuate and even gets weaker in longer distance as show in Figure 5.4.

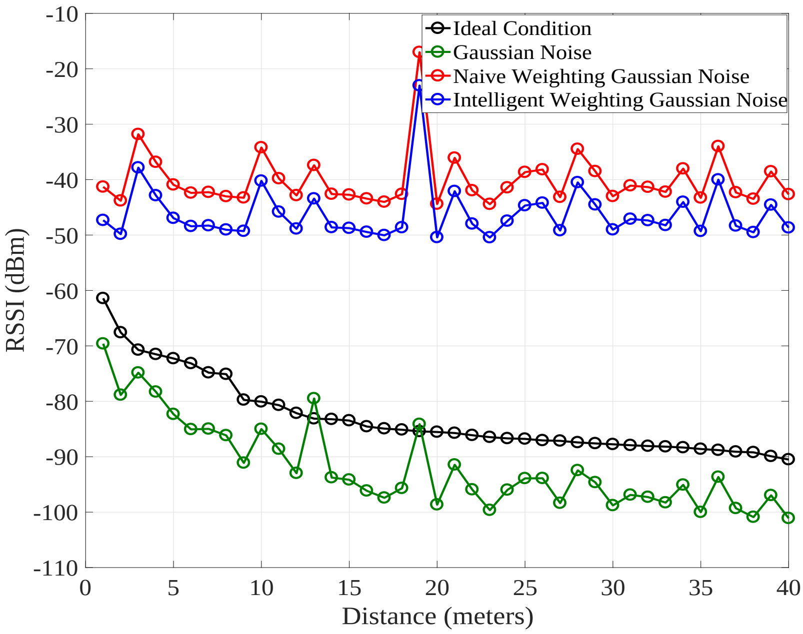

Figure 5.4: Distance vs RSSI.

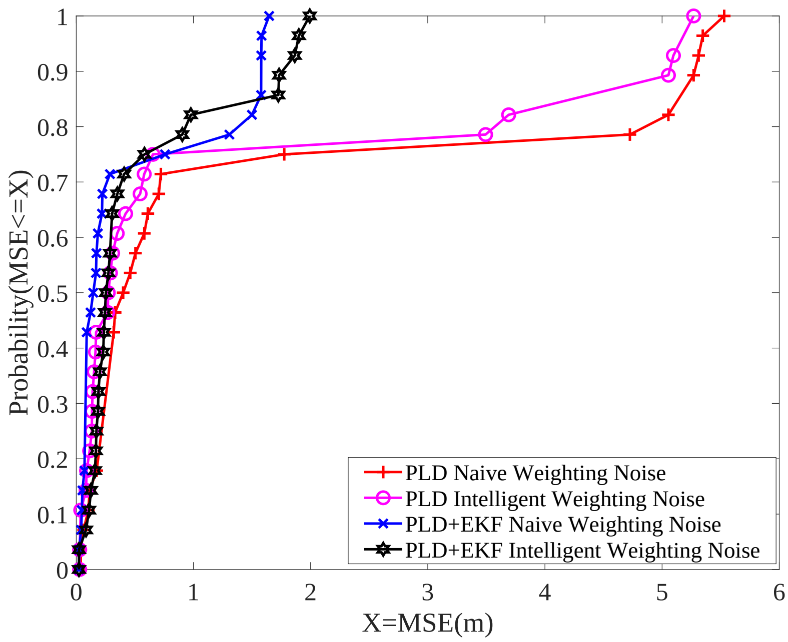

Figure 5.5: CDF of MSE for 5 anchor nodes.

The Gaussian noise gives small fluctuation in longer distance. The error distance is checked for all noise modelled using CDF for analyzing MSE values. The three main factors that affect the localization computation are the number of anchor nodes, the kind of noise and the type of algorithm used along with noise refinement framework.

PLD gives high refinement accuracy with EKF framework. With 5 anchor nodes, the combination of PLD and EKF algorithm with naive noise has error estimation range between $0.042m$ to $1.64m$ as shown in Figure 5.5. While adding intelligent noise to the PLD with EKF algorithm has almost same error estimation range between $0.023m$ to $1.99m$. It is very different with the classic PLD algorithm without refinement process by EKF algorithm, the estimation error can reach $2.53m$.

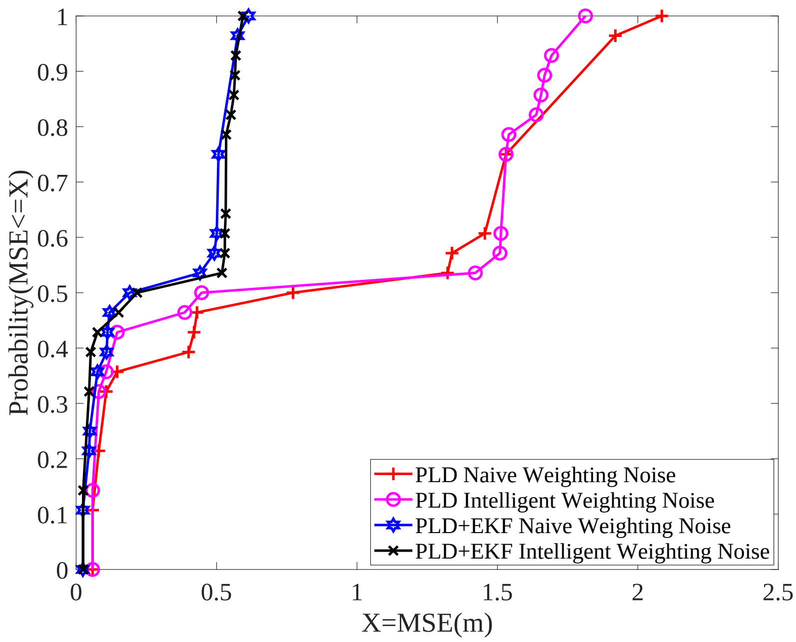

Figure 5.6: CDF of MSE for 6 anchor nodes.

With 6 anchor nodes, the results are shown in Figure 5.6, with estimated data in Table 5.2 and Table 5.3. It is being observed that localization error in case of naive and intelligent noise is decreasing. The use of EKF framework can gather the data elements on the central point that helps to minimize the localization error.

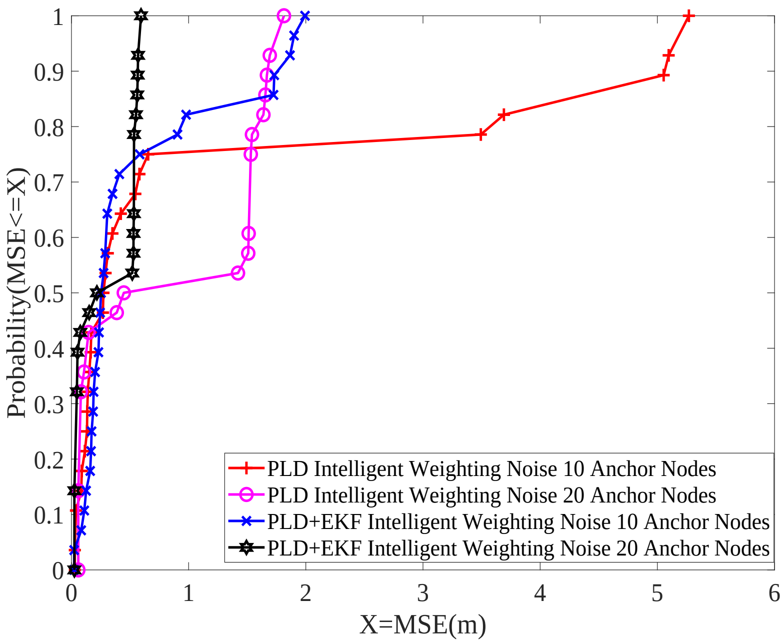

Figure 5.7: CDF of MSE with intelligent weighting noise.

However, the estimation error is the same for both naive and intelligent noise, i.e., $0.305m$. The range is slightly different, adding naive noise the estimation error is $0.99m$ that is higher as compared to intelligent noise having error of $0.65m$. Second factor, the number of anchor nodes also affects the localization error. We gradually increased the number of anchor nodes in the same deployment region, the effect is shown in Figure 5.7 and Figure 5.8. The results shows that increasing number of anchor nodes will gives favourable effect for both classic PLD and PLD with EKF framework.

Simulation results show that by increasing anchor percentage with intelligent noise the PLD algorithm has maximum error of $0.57m$ as shown in Table 5.4. Similarly, in case of naive noise addition, PLD algorithm with EKF framework achieves a maximum error of $o.61m$ as shown in Table 5.5.

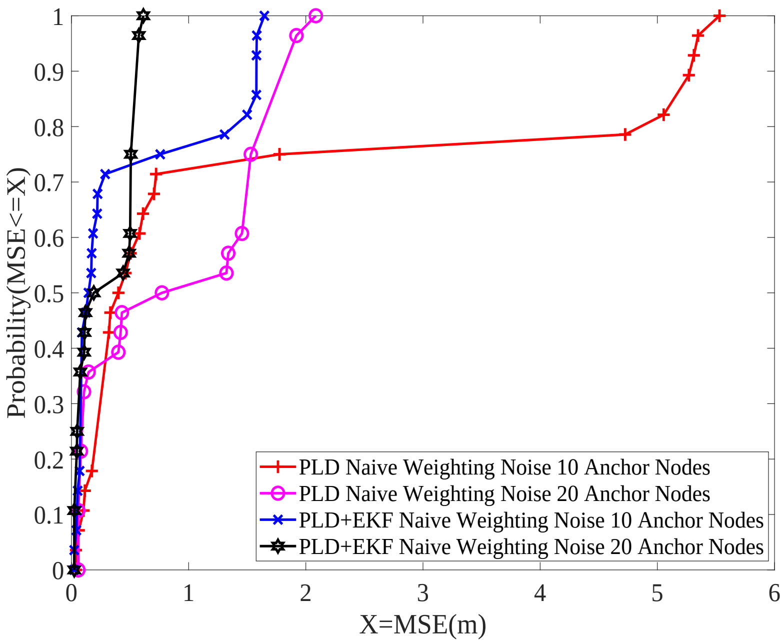

Figure 5.8: CDF of MSE with naive weighting noise.

The overall average estimation error is less than 1.8 m in the presence of naive and intelligent noise. The result from output state shows that using the combination of EKF framework along with PLD and intelligent and naive noise give higher accuracy up to 89.57% as shown in Fig 5.9. The PLD algorithm also tested by increasing the number of anchor nodes gradually. We observed that the scheme even gains accuracy up to 90.84% by using only 20 anchor nodes as shown in Figure 5.10. Comparison of classic PLD algorithm and PLD with denoising scheme by EKF frame work with $A = 5$ and $A = 6$ is given in Table 5.1.

Table 5.1: comparison of MSE, based on additive and multiplicative noise.

Nature of Experiment	$A = 5$	$A = 6$
Classic PLD Algorithm	1.435m	0.897m
PLD + Naive weighting noise	1.619m	0.955m
PLD + Intelligent weighting noise	1.353m	0.966m
PLD + EKF + Naive weighting noise	0.496m	0.263m
PLD + EKF + Intelligent weighting noise	0.571m	0.263m

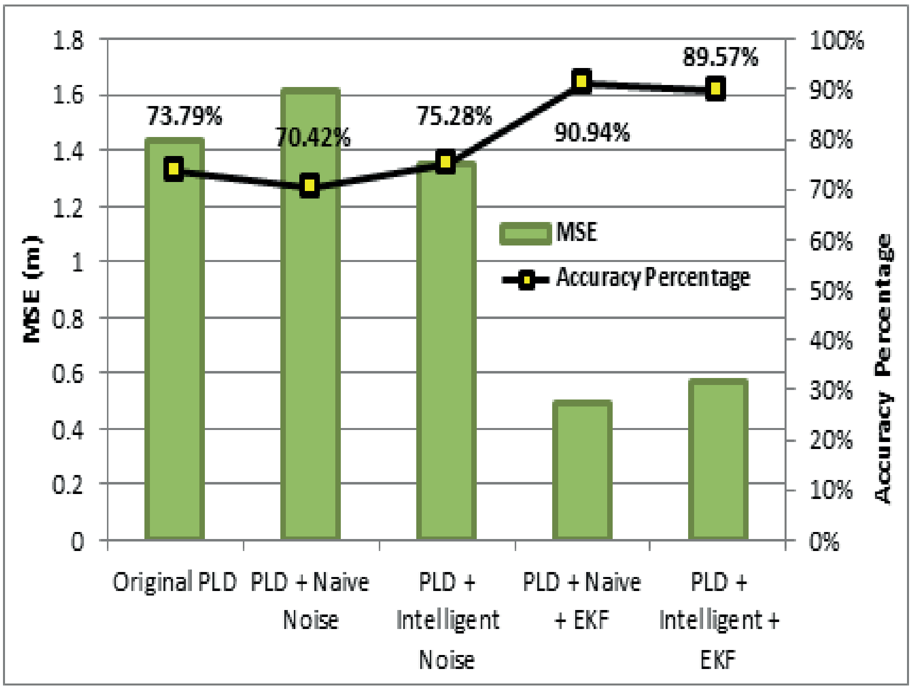

Figure 5.9: Estimated error vs accuracy with 6 anchor nodes.

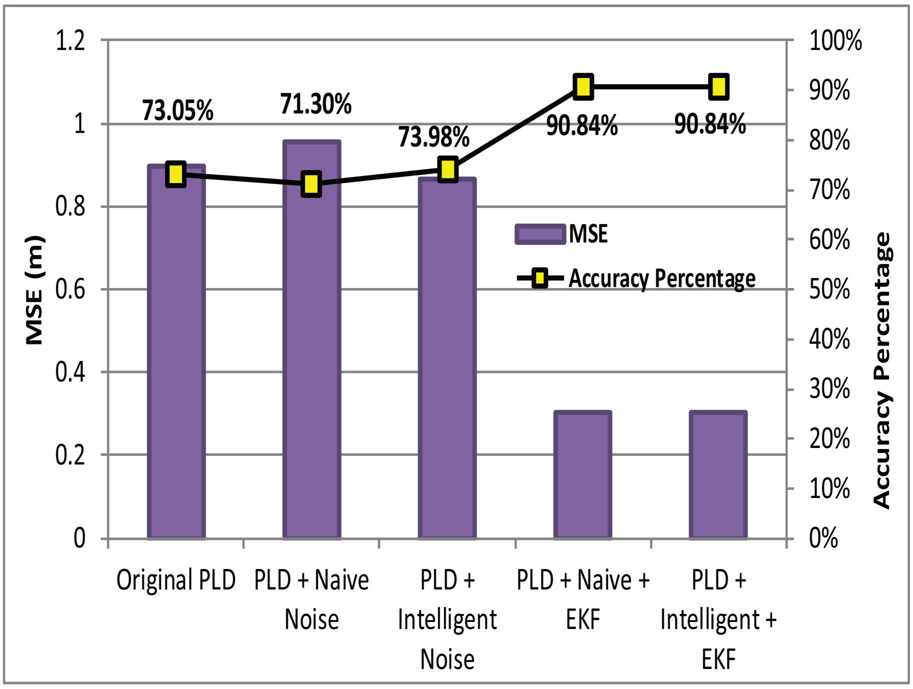

Figure 5.10: Estimated error vs accuracy with 20 anchor nodes.

The PLD algorithm is tested with combination of EKF framework in the presence of naive noise, the naive noise factor was considered as 0.1 during the initial simulation with a mean of zero and standard deviation is set to be 5% of the distance. Six anchor nodes were deployed with a 10 target points in each iteration. The data elements were spreads in case of naive noise and EKF framework. Therefore, the standard deviation is higher than the mean value.

Table 5.2: comparison of classic PLD with Naive noise and Refine EKF PLD algorithm, $A = 6$ and $N = 1, 2, ...10$.

True Position			**Estimated Location (PLD + Naive Noise)**			**Error (m)**	**Refined Coordinates (PLD+EKF+Noise)**			**Error (m)**
x	y	z	$\hat{x}$	$\hat{y}$	$\hat{z}$	MSE	$\hat{x}$	$\hat{y}$	$\hat{z}$	MSE
10.99	11.95	14.45	11.18	12.13	14.63	0.32	11.02	12.01	14.51	0.09
11.31	12.10	14.76	14.53	15.15	17.68	5.31	11.68	13.30	15.73	1.58
17.80	18.47	20.97	17.83	18.46	21.00	0.04	17.81	18.45	20.99	0.02
20.18	20.76	23.26	20.51	20.95	23.53	0.46	20.26	20.82	23.40	0.17
11.35	12.13	14.74	14.71	15.27	17.82	5.53	11.73	13.34	15.79	1.65
17.12	17.91	20.34	17.60	18.22	20.75	0.70	17.20	18.01	20.52	0.22
11.62	12.44	15.03	14.69	15.30	17.85	5.05	11.97	13.53	15.99	1.50
17.29	17.67	20.22	17.50	17.99	20.55	0.51	17.26	17.82	20.38	0.22
19.28	19.64	22.11	20.21	20.66	23.22	1.78	19.34	20.09	22.71	0.76
20.85	21.56	24.07	20.83	21.46	24.01	0.11	20.85	21.51	24.04	0.05

The PLD algorithm is also tested with combination of EKF framework in presence of intelligent noise, and the intelligent noise factor was consider as 0.1 as we used for naive noise for the whole simulation process. Six anchor nodes were deployed with a 10 target points in each iteration. The data elements were scattered in case of intelligent noise and EKF framework. The reason behind is that intelligent noise does not affect a mutual distance collection. Therefore, the standard deviation was lower values over than mean, which shows the good performance of EKF framework over noise PLD algorithm.

Table 5.3: comparison of classic PLD with Intelligent noise and Refine EKF PLD algorithm, $A = 6$ and $N = 1, 2, ..., 10$.

True Position			**Estimated Location (PLD + Intelligent Noise)**			**Error (m)**	**Refined Coordinates (PLD+EKF+Noise)**			**Error (m)**
x	y	z	$\hat{x}$	$\hat{y}$	$\hat{z}$	MSE	$\hat{x}$	$\hat{y}$	$\hat{z}$	MSE
17.63	18.14	20.74	17.57	18.08	20.64	0.13	17.65	18.17	20.67	0.08
20.18	20.76	23.26	20.53	21.03	23.59	0.55	20.27	20.99	23.39	0.27
20.02	20.43	22.99	19.99	20.45	22.99	0.03	20.00	20.44	23.00	0.02
11.62	12.44	15.03	14.69	15.30	17.85	5.05	12.31	13.45	16.24	1.72
17.23	17.82	20.32	17.46	17.98	20.52	0.35	17.29	17.86	20.42	0.13
20.85	21.29	23.90	20.65	21.18	23.74	0.27	20.77	21.13	23.88	0.17
17.81	17.82	20.55	17.66	18.06	20.64	0.29	17.59	17.91	20.65	0.25
11.64	12.57	15.08	11.89	12.81	15.32	0.42	11.53	12.42	15.21	0.23
12.50	13.30	15.98	14.79	15.23	17.77	3.49	12.93	13.53	16.74	0.91
20.29	20.98	23.41	20.56	20.94	23.56	0.31	20.43	20.87	23.51	0.20

Similarly, we increased in number of anchor nodes and test the validity of PLD algorithm in the presence of intelligent noise. We observed that only an increase of few anchor nodes and anchor density the localization error decreases by 90.84%. EKF framework along with 20 nodes and intelligent noise can reduce the localization error with scattered data item over a region bounded by the anchor nodes.

Table 5.4: comparison of classic PLD with Intelligent noise and Refine EKF PLD algorithm, $A = 20$.

True Position			**Estimated Location (PLD + Intelligent Noise)**			**Error (m)**	**Refined Coordinates (PLD+EKF+Noise)**			**Error (m)**
x	y	z	$\hat{x}$	$\hat{y}$	$\hat{z}$	MSE	$\hat{x}$	$\hat{y}$	$\hat{z}$	MSE
15.90	8.27	15.32	14.66	7.96	14.28	1.66	15.56	8.38	14.91	0.55
16.43	9.56	16.09	15.54	9.93	14.91	1.53	16.20	9.64	15.62	0.53
14.95	10.71	14.85	15.39	10.77	14.92	0.45	15.14	10.60	14.82	0.22
16.94	11.84	16.53	16.94	11.85	16.45	0.08	16.96	11.83	16.49	0.05
15.79	10.64	15.27	15.74	10.65	15.25	0.06	15.77	10.65	15.27	0.03
16.47	9.56	16.06	15.55	9.98	14.90	1.54	16.22	9.66	15.60	0.53
15.92	8.21	15.27	14.59	7.91	14.27	1.69	15.53	8.35	14.88	0.57
15.79	8.23	12.45	15.74	11.84	16.45	0.08	12.32	6.76	17.21	0.43
10.64	10.37	16.09	15.61	10.25	14.92	1.34	16.19	10.31	15.60	0.58
15.27	20.98	23.41	20.56	20.94	23.56	0.31	20.43	20.87	23.51	0.56

In a same context, we increased in number of anchor nodes and test the validity of PLD algorithm in the presence of naive noise. Naive noise does not gives higher accuracy, but few anchor nodes density along with EKF framework also decreases the localization error to some percent. However, the accuracy is always low for naive noise due to data elements scattered over a boundary of region.

Table 5.5: comparison of classic PLD with naive noise and Refine EKF PLD algorithm, $A = 20$.

True Position			**Estimated Location (PLD + Naive Noise)**			**Error (m)**	**Refined Coordinates (PLD+EKF+Noise)**			**Error (m)**
x	y	z	$\hat{x}$	$\hat{y}$	$\hat{z}$	MSE	$\hat{x}$	$\hat{y}$	$\hat{z}$	MSE
15.90	8.21	15.27	14.47	7.67	14.11	1.92	15.56	8.31	14.82	0.58
16.43	9.56	16.09	15.54	9.93	14.91	1.53	16.23	9.64	15.63	0.51
15.79	10.64	15.27	15.74	10.65	15.25	0.06	15.77	10.65	15.27	0.02
16.94	11.84	16.53	16.94	11.85	16.45	0.08	16.96	11.83	16.49	0.05
16.43	9.56	16.09	15.54	9.93	14.91	1.53	16.23	9.64	15.63	0.51
16.04	8.38	15.40	14.51	7.72	14.15	2.09	15.70	8.47	14.90	0.61
15.96	9.36	15.95	15.41	9.88	14.87	1.32	15.85	9.40	15.52	0.44
15.17	10.64	15.11	15.56	10.63	15.19	0.40	15.33	10.54	15.09	0.19
16.24	10.37	16.09	15.61	10.25	14.92	1.34	16.19	10.31	15.60	0.50
20.29	20.98	23.41	20.56	20.94	23.56	0.31	20.43	20.87	23.51	0.20

We have compared PLD algorithm with naive and intelligent noise, with higher number of anchor nodes with different radio range. Both the framework gives comparable performance as shown in Table 5.6. The number of anchor were increased in each iteration. The number of PLD network also increases with the increase in anchor node density. Furthermore, the noisy distance is also computed along with different noises and EKF framework as shown in Figure 5.11.

Table 5.6: Comparison of naive and intelligent noise with different anchor node density.

Number of nodes	Radio Range	Error with naive noise	Error with Intelligent noise	Number of PLD networks
5	2.23	0.42	0.266	2
6	1.1	0.41	0.264	3
10	0.74	0.38	0.251	4
20	0.56	0.376	0.234	5
25	0.44	0.24	0.221	6
35	0.39	0.254	0.209	7
45	0.5	0.289	0.208	8
55	0.45	0.2454	0.194	9
65	0.41	0.278	0.193	10
75	0.39	0.265	0.188	11
85	0.37	0.243	0.177	12
95	0.36	0.232	0.123	13
105	0.31	0.255	0.198	14

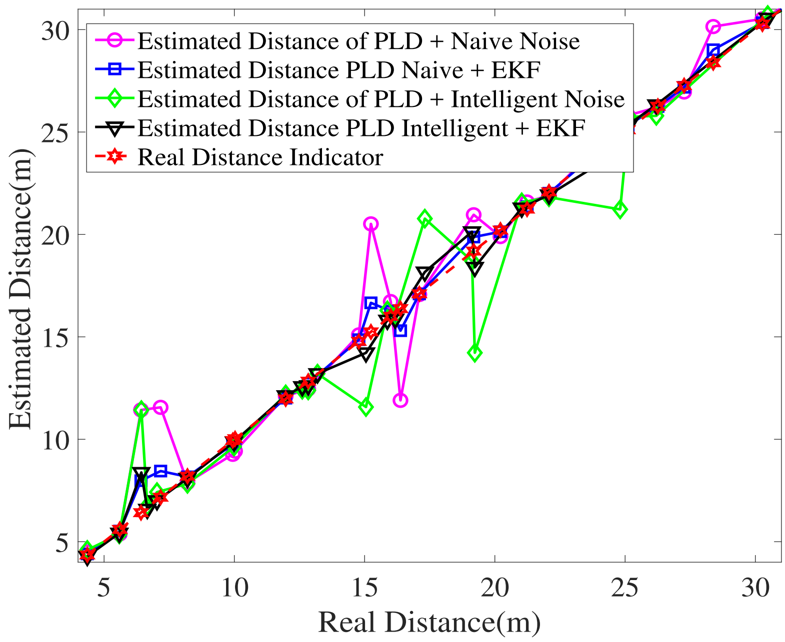

Figure 5.11: Estimated Distance Performance Analysis for 5 anchor nodes.

5.6 Summary

In this chapter, we have analyzed the performance of PLD algorithm in the presence of various noise factors. AGN, AWGN, naive and intelligent noise is added to the distance to check the performance of PLD algorithm. PLD algorithm provides a non-linear computation, thus we added EKF framework along with noise addition to scatter the node coordinates into bounded region. EKF framework also refine the coordinates of the target nodes, which also refines the accuracy of the entire system. The performance of PLD is improved by using the EKF framework, which helps to scattered the data elements within a region.

Chapter 6

Mobile Assisted Localization based on Fuzzy Logic

With the recent advancement in technology, mobile based WSN becomes popular. A comprehensive survey of mobile based system is already presented in Chapter 3. The literature shows that equipping each sensor node with GPS unit makes system costly with high consumption of power, especially for large scale WSNs. A better approach to localize unknown nodes is to use many mobile nodes with GPS units and rove along a known trajectory broadcasting their location coordinates periodically as shown in Figure 6.1. This kind of network structure provides many practical advantages because mobile node is not energy constrained as compared to unknown nodes. Also the accuracy of such system is totally dependent to the design trajectories [324]. Therefore, path planning is a main factor for mobile assisted localization algorithms. As path planning is beyond the scope of this thesis, we only study a mobile assisted localization scheme on fuzzy logic control.

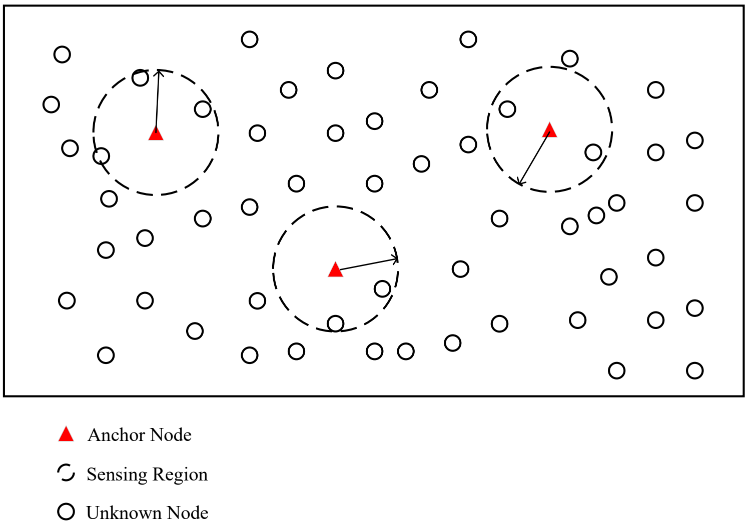

Figure 6.1: Mobile anchor assisted localization.

6.1 Fuzzy Logic

The mathematics of Fuzzy Logic (FL) was introduced in 1965 to model conditions that describe incorrect information [325]. FL is a multi- valued logic control that allows to define intermediate data between conventional system in the form of "High" or "Low", "Yes" or "No"or "True" or "False". In a broader sense, FL is an extension to the multi valued logic with two different meanings. FL gives the same meaning with theory of fuzzy sets which contains classes similar to object oriented programming.

It is also narrated that FL works like a human mind in operative modes based on reasoning and logic. In case of hard computing, the precision and certainty can increase the cost while in soft computing the tolerance for preciseness, low cost solution and uncertainty are handled by FL to achieve the control of characteristics of the problem. FL cannot describe the working of a system while it only explain, what the system must do. Therefore, FL only concentrates with solution of the problem not the mathematical modelling of the system. By this context, we can say that FL is a trade off between exactness and significance. A map of input is reasonably stated to output space, where mapping is a initial point. In case of WSN localization, this initial point is referred to as reference point or an initiator in a system [326]. A simple example of FL is if-then rules explained in artificial intelligence to achieve fuzzy control. However, this solution is man-made interpretation, so the chance of error is always there. Same like EKF, FL also used to model non-linear functions with elective complication to a adequate degree of exactness. Shortly, FL is an inference system contains if-then rules, fuzzy inference engine, fuzzifier and defuzzifier as shown in Figure 6.2.

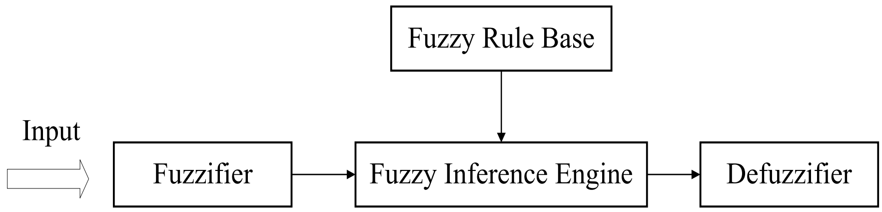

Figure 6.2: The Fuzzy Logic System.

6.2 Benefits of using Fuzzy Logic

In [325], the authors stated that in every research and problem we can derived the same solution without the use of FL. But FL is cheaper and faster. Other benefits of FL include [327].

1. FL provides a flexible solution for almost every problem.
2. The input-output of any problem can be matched with fuzzy system, thus FL can model any nonlinear system.
3. FL is easy to implement and understand because of its simple mathematics. The complexity of FL is low.
4. FL is based on any programming structural derivation, thus it is easy to use. FL can be written in any language.

5. It can be easily combined with a conventional system.

However, FL does not apply to all systems, because for some systems, like image processing do not have a useful way to implement FL.

6.3 Fuzzy Rules

The interpretative values are known as crisp values, which are completely explained and computable. These are also known as singleton values, which are basically the set of fuzzy values. Fuzzy values have several interpretations with different set of values with unclear control setting, where a set of several values are a subset of fuzzy set [328]. To understand a fuzzy set in a given system, one needs to know the description of classical set in a given problem. This classical set is basically a container that includes all the elements used in a system. The membership function in a FL is acting like a curve on which all data sets, including input and output, are mapped. The mapping degree is between 0 and 1. Thus, the crisp value only provides correction to incorrect interpretation.

6.3.1 Connection with Logical Operations

Boolean operator is well known to understand the FL operator. For example, if a crisp value is true or false, the Boolean operator "0" or "1" is used for representation. In uncertain environment, it may be considered like X-AND-Y or X-OR-Y. The OR operator interprets max operation, equivalent to $max(X, Y)$. Another operator is NOT, used for $1 - x$. In summary, in FL, intersection or conjunction is represented by AND, the union and disjunction represented by OR and NOT operator is used to express fuzzy complement.

6.3.2 Conditional Statement in Fuzzy Logic

The conditional statement of if-then rules in FL are similar to the ordinary programming logic. The simple syntax of if-then is $if\ X\ is\ "1"\ then\ Y\ is\ "0"$, where X and Y are the variables with the range of conditions. Conditional statement have three steps:

1. Input fuzification, used to minimize all fuzzy statements into some degree, where "if" is a part of antecedent followed by the fuzified rules.

2. Multiple or nested antecedent is needed to be compressed into single or nested fuzzifier.

3. Implementation of technique, which becomes the membership of the fuzification function.

6.3.3 Fuzzification and Defuzzification

Fuzzification is a process of converting input variables to output variables along with membership function. These are the resultant values also expressing degree of membership values. Defuzzification is used to represent a single value in the set of output data.

6.3.4 Fuzzy Inference Rule

Formulation of input map to output map in FL is known as fuzzy inference. Truth table is used to represents these rules stored in a Boolean operator. A simple representation of such rules based on different input and output values is as follows:

$$\left[\begin{array}{c} if < cond. > then < consequence > \\ if < condition\ 1\ and\ (or)\ cond.\ 2 > then < consequence > \\ if < cond.\ 1\ and\ (or)\ cond.\ 2 > then < cons.\ 1\ and\ (or)\ cons.\ 2 > \end{array}\right]$$

Fuzzy inference in the context of several input variables or rules with one output is shown in Figure 6.3.

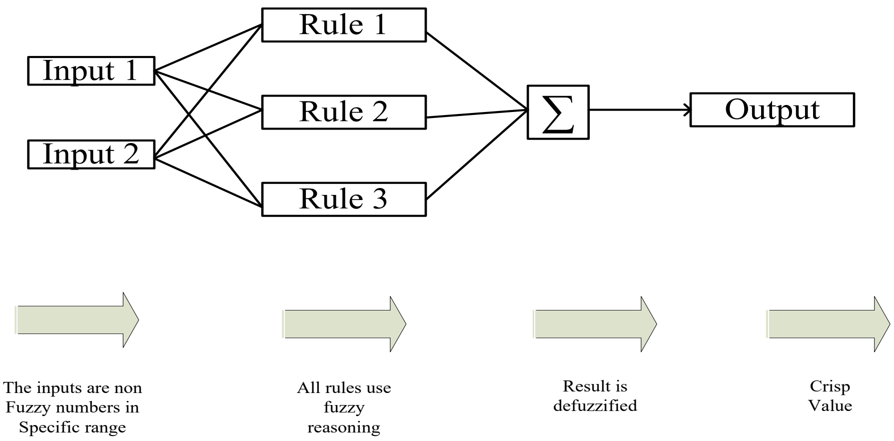

Figure 6.3: The process of Fuzzy Inference.

The process of inference is accomplished in five steps such as the fuzification of the input values, applying fuzzy operator, execution of the conditions and then aggregation of the consequences in defuzzified state.

6.4 Definition and Problem Formulation

The following definitions are used in this Chapter :

Definition 11. Unknown Nodes are those nodes whose location is not known and estimation of their location will be solved as localization problem.

Definition 12. Mobile Anchor Nodes are those nodes that move in predefined manner to assist unknown nodes in their localization process. Their location information is known apriori throughout their trajectory.

Definition 13. Training means the phase in which we find mapping data between RSSI values and their corresponding distances.

Let us consider a set of deployed randomly in a 3D indoor environment. The graph or a topology diagram is denoted by $\sum(N, M)$ with N target nodes and M mobile anchors with known position. The network is arranged in a square area using spherical method as shown in Figure 6.4.

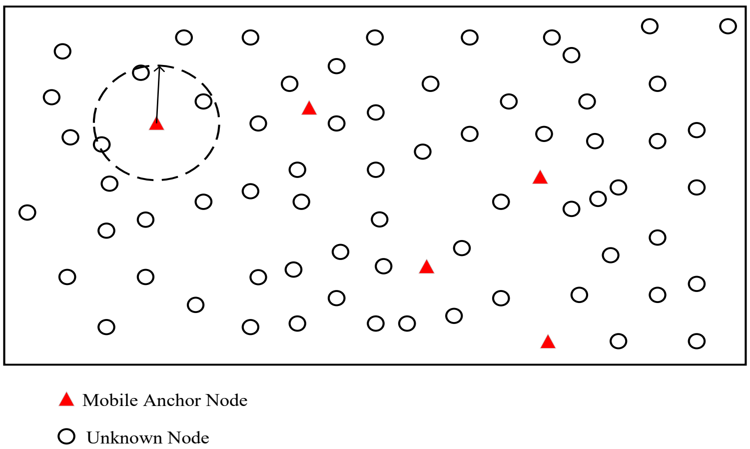

Figure 6.4: Problem formulation scenario for mobile based network.

These sensor nodes can communicate with their neighbours in the sensing range. For the sake of simplicity, we assume that the communication range of unknown and reference mobile anchors is $R \in \mathbb{R}$. Moreover, we assume spherical shape for area of communication of sensor which means the sensor nodes can receive radio signals from other sensors in this area. The target nodes N is represented in Cartesian coordinates form we have:

$$(x_i, y_i, z_i) \in \mathbb{R}^3, i \in (1, 2, 3, \ldots, N) \tag{6.1}$$

The 3D coordinates take any real number including decimals and fractions. In our system model, we have M reference mobile anchors whose coordinates are denoted as follows:

$$(x_{rj}, y_{rj}, z_{rj}) \in \mathbb{R}^3, j \in (1, 2, 3, \ldots, M) \tag{6.2}$$

The coordinates of reference mobile anchors are known apriori and these coordinates are broadcast to static unknown nodes for estimating their location with the help of radio signals. It is assumed that sensor nodes contain radio transmitter/receiver circuits for exchanging beacons in a particular frequency range.

The mobile anchor nodes move along with their predefined path to broadcast beacons to all target nodes within a sensing range periodically. At any instant, only a particular set of anchor nodes are transmitting and the rest are receiving. Mobile anchors along with a trajectory and sensing range also receive RSSI and compute Euclidean distance D_{ij} where $\forall(i, j) \in [1, M]$ as:

$$D_{ij} = \sqrt{(x_i - x_{rj})^2 + (y_i - y_{rj})^2 + (z_i - z_{rj})^2}, \forall(i, j) \in [1, M] \tag{6.3}$$

A fuzzy mapping of RSSI set is taken from anchor nodes versus Euclidean distance. This is known as training phase. At the end of training phase, anchor nodes share a table with all target nodes for completing the mapping function.

$$D_{est} = \digamma(\text{RSSI}) = a_n \text{RSSI}^n + a_{n-1}\text{RSSI}^{n-1} + \cdots + a_1 \text{RSSI} + a_0 \tag{6.4}$$

where D_{est} is the estimated distance. $\digamma$ is the mapping function obtained from interpolation of n^{th} order as provided in (6.4). $a_i, i \in [1, N]$ are the coefficients obtained from interpolation. n will be greater than 3 or more so as to reduce the interpolation error.

The relationship between Euclidean distance and RSSI is nonlinear, thus to complete a mapping between these values, a third or higher order of polynomial is required to complete the training phase. The mapping function is computed as follows:

$$F : RSSI \rightarrow D_{est} = \sum_{i=1}^{n} a_i RSSI^i \tag{6.5}$$

6.5 Proposed Localization Algorithm

The proposed localization algorithm works in four phases as described below:

6.5.1 Training Phase

This is the calibration or mapping phase to obtain the function data that would give us distance between transmitting node and receiving node in the form of RSSI. The phase starts when mobile anchor nodes start moving in random walk way to cover the entire WSN. During their motion, they transmit beacons for some time period and listen to transmissions from other nodes for rest of the time as shown in Figure 6.5. The message signal will be encoded in the form of radio signals with proper modulation technique like Amplitude, Phase, or Frequency.

Since the location of reference anchors are predetermined, so parameters of received signals could be easily correlated to the distance between transmitting node and receiving node. We have chosen RSSI as signal parameter to map against distance. Each anchor node maintains a table of received RSSI from other anchors measured against respective distances.

Once training phase is complete after motion of anchor nodes has covered entire WSN, the mapping tables are exchanged with one another to find the required interpolation function F.

$$D_{est} = F(\text{RSSI}) = \sum_{i=0}^{n} a_i \text{RSSI}^i$$

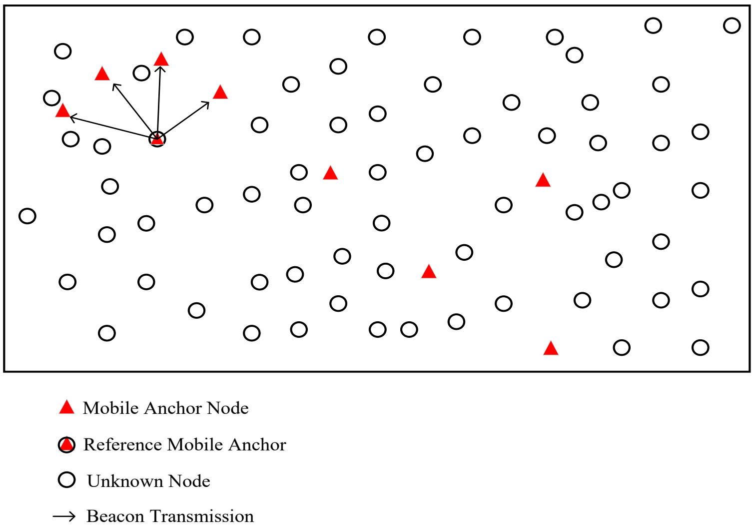

Figure 6.5: Beacon transmission in Training phase.

After training phase, the mobile anchors nodes start moving along their random-walk method again throughout the network and keep sending beacons to unknown nodes periodically. The trajectory of mobile beacons can be modelled as:

$$\xi(t) = \text{RAND}((x_{rj}(t), y_{rj}(t), z_{rj}(t))) \in \mathbb{R}^3, j \in (1, 2, 3, \ldots, M) \tag{6.6}$$

where t is a time factor represents the dynamic behaviour of anchor locations and their corresponding coordinates. ξ is used to describe the path of random-walk using random function of locations "**RAND**". All the nodes in sensing region receive beacons from all the reference anchors within the region. Unknown nodes find the maximum RSSI that they receive from their neighbouring K anchors.

$$\text{RSSI}_{imax} = \max(\text{RSSI}_1, \text{RSSI}_2, \ldots, \text{RSSI}_K), i \in [1, N] \tag{6.7}$$

6.5.2 Position Estimation

The data obtained from training phase as function $\digamma$ is applied in this phase. The reference anchor nodes move along their random walk while transmitting beacons containing their coordinates and the mapping function $\digamma$. The unknown nodes will receive the beacons and find the value of estimated distance from received RSSI. The maximum value of RSSI is used to draw a circle with center as reference location from where maximum RSSI is obtained and radius as estimated distance mapped to maximum RSSI. This circle will contain unknown node but the exact position is uncertain as shown in Figure 6.6. It will be estimated in the last phase.

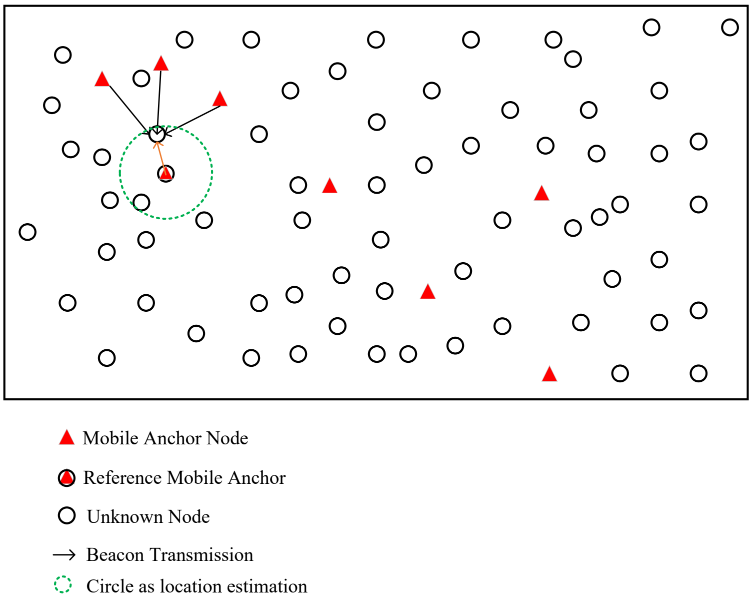

Figure 6.6: Position Estimation as Circle.

The RSSI within a sensing circle provides a center on which unknown node is located as a raw estimation of its location. The mapping function $\digamma$ is used to compute the radius of circle. Then, we have:

$$(x - x_r)^2 + (y - y_r)^2 + (z - z_r)^2 = (D_{est})_i^2, i \in [1, N] \tag{6.8}$$

Where x_r, y_r, z_r are the coordinates of the reference anchor that yields maximum RSSI. The circle interpretation extended to sphere for easy computation for 3D space. The equation of circle is transformed accordingly. Once circle is available as rough location about unknown nodes, the next raw estimation is computed through centroid method. The quality factor for weighing coordinates is computed by fuzzy function used for centroid computing. The basic formula for computing centroid from K reference anchors are:

$$(\hat{x}_i, \hat{y}_i, \hat{z}_i) = (\frac{1}{K}\sum_{j=1}^{K} x_j, \frac{1}{K}\sum_{j=1}^{K} y_j, \frac{1}{K}\sum_{j=1}^{K} z_j)$$

where $(X_{i-est}, Y_{i-est}, Z_{i-est})$ is the estimated location of i^{th} unknown node containing K reference anchors in its radio range.

6.5.3 Position Estimation as Extended Weighted Centroid

In this phase, the unknown nodes use reference anchors beacons to find centroid with the aid of weighted fuzzy functions. The basic form of fuzzy function is (6.12). It contains two membership functions μ_1, μ_2 for fuzzification of input variables. We have selected received signal power and received RSSI as input fuzzy parameters. The first function μ_1 maps received signal power to a specific number as follows:

$$\mu_1 = \begin{cases} 0(\text{Low}) \;\; P_R \in [0, P_{Rmax}/3] \\ 1(\text{Medium}) \;\; P_R \in [P_{Rmax}/3, 2P_{Rmax}/3] \\ 2(\text{High}) \;\; P_R \in [2P_{Rmax}/3, P_{Rmax}] \end{cases} \tag{6.9}$$

Where P_R refers to the received signal power at the unknown node. The fuzzy levels 0, 1, and 2 for different ranges of received signal power and they are scaled as low, medium, and high. Received power is scaled in three equal ranges for this function.

Similar sort of fuzzy function is set for received RSSI as follows:

$$\mu_2 = \begin{cases} 0(\text{Low}) \ \ \text{RSSI} \in [0, \text{RSSI}_{max}/3] \\ 1(\text{Medium}) \ \ \text{RSSI} \in [\text{RSSI}_{max}/3, 2\text{RSSI}_{max}/3] \\ 2(\text{High}) \ \ \text{RSSI} \in [2\text{RSSI}_{max}/3, \text{RSSI}_{max}] \end{cases} \tag{6.10}$$

Like received signal power, RSSI is also divided into three equal ranges that are mapped to three distinct levels as low, medium, and high.

The output function Ω defuzzifies the fuzzy functions. It provides the quality factor as weight for multiplying them with coordinates of reference locations for a certain unknown node. It will be of the following form:

$$\Omega \in [0, 1] \ \text{ for } \ \mu_1, \mu_2 \in [0, 2] \tag{6.11}$$

The value of the output function varies between 0 and 1. Its value depends on levels of its input variables μ_1, μ_2. For example, if $\mu_1 = 0, \mu_2 = 0$, then $\Omega = 0$. Rules can be developed to map input fuzzy levels to output value in the given range. The estimated centroid will be obtained from the following equation:

$$(\hat{x}_i, \hat{y}_i, \hat{z}_i) = (\frac{1}{K}\sum_{j=1}^{K}\Omega_j x_j, \frac{1}{K}\sum_{j=1}^{K}\Omega_j y_j, \frac{1}{K}\sum_{j=1}^{K}\Omega_j z_j)$$

where Ω_j is the fuzzy output for the given beacon received at the unknown node. It is evident that the fuzzy output provides suitable weights to anchor locations based on their RSSI, and received power.

In formulation of basic centroid, each reference location is equally weighted. However, radio signals suffer from several deterioration effects in indoor environment so probability of receiving accurate signal from far reference mobile anchor node is rather low. Signal parameters like RSSI and received power indicate the reliability of the received signal. Hence, these factors must indicate which reference anchor should have more significance towards finding centroid location. The weight to locations is found from objective functions using Fuzzy logic. The fuzzy function Γ will have the following form:

$$\Gamma(i) = \Omega(\mu_1(\text{RSSI}), \mu_2(P_R)), i \in [1, K] \tag{6.12}$$

Where μ represents the membership function or fuzzifier, Ω denotes the output function or defuzzifier. These functions will be explained in algorithm description.

Fuzzy logic based centroid gives second raw estimate of unknown nodes' location. Now, we use these two estimates to arrive at accurate location. Draw a line segment from centroids of respective unknown nodes to their circles that has minimum length such that angle made at centroid with this line segment is right angle. The final location is proposed to be center point of the resulting line segments. It will be the average of centroid location and the point on circle $(x_{min}, y_{min}, z_{min})$ that has minimum Euclidean distance from centroid:

$$(x_i, y_i, z_i) = \frac{1}{2}(\hat{x}_i + x_{min}, \hat{y}_i + y_{min}, \hat{z}_i + z_{min}) \tag{6.13}$$

Hence, two raw estimates of locations of unknown nodes are found, which are used to find the final location estimation that is accurate to a given level.

6.5.4 Accurate Location Estimation

In the final stage, we have two raw estimations to compute the position of unknown nodes.

- The estimation between Circles with center at the exact position of anchor nodes along with maximum RSSI.

- Centroid using weighted average of locations of references anchors in radio range of unknown sensors.

These two raw location estimations will provide us the final solution to the localization problem. For this purpose, we draw a line segment that connects the centroid with the circle such that length of the line segment is minimum. The line segment will intersect circle at the point for which its distance from centroid is minimum. Let that point on the circle have coordinates $x_{min}, y_{min}, z_{min}$. Then, location of unknown nodes will be computed by (6.13).

Algorithm 4 Description of Mobile anchor based localization

Data: Beacons Transmitted by Mobile Anchor Nodes

Results: Localization coordinates of unknown nodes $(x_i, y_i, z_i), i \in [1, N]$

while Training session not completed **do**
Transmit/receive beacons
Get mapping of RSSI with known distance.
Find interpolated function that finds distance for given RSSI.
end while
while Unknown Nodes Not Received Beacons, $i = 1$ to N **do**
while Mobile beacons $\neq K$ **do**
Keep sensing radio frequencies in passive mode.
if Beacon Received **then**
Estimate Received RSSI.
Estimate Distance from RSSI through F.
else
Keep searching for beacons.
end if
end while
end while
Find Maximum RSSI_{max} and corresponding distance D_0
Draw circles at anchor with RSSI_{max} and radius as D_0.
while Fuzzy Functions Evaluation in Process **do**
while Membership functions under process μ_1, μ_2 **do**
Find membership functions using equations (6.9) and (6.10)
Find fuzzy output from defuzzifier using equation (6.11)
Find weighted centroids using equation (6.5.3).
end while
Find actual coordinates of unknown sensors using equation (6.13)
end while

6.6 Simulation Results

In this section, we can briefly explain the simulation process of our proposed method using Mamdani fuzzy method. The estimation is performed by the centroid methods, where weight on the distance estimation is a main variable for centroid relation that latter used to compute the output of the fuzzy system. The simulation is performed in Matlab with fuzzy logic toolbox. The total of $1000m \times 1000m \times 1000m$ is taken for initial simulation. The 10 mobile anchor nodes and 20 to 80 target nodes are deployed which traverse the whole 3D region and transmit beacons to target nodes. The communication range is fixed during the simulation and set to $100m$. The major contribution is to analyze localization error through fuzzy inference system, which provide weighting factor for signal power and RSSI. The example weight output and its relation with RSSI is shown in Figure 6.7.

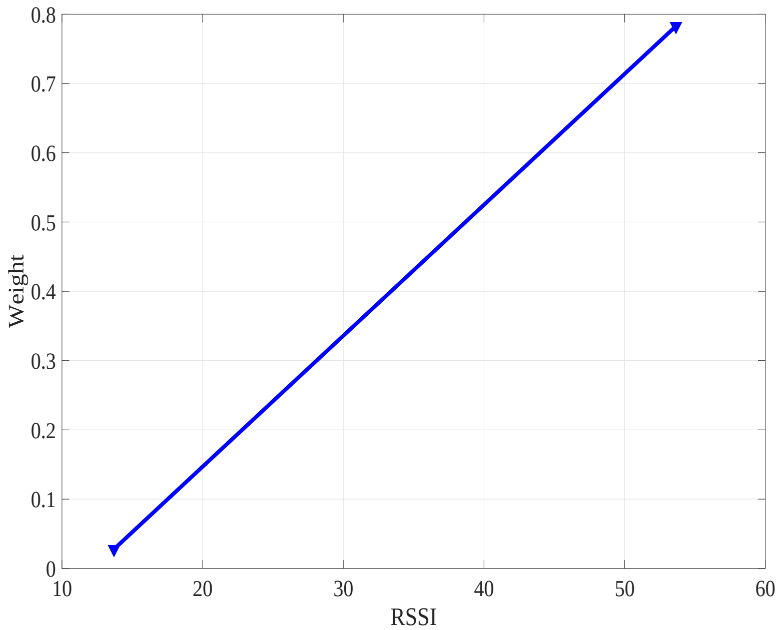

Figure 6.7: Relationship between RSSI and weight.

In our proposed system, the fuzzy sets qualify the RSSI as "HIGH", "MEDIUM" and "LOW" for each input as shown in Figure 6.8 and Figure 6.9. Signal power and RSSI are used as input and weight as a output function. Crisp values are accepted by fuzzy controller. The membership functions can used these crisp values as a input, and all input values are mapped with the degree of membership between 0 and 1. In next phase, the crisp values are converted from crisp input into fuzzy input using fuzzification process. We select receive RSSI and signal power as a fuzzy input parameter. The function μ_1 maps received signal power as described in (6.9).

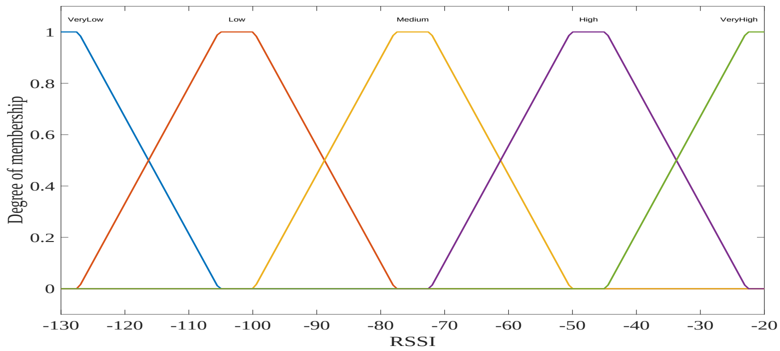

Figure 6.8: RSSI as an input for fuzzy membership function.

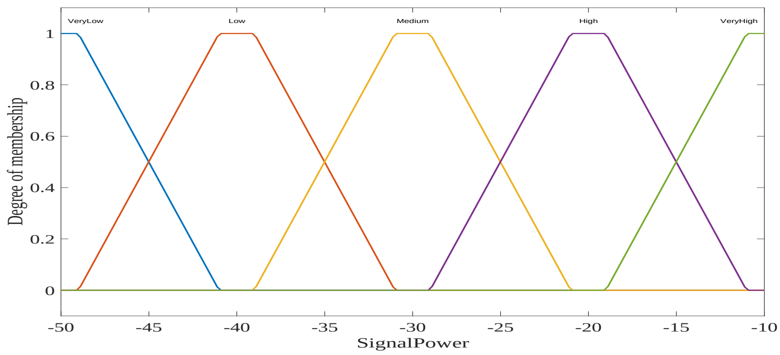

Figure 6.9: Signal power as an input for fuzzy membership function.

The fuzzy levels 0, 1, and 2 are considered as "LOW", "MEDIUM" and "HIGH" for different ranges of received power. The fuzzy function is set up for RSSI as (6.10). Similarly, the weight is used as an output membership function as shown in Figure 6.10 along with fuzzy weighting function in Figure 6.11.

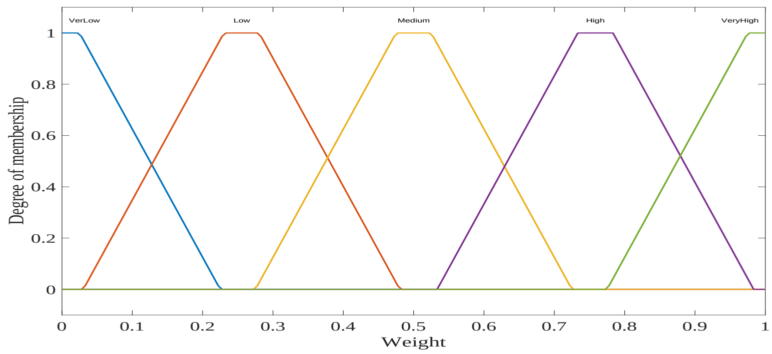

Figure 6.10: weight as an output for fuzzy membership function.

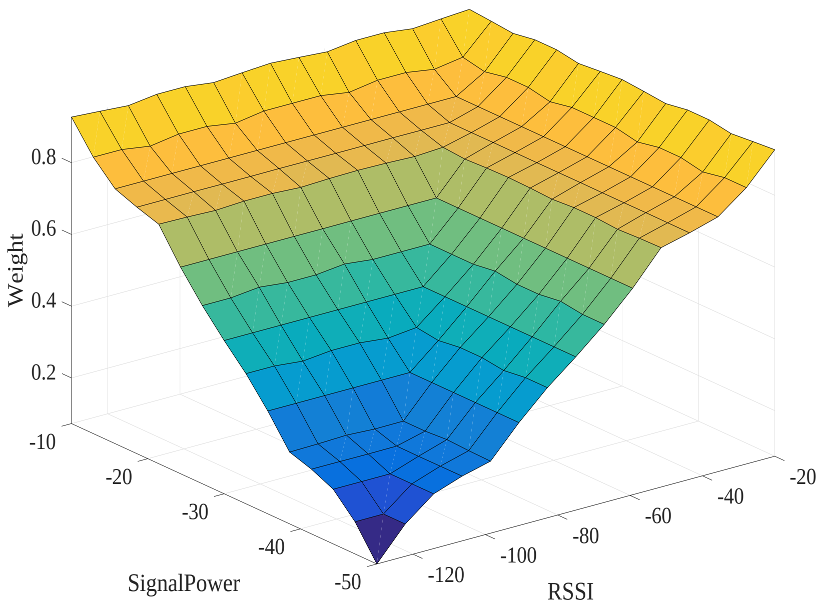

Figure 6.11: The fuzzy inference weighting system.

The whole implementation is done by Mamdani type fuzzy inference, which is much similar to sugeno type fuzzy inference method. However, the membership function in sugeno method is always linear or constant.

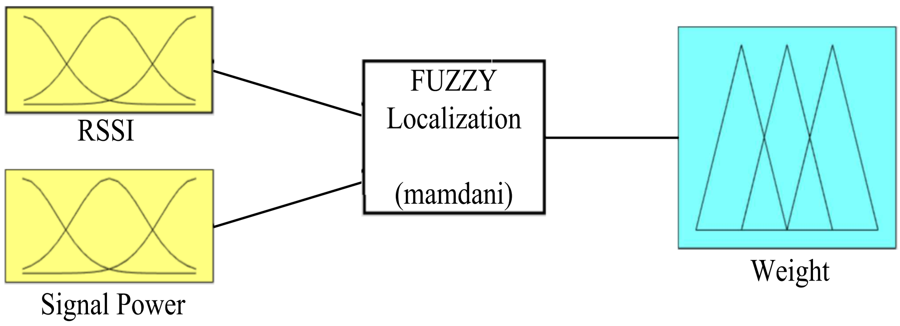

Figure 6.12: Mamadani fuzzy inference (2 input 1 output).

The simulation was run for 1000 times for estimating the average localization error. Initially, we deploy 20 target nodes with 10 anchor nodes. The Mamdani fuzzy inference combined with the input values provides an overall accuracy of $(0.7 - 0.9)m$. The weight is also included in simulation process for checking the centroid accuracy with our proposed techniques. The input membership functions of Mamadani method is the received signal from anchor nodes, which are producing different triangles membership functions from "very LOW" to "very HIGH". The membership functions take the minimum and maximum signal strength values that an anchor broadcast to other target nodes.

The number of sensor nodes are increased gradually and check the accuracy of the proposed algorithm. We noticed that with 60 target nodes and 10 mobile anchor nodes the error was $(0.9 - 1.1)m$. All nodes have a communication range of $250m$. The average result is shown in Figure 6.13.

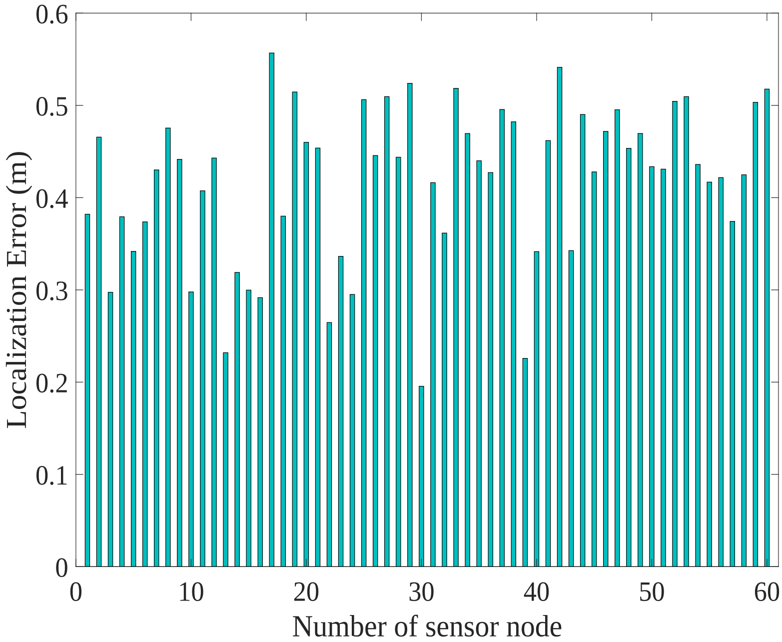

Figure 6.13: Localization Error vs number of unknown nodes.

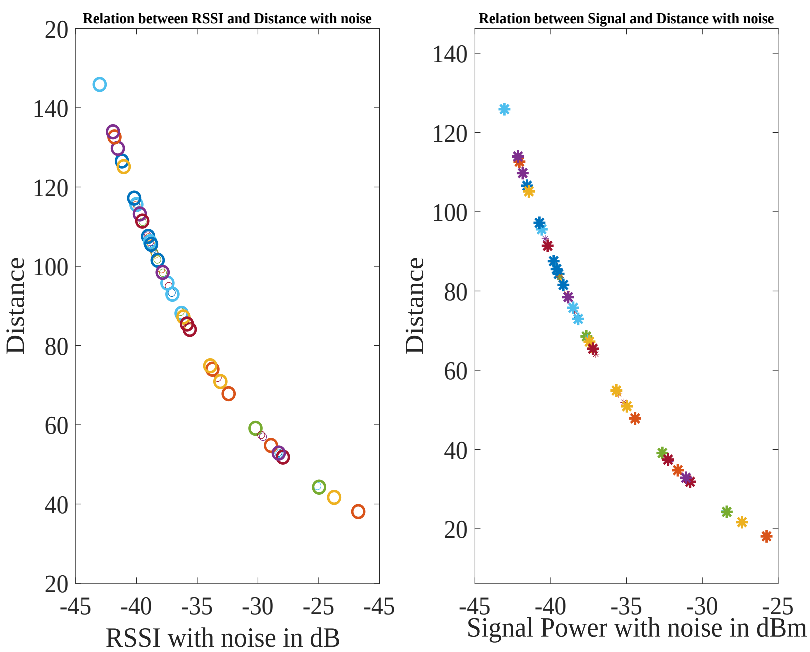

Figure 6.14: RSSI and Received power with Distance.

The received signal power and RSSI are decreasing logarithmically as a function of membership function as shown in Figure 6.14. This plot is generated and obtained from training phase. Furthermore, we observed that the proposed solution is robust against noise factors. However, all the noises are not considered because of nonlinear state of the fuzzy inference. AWGN is added in RSSI with a fixed $SNR = 20dB$. The sensor location in the presence of AWGN is shown in Figure 6.15.

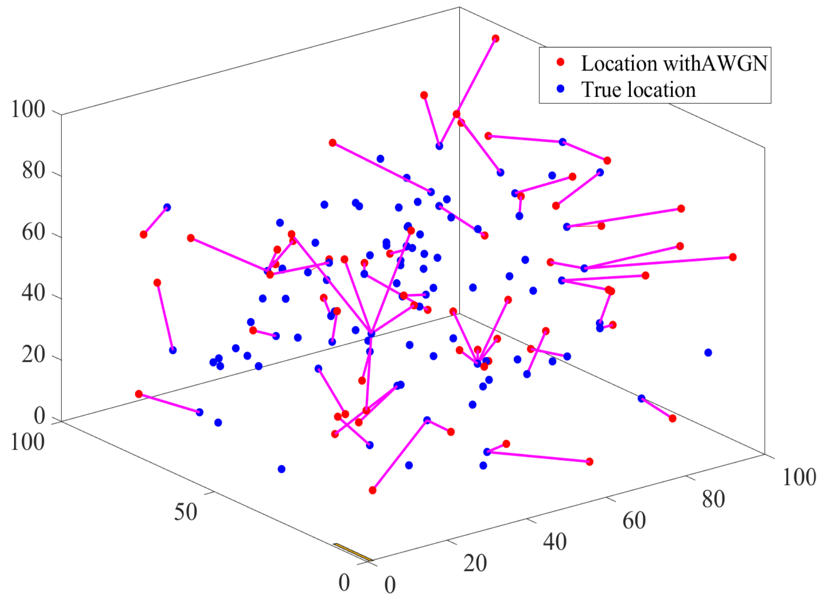

Figure 6.15: Sensor location in presence of AWGN.

The proposed algorithm is also tested and observed at different stages of Fuzzy implementation. Initially 60 anchor nodes were deployed to compute the localization errorfor simple centroid localization algorithms [329]. According to this technique nodes are moving continuously without pausing at any stage with an average speed. Initial coordinates are obtained by using uniform distribution however, with a constant speed of mobile anchor nodes some nodes got duplicate RSSI values causing an extra overhead for reference anchor with extra space. RSSI data set is not stored at any point so each node needed to compute its location dependent on the mobile anchor nodes density. With a large localization error, the size of RSSI request will increases with in a 1000 unit $\times$ 1000 unit of network region. The weight function also implemented as a member ship function in Mamdani fuzzy localization algorithm [320] and Sugeno fuzzy algorithm [228] to test the affect of weight as a membership function. The weight function. Initially, 100 sensor nodes are randomly deployed in the region. Each sensor node receives four different RSSI from each of the four anchor nodes, therefore, RSSI reflect the distance of the sensor node to each of the anchor nodes. After estimating the RSSIs, each sensor node has four weights that are estimated by Sugeno fuzzy system. The entire experiment was done in a square region with $10m$ side length. The RSSI taken from each node in this experiment have slightly different values compared to the RSSI obtained in the simulation. A log normal based adaptive neural fuzzy inference system (ANFIS) is proposed in [326] in which error even goes higher in case of fewer mobile anchor deployment. For a fair trial of errors the localization algorithm was even upto $12m$.

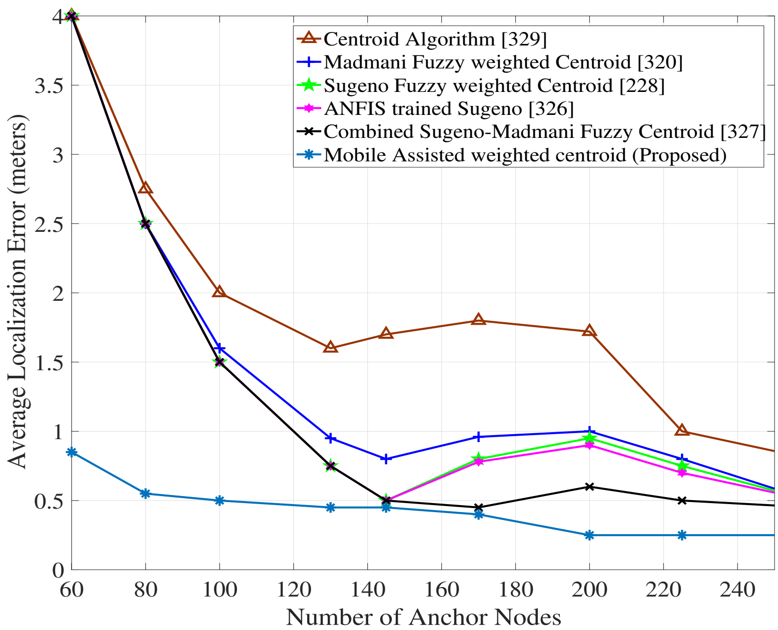

Figure 6.16: Comparison of proposed solution at different stages of Fuzzy implementation.

After computing the sensor node position by using Sugeno and Mamdani fuzzy inference system, an author in [327] assume that the node coordinates for Sugeno and Mamdani system are $(X_{est-sug}, Y_{est-sug})$ and $(X_{est-mam}, Y_{est-mam})$ respectively, then by combining the sugeno and mamdani approaches the author compute the final node coordinates by taking the average as follows [327]:

$$(X_{est-final}, Y_{est-final}) = \left(\frac{X_{est-sug} + X_{est-mam}}{2}, \frac{Y_{est-sug} + Y_{est-mam}}{2} \right) \tag{6.14}$$

The RSS information between sensor nodes and its neighbor anchor nodes is used to estimate the positions without any complicated hardware. Fuzzy logic system is the main component of the proposed schemes. First of all, the edge weight of each anchor node which is adjacent and within the range the sensor node, are found out using Mamdani fuzzy system and the weighted centroid theorem is applied to estimate the sensor node position, then the edge weights are calculated using Sugeno fuzzy system and the localization of node is carried out by weighted centroid theorem. Proposed Combined Mamdani-Sugeno approach, localize the node by taking the average of the location obtained from first two schemes. This approach is able to work for a large network to estimate the node position independently. All of these approaches are then compared with our proposed solution. The propose algorithm gives very high accuracy while increasing the anchor node density. As we have introduce the weigh function after training phase when all the mobile anchors stop their first trial of sending beacons to the unknown nodes. The weight is then mapped to weighted fuzzy functions. This weight will refine the node coordinates in presence of mamdani and sugeno variables. This is why the proposed algorithm obtained a high accuracy as compared to other algorithms using fuzzy logic framework as shown in Figure 6.16. Furthermore, we have also compared our algorithm with the well-known mobile anchor based localization techniques SCAN. DUALSCAN and HILBERT presented in [300]. The disparity between the localization error between the proposed trajectories can be seen in Figure 6.17.

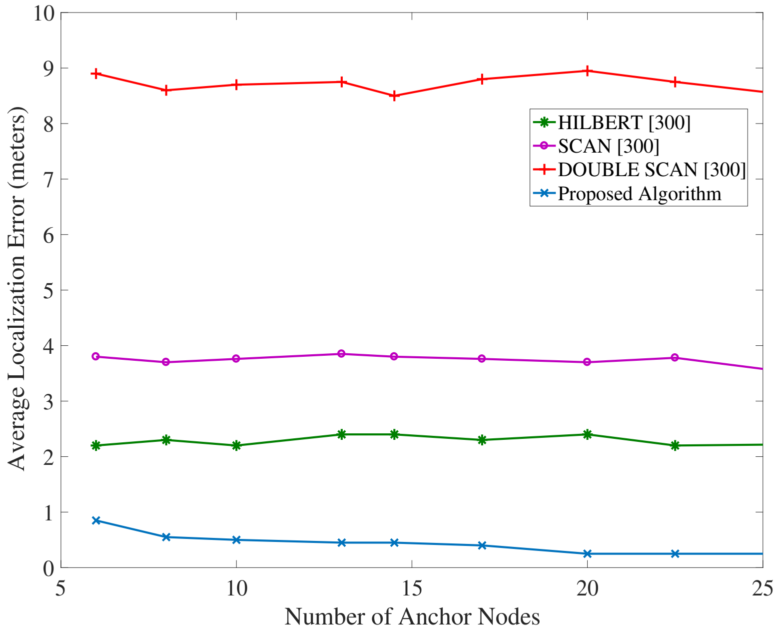

Figure 6.17: Comparison between SCAN, DOUBLE SCAN, HILBERT and proposed algorithm.

We have observed that the error in SCAN algorithm is 2 times larger than the HILBERT algorithm. Whereas, DOUBLE SCAN trajectory have very large error on each axis. The experiment ws performed over $45m$ resolution of mobile anchor nodes that cover a total area of $60m$. The CDF is much better for HILBERT algorithm even the trajectory was very complex in this case. Hence the use of membership function helps the propose solution to provide high accuracy as compared to existing solutions.

6.7 Summary

In this chapter, we present a novel algorithm for solving localization problem using extended centroid approach based on fuzzy logic inference. The problem is solved in four phases: the data is collected to map the distance between nodes and their respective RSSI. The estimation of nodes is computed in the form of circle and then we finds centroid of all nodes using weighted approach, derived by fuzzy logic approach with input parameters (RSSI and signal power) and weight as a output. The use of FL approach can helps to localize the nodes using mobile anchors with low computation cost.

Chapter 7

Conclusion and Future Work

The main function of WSN includes tracking, navigation, localization and sensing. Sensor localization is always crucial because position information is prerequisite for localizing nodes. This thesis focuses on the design and development of localization algorithm for 3D static and mobile anchor based sensor network. In particular, it focuses on the development of low-cost, accurate and efficient algorithm. In particular, we completely studied the issue of sensor network localization in two approaches. One is 3D static node localization and the other is mobile anchor based localization algorithm. We identified the localization challenges, proposed new algorithms and analyzed their performance with simulation in Matlab. To do this, we surveyed state-of-the art algorithms presented in the literature, and highlighted different factors to design robust localization algorithm. Most of the challenges in WSN are caused by network topology, network nature (heterogeneous of homogeneous), radio pattern, network coverage and computation cost in term of communication and energy. We proposed a localization algorithms based on parametric Loop division and refined the coordinates of the nodes using extended kalman filtering process in the presence of noise. The proposed algorithms have the benefit of accurate distance measurement, reduced localization error, improved network coverage and reduced computation cost.

Furthermore, a mobile anchor based localization algorithm is presented with the help of centroid based function and fuzzy logic control to localize static sensor nodes.

7.1 Conclusions

- We performed a comprehensive literature survey and we analyzed that most of the research work proposed for 2D based sensor network. However, most localization schemes are based on assumptions of accurate synchronization between sensor nodes, which is almost impossible to achieve in certain environment. Then, we propose a method based on Parametric Loop Division. The method of PLD is free from node synchronization and only needs to compute mid-point to form a working boundary. With the help of step size and parametric points, the whole network region will be divided into different networks. The subdivision helps to reduce the communication cost and computational overhead.

  PLD also helps to compute its own pre-localized node within a region. An initiator or reference point that start the process to estimate mid-point, parametric point and step size helps transfer the control of iteration to the next reference node. This helps PLD to work in a different network in continuous form. We have compared the PLD algorithm with DV-Hop, MDS-MAP and APIT scheme. The simulation results affirmed superior performance for the proposed algorithm. With a communication range of $200m$ and 6 number of anchor nodes, we noticed an overall average error of $0.89m$ which is far better in range-free localization algorithms. By increasing the number of anchor nodes in each iteration, the accuracy of PLD can be further improved.

- Then, we considered the performance of PLD in the presence of noise. We proposed to use Extended Kalman Filters (EKF) to perform denoising. PLD is capable of finding its own localized node within its working boundary. Reference points are considered to produce mid-points, parametric points and step size, which helps the iterative control to be transferred to inner parametric points. This enables PLD to work in different networks, within the working boundary. At each reference point, sum of RSSI value is computed for pre-localized nodes, compared to a threshold value, and stored in a storage matrix. Furthermore, the localization volume is obtained with maximum and minimum coordinates, stored in a storage matrix. Compared with the refined coordinates, PLD, provide an overall efficiency of 90.84% even in noisy condition.

- Finally, we developed a mobile anchor based localization algorithm for localizing the static sensor nodes. In this algorithm, we extend a centroid based localization algorithm with an extension of fuzzy logic inference. The algorithm operated in four difference phases, and a training phase is used to collect and map data (distance) from corresponding sensor nodes. In a phase 2, node position is estimated in the form of cicular region. We introduce a weighting factor with centroid method from fuzzy logic system with RSSI and signal power as input parameter and weight as output. In the last phase, the results of phases 2 and 3 are used to estimate the node location. This system provides a reasonable accuracy as the nodes always falls within the sensing region.

7.2 Future Work

The importance of localization in WSNs is paramount and this thesis significantly contributes to the fast development of this topic. However, there are still many open issues to be addressed. Along the preparation of this thesis, we have identified the following topics for future work.

1. PLD provides good accuracy in 3D range free localization systems. However, anchor node localization error is not considered. The accuracy of the anchor node position will affect the performance of the PLD scheme.

2. A mobile anchor node can be introduced in PLD algorithm to verify whether further improvement in localization accuracy and efficiency is possible.

3. It is also worth studying the energy consumption of PLD algorithm. The trade-off between energy consumption and localization accuracy can be considered.

4. Does the integration is possible with other technique. Can we make a PLD as hybrid by using it with other algorithms?

5. EKF and fuzzy logic both provides simple solution to be opt out with other techniques. Both techniques are suitable for non-linear computation that make it easy to linearize the system. This is another point that can we make a system that does not need any external frameworks for linearization.

6. Finally, in mobile-assisted localization schemes, many challenging issues are worth studying, like topology construction, path planning and energy consumption.

References

[1] I. F. Akyildiz, W. Su, Y. Sankarasubramaniam, and E. Cayirci, “A survey on sensor networks,” *IEEE Communications Magazine*, vol. 40, no. 8, pp. 102–114, 2002.

[2] S. O. Olatinwo and T.-H. Joubert, “Energy efficient solutions in wireless sensor systems for water quality monitoring: A review,” *IEEE Sensors Journal*, vol. 19, no. 5, pp. 1596–1625, 2018.

[3] K. Zarifi, A. Ghrayeb, and S. Affes, “Distributed beamforming for wireless sensor networks with improved graph connectivity and energy efficiency,” *IEEE Transactions on Signal Processing*, vol. 58, no. 3, pp. 1904–1921, 2009.

[4] J. Hill, M. Horton, R. Kling, L. Krishnamurthy, and L. Krishnamurthy, “The platforms enabling wireless sensor networks,” *Communications of the ACM*, vol. 47, no. 6, pp. 41–46, 2004.

[5] J.-P. Sheu, W.-K. Hu, and J.-C. Lin, “Distributed localization scheme for mobile sensor networks,” *IEEE Transactions on Mobile Computing*, vol. 9, no. 4, pp. 516–526, 2009.

[6] C. Wang, S. Guo, and Y. Yang, “An optimization framework for mobile data collection in energy-harvesting wireless sensor networks,” *IEEE Transactions on Mobile Computing*, vol. 15, no. 12, pp. 2969–2986, 2016.

[7] T. Rault, A. Bouabdallah, and Y. Challal, “Energy efficiency in wireless sensor networks: A top-down survey,” *Computer Networks*, vol. 67, pp. 104–122, 2014.

[8] S. K. Singh, M. Singh, and D. Singh, “A survey of energy-efficient hierarchical cluster-based routing in wireless sensor networks,” *International Journal of Advanced Networking and Application*, vol. 2, no. 02, pp. 570–580, 2010.

[9] P. Park, S. C. Ergen, C. Fischione, C. Lu, and K. H. Johansson, “Wireless network design for control systems: A survey,” *IEEE Communications Surveys & Tutorials*, vol. 20, no. 2, pp. 978–1013, 2017.

[10] C. Soo-Hwan, K. Byung-Kug, P. Jinwo, K. Chul-Hee, and E. Doo-Seop, “An implementation of wireless sensor network,” *IEEE Transactions on Consumer Electronics*, vol. 50, no. 1, pp. 236–244, 2004.

[11] R. Glidden, C. Bockorick, S. Cooper, C. Diorio, D. Dressler, V. Gutnik, C. Hagen, D. Hara, T. Hass, T. Humes *et al.*, "Design of ultra-low-cost uhf rfid tags for supply chain applications," *IEEE Communications Magazine*, vol. 42, no. 8, pp. 140–151, 2004.

[12] R. Morais, M. A. Fernandes, S. G. Matos, C. Serôdio, P. Ferreira, and M. Reis, "A zigbee multi-powered wireless acquisition device for remote sensing applications in precision viticulture," *Computers and Electronics in Agriculture*, vol. 62, no. 2, pp. 94–106, 2008.

[13] J. Eriksson, L. Girod, B. Hull, R. Newton, S. Madden, and H. Balakrishnan, "The pothole patrol: using a mobile sensor network for road surface monitoring," in *Proc. of ACM MobiSys '08*, 2008, pp. 29–39.

[14] V. C. Gungor and G. P. Hancke, "Industrial wireless sensor networks: Challenges, design principles, and technical approaches," *IEEE Transactions on Industrial Electronics*, vol. 56, no. 10, pp. 4258–4265, 2009.

[15] C.-W. Tsai, T.-P. Hong, and G.-N. Shiu, "Metaheuristics for the lifetime of wsn: A review," *IEEE Sensors Journal*, vol. 16, no. 9, pp. 2812–2831, 2016.

[16] G. Simon, M. Maróti, Á. Lédeczi, G. Balogh, B. Kusy, A. Nádas, G. Pap, J. Sallai, and K. Frampton, "Sensor network-based countersniper system," in *Proc. of ACM SenSys'04*. ACM, 2004, pp. 1–12.

[17] A. Arora, P. Dutta, S. Bapat, V. Kulathumani, H. Zhang, V. Naik, V. Mittal, H. Cao, M. Demirbas, M. Gouda *et al.*, "A line in the sand: a wireless sensor network for target detection, classification, and tracking," *Computer Networks*, vol. 46, no. 5, pp. 605–634, 2004.

[18] Á. Lédeczi, A. Nádas, P. Völgyesi, G. Balogh, B. Kusy, J. Sallai, G. Pap, S. Dóra, K. Molnár, M. Maróti *et al.*, "Countersniper system for urban warfare," *ACM Transactions on Sensor Networks*, vol. 1, no. 2, pp. 153–177, 2005.

[19] T. He, S. Krishnamurthy, L. Luo, T. Yan, L. Gu, R. Stoleru, G. Zhou, Q. Cao, P. Vicaire, J. A. Stankovic *et al.*, "Vigilnet: An integrated sensor network system for energy-efficient surveillance," *ACM Transactions on Sensor Networks*, vol. 2, no. 1, pp. 1–38, 2006.

[20] P. Volgyesi, G. Balogh, A. Nadas, C. B. Nash, and A. Ledeczi, "Shooter localization and weapon classification with soldier-wearable networked sensors," in *Proc. of ACM Mobisys'07*. ACM, 2007, pp. 113–126.

[21] P. Juang, H. Oki, Y. Wang, M. Martonosi, L. S. Peh, and D. Rubenstein, "Energy-efficient computing for wildlife tracking: Design tradeoffs and early experiences with zebranet," *ACM SIGARCH Computer Architecture News*, vol. 30, no. 5, pp. 96–107, 2002.

[22] J. Polastre, R. Szewczyk, A. Mainwaring, D. Culler, and J. Anderson, “Analysis of wireless sensor networks for habitat monitoring,” in *Wireless sensor networks*. Springer, 2004, pp. 399–423.

[23] G. Tolle, D. Gay, W. Hong, J. Polastre, R. Szewczyk, D. Culler, N. Turner, K. Tu, S. Burgess, T. Dawson, and P. Buonadonna, “A macroscope in the redwoods,” in *Proc. of ACM SenSys’05,*. ACM Press, 2005. [Online]. Available: https://doi.org/10.1145/1098918.1098925

[24] G. Werner-Allen, K. Lorincz, M. Ruiz, O. Marcillo, J. Johnson, J. Lees, and M. Welsh, “Deploying a wireless sensor network on an active volcano,” *IEEE Internet Computing*, vol. 10, no. 2, pp. 18–25, Mar. 2006. [Online]. Available: https://doi.org/10.1109/mic.2006.26

[25] L. Mo, Y. He, Y. Liu, J. Zhao, S.-J. Tang, X.-Y. Li, and G. Dai, “Canopy closure estimates with GreenOrbs,” in *Proc. of ACM SenSys’09*. ACM Press, 2009. [Online]. Available: https://doi.org/10.1145/1644038.1644049

[26] P. Tokekar, D. Bhadauria, A. Studenski, and V. Isler, “A robotic system for monitoring carp in minnesota lakes,” *Journal of Field Robotics*, vol. 27, no. 6, pp. 779–789, Sep. 2010. [Online]. Available: https://doi.org/10.1002/rob.20364

[27] N. Xu, S. Rangwala, K. K. Chintalapudi, D. Ganesan, A. Broad, R. Govindan, and D. Estrin, “A wireless sensor network for structural monitoring,” in *Proc. of ACM SenSys’04*. ACM Press, 2004. [Online]. Available: https://doi.org/10.1145/1031495.1031498

[28] K. Chintalapudi, T. Fu, J. Paek, N. Kothari, S. Rangwala, J. Caffrey, R. Govindan, E. Johnson, and S. Masri, “Monitoring civil structures with a wireless sensor network,” *IEEE Internet Computing*, vol. 10, no. 2, pp. 26–34, Mar. 2006. [Online]. Available: https://doi.org/10.1109/mic.2006.38

[29] M. Z. A. Bhuiyan, G. Wang, J. Cao, and J. Wu, “Deploying wireless sensor networks with fault-tolerance for structural health monitoring,” *IEEE Transactions on Computers*, vol. 64, no. 2, pp. 382–395, Feb 2015.

[30] K. Chebrolu, B. Raman, N. Mishra, P. K. Valiveti, and R. Kumar, “Brimon: a sensor network system for railway bridge monitoring,” in *Proc. of ACM MobiSys’08*. ACM, 2008, pp. 2–14.

[31] F. Stajano, N. Hoult, I. Wassell, P. Bennett, C. Middleton, and K. Soga, “Smart bridges, smart tunnels: Transforming wireless sensor networks from research prototypes into robust engineering infrastructure,” *Ad Hoc Networks*, vol. 8, no. 8, pp. 872–888, Nov. 2010. [Online]. Available: https://doi.org/10.1016/j.adhoc.2010.04.002

[32] J. M. Kahn, R. H. Katz, and K. S. J. Pister, "Emerging challenges: Mobile networking for "smart dust"," *Journal of Communications and Networks*, vol. 2, no. 3, pp. 188–196, Sep. 2000.

[33] S. Intille, "Designing a home of the future," *IEEE Pervasive Computing*, vol. 1, no. 2, pp. 76–82, Apr. 2002. [Online]. Available: https://doi.org/10.1109/mprv.2002.1012340

[34] K.-K. Yap, V. Srinivasan, and M. Motani, "MAX: Wide area human-centric search of the physical world ," *ACM Transactions on Sensor Networks*, vol. 4, no. 4, pp. 1–34, Aug. 2008. [Online]. Available: https://doi.org/10.1145/1387663.1387672

[35] C.-Y. Lin, S.-C. Wang, S.-Y. Kuo, and C.-Y. Chen, "Increasing service availability in a wireless home network environment," *The Computer Journal*, vol. 52, no. 8, pp. 851–860, Oct. 2008. [Online]. Available: https://doi.org/10.1093/comjnl/bxn050

[36] A. J. Marszal and P. Heiselberg, "Life cycle cost analysis of a multi-storey residential net zero energy building in denmark," *Energy*, vol. 36, no. 9, pp. 5600–5609, Sep. 2011. [Online]. Available: https://doi.org/10.1016/j.energy.2011.07.010

[37] L. Schwiebert, S. K. Gupta, and J. Weinmann, "Research challenges in wireless networks of biomedical sensors," in *Proceedings of the 7th annual international conference on Mobile computing and networking - MobiCom 01*. ACM Press, 2001. [Online]. Available: https://doi.org/10.1145/381677.381692

[38] Y. Zhang, L. Sun, H. Song, and X. Cao, "Ubiquitous wsn for healthcare: Recent advances and future prospects," *IEEE Internet of Things Journal*, vol. 1, no. 4, pp. 311–318, Aug 2014.

[39] C. Efstratiou, N. Davies, G. Kortuem, J. Finney, R. Hooper, and M. Lowton, "Experiences of designing and deploying intelligent sensor nodes to monitor hand-arm vibrations in the field," in *Proc. of ACM MobiSys'07*. ACM Press, 2007. [Online]. Available: https://doi.org/10.1145/1247660.1247677

[40] S. Iyengar, F. T. Bonda, R. Gravina, A. Guerrieri, G. Fortino, and A. Sangiovanni-Vincentelli, "A framework for creating healthcare monitoring applications using wireless body sensor networks," in *Proc. of BodyNets'08*. ICST, 2008. [Online]. Available: https://doi.org/10.4108/icst.bodynets2008.2969

[41] K. Lorincz, B. rong Chen, G. W. Challen, A. R. Chowdhury, S. Patel, P. Bonato, and M. Welsh, "Mercury: A wearable sensor network platform for high-fidelity motion analysis," in *Proc. of ACM Sensys'09*. ACM Press, 2009. [Online]. Available: https://doi.org/10.1145/1644038.1644057

[42] E. I. Shih, A. H. Shoeb, and J. V. Guttag, "Sensor selection for energy-efficient ambulatory medical monitoring," in *Proc. of ACM MobiSys'09*. ACM Press, 2009. [Online]. Available: https://doi.org/10.1145/1555816.1555851

[43] J. Jeong, S. Guo, T. He, and D. Du, "APL: Autonomous passive localization for wireless sensors deployed in road networks," in *Proc. of IEEE INFOCOM'08*. IEEE, Apr. 2008. [Online]. Available: https://doi.org/10.1109/infocom.2008.107

[44] X. Li, W. Shu, M. Li, H.-Y. Huang, P.-E. Luo, and M.-Y. Wu, "Performance evaluation of vehicle-based mobile sensor networks for traffic monitoring," *IEEE Transactions on Vehicular Technology*, vol. 58, no. 4, pp. 1647–1653, May 2009. [Online]. Available: https://doi.org/10.1109/tvt.2008.2005775

[45] M. Franceschinis, L. Gioanola, M. Messere, R. Tomasi, M. A. Spirito, and P. Civera, "Wireless sensor networks for intelligent transportation systems," in *Proc. of IEEE VTC Spring'09*. IEEE, Apr. 2009. [Online]. Available: https://doi.org/10.1109/vetecs.2009.5073915

[46] T. Semertzidis, K. Dimitropoulos, A. Koutsia, and N. Grammalidis, "Video sensor network for real-time traffic monitoring and surveillance," *IET Intelligent Transport Systems*, vol. 4, no. 2, p. 103, 2010. [Online]. Available: https://doi.org/10.1049/iet-its.2008.0092

[47] C. Harrison, B. Eckman, R. Hamilton, P. Hartswick, J. Kalagnanam, J. Paraszczak, and P. Williams, "Foundations for smarter cities," *IBM Journal of Research and Development*, vol. 54, no. 4, pp. 1–16, Jul. 2010. [Online]. Available: https://doi.org/10.1147/jrd.2010.2048257

[48] C. Karlof, N. Sastry, and D. Wagner, "TinySec: a link layer security architecture for wireless sensor networks," in *Proc. of ACM SenSys'04*. ACM Press, 2004. [Online]. Available: https://doi.org/10.1145/1031495.1031515

[49] G. R. Bauer, P. Potisk, and S. Tillich, "Comparing block cipher modes of operation on MICAz sensor nodes," in *Proc. of PDP'09*. IEEE, 2009. [Online]. Available: https://doi.org/10.1109/pdp.2009.16

[50] W. Dargie and C. Poellabauer, *Fundamentals of Wireless Sensor Networks*. John Wiley & Sons, Ltd, Jul. 2010. [Online]. Available: https://doi.org/10.1002/9780470666388

[51] T. M. Johnson and M. Margalho, "Wireless sensor networks for agroclimatology monitoring in the brazilian amazon," in *Proc. of IEEE ICCT'06*. IEEE, 2006, pp. 1–4.

[52] Y. Chen, J. Shu, S. Zhang, L. Liu, and L. Sun, "Data fusion in wireless sensor networks," in *2009 Second International Symposium on Electronic Commerce and Security*, vol. 2, May 2009, pp. 504–509.

[53] M. Arattano and L. Marchi, "Systems and sensors for debris-flow monitoring and warning," *Sensors*, vol. 8, no. 4, pp. 2436–2452, 2008.

[54] T. Ahmad, X. J. Li, and B.-C. Seet, "3d localization using social network analysis for wireless sensor networks," in *Proc. of IEEE ICCIS'18*. IEEE, 2018, pp. 88–92.

[55] I. Chen, A. P. Speer, and M. Eltoweissy, "Adaptive fault-tolerant qos control algorithms for maximizing system lifetime of query-based wireless sensor networks," *IEEE Transactions on Dependable and Secure Computing*, vol. 8, no. 2, pp. 161–176, March 2011.

[56] T. Ahmad, X. Li, and B.-C. Seet, "Parametric loop division for 3d localization in wireless sensor networks," *Sensors*, vol. 17, no. 7, p. 1697, 2017.

[57] B. Hofmann-Wellenhof, H. Lichtenegger, and J. Collins, *Global positioning system: theory and practice*. Springer Science & Business Media, 2012.

[58] R. Mautz, "Indoor positioning technologies," Ph.D. dissertation, ETH, 2012.

[59] M. Cardei and J. Wu, "Coverage in wireless sensor networks," *Handbook of Sensor Networks*, vol. 21, pp. 201–202, 2004.

[60] F. Viani, M. Salucci, P. Rocca, G. Oliveri, and A. Massa, "A multi-sensor wsn backbone for museum monitoring and surveillance," in *in Proc. of EUCAP'12*. IEEE, 2012.

[61] N. Abu-Ghazaleh, K.-D. Kang, and K. Liu, "Towards resilient geographic routing in wsns," in *Proc. of Q2SWinet '05*. ACM, 2005, pp. 71–78.

[62] C. Zhu, C. Zheng, L. Shu, and G. Han, "A survey on coverage and connectivity issues in wireless sensor networks," *Journal of Network and Computer Applications*, vol. 35, no. 2, pp. 619–632, 2012.

[63] T. Ahmad, X. J. Li, and B.-C. Seet, "3d localization based on parametric loop division and subdivision surfaces for wireless sensor networks," in *Proc. of IEEE WOCC'16*. IEEE, 2016, pp. 1–6.

[64] T. Ahmad, X. J. Li, and B. C. Seet, "Noise reduction scheme for parametric loop division 3d wireless localization algorithm based on extended kalman filtering," *Journal of Sensor and Actuator Networks*, vol. 8, no. 2, p. 24, 2019.

[65] T. Ahmad, X. J. Li, and B.-C. Seet, "Fuzzy-logic based localization for mobile sensor networks," in *2019 2nd International Conference on Communication, Computing and Digital systems (C-CODE)*. IEEE, 2019, pp. 43–47.

[66] M. Z. Hasan, H. Al-Rizzo, and F. Al-Turjman, “A survey on multipath routing protocols for qos assurances in real-time wireless multimedia sensor networks,” *IEEE Communications Surveys Tutorials*, vol. 19, no. 3, pp. 1424–1456, thirdquarter 2017.

[67] L. B. Ruiz, T. R. Braga, F. A. Silva, H. P. Assunção, J. M. S. Nogueira, and A. A. Loureiro, “On the design of a self-managed wireless sensor network,” *IEEE Communications Magazine*, vol. 43, no. 8, pp. 95–102, 2005.

[68] B. Warneke, M. Last, B. Liebowitz, and K. S. Pister, “Smart dust: Communicating with a cubic-millimeter computer,” *Computer*, vol. 34, no. 1, pp. 44–51, 2001.

[69] H. Wang, H. Zeng, and P. Wang, “Linear estimation of clock frequency offset for time synchronization based on overhearing in wireless sensor networks,” *IEEE Communications Letters*, vol. 20, no. 2, pp. 288–291, Feb 2016.

[70] T. Ahmad, X. J. Li, and B.-C. Seet, “A self-calibrated centroid localization algorithm for indoor zigbee wsns,” in *Proc. of IEEE ICCSN’16*. IEEE, 2016, pp. 455–461.

[71] A. Howard, M. J. Matarić, and G. S. Sukhatme, “An incremental self-deployment algorithm for mobile sensor networks,” *Autonomous Robots*, vol. 13, no. 2, pp. 113–126, 2002.

[72] J. J. Pan, S. J. Pan, J. Yin, L. M. Ni, and Q. Yang, “Tracking mobile users in wireless networks via semi-supervised colocalization,” *IEEE Transactions on Pattern Analysis and Machine Intelligence*, vol. 34, no. 3, pp. 587–600, March 2012.

[73] X. Bai, Z. Yun, D. Xuan, T. H. Lai, and W. Jia, “Optimal patterns for four-connectivity and full coverage in wireless sensor networks,” *IEEE Transactions on Mobile Computing*, vol. 9, no. 3, pp. 435–448, 2010.

[74] S. Poduri and G. S. Sukhatme, “Constrained coverage for mobile sensor networks,” in *IEEE International Conference on Robotics and Automation, 2004. Proceedings. ICRA’04. 2004*, vol. 1. IEEE, 2004, pp. 165–171.

[75] S. Phoemphon, C. So-In, and N. Leelathakul, “Fuzzy weighted centroid localization with virtual node approximation in wireless sensor networks,” *IEEE Internet of Things Journal*, vol. 5, no. 6, pp. 4728–4752, Dec 2018.

[76] G. Wang, G. Cao, and T. F. La Porta, “Movement-assisted sensor deployment,” *IEEE Transactions on Mobile Computing*, vol. 5, no. 6, pp. 640–652, 2006.

[77] M. Vlachos, D. Gunopulos, and G. Kollios, “Robust similarity measures for mobile object trajectories,” in *Proc. of IEEE IWDESA’02*. IEEE, 2002, pp. 721–726.

[78] K. Dantu, M. Rahimi, H. Shah, S. Babel, A. Dhariwal, and G. S. Sukhatme, "Robomote: enabling mobility in sensor networks," in *Proc. of IEEE ISIPSN'05*. IEEE Press, 2005, p. 55.

[79] A. Achour, L. Deru, and J. C. Deprez, "Mobility management for wireless sensor networks a state-of-the-art," *Procedia Computer Science*, vol. 52, pp. 1101–1107, 2015.

[80] D. L. Guidoni, R. A. F. Mini, and A. A. F. Loureiro, "Applying the small world concepts in the design of heterogeneous wireless sensor networks," *IEEE Communications Letters*, vol. 16, no. 7, pp. 953–955, July 2012.

[81] F. S. Bao, Y. Pang, W. Zhou, W. Jiang, Y. Yang, Y. Liu, and C. Qian, "Coverage-based lossy node localization for wireless sensor networks," *IEEE Sensors Journal*, vol. 16, no. 11, pp. 4648–4656, June 2016.

[82] A. Chen, S. Kumar, and T. H. Lai, "Designing localized algorithms for barrier coverage," in *Proc. of ACM ICMCN'07*. ACM, 2007, pp. 63–74.

[83] J. M. Kahn, R. H. Katz, and K. S. Pister, "Emerging challenges: mobile networking for" smart dust"," *Journal of Communications and Networks*, vol. 2, no. 3, pp. 188–196, 2000.

[84] A. Srinivasan and J. Wu, "Track: A novel connected dominating set based sink mobility model for wsns," in *Proc. of IEEE ICCCN'08*. IEEE, 2008, pp. 1–8.

[85] A. A. Aziz, Y. A. Sekercioglu, P. Fitzpatrick, and M. Ivanovich, "A survey on distributed topology control techniques for extending the lifetime of battery powered wireless sensor networks," *IEEE Communications Surveys Tutorials*, vol. 15, no. 1, pp. 121–144, First 2013.

[86] N. A. A. Aziz, K. A. Aziz, and W. Z. W. Ismail, "Coverage strategies for wireless sensor networks," *World academy of science, Engineering and technology*, vol. 50, pp. 145–150, 2009.

[87] K. Kar and S. Banerjee, "Node placement for connected coverage in sensor networks," in *WiOpt'03: Modeling and Optimization in Mobile, Ad Hoc and Wireless Networks*, 2003, pp. 2–pages.

[88] A. Arora, P. Dutta, S. Bapat, V. Kulathumani, H. Zhang, V. Naik, V. Mittal, H. Cao, M. Demirbas, M. Gouda *et al.*, "A line in the sand: a wireless sensor network for target detection, classification, and tracking," *Computer Networks*, vol. 46, no. 5, pp. 605–634, 2004.

[89] M. Cardei, M. T. Thai, Y. Li, and W. Wu, "Energy-efficient target coverage in wireless sensor networks," in *Proc. of IEEE C&CS'05*, vol. 3. IEEE, 2005, pp. 1976–1984.

[90] M. Cardei and D.-Z. Du, "Improving wireless sensor network lifetime through power aware organization," *Wireless Networks*, vol. 11, no. 3, pp. 333–340, 2005.

[91] M. Cardei, J. Wu, M. Lu, and M. O. Pervaiz, "Maximum network lifetime in wireless sensor networks with adjustable sensing ranges," in *Proc. of IEEE WiMob'05*, vol. 3. IEEE, 2005, pp. 438–445.

[92] H. Zhang, H. Wang, and H. Feng, "A distributed optimum algorithm for target coverage in wireless sensor networks," in *Proc. of IEEE APCIP'09*, vol. 2. IEEE, 2009, pp. 144–147.

[93] H. Zhang, "Energy-balance heuristic distributed algorithm for target coverage in wireless sensor networks with adjustable sensing ranges," in *Proc. of IEEE APCIP'09*, vol. 2. IEEE, 2009, pp. 452–455.

[94] S. Meguerdichian, F. Koushanfar, M. Potkonjak, and M. B. Srivastava, "Coverage problems in wireless ad-hoc sensor networks," in *Proc. IEEE INFOCOM 01*, vol. 3. IEEE, 2001, pp. 1380–1387.

[95] K. Romer and F. Mattern, "The design space of wireless sensor networks," *IEEE Wireless Communications*, vol. 11, no. 6, pp. 54–61, 2004.

[96] C. Alcaraz, J. Lopez, R. Roman, and H.-H. Chen, "Selecting key management schemes for wsn applications," *Computers & Security*, vol. 31, no. 8, pp. 956–966, 2012.

[97] P. Nayak and A. Devulapalli, "A fuzzy logic-based clustering algorithm for wsn to extend the network lifetime," *IEEE sensors journal*, vol. 16, no. 1, pp. 137–144, 2016.

[98] T. Ho, "Urban location estimation for mobile cellular networks: A fuzzy-tuned hybrid systems approach," *IEEE Transactions on Wireless Communications*, vol. 12, no. 5, pp. 2389–2399, May 2013.

[99] L. Gavrilovska, S. Krco, V. Milutinović, I. Stojmenovic, and R. Trobec, *Application and multidisciplinary aspects of Wireless Sensor Networks: concepts, integration, and case studies*. Springer Science & Business Media, 2010.

[100] J. Agre and L. Clare, "An integrated architecture for cooperative sensing networks," *Computer*, vol. 33, no. 5, pp. 106–108, 2000.

[101] I. F. Akyildiz, W. Su, Y. Sankarasubramaniam, and E. Cayirci, "Wireless sensor networks: a survey," *Computer Networks*, vol. 38, no. 4, pp. 393–422, 2002.

[102] K. A. Sudduth, "Engineering technologies for precision farming," in *International Seminar on Agricultural Mechanization Technology for Precision Farming*. Rural Development Admin Suwon, 1999, pp. 5–27.

[103] C. Locke, G. Carbone, A. Filippi, E. Sadler, B. Gerwig, D. Evans *et al.*, "Using remote sensing and modeling to measure crop biophysical variability," in *Proc. of ICPA'16*, vol. 16, 2000.

[104] P. Bonnet, J. Gehrke, and P. Seshadri, "Querying the physical world," *IEEE Personal Communications*, vol. 7, no. 5, pp. 10–15, 2000.

[105] M. A. Hussain, K. kyung Sup *et al.*, "Wsn research activities for military application," in *Proc. of IEEE ICACT'09*, vol. 1. IEEE, 2009, pp. 271–274.

[106] A. Chatterjee and M. Pandey, "Practical applications of wireless sensor network based on military, environmental, health and home applications: A survey," *International Journal of Scientific & Engineering Research*, vol. 5, no. 1, pp. 1043–1050, 2014.

[107] F. Ye, H. Luo, J. Cheng, S. Lu, and L. Zhang, "A two-tier data dissemination model for large-scale wireless sensor networks," in *Proc. of ACM ICMCN'02*. ACM, 2002, pp. 148–159.

[108] L. Schwiebert, S. K. Gupta, and J. Weinmann, "Research challenges in wireless networks of biomedical sensors," in *Proc. of ACM ICMCN'01*. ACM, 2001, pp. 151–165.

[109] R. Beckwith, D. Teibel, and P. Bowen, *Pervasive computing and proactive agriculture*. springer, 2004.

[110] Z. Butler, P. Corke, R. Peterson, and D. Rus, "Virtual fences for controlling cows," in *Proc. of IEEE ICRA'04*, vol. 5. IEEE, 2004, pp. 4429–4436.

[111] A. LaMarca, W. Brunette, D. Koizumi, M. Lease, S. B. Sigurdsson, K. Sikorski, D. Fox, and G. Borriello, "Plantcare: An investigation in practical ubiquitous systems," in *Proc. of ICUC'02*. Springer, 2002, pp. 316–332.

[112] G. Molina and E. Alba, "Location discovery in wireless sensor networks using metaheuristics," *Applied Soft Computing*, vol. 11, no. 1, pp. 1223–1240, 2011.

[113] J. Heidemann, F. Silva, C. Intanagonwiwat, R. Govindan, D. Estrin, and D. Ganesan, "Building efficient wireless sensor networks with low-level naming," in *ACM SIGOPS Operating Systems Review*, vol. 35, no. 5. ACM, 2001, pp. 146–159.

[114] B. Krishnamachari, D. Estrin, S. B. Wicker *et al.*, "The impact of data aggregation in wireless sensor networks." in *Proc. of ICDCS workshops*, vol. 578, 2002.

[115] F. Sivrikaya and B. Yener, "Time synchronization in sensor networks: a survey," *IEEE network*, vol. 18, no. 4, pp. 45–50, 2004.

[116] J. Elson, L. Girod, and D. Estrin, “Fine-grained network time synchronization using reference broadcasts,” *ACM SIGOPS Operating Systems Review*, vol. 36, no. SI, pp. 147–163, 2002.

[117] D. L. Mills, “Internet time synchronization: the network time protocol,” *IEEE Transactions on Communications*, vol. 39, no. 10, pp. 1482–1493, 1991.

[118] L. Lamport, “Time, clocks, and the ordering of events in a distributed system,” *Communications of the ACM*, vol. 21, no. 7, pp. 558–565, 1978.

[119] J. van Greunen and J. Rabaey, “Lightweight time synchronization for sensor networks,” in *Proc. of ACM WSNA'03*. ACM Press, 2003. [Online]. Available: https://doi.org/10.1145/941350.941353

[120] S. Ganeriwal, R. Kumar, and M. B. Srivastava, “Timing-sync protocol for sensor networks,” in *Proc. of ACM SenSys'03*. ACM Press, 2003. [Online]. Available: https://doi.org/10.1145/958491.958508

[121] X. Lai, J. Wang, G. Zeng, M. Wu, J. She, and S. Yang, “Distributed positioning algorithm based on centroid of three-dimension graph for wireless sensor networks,” *Journal of System Simulation*, vol. 20, no. 15, pp. 4104–4111, 2008.

[122] S. Tilak, N. B. Abu-Ghazaleh, and W. Heinzelman, “Infrastructure tradeoffs for sensor networks,” in *Proc. of ACM WSNA'02*. ACM Press, 2002. [Online]. Available: https://doi.org/10.1145/570738.570746

[123] N. F. Shah, Amritanjali, S. Gautam, and D. Gosain, “EERA: Energy efficient reliable routing algorithm for WSN,” in *Proc. of IEEE IICIP'16*. IEEE, Aug. 2016. [Online]. Available: https://doi.org/10.1109/iicip.2016.7975384

[124] J. Hill, R. Szewczyk, A. Woo, S. Hollar, D. Culler, and K. Pister, “System architecture directions for networked sensors,” in *Proc. of ACM ASPLOS'00*. ACM Press, 2000. [Online]. Available: https://doi.org/10.1145/378993.379006

[125] “Crossbow technology inc.” https://patents.google.com/patent/US7506643B2/en, accessed: 2019-04-19.

[126] K. Langendoen and N. Reijers, “Distributed localization in wireless sensor networks: a quantitative comparison,” *Computer Networks*, vol. 43, no. 4, pp. 499–518, Nov. 2003. [Online]. Available: https://doi.org/10.1016/s1389-1286(03)00356-6

[127] M. Weiser, “Hot topics-ubiquitous computing,” *Computer*, vol. 26, no. 10, pp. 71–72, 1993. [Online]. Available: https://doi.org/10.1109/2.237456

[128] N. B. Priyantha, A. K. Miu, H. Balakrishnan, and S. Teller, “The cricket compass for context-aware mobile applications,” in *Proc. of ACM MobiCom'01*. ACM Press, 2001. [Online]. Available: https://doi.org/10.1145/381677.381679

[129] "Sensing technologies." https://www.nap.edu/read/10661/chapter/4#28, accessed: 2019-04-19.

[130] C. Hofner and G. Schmidt, "Path planning and guidance techniques for an autonomous mobile cleaning robot," *Robotics and Autonomous Systems*, vol. 14, no. 2-3, pp. 199–212, 1995.

[131] B. Hofmann-Wellenhof, H. Lichtenegger, and J. Collins, *Global Positioning System: theory and practice*. Springer Science & Business Media, 2012.

[132] G. Welch, G. Bishop, L. Vicci, S. Brumback, K. Keller, and D. Colucci, "High-performance wide-area optical tracking: The hiball tracking system," *Presence: Teleoperators & Virtual Environments*, vol. 10, no. 1, pp. 1–21, 2001.

[133] S. Thrun, D. Fox, W. Burgard, and F. Dellaert, "Robust monte carlo localization for mobile robots," *Artificial Intelligence*, vol. 128, no. 1-2, pp. 99–141, 2001.

[134] S. Tabbane, "Location management methods for third generation mobile systems," *IEEE Communications Magazine*, vol. 35, no. 8, pp. 72–78, 1997.

[135] F. Ye, H. Luo, J. Cheng, S. Lu, and L. Zhang, "A two-tier data dissemination model for large-scale wireless sensor networks," in *Proc. of ACM ICMCN'02*. ACM, 2002, pp. 148–159.

[136] B. Karp and H.-T. Kung, "Gpsr: Greedy perimeter stateless routing for wireless networks," in *Proc. of ACM ICMCN'00*. ACM, 2000, pp. 243–254.

[137] S. Ratnasamy, M. Handley, R. Karp, and S. Shenker, "Topologically-aware overlay construction and server selection," in *Proc. of IEEE INFOCOM'02*, vol. 3. IEEE, 2002, pp. 1190–1199.

[138] T. Wark, W. Hu, P. Corke, J. Hodge, A. Keto, B. Mackey, G. Foley, P. Sikka, and M. Brunig, "Springbrook: Challenges in developing a long-term, rainforest wireless sensor network," in *Proc. of IEEE ICISSNIP'02*. IEEE, Dec. 2008. [Online]. Available: https://doi.org/10.1109/issnip.2008.4762055

[139] "Gps, gnss and segmentations." https://www.novatel.com/an-introduction-to-gnss/chapter-1-gnss-overview/section-1/, accessed: 2019-04-19.

[140] F. Fell and M. Tanenbaum, "Preliminary comparisons of the WGS84(EGM 96) geoid with national vertical datums," in *Proc. of IEEE MTS'01*. Marine Technol. Soc. [Online]. Available: https://doi.org/10.1109/oceans.2001.968784

[141] H. P. Li, S. F. Bian, and Z. M. Li, "Chinese geodetic coordinate system 2000 and its comparison with WGS84," *Applied Mechanics and Materials*, vol. 580-583, pp. 2793–2796, Jul. 2014. [Online]. Available: https://doi.org/10.4028/www.scientific.net/amm.580-583.2793

[142] T. G. Grubb and W. L. Eakle, "Recording wildlife locations with the universal transverse mercator (UTM) grid system," Tech. Rep., 1988. [Online]. Available: https://doi.org/10.2737/rm-rn-483

[143] R. B. Langley *et al.*, "Dilution of precision," *GPS World*, vol. 10, no. 5, pp. 52–59, 1999.

[144] N. S. Alagha, "Cramer-rao bounds of snr estimates for bpsk and qpsk modulated signals," *IEEE Communications Letters*, vol. 5, no. 1, pp. 10–12, 2001.

[145] H. White, "Maximum likelihood estimation of misspecified models," *Econometrica: Journal of the Econometric Society*, pp. 1–25, 1982.

[146] J. Neering, "Optimization and estimation techniques for passive acoustic source localization," Ph.D. dissertation, École Nationale Supérieure des Mines de Paris, 2009.

[147] S. M. Kay, *Fundamentals of Statistical Signal Processing*. Prentice Hall PTR, 1993.

[148] X. Sheng and Y.-H. Hu, "Maximum likelihood multiple-source localization using acoustic energy measurements with wireless sensor networks," *IEEE Transactions on Signal Processing*, vol. 53, no. 1, pp. 44–53, 2005.

[149] S. P. Chepuri, R. T. Rajan, G. Leus, and A.-J. van der Veen, "Joint clock synchronization and ranging: Asymmetrical time-stamping and passive listening," *IEEE Signal Processing Letters*, vol. 20, no. 1, pp. 51–54, 2013.

[150] R. M. Vaghefi, M. R. Gholami, R. M. Buehrer, and E. G. Strom, "Cooperative received signal strength-based sensor localization with unknown transmit powers," *IEEE Transactions on Signal Processing*, vol. 61, no. 6, pp. 1389–1403, 2013.

[151] M. R. Gholami, S. Gezici, and E. G. Strom, "Tdoa based positioning in the presence of unknown clock skew," *IEEE Transactions on Communications*, vol. 61, no. 6, pp. 2522–2534, 2013.

[152] G. M. R, G. S, and S. E. G, "Improved position estimation using hybrid TW-TOA and TDOA in cooperative networks," *IEEE Transactions on Signal Processing*, vol. 60, no. 7, pp. 3770–3785, Jul. 2012. [Online]. Available: https://doi.org/10.1109/tsp.2012.2194705

[153] R. M. Vaghefi, M. R. Gholami, and E. G. Strom, "RSS-based sensor localization with unknown transmit power," in *Proc. of IEEE ICASSP'11*. IEEE, May 2011. [Online]. Available: https://doi.org/10.1109/icassp.2011.5946987

[154] M. R. Gholami, S. Gezici, and E. G. Strom, "Range based sensor node localization in the presence of unknown clock skews," in *Proc. of IEEE ICASSP'13*. IEEE, May 2013. [Online]. Available: https://doi.org/10.1109/icassp.2013.6638419

[155] M. R. Gholami, S. Gezici, E. G. Strom, and M. Rydstrom, “Positioning algorithms for cooperative networks in the presence of an unknown turn-around time,” in *Proc. of IEEE IWSPAWC’11*. IEEE, Jun. 2011. [Online]. Available: https://doi.org/10.1109/spawc.2011.5990386

[156] C. Meesookho, U. Mitra, and S. Narayanan, “On energy-based acoustic source localization for sensor networks,” *IEEE Transactions on Signal Processing*, vol. 56, no. 1, pp. 365–377, Jan. 2008. [Online]. Available: https://doi.org/10.1109/tsp.2007.900757

[157] M. Sun and K. Ho, “Successive and asymptotically efficient localization of sensor nodes in closed-form,” *IEEE Transactions on Signal Processing*, vol. 57, no. 11, pp. 4522–4537, Nov. 2009. [Online]. Available: https://doi.org/10.1109/tsp.2009.2025821

[158] S. Gezici, I. Guvenc, and Z. Sahinoglu, “On the performance of linear least-squares estimation in wireless positioning systems,” in *Proc. of IEEE ICC’08*. IEEE, 2008. [Online]. Available: https://doi.org/10.1109/icc.2008.789

[159] K. C. Ho, X. Lu, and L. Kovavisaruch, “Source localization using TDOA and FDOA measurements in the presence of receiver location errors: Analysis and solution,” *IEEE Transactions on Signal Processing*, vol. 55, no. 2, pp. 684–696, Feb. 2007. [Online]. Available: https://doi.org/10.1109/tsp.2006.885744

[160] S. D. Xie, A. Q. Hu, and Y. Huang, “Nonlinear least square localization algorithm based on time difference of arrival,” *Applied Mechanics and Materials*, vol. 411-414, pp. 903–906, Sep. 2013. [Online]. Available: https://doi.org/10.4028/www.scientific.net/amm.411-414.903

[161] L. Gubin, B. Polyak, and E. Raik, “The method of projections for finding the common point of convex sets,” *USSR Computational Mathematics and Mathematical Physics*, vol. 7, no. 6, pp. 1–24, Jan. 1967. [Online]. Available: https://doi.org/10.1016/0041-5553(67)90113-9

[162] P. Oskoui-Fard and H. Stark, “Tomographic image reconstruction using the theory of convex projections,” *IEEE Transactions on Medical Imaging*, vol. 7, no. 1, pp. 45–58, Mar. 1988. [Online]. Available: https://doi.org/10.1109/42.3928

[163] G. Herman and L. Meyer, “Algebraic reconstruction techniques can be made computationally efficient (positron emission tomography application),” *IEEE Transactions on Medical Imaging*, vol. 12, no. 3, pp. 600–609, 1993. [Online]. Available: https://doi.org/10.1109/42.241889

[164] D. C. Youla and H. Webb, “Image restoration by the method of convex projections: Part 1theory,” *IEEE Transactions on Medical Imaging*, vol. 1, no. 2, pp. 81–94, Oct. 1982. [Online]. Available: https://doi.org/10.1109/tmi.1982.4307555

[165] A. O. Hero and D. Blatt, "Sensor network source localization via projection onto convex sets (pocs)," in *Proc. of IEEE ICASSP'05*, vol. 3. IEEE, 2005, pp. iii–689.

[166] D. Blatt and A. Hero, "Energy-based sensor network source localization via projection onto convex sets," *IEEE Transactions on Signal Processing*, vol. 54, no. 9, pp. 3614–3619, Sep. 2006. [Online]. Available: https://doi.org/10.1109/tsp.2006.879312

[167] B. D and H. A.O, "APOCS: a rapidly convergent source localization algorithm for sensor networks," in *Proc. of IEEE WSSP'05*. IEEE, 2005. [Online]. Available: https://doi.org/10.1109/ssp.2005.1628781

[168] Y. Censor, A. R. D. Pierro, and M. Zaknoon, "Steered sequential projections for the inconsistent convex feasibility problem," *Nonlinear Analysis: Theory, Methods & Applications*, vol. 59, no. 3, pp. 385–405, Nov. 2004. [Online]. Available: https://doi.org/10.1016/j.na.2004.07.018

[169] L. Lin, H. So, and F. K. Chan, "Multidimensional scaling approach for node localization using received signal strength measurements," *Digital Signal Processing*, vol. 34, pp. 39–47, Nov. 2014. [Online]. Available: https://doi.org/10.1016/j.dsp.2014.07.008

[170] I. Kadayif, M. Kandemir, N. Vijaykrishnan, and M. Irwin, "An integer linear programming-based tool for wireless sensor networks," *Journal of Parallel and Distributed Computing*, vol. 65, no. 3, pp. 247–260, Mar. 2005. [Online]. Available: https://doi.org/10.1016/j.jpdc.2004.04.004

[171] M. Marks and E. Niewiadomska-Szynkiewicz, "Localization based on stochastic optimization and RSSI measurements," in *Proc. of ACM/IEEE IPSN'10*. ACM Press, 2010. [Online]. Available: https://doi.org/10.1145/1791212.1791275

[172] G. Mao, B. Fidan, and B. D. Anderson, "Wireless sensor network localization techniques," *Computer Networks*, vol. 51, no. 10, pp. 2529–2553, Jul. 2007. [Online]. Available: https://doi.org/10.1016/j.comnet.2006.11.018

[173] G. J. Pottie and W. J. Kaiser, "Wireless integrated network sensors," *Communications of the ACM*, vol. 43, no. 5, pp. 51–58, May 2000. [Online]. Available: https://doi.org/10.1145/332833.332838

[174] F. Mekelleche and H. Haffaf, "Classification and comparison of range-based localization techniques in wireless sensor networks," *Journal of Communications*, vol. 12, no. 4, pp. 221–227, 2017.

[175] S. P. Singh, , and S. C. Sharma, "Critical analysis of distributed localization algorithms for wireless sensor networks," *International Journal of Wireless and Microwave Technologies*, vol. 6, no. 4, pp. 72–83, Jul. 2016. [Online]. Available: https://doi.org/10.5815/ijwmt.2016.04.07

[176] W. Jianguo, W. Zhongsheng, Z. Ling, S. Fei, and S. Guohua, “A new anchor-based localization algorithm for wireless sensor network,” in *Proc. of IEEE DCABES’11*. IEEE, Oct. 2011. [Online]. Available: https://doi.org/10.1109/dcabes.2011.5

[177] T. Du, S. Qu, Q. Guo, and L. Zhu, “A simple efficient anchor-free node localization algorithm for wireless sensor networks,” *International Journal of Distributed Sensor Networks*, vol. 13, no. 4, p. 155014771770578, Apr. 2017. [Online]. Available: https://doi.org/10.1177/1550147717705784

[178] C. Savarese, J. M. Rabaey, and J. Beutel, “Location in distributed ad-hoc wireless sensor networks,” in *Proc. of IEEE ICASSP’01*, vol. 4. IEEE, 2001, pp. 2037–2040.

[179] D. Moore, J. Leonard, D. Rus, and S. Teller, “Robust distributed network localization with noisy range measurements,” in *Proc. of ACM SenSys’04*. ACM Press, 2004. [Online]. Available: https://doi.org/10.1145/1031495.1031502

[180] S. Lee, H. Woo, and C. Lee, “Wireless sensor network localization with connectivity-based refinement using mass spring and kalman filtering,” *EURASIP Journal on Wireless Communications and Networking*, vol. 2012, no. 1, Apr. 2012. [Online]. Available: https://doi.org/10.1186/1687-1499-2012-152

[181] W. Qin, Y. Feng, and X. Zhang, “Localization algorithm for wireless sensor network based on characteristics of energy attenuation,” *Journal of Chinese Computer Systems*, vol. 30, no. 6, pp. 1082–1088, 2009.

[182] B. Cheng, R. Du, B. Yang, W. Yu, C. Chen, and X. Guan, “An accurate GPS-based localization in wireless sensor networks: A GM-WLS method,” in *Proc. of IEEE ICPPW’11*. IEEE, Sep. 2011. [Online]. Available: https://doi.org/10.1109/icppw.2011.32

[183] I. Mahjri, A. Dhraief, A. Belghith, K. Drira, and H. Mathkour, “A gps-less framework for localization and coverage maintenance in wireless sensor networks,” *KSII Transactions on internet and information systems*, vol. 10, no. 1, pp. 96–116, 2016.

[184] Z. Yang, Z. Zhou, and Y. Liu, “From RSSI to CSI,” *ACM Computing Surveys*, vol. 46, no. 2, pp. 1–32, Nov. 2013. [Online]. Available: https://doi.org/10.1145/2543581.2543592

[185] Y.-H. Wu and W.-M. Chen, “An intelligent target localization in wireless sensor networks,” in *Proc. of IEEE IGBSG’14*. IEEE, Apr. 2014. [Online]. Available: https://doi.org/10.1109/igbsg.2014.6835263

[186] H. P. Mistry and N. H. Mistry, “RSSI based localization scheme in wireless sensor networks: A survey,” in *Proc. of IEEE ICACC’15*. IEEE, Feb. 2015. [Online]. Available: https://doi.org/10.1109/acct.2015.105

[187] J. Xu, W. Liu, F. Lang, Y. Zhang, and C. Wang, "Distance measurement model based on RSSI in WSN," *Wireless Sensor Network*, vol. 02, no. 08, pp. 606–611, 2010. [Online]. Available: https://doi.org/10.4236/wsn.2010.28072

[188] K. C. Tran and E. G. Tsionas, "Gmm estimation of stochastic frontier model with endogenous regressors," *Economics Letters*, vol. 118, no. 1, pp. 233–236, 2013.

[189] R. Luo, O. Chen, and S. Pan, "Mobile user localization in wireless sensor network using grey prediction method," in *Proc. of IEEE IECON'05*. IEEE, 2005. [Online]. Available: https://doi.org/10.1109/iecon.2005.1569330

[190] D. Niculescu and B. Nath, "Dv based positioning in ad hoc networks," *Telecommunication Systems*, vol. 22, no. 1-4, pp. 267–280, 2003.

[191] M. Jin, S. Xia, H. Wu, and X. Gu, "Scalable and fully distributed localization with mere connectivity," in *Proc. of IEEE INFOCOM'11*. IEEE, Apr. 2011. [Online]. Available: https://doi.org/10.1109/infcom.2011.5935163

[192] E. Stevens-Navarro, V. Vivekanandan, and V. W. S. Wong, "Dual and mixture monte carlo localization algorithms for mobile wireless sensor networks," in *Proc. of IEEE WCNC'07*. IEEE, 2007. [Online]. Available: https://doi.org/10.1109/wcnc.2007.735

[193] Y. Shang and W. Ruml, "Improved mds-based localization," in *IEEE INFOCOM 2004*, vol. 4. IEEE, 2004, pp. 2640–2651.

[194] Y. Shang, W. Ruml, Y. Zhang, and M. P. J. Fromherz, "Localization from mere connectivity," in *Proc. of ACM MobiHoc'03*. ACM Press, 2003. [Online]. Available: https://doi.org/10.1145/778415.778439

[195] A. A. Kannan, G. Mao, and B. Vucetic, "Simulated annealing based wireless sensor network localization." *JCP*, vol. 1, no. 2, pp. 15–22, 2006.

[196] C. Alippi and G. Vanini, "A rssi-based and calibrated centralized localization technique for wireless sensor networks," in *Proc. of IEEE PERCOMW'06*. IEEE, 2006, pp. 5–pp.

[197] T. He, C. Huang, B. M. Blum, J. A. Stankovic, and T. Abdelzaher, "Range-free localization schemes for large scale sensor networks," in *Proc. of ACM MobiCom'03*. ACM Press, 2003. [Online]. Available: https://doi.org/10.1145/938985.938995

[198] A. Savvides, H. Park, and M. B. Srivastava, "The bits and flops of the n-hop multilateration primitive for node localization problems," in *Proc. of ACM WSNA'02*. ACM Press, 2002. [Online]. Available: https://doi.org/10.1145/570738.570755

[199] S. Simic and S. Sastry, "Distributed localization in wireless ad hoc networks," Technical Report UCB/ERL, Tech. Rep., 2002.

[200] J. Bachrach, R. Nagpal, M. Salib, and H. Shrobe, "Experimental results for and theoretical analysis of a self-organizing global coordinate system for ad hoc sensor networks," *Telecommunication Systems*, vol. 26, no. 2-4, pp. 213–233, Jun. 2004. [Online]. Available: https://doi.org/10.1023/b:tels.0000029040.85449.7b

[201] N. B. Priyantha, H. Balakrishnan, E. D. Demaine, and S. J. Teller, "Anchor-free distributed localization in sensor networks." in *SenSys*, vol. 3, 2003, pp. 340–341.

[202] L. Meertens and S. Fitzpatrick, "The distributed construction of a global coordinate system in a network of static computational nodes from inter-node distances," *Kestrel Institute TR KES. U*, vol. 4, 2004.

[203] K.-Y. Cheng, K.-S. Lui, and V. Tam, "Localization in sensor networks with limited number of anchors and clustered placement," in *Proc. of IEEE WSNC'07*. IEEE, 2007. [Online]. Available: https://doi.org/10.1109/wcnc.2007.806

[204] A. A. Ahmed, H. Shi, and Y. Shang, "Sharp: A new approach to relative localization in wireless sensor networks," in *25th IEEE International Conference on Distributed Computing Systems Workshops*. IEEE, 2005, pp. 892–898.

[205] M. Maróti, P. Völgyesi, S. Dóra, B. Kusỳ, A. Nádas, Á. Lédeczi, G. Balogh, and K. Molnár, "Radio interferometric geolocation," in *Proceedings of the 3rd international conference on Embedded networked sensor systems*. ACM, 2005, pp. 1–12.

[206] N. Patwari and A. Hero, "Indirect radio interferometric localization via pairwise distances," in *Proc. of IEEE EmNets'06*. Citeseer, 2006, pp. 26–30.

[207] R. Huang, G. V. Zaruba, and M. Huber, "Complexity and error propagation of localization using interferometric ranging," in *Proc. of IEEE ICC'07*. IEEE, 2007, pp. 3063–3069.

[208] N. Alsindi, K. Pahlavan, and B. Alavi, "An error propagation aware algorithm for precise cooperative indoor localization," in *Proc. of IEEE MILCOM'06*. IEEE, Oct. 2006. [Online]. Available: https://doi.org/10.1109/milcom.2006.302311

[209] J. Lloret, J. Tomas, M. Garcia, and A. Canovas, "A hybrid stochastic approach for self-location of wireless sensors in indoor environments," *Sensors*, vol. 9, no. 5, pp. 3695–3712, May 2009. [Online]. Available: https://doi.org/10.3390/s90503695

[210] T. He, C. Huang, B. M. Blum, J. A. Stankovic, and T. Abdelzaher, "Range-free localization schemes for large scale sensor networks," in *Proc. of ACM Mobicom'03*. ACM Press, 2003. [Online]. Available: https://doi.org/10.1145/938985.938995

[211] J. R. Agre, L. P. Clare, G. J. Pottie, and N. P. Romanov, "Development platform for self-organizing wireless sensor networks," in *Unattended Ground Sensor Technologies and Applications*, vol. 3713. International Society for Optics and Photonics, 1999, pp. 257–269.

[212] X. Li, Z. D. Deng, L. T. Rauchenstein, and T. J. Carlson, "Contributed review: Source-localization algorithms and applications using time of arrival and time difference of arrival measurements," *Review of Scientific Instruments*, vol. 87, no. 4, p. 041502, Apr. 2016. [Online]. Available: https://doi.org/10.1063/1.4947001

[213] "Smart floor," http://www3.cc.gatech.edu/fce/smartfloor/, accessed: 2010-09-30.

[214] N. Bulusu, J. Heidemann, and D. Estrin, "GPS-less low-cost outdoor localization for very small devices," *IEEE Personal Communications*, vol. 7, no. 5, pp. 28–34, 2000. [Online]. Available: https://doi.org/10.1109/98.878533

[215] H. Chen, P. Huang, M. Martins, H. C. So, and K. Sezaki, "Novel centroid localization algorithm for three-dimensional wireless sensor networks," in *Proc. of IEEE ICWCNMC'08*. IEEE, 2008, pp. 1–4.

[216] M. Rudafshani and S. Datta, "Localization in wireless sensor networks," in *Proc. of ACM IPSN'07*. ACM Press, 2007. [Online]. Available: https://doi.org/10.1145/1236360.1236368

[217] L. M. Ni, Y. Liu, Y. C. Lau, and A. P. Patil, "Landmarc: indoor location sensing using active rfid," in *Proc. of IEEE PerCom'03*. IEEE, 2003, pp. 407–415.

[218] T. He, C. Huang, B. M. Blum, J. A. Stankovic, and T. Abdelzaher, "Range-free localization schemes for large scale sensor networks," in *Proc. of ACM MobiCom'03*. ACM Press, 2003. [Online]. Available: https://doi.org/10.1145/938985.938995

[219] W. Tie-zhou, Z. Yi-shi, Z. Hui-Jun, and L. Biao, "Wireless sensor network node location based on improved apit," *The Journal of Surveying and Mapping Engineering*, vol. 1, no. 1, pp. 15–19, 2013.

[220] "Zigbee specifications," https://www.zigbee.org/zigbee-products-2/, accessed: 2010-09-30.

[221] J. Blumenthal, F. Reichenbach, and D. Timmermann, "Position estimation in ad hoc wireless sensor networks with low complexity," in *Proc. of IEEE IPNC'05*, 2005, pp. 41–49.

[222] R. Grossmann, J. Blumenthal, F. Golatowski, and D. Timmermann, "Localization in zigbee-based sensor networks," in *Proc. of IEEE EuZDC'07*. Citeseer, 2007.

[223] P. Krishnan, A. Krishnakumar, W.-H. Ju, C. Mallows, and S. Gamt, "A system for lease: Location estimation assisted by stationary emitters for indoor rf wireless networks," in *Proc. of IEEE INFOCOM'04*, vol. 2. IEEE, 2004, pp. 1001–1011.

[224] P. Bahl, V. N. Padmanabhan, V. Bahl, and V. Padmanabhan, "Radar: An in-building rf-based user location and tracking system," 2000.

[225] G. Arditi, A. J. Weiss, and Y. Yovel, "Object localization using a biosonar beam: how opening your mouth improves localization," *Royal Society Open Science*, vol. 2, no. 8, p. 150225, Aug. 2015. [Online]. Available: https://doi.org/10.1098/rsos.150225

[226] E. Elnahrawy, X. Li, and R. P. Martin, "The limits of localization using signal strength: A comparative study," in *Proc of IEEE SECON'04*. IEEE, 2004, pp. 406–414.

[227] C.-L. Wang, Y.-W. Hong, and Y.-S. Dai, "A decentralized positioning method for wireless sensor networks based on weighted interpolation," in *Proc. of IEEE ICC'07*. IEEE, Jun. 2007. [Online]. Available: https://doi.org/10.1109/icc.2007.525

[228] M. A. Monfared, R. Abrishambaf, and S. Uysal, "Range free localization of wireless sensor networks based on sugeno fuzzy inference," in *The Sixth International Conference on Sensor Technologies and Applications (SENSORCOMM)*, 2012, pp. 36–41.

[229] S. Hamdoun, A. Rachedi, and A. Benslimane, "RSSI-based localisation algorithms using spatial diversity in wireless sensor networks," *International Journal of Ad Hoc and Ubiquitous Computing*, vol. 19, no. 3/4, p. 157, 2015. [Online]. Available: https://doi.org/10.1504/ijahuc.2015.070592

[230] P. Barsocchi, S. Lenzi, S. Chessa, and G. Giunta, "A novel approach to indoor RSSI localization by automatic calibration of the wireless propagation model," in *Proc. of IEEE VTC'09*. IEEE, Apr. 2009. [Online]. Available: https://doi.org/10.1109/vetecs.2009.5073315

[231] X. Huang, "Antenna polarization as complementarities on RSSI based location identification," in *Proc. of IEEE ISWPC'09*. IEEE, Feb. 2009. [Online]. Available: https://doi.org/10.1109/iswpc.2009.4800570

[232] J. Chen, X. jun Wu, F. Ye, P. Song, and J. wei Liu, "Improved RSSI-based localization algorithm for park lighting control and child location tracking," in *Proc. of IEEE ICIA'09*. IEEE, Jun. 2009. [Online]. Available: https://doi.org/10.1109/icinfa.2009.5205159

[233] N. Chuku, A. Pal, and A. Nasipuri, "An RSSI based localization scheme for wireless sensor networks to mitigate shadowing effects," in

Proc. of IEEE SoutheastCon'13. IEEE, Apr. 2013. [Online]. Available: https://doi.org/10.1109/secon.2013.6567451

[234] K. Heurtefeux and F. Valois, "Is RSSI a good choice for localization in wireless sensor network?" in *Proc. of IEEE ICAINA'12*. IEEE, Mar. 2012. [Online]. Available: https://doi.org/10.1109/aina.2012.19

[235] N. A. Dieng, M. Charbit, C. Chaudet, L. Toutain, and T. B. Meriem, "A multi-path data exclusion model for rssi-based indoor localization," *Proc of IEEE WPMC'12*, pp. 336–340, 2012.

[236] J.-A. Jiang, C.-L. Chuang, T.-S. Lin, C.-P. Chen, C.-H. Hung, J.-Y. Wang, C.-W. Liu, and T.-Y. Lai, "Collaborative localization in wireless sensor networks via pattern recognition in radio irregularity using omnidirectional antennas," *Sensors*, vol. 10, no. 1, pp. 400–427, Jan. 2010. [Online]. Available: https://doi.org/10.3390/s100100400

[237] S. Jauregui-Ortiz, M. Siller, and F. Ramos, "Node localization in WSN using trigonometric figures," in *Proc. of IEEE WSSN'11*. IEEE, Jan. 2011. [Online]. Available: https://doi.org/10.1109/wisnet.2011.5725030

[238] C. Hai-qing, W. Hua, and W. Hua-kui, "An improved centroid localization algorithm based on weighted average in WSN," in *Proc. of IEEE ICECT'11*. IEEE, Apr. 2011. [Online]. Available: https://doi.org/10.1109/icectech.2011.5941899

[239] R. Vera, S. F. Ochoa, and R. G. Aldunate, "EDIPS: an easy to deploy indoor positioning system to support loosely coupled mobile work," *Personal and Ubiquitous Computing*, vol. 15, no. 4, pp. 365–376, Jan. 2011. [Online]. Available: https://doi.org/10.1007/s00779-010-0357-x

[240] L. Lazos, R. Poovendran, and S. Čapkun, "Rope: robust position estimation in wireless sensor networks," in *Proc. of IEEE IPSN'05*. IEEE Press, 2005, p. 43.

[241] N. A. Dieng, M. Charbit, C. Chaudet, L. Toutain, and T. B. Meriem, "Indoor localization in wireless networks based on a two-modes gaussian mixture model," in *Proc. of IEEE VTC'13*. IEEE, Sep. 2013. [Online]. Available: https://doi.org/10.1109/vtcfall.2013.6692240

[242] Z. M. Livinsa and S. Jayashri, "Performance analysis of diverse environment based on RSSI localization algorithms in wsns," in *Proc. of IEEE ICICT'13*. IEEE, Apr. 2013. [Online]. Available: https://doi.org/10.1109/cict.2013.6558160

[243] M. Kolakowski and V. Djaja-Josko, "TDOA-TWR based positioning algorithm for UWB localization system," in *Proc. of IEEE MIKON'16*. IEEE, May 2016. [Online]. Available: https://doi.org/10.1109/mikon.2016.7491981

[244] W. Meng, L. Xie, and W. Xiao, "TDOA sensor pairing in multi-hop sensor networks," in *Proc. of ACM IPSN'12*. ACM Press, 2012. [Online]. Available: https://doi.org/10.1145/2185677.2185692

[245] A. Savvides, C.-C. Han, and M. B. Strivastava, "Dynamic fine-grained localization in ad-hoc networks of sensors," in *Proc. of ACM MobiCom'01*. ACM Press, 2001. [Online]. Available: https://doi.org/10.1145/381677.381693

[246] A. Ihler, J. Fisher, R. Moses, and A. Willsky, "Nonparametric belief propagation for self-localization of sensor networks," *IEEE Journal on Selected Areas in Communications*, vol. 23, no. 4, pp. 809–819, Apr. 2005. [Online]. Available: https://doi.org/10.1109/jsac.2005.843548

[247] D. Niculescu and B. Nath, "Ad hoc positioning system (aps) using aoa," in *Proc. of IEEE INFOCOM'03*, vol. 3. Ieee, 2003, pp. 1734–1743.

[248] M. Boushaba, A. Hafid, and A. Benslimane, "High accuracy localization method using AoA in sensor networks," *Computer Networks*, vol. 53, no. 18, pp. 3076–3088, Dec. 2009. [Online]. Available: https://doi.org/10.1016/j.comnet.2009.07.015

[249] A. Basu, J. Gao, J. S. B. Mitchell, and G. Sabhnani, "Distributed localization using noisy distance and angle information," in *Proc. of ACM MobiHoc'06*. ACM Press, 2006. [Online]. Available: https://doi.org/10.1145/1132905.1132934

[250] R. Roy and T. Kailath, "ESPRIT-estimation of signal parameters via rotational invariance techniques," *IEEE Transactions on Acoustics, Speech, and Signal Processing*, vol. 37, no. 7, pp. 984–995, Jul. 1989. [Online]. Available: https://doi.org/10.1109/29.32276

[251] H. lin Chang, J. ben Tian, T.-T. Lai, H.-H. Chu, and P. Huang, "Spinning beacons for precise indoor localization," in *Proc. of ACM SenSys'08*. ACM Press, 2008. [Online]. Available: https://doi.org/10.1145/1460412.1460426

[252] R. Stoleru, P. Vicaire, T. He, and J. A. Stankovic, "StarDust: A flexible architecture for passive localization in wireless sensor networks," in *Proc. of ACM SenSys'06*. ACM Press, 2006. [Online]. Available: https://doi.org/10.1145/1182807.1182814

[253] K. Doğançay and H. Hmam, "Optimal angular sensor separation for AOA localization," *Signal Processing*, vol. 88, no. 5, pp. 1248–1260, May 2008. [Online]. Available: https://doi.org/10.1016/j.sigpro.2007.11.013

[254] R. Pregla, *Analysis of Electromagnetic Fields and Waves*. John Wiley & Sons, Ltd, Apr. 2008. [Online]. Available: https://doi.org/10.1002/9780470058503

[255] J.-R. Jiang, C.-M. Lin, F.-Y. Lin, and S.-T. Huang, "ALRD: AoA localization with RSSI differences of directional antennas for wireless sensor networks," *International Journal of Distributed Sensor Networks*, vol. 9, no. 3, p. 529489, Jan. 2013. [Online]. Available: https://doi.org/10.1155/2013/529489

[256] S. Jeong, T.-K. Sung, K. E. Lee, and J. Kang, "Joint TOA/AOA-based localization in wireless sensor networks," in *Proc. of IEEE ICSPCS'14*. IEEE, Dec. 2014. [Online]. Available: https://doi.org/10.1109/icspcs.2014.7021103

[257] H.-J. Shao, X.-P. Zhang, and Z. Wang, "Novel closed-form auxiliary variables based algorithms for sensor node localization using AOA," in *Proc. of IEEE ICASSP'14*. IEEE, May 2014. [Online]. Available: https://doi.org/10.1109/icassp.2014.6853830

[258] E. Y. Menta, N. Malm, R. Jantti, K. Ruttik, M. Costa, and K. Leppanen, "On the performance of AoA–based localization in 5g ultra–dense networks," *IEEE Access*, vol. 7, pp. 33 870–33 880, 2019. [Online]. Available: https://doi.org/10.1109/access.2019.2903633

[259] S. Aditya, H. S. Dhillon, A. F. Molisch, R. M. Buehrer, and H. M. Behairy, "Characterizing the impact of SNR heterogeneity on time-of-arrival-based localization outage probability," *IEEE Transactions on Wireless Communications*, vol. 18, no. 1, pp. 637–649, Jan. 2019. [Online]. Available: https://doi.org/10.1109/twc.2018.2883726

[260] R. S and J. S. N, "Time of arrival based localization in wireless sensor networks: A linear approach," *Signal & Image Processing : An International Journal*, vol. 4, no. 4, pp. 13–30, Aug. 2013. [Online]. Available: https://doi.org/10.5121/sipij.2013.4402

[261] J. Jiang, G. Wang, and K. C. Ho, "Sensor network-based rigid body localization via semi-definite relaxation using arrival time and doppler measurements," *IEEE Transactions on Wireless Communications*, vol. 18, no. 2, pp. 1011–1025, Feb. 2019. [Online]. Available: https://doi.org/10.1109/twc.2018.2889051

[262] H. Shen, Z. Ding, S. Dasgupta, and C. Zhao, "Multiple source localization in wireless sensor networks based on time of arrival measurement," *IEEE Transactions on Signal Processing*, vol. 62, no. 8, pp. 1938–1949, Apr. 2014. [Online]. Available: https://doi.org/10.1109/tsp.2014.2304433

[263] C. Anastopoulos and N. Savvidou, "Time of arrival and localization of relativistic particles," *Journal of Mathematical Physics*, vol. 60, no. 3, p. 032301, Mar. 2019. [Online]. Available: https://doi.org/10.1063/1.5080930

[264] R. Eickhoff, F. Ellinger, R. Mosshammer, R. Weigel, A. Ziroff, and M. Huemer, "3d-accuracy improvements for TDoA based wireless local positioning systems,"

in *Proc. of IEEE GlobeCom'08*. IEEE, Nov. 2008. [Online]. Available: https://doi.org/10.1109/glocomw.2008.ecp.33

[265] W. Meng, L. Xie, and W. Xiao, "Poster abstract: TDOA sensor pairing in multi-hop sensor networks," in *Proc. of ACM IPSN'12*. IEEE, Apr. 2012. [Online]. Available: https://doi.org/10.1109/ipsn.2012.6920969

[266] C. Jia, D. Wang, J. Yin, X. Chen, and L. Zhang, "Joint multiple sources localization using toa measurements based on lagrange programming neural network," *IEEE Access*, vol. 7, pp. 3247–3263, 2019.

[267] V. Kumar, R. Arablouei, F. de Hoog, R. Jurdak, B. Kusy, and N. W. Bergmann, "Pseudo-linear localization using perturbed rssi measurements and inaccurate anchor positions," *Pervasive and Mobile Computing*, vol. 52, pp. 46–59, 2019.

[268] I. Memon, D. Jamro, F. A. Mangi, M. Basit, and M. Memon, "Source localization wireless sensor network using time difference of arrivals (tdoa)," *International Journal of Scientific and Engineering Research*, vol. 4, no. 7, pp. 1046–1054, 2013.

[269] B. Xu, G. Sun, R. Yu, and Z. Yang, "High-accuracy tdoa-based localization without time synchronization," *IEEE Transactions on Parallel and Distributed Systems*, vol. 24, no. 8, pp. 1567–1576, 2013.

[270] O. Tekdas and V. Isler, "Sensor placement for triangulation-based localization," *IEEE transactions on Automation Science and Engineering*, vol. 7, no. 3, pp. 681–685, 2010.

[271] J. S. Esteves, A. Carvalho, and C. Couto, "Generalized geometric triangulation algorithm for mobile robot absolute self-localization," in *Proc. of IEEE ISIE'03*, vol. 1. IEEE, 2003, pp. 346–351.

[272] D. Niculescu and B. Nath, "Dv based positioning in ad hoc networks," *Telecommunication Systems*, vol. 22, no. 1-4, pp. 267–280, 2003.

[273] Z. Luo, X. Cui, W. Zhang, and J. Lu, "Calculation of the 3-d ionized field under hvdc transmission lines," *IEEE Transactions on Magnetics*, vol. 47, no. 5, pp. 1406–1409, 2011.

[274] G. V. Zàruba, M. Huber, F. Kamangar, and I. Chlamtac, "Indoor location tracking using rssi readings from a single wi-fi access point," *Wireless Networks*, vol. 13, no. 2, pp. 221–235, 2007.

[275] C.-L. Wu, L.-C. Fu, and F.-L. Lian, "Wlan location determination in e-home via support vector classification," in *Proc. of IEEE ICNSC'04*, vol. 2. IEEE, 2004, pp. 1026–1031.

[276] P. Cellier, M. Ducassé, S. Ferré, and O. Ridoux, "Multiple fault localization with data mining." in *Proc. of IEEE SEKE'11*, 2011, pp. 238–243.

[277] M. Cummins and P. Newman, "Fab-map: Probabilistic localization and mapping in the space of appearance," *The International Journal of Robotics Research*, vol. 27, no. 6, pp. 647–665, 2008.

[278] S. Chaudhari and D. Cabric, "Cyclic weighted centroid algorithm for transmitter localization in the presence of interference," *IEEE Transactions on Cognitive Communications and Networking*, vol. 2, no. 2, pp. 162–177, June 2016.

[279] H. Chen, Y.-T. Chan, H. V. Poor, and K. Sezaki, "Range-free localization with the radical line," in *Proc. of IEEE ICC'10*. IEEE, 2010, pp. 1–5.

[280] S. Liu, Y. Chen, W. Trappe, and L. J. Greenstein, "Non-interactive localization of cognitive radios based on dynamic signal strength mapping," in *Proc. of IEEE WDNSS'09*. IEEE, 2009, pp. 85–92.

[281] S. Jauregui-Ortiz, M. Siller, and F. Ramos, "Node localization in WSN using trigonometric figures," in *Proc. of IEEE WSSN'11*. IEEE, Jan. 2011. [Online]. Available: https://doi.org/10.1109/wisnet.2011.5725030

[282] "Eurocae-wg-41: Ed-117, mops for mode s multilateration systems for use in advanced surface movement guidance and control systems (a-smgcs)." https://global.ihs.com, accessed: 2019-04-19.

[283] C. S. J. Rabaey, K. Langendoen *et al.*, "Robust positioning algorithms for distributed ad-hoc wireless sensor networks," in *Proc. of USENIX-TAC'02*, 2002, pp. 317–327.

[284] R. Nagpal, H. Shrobe, and J. Bachrach, "Organizing a global coordinate system from local information on an ad hoc sensor network," in *Information processing in sensor networks*. Springer, 2003, pp. 333–348.

[285] J. zeng Wang and H. Jin, "Improvement on apit localization algorithms for wireless sensor networks," in *Proc. of IEEE NSWCTC'09*, vol. 1. IEEE, 2009, pp. 719–723.

[286] W. Jichun, H. Liusheng, X. Hongli, X. Ben, and L. Shanliang, "A novel range free localization scheme based on voronoi diagrams in wireless sensor networks [j]," *Journal of Computer Research and Development*, vol. 1, p. 014, 2008.

[287] K. Kaemarungsi and P. Krishnamurthy, "Modeling of indoor positioning systems based on location fingerprinting," in *Proc. of IEEE INFOCOM'04*, vol. 2. IEEE, 2004, pp. 1012–1022.

[288] N. Patwari, "Location estimation in sensor networks," Ph.D. dissertation, Citeseer, 2005.

[289] G.-J. Yu and S.-C. Wang, “A hierarchical mds-based localization algorithm for wireless sensor networks,” in *Proc. of IEEE AINA’08*. IEEE, 2008, pp. 748–754.

[290] L. Lazos and R. Poovendran, “Hirloc: high-resolution robust localization for wireless sensor networks,” *IEEE Journal on Selected Areas in Communications*, vol. 24, no. 2, pp. 233–246, 2006.

[291] L. Liangbin, C. Yang, G. Xun, and L. Hui, “Three dimensional localization schemes based on sphere intersections in wireless sensor network,” *Journal of Beijing University of Posts and Telecommunications*, vol. 29, no. 5, pp. 48–51, 2006.

[292] G.-L. Dai, C.-C. Zhao, and Y. Qiu, “A localization scheme based on sphere for wireless sensor network in 3d,” *Acta Electronica Sinica*, vol. 36, no. 7, pp. 1297–1303, 2008.

[293] C.-H. Ou and K.-F. Ssu, “Sensor position determination with flying anchors in three-dimensional wireless sensor networks,” *IEEE Transactions on Mobile Computing*, vol. 7, no. 9, pp. 1084–1097, 2008.

[294] G. Yu, F. Yu, and L. Feng, “A three dimensional localization algorithm using a mobile anchor node under wireless channel,” in *Proc. of IEEE WCCI’08*. IEEE, 2008, pp. 477–483.

[295] L. Zhang, X. Zhou, and Q. Cheng, “Landscape-3d; a robust localization scheme for sensor networks over complex 3d terrains,” in *Proc. of IEEE LCN’06*. IEEE, 2006, pp. 239–246.

[296] Z. Hu, D. Gu, Z. Song, and H. Li, “Localization in wireless sensor networks using a mobile anchor node,” in *Proc. of IEEE ASME’08*. IEEE, Jul. 2008. [Online]. Available: https://doi.org/10.1109/aim.2008.4601728

[297] R. Huang and G. V. Zaruba, “Static path planning for mobile beacons to localize sensor networks,” in *Proc. of IEEE PerComw’07*. IEEE, Mar. 2007. [Online]. Available: https://doi.org/10.1109/percomw.2007.109

[298] B. Neuwinger, U. Witkowski, and U. Rückert, “Ad-hoc communication and localization system for mobile robots,” in *Advances in Robotics*. Springer Berlin Heidelberg, 2009, pp. 220–229. [Online]. Available: https://doi.org/10.1007/978-3-642-03983-6_26

[299] R. Huang and G. V. Zaruba, “Static path planning for mobile beacons to localize sensor networks,” in *Proc. of IEEE PerComw’07*. IEEE, Mar. 2007. [Online]. Available: https://doi.org/10.1109/percomw.2007.109

[300] D. Koutsonikolas, S. M. Das, and Y. C. Hu, “Path planning of mobile landmarks for localization in wireless sensor networks,” *Computer*

Communications, vol. 30, no. 13, pp. 2577–2592, Sep. 2007. [Online]. Available: https://doi.org/10.1016/j.comcom.2007.05.048

[301] A. Uchiyama, S. Fujii, K. Maeda, T. Umedu, H. Yamaguchi, and T. Higashino, "Ad-hoc localization in urban district," in *Proc. of IEEE INFOCOM'07*. IEEE, 2007. [Online]. Available: https://doi.org/10.1109/infcom.2007.270

[302] D. Doo and M. Sabin, "Behaviour of recursive division surfaces near extraordinary points," *Computer-Aided Design*, vol. 10, no. 6, pp. 356–360, 1978.

[303] E. Catmull and J. Clark, "Recursively generated b-spline surfaces on arbitrary topological meshes," *Computer-Aided Design*, vol. 10, no. 6, pp. 350–355, 1978.

[304] C. Loop, "Smooth subdivision surfaces based on triangles," *Master's thesis, University of Utah, Department of Mathematics*, 1987.

[305] N. Dyn, D. Levine, and J. A. Gregory, "A butterfly subdivision scheme for surface interpolation with tension control," *ACM transactions on Graphics (TOG)*, vol. 9, no. 2, pp. 160–169, 1990.

[306] L. Kobbelt, "Interpolatory subdivision on open quadrilateral nets with arbitrary topology," in *Computer Graphics Forum*, vol. 15, no. 3. Wiley Online Library, 1996, pp. 409–420.

[307] M. Halstead, M. Kass, and T. DeRose, "Efficient, fair interpolation using catmull-clark surfaces," in *Proc. of ACM SIGGRAPH'93*. ACM, 1993, pp. 35–44.

[308] A. H. Nasri, "Surface interpolation on irregular networks with normal conditions," *Computer Aided Geometric Design*, vol. 8, no. 1, pp. 89–96, 1991.

[309] J. Zheng and Y. Cai, "Interpolation over arbitrary topology meshes using a two-phase subdivision scheme," *IEEE Transactions on Visualization and Computer Graphics*, vol. 12, no. 3, pp. 301–310, 2006.

[310] S. Lai and F. F. Cheng, "Similarity based interpolation using catmull–clark subdivision surfaces," *The Visual Computer*, vol. 22, no. 9, pp. 865–873, Sep 2006. [Online]. Available: https://doi.org/10.1007/s00371-006-0072-9

[311] F.-H. F. Cheng, F.-T. Fan, S.-H. Lai, C.-L. Huang, J.-X. Wang, and J.-H. Yong, "Loop subdivision surface based progressive interpolation," *Journal of Computer Science and Technology*, vol. 24, no. 1, pp. 39–46, Jan 2009. [Online]. Available: https://doi.org/10.1007/s11390-009-9199-2

[312] J. M. Lane and R. F. Riesenfeld, "A theoretical development for the computer generation and display of piecewise polynomial surfaces," *IEEE Transactions on Pattern Analysis and Machine Intelligence*, vol. PAMI-2, no. 1, pp. 35–46, Jan. 1980. [Online]. Available: https://doi.org/10.1109/tpami.1980.4766968

[313] M. Saxena, P. Gupta, and B. N. Jain, "Experimental analysis of rssi-based location estimation in wireless sensor networks," in *Proc. of IEEE COMSWARE'08*. IEEE, 2008, pp. 503–510.

[314] X. J. Li, "An analytical method for centroid computing and its application in wireless localization," in *Proc. of IEEE ICON'13*. IEEE, 2013, pp. 1–5.

[315] H.-C. Chu and R.-H. Jan, "A gps-less, outdoor, self-positioning method for wireless sensor networks," *Ad Hoc Networks*, vol. 5, no. 5, pp. 547–557, 2007.

[316] D. Moore, J. Leonard, D. Rus, and S. Teller, "Robust distributed network localization with noisy range measurements," in *Proc. of ACM ICENSS'04*. ACM, 2004, pp. 50–61.

[317] Z. Sahinoglu, S. Gezici, and I. Guvenc, "Ultra-wideband positioning systems," *Cambridge, New York*, 2008.

[318] S. S. Haykin and M. Moher, *Modern wireless communications*. Pearson Education India, 2011.

[319] K. R. Anne, K. Kyamakya, F. Erbas, C. Takenga, and J. C. Chedjou, "Gsm rssi-based positioning using extended kalman filter for training artificial neural networks," in *Proc. of IEEE VTC'04*, vol. 6. IEEE, 2004, pp. 4141–4145.

[320] I. Iancu and C.-I. Popirlan, "Mamdani fuzzy logic controller with mobile agents for matching," in *Proceedings of the 11th WSEAS international conference on nural networks and 11th WSEAS international conference on evolutionary computing and 11th WSEAS international conference on Fuzzy systems*. World Scientific and Engineering Academy and Society (WSEAS), 2010, pp. 117–122.

[321] P. Chalimbaud, F. Marmoiton, and F. Berry, "Towards an embedded visuo-inertial smart sensor," *The International Journal of Robotics Research*, vol. 26, no. 6, pp. 537–546, 2007.

[322] J. Albukerque, J. Lair, B. Govin, G. Muller, P. Riant, D. Berton, and D. Godart, "Autonomous satellite navigation using optico-inertial instruments," in *Automatic Control in Space 1985*. Elsevier, 1986, pp. 183–188.

[323] Y. Zhu and A. Shareef, "Comparisons of three kalman filter tracking algorithms in sensor network," in *2006 International Workshop on Networking, Architecture, and Storages (IWNAS'06)*. IEEE, 2006, pp. 2–pp.

[324] C.-H. Ou and W.-L. He, "Path planning algorithm for mobile anchor-based localization in wireless sensor networks," *IEEE Sensors Journal*, vol. 13, no. 2, pp. 466–475, 2012.

[325] G. J. Klir and B. Yuan, *Fuzzy Sets and Fuzzy Logic: Theory and Applications*. Prentice Hall PTR New Jersey, 1995, vol. 574.

[326] S. K. Gharghan, R. Nordin, A. M. Jawad, H. M. Jawad, and M. Ismail, "Adaptive neural fuzzy inference system for accurate localization of wireless sensor network in outdoor and indoor cycling applications," *IEEE Access*, vol. 6, pp. 38 475–38 489, 2018.

[327] V. Kumar, A. Kumar, and S. Soni, "A combined mamdani-sugeno fuzzy approach for localization in wireless sensor networks," in *Proceedings of the International Conference & Workshop on Emerging Trends in Technology*. ACM, 2011, pp. 798–803.

[328] J. Dombi, "A general class of fuzzy operators, the demorgan class of fuzzy operators and fuzziness measures induced by fuzzy operators," *Fuzzy Sets and Systems*, vol. 8, no. 2, pp. 149–163, 1982.

[329] Y.-B. Ko and N. H. Vaidya, "Location-aided routing (lar) in mobile ad hoc networks," *Wireless networks*, vol. 6, no. 4, pp. 307–321, 2000.

Appendix A

Irregular node distribution in PLD

Let the parametric points be

$$P_{ik} = \{P_{11}, P_{12}, ..., P_{1k}\} \tag{A.1}$$

New center points are calculated by using parametric factor. The new center points which is less dependent with irregular distribution of anchor node, can be calculated as:

$$\acute{M_1} = \alpha_k M_1 + \frac{(1-\alpha_k)}{k}\sum_{k=1}^{K} P_{ik} \tag{A.2}$$

where α_k represents parametric function of PLD network obtained from [315] whose value is constant if anchor node has regular distribution. Due to symmetry, we can also write this for anchor node distribution

$$\acute{M_1} = \alpha_k M_1 + \frac{(1-\alpha_k)}{k}\sum_{k=1}^{k} A_{ik} \tag{A.3}$$

$$\acute{M_1} = \alpha_k M_1 + (1-\alpha_k)\frac{\sum_{k=1}^{K}(A_{ik})}{k} \tag{A.4}$$

$$\acute{M_1} = \alpha_k M_1 + (1-\alpha_k) M_1 \tag{A.5}$$

Thus, for regular distribution the centroid of points lies in centre i.e. $\acute{M_1} = M_1$. In case of irregular distribution the value of α_k lies between 0.5 to 0.75. Hence,

$$\alpha_k = \frac{3}{8} + (\frac{3}{8} + \frac{1}{4}\cos\frac{2\pi}{k})^2 \tag{A.6}$$

To compute radio irregularity, we take two different values of α_k. One is 0.5 for assuming center value and 0.75 for anchor nodes. α_k has direct effect on cosine angle that is between two anchor nodes from the center points in triangulation. Suppose the difference in angle is $(0-90)^{\circ}$, then the value of α_k ranges from 0.516 to 0.765.
M_1 has a parametric factor $\alpha_m = \alpha_k = \frac{2\pi}{k}$ and $\alpha_p = \alpha_k = \frac{\alpha_1, \alpha_2, ..., \alpha_p}{k}$. So the next mid

point is

$$\acute{M}_1 = \alpha_m M_1 + (1 - \alpha_p) M_1 \tag{A.7}$$

$$\acute{M}_1 = (1 + \alpha_m - \alpha_p) M_1 \tag{A.8}$$

Appendix B

Shifting of center point in PLD

For perfect mathematical modelling, we assume that anchor nodes are regularly distributed, the sum of acute angle making with center is equal to $360°$.
If $k = 5$ $A = 5$, $\cos\theta$ has value of 0.3090 and $\theta = 72°$. And the value of $\alpha_k = 0.5795$.
If $k = 6$ $A = 6$, $\cos\theta$ has value of 0.5 and $\theta = 60°$. And the value of $\alpha_k = 0.625$.
If irregular anchor node distribution occurs, then we consider irregular distribution of angle between anchor nodes. The angle effect on parametric factor is significant only when it has significant difference between angles.
If angle varies by $10°$ at $k = 5$ then the value of θ lies between $\theta = (67° - 77°)$ and the value of $\alpha_k = (0.5984 - 0.5610)$. Hence localization error = $0.0374m$. Similarly, if angle varies by $10°$ at $k = 6$ then the value of θ lies between $\theta = (55° - 65°)$ and the value of $\alpha_k = 0.6437 - 0.6060$. Hence localization error = $0.0377m$. This shows that anchor node irregularity produces some considerable error but we can minimize it. The minimization occurs because we calculate only midpoint of each iteration by using this parametric function. The difference of shifting is greatly minimized by:

$$\acute{M_1} = (1 + \alpha_p - \alpha_m)M_1 \tag{B.1}$$

With the localization error of 0.0377 in a parametric factor equation, we get; $\acute{M_1} = (1 - 0.0377)M_1 = 0.9623M_1$.

From the numeric parametric analysis, it is clearly seen that less angle gives higher parametric value α_p and higher angle gives lower parametric constant α_m.

Appendix C

Multipath transmission model in EKF-PLD

The noise includes additive noise to the distances:

$$d_{i,j} = \sqrt{(x_i - x_j)^2 + (y_i - y_j)^2 + (z_i - z_j)^2} + \Im_{i,j} \tag{C.1}$$

while the noise model widely used is multiplicative as follows:

$$d_{i,j} = \sqrt{(x_i - x_j)^2 + (y_i - y_j)^2 + (z_i - z_j)^2} + \parallel 1 + \Im_{i,j} \parallel \tag{C.2}$$

$$= \Im_{i,j} - \Im_{LOS}\left(0, \parallel \sqrt{(x_i - x_j)^2 + (y_i - y_j)^2 + (z_i - z_j)^2} \parallel^2 \sigma_{i,j}^2\right) \tag{C.3}$$

$$= \Im_{i,j} - \Im_{NLOS}\left(\left[\parallel \sqrt{(x_i - x_j)^2 + (y_i - y_j)^2 + (z_i - z_j)^2} \parallel^2 \sigma_{i,j}^2\right]_{min}, \left[\parallel \sqrt{(x_i - x_j)^2 + (y_i - y_j)^2 + (z_i - z_j)^2} \parallel^2 \sigma_{i,j}^2\right]_{max}\right) \tag{C.4}$$

Let us assume the $dl_{i,j} = \sqrt{(x_i - x_j)^2 + (y_i - y_j)^2 + (z_i - z_j)^2}$ as the ideal distance without noise influence. Practical RSSI data have high noise variations and it is suitable for adding the weight that can develop approximations of log-likehood function in the sophisticated noise model. The weights can be written as $\gamma = \frac{1}{\sigma_{i,j}^2 d_{i,j}^2}$, so this noise modeling system is known as intelligent noise as:

$$= \sum_{i,j\epsilon 1,2,3\ldots N} \frac{1}{\parallel dl_{i,j} \parallel^2 \sigma_{i,j}^2} (\parallel dl_{i,j} \parallel - d_{i,j}) \tag{C.5}$$

In case of intelligent weighting, the noise is scaled based on the distance that is not reliable for long distances due to less weight. In that case, naive Bayesian noise model is a good solution expressed as:

$$= \sum_{i,j\epsilon 1,2,3\ldots N} \frac{1}{\parallel dl_{i,j} \parallel^2 \sigma_{i,j}^2} (\log \parallel dl_{i,j} \parallel - \log d_{i,j}) \tag{C.6}$$

Appendix D

AGN and AWGN noise derivations

Intelligent noise:

$$|\ \vec{D}_{int.noise}\ |= \sum_{k=1}^{m} D_{ik} + \frac{1}{D_k^2 + var(D_k^2)} x(lD_k - D_k)^2 \tag{D.1}$$

Naive noise:

$$|\ \vec{D}_{naive.noise}\ |= \sum_{k=1}^{m} D_{ik} + \frac{1}{D_k^2 + var(D_k^2)} x(\log lD_k - \log D_k)^2 \tag{D.2}$$

Then the combination of intelligent and noise model that forms the multiplicative noise that can be calculated as:

$$|\ \vec{D}_{mul.noise}\ |= \sum_{k=1}^{m} [\frac{1}{D_k^2 + var(D_k^2)} x(lD_k - D_k)^2 + \frac{1}{D_k^2 + var(D_k^2)} x(\log lD_k - \log D_k)^2] \tag{D.3}$$